UNIVERSIDAD AUTÓNOMA DE MADRID
FACULTAD DE MEDICINA
Departamento de Anatomía, Histología y Neurociencia

Implicación de los receptores dopaminérgicos D1 y D2 en la neurotoxicidad inducida por metanfetamina

TESIS DOCTORAL

Sara Ares Santos

Madrid, 2013

INSTITUTO CAJAL
CONSEJO SUPERIOR DE INVESTIGACIONES CIENTÍFICAS
(CSIC)

Implicación de los receptores dopaminérgicos D1 y D2 en la neurotoxicidad inducida por metanfetamina

Memoria presentada por Sara Ares Santos

para optar al título de Doctor,

elaborada a partir del trabajo realizado bajo la dirección de la Dra. Rosario Moratalla Villalba, en el Instituto Cajal, (CSIC), Madrid.

MINISTERIO
DE CIENCIA
E INNOVACIÓN

CSIC
CONSEJO SUPERIOR DE INVESTIGACIONES CIENTÍFICAS

Doña Rosario Moratalla Villalba, Profesor Titular del Instituto Cajal en el CSIC de Madrid

CERTIFICA

Que Doña Sara Ares Santos ha realizado en el departamento de Neurobiología Funcional y de Sistemas, del Instituto Cajal, bajo mi dirección, el presente trabajo de investigación correspondiente a la Tesis Doctoral: “Implicación de los receptores dopaminérgicos D1 y D2 en la neurotoxicidad inducida por metanfetamina”.

Revisado el presente trabajo, considero que la presente memoria reúne todos los requisitos necesarios para ser sometida a juicio de la Comisión correspondiente

Y para que así conste y surta los efectos oportunos, firmo la presente en Madrid a …… de ……...de 2013.

Fdo. Rosario Moratalla Villalba

<<Las ideas no duran mucho.
Hay que hacer algo con ellas.>>

Santiago Ramón y Cajal

A mis padres,
A Juan,
A Gabi

Quiero expresar mi más sincero agradecimiento a todas las personas e instituciones que, en mayor o menor medida, han contribuido a la realización de esta Tesis Doctoral con su trabajo, apoyo, consejos y confianza, en especial:

A mi directora de Tesis, la Dra. Rosario Moratalla Villalba, por confiar en mí desde el primer momento cuando llegué al laboratorio llena de motivación y vacía de experiencia. Por brindarme la oportunidad de desarrollarme como investigadora en su laboratorio, por su orientación, su apoyo y sus consejos en el conjunto de este trabajo. Por no escatimar en gastos para mi formación permitiéndome además presentar en congresos nacionales e internacionales los trabajos que componen esta Tesis.

A todas las instituciones que han financiado este trabajo con los proyectos de investigación concedidos a la Dra. Moratalla: Ministerio de Sanidad, Servicios Sociales e Igualdad, Plan Nacional Sobre Drogas PNSD #2012/071, Ministerio de Economía y Competitividad # BFU2010-20664, CIBERNED #CB06/05/0055 , Ministerios de Ciencia e Innovación y de Sanidad y Política Social ISCIII: BFU2010-20664 , RedRTA (RD06/0001/1011) y por la Comunidad de Madrid ref S2010/BMD-2336 concedidos a la Dra. Rosario Moratalla.. Al Consejo Superior de Investigaciones Científicas (CSIC), por concederme una beca predoctoral JAE-predoc y una beca JAE-estancia breve que posibilitó mi estancia en Argentina para aprender la tinción de plata que empleamos en este trabajo. Al CIBERNED del que también disfruté de un contrato de investigación.

A la Dra. Lucía Prensa Sepúlveda, mi tutora de la Universidad Autónoma de Madrid (UAM), y al responsable de la Comisión Académica del programa de Doctorado en Neurociencias de la UAM el Dr. Carlos Avendaño, por su ayuda y asesoramiento, su cercanía y su disponibilidad.

A la Dra. Soledad de Olmos, del Laboratorio de Neurofisiología Experimental e Histología, del Instituto de Investigación Médica Mercedes Martín y Ferreyra (IMMF), en Córdoba, (Argentina), por enseñarme todo lo que sabe de la técnica de Olmos, que ha sido fundamental para el desarrollo de este trabajo, por sus consejos científicos, turísticos y gastronómicos. Y a toda su familia por invitarme a compartir con ellos sus deliciosos asados argentinos. A todos aquellos con los que me crucé en el Ferreyra que me hicieron sentirme tan a gusto durante mi estancia allí. A los Cordobeses que me acompañaron en mi viaje a Iguazú y me llevaron de domingueo a las sierras de Córdoba. A Santiago Salim, el mejor guía de Buenos Aires y conductor raudo y veloz que casi estrella su coche con tal de que no perdiera el bus de vuelta.

A todos los colaboradores que han hecho posible las publicaciones recogidas en esta tesis doctoral: Al Dr. Eduardo D. Martin, del Laboratorio de Neurofisiología y Plasticidad Sináptica, del Parque Científico y Tecnológico de Albacete (PCYTA), por sus agradables conversaciones en cada visita a nuestro laboratorio, y a él y a la Dra. Idaira Oliva por su ayuda con los experimentos de voltametría. Al Dr. Antonio Cuadrado y la Dra. Isabel Lastres-Becker, del Instituto de Investigaciones Biológicas (IIB), por su interés por nuestro trabajo y su colaboración en el estudio con los animales knockout de Nrf2. A las Dr. Maribel Colado, Esther O'Shea y la gente de su laboratorio, especialmente a las Dras. Noemí Llopis e Inés Peraile y al Dr. Andrés Urrutia, por su colaboración y ayuda con los experimentos de HPLC, aunque significara perderse una clase de baile por quedarse en el laboratorio ayudándome. Al Dr. Ricardo Martínez, del Instituto Cajal, por su ayuda con los experimentos de microscopía electrónica y por compartir con nosotros sus valiosísismos anticuerpos de iNos y 3NT. A Andrea Pozo del laboratorio

de Ricardo Martínez, y a Martin Ian Maher, del servicio de microscopía electrónica del Instituto Cajal, por su entrega, dedicación y afán con nuestros experimentos. Al Dr. Miquel Vila, del instituto de Investigación Vall d'Hebron en Barcelona, por su ayuda con la identificación de los cuerpos apoptóticos. Al Dr. Carlos Vicario, por ayudarme a presentar cada charla sobre este trabajo con sus críticas constructivas.

A mis compañeros del B-01 (ó C-15 para los añejos), por su apoyo, amistad y los buenos momentos que hemos compartido dentro y fuera del laboratorio: en primer lugar, a la Dra. Noelia Granado, Noe, responsable en gran medida de que esta Tesis sea lo que es. Por haberme enseñado desde cero como trabajar en un laboratorio dejándome ser su pequeño saltamontes durante estos 5 años. Porque trabajar contigo es un verdadero placer, no eres una "jefa", sino la mejor compañera que se puede tener. Porque quien quiera ser líder, debe ser puente. Por conseguir que formásemos un gran equipo. Por apoyarme siempre, en los momentos buenos y en los no tan buenos. Por tus consejos dentro y fuera del laboratorio. A Irene, mi "alter ego" del B01, por acompañarme en este camino desde el primer día en el laboratorio, por estar siempre dispuesta a escuchar y a echar una mano cuando alguien lo necesita, porque sin ella hay demasiado silencio en el laboratorio, por su inigualable, enérgico y en ocasiones deliciosamente inaguantable "modo viernes" y por ser la líder de muchas salidas y cañas cajalianas. A Marco, por ser un gran técnico de laboratorio y un gran compañero, eficaz, generoso, risueño y cercano, facilitando siempre tanto las cosas. Por hacernos reír tanto y por afrontar la vida con valentía. A Isa, por ser tan humilde, por su buen humor y su risa tremendamente contagiosa. Al sector sevillano del labo: a Ramiro, por llevar buena cuenta de mis suspiros desesperados y a Patri, por ser tan *saláa* y tan poco *saboría*, especialmente cuando entra en colapso y por sacarnos de fiesta ya sea por la feria de Abril o por Vallecas. A Lula, LuzMaligna para los amigos, por inventar el concepto de Corchopán y porque tener siempre algo de que hablar, haciendo que un viaje en tren a Oviedo pueda pasarse en un pispas. Al sector Mejicano: A Rubén, por deleitarnos con su comida de Sinaloa y alrededores y a Óscar, el Mejicano de Oro, por haber venido desde Méjico sólo para bailar con Charo. A todos aquellos a los que he tenido la oportunidad de enseñar algo, por su paciencia conmigo: A Flo, por ser el primero en superar la fase de entrenamiento de monje budista con la técnica de plata, ganando el suficiente buen karma para alcanzar el Nirvana y proseguir con su vida en su Francia natal. A María Zazu, por no entender que nos dé asco desatascar un fregadero pero no coger ratones. A Ana por ser tan buena en lo personal y en lo profesional, por aprender a no desesperar y por su gran dedicación. A Lorena, con quien es un placer ver un partido del Atleti aunque por mi culpa casi nos peguen en el Calderón. A Chema, por ayudarnos verano tras verano y acabar quedándose con nosotros. A Marco vallecano, por ser tan entregado ayudándome con el vibratomo incluso cuando su nuevo tatuaje se lo ponía difícil. A Samuel por darnos cada día lecciones de cocina creativa con sus recetas inimaginables. A Guille, el master chef del labo, por sus palmeritas, por su sonrisa perenne y por ser él quien me enseñó por fin a mí a hacer western Blots. A Pablo, que vino a hacer una inmuno y se quedó tres meses, por enseñarme a coger una rata sin asustarme más que ella. A Víctor, siempre tan risueño, que con su forma de cerrar las botellas nos ahorraba el gimnasio. A Bea, la nueva incorporación del labo, por ser tan abierta y comprensiva. A Tao, porque su sombra es alargada…porque ni mis suspiros superan sus ruiditos de sorpresa y exaltación: uuuuuuooooooh! A Julia, a la que le gustaba disfrutar de la vida fuera del laboratorio. A Sanja, de la que aprendí tantas cosas. A Oskar, así con ka, por haberme enseñado a perfundir desde el primer día y bla, bla bla, bla bla,

bla bla… A Emy, por ser la voz de la experiencia en el laboratorio.

A mis compañeros del Cajal: A Carmen Ovejero, por elegir para ella una beca FPU permitiéndome disfrutar a mí de la JAE-predoc. Sin esa decisión tuya esta tesis no habría sido posible. Gracias a la gente de confocal, especialmente a Carmen y Belén, y de la unidad de Biología molecular y celular, especialmente a Silvia, por su ayuda con las RT-PCR's y el genotipado de los transgénicos. A Aurelio, por estar siempre tan pendiente de todos y ser el primero en echarnos de menos cuando desaparecemos una temporada. A la gente del C-15, por estar siempre disponibles para ayudarnos en nuestras necesidades técnico-científicas o fuera del laboratorio, especialmente a Vanesa, que ha respondido sin quejarse a mis múltiples dudas de última hora en el proceso de entrega y defensa de la tesis. A los del labo de enfrente, siempre dispuestos a ayudar aunque sea a encontrar una garrafa de agua milliQ desaparecida en combate. A Paloma, por entretenerme las horas y horas pasadas en el cuarto del Neurolúcida con sus insaciables ganas de hablar y por cuidar tanto de mi amiga Cristina. A la gente del comedor que ya emigró o está en ello para proseguir con sus carreras científicas: A María Pedraza, por su compañía y conversación en los viajes matutinos en autobús al Cajal, su inestimable ayuda con la maquetación de la tesis. A Jorge, por ser un ejemplo de lo que es ser bueno en lo que te gusta. A Wolfi, por sus grandes historias. A Eduardo, porque aunque sea un cascarrabias siempre está dispuesto a echar una mano, por su valiosa ayuda con la H&E. A Diego, por dejarnos el anticuerpo de IL -15 y por ser un científico ejemplar. A Bea por su envidiable forma de ilusionarse con los retos. A los chicos del almacén, por hacer tan divertidas mis visitas al sótano, sin dejar de ser eficaces. A la gente del animalario, especialmente a Laude y Mario, por lidiar con nuestros requerimientos durante todos estos años y no morir en el intento. Y a todos los demás Cajalianos que me habéis ayudado de una u otra forma.

A mis compañeros de los cursos de Doctorado de la UAM, por compartir siestas entre clase y clase y celebraciones fuera de ellas.

A mis chicas Pino, Laura, Ana, Marilena, Nieves, Trillo, Carmenma y Cristina, por ser mi familia en Madrid desde hace ya más de 10 años.

A mis Parisinas más auténticas, aunque sean de Barcelona, Madrid, Salamanca y Andalucía. Isa, Lole, Maribel, Carol, Pili, Lucía y Henar. Porque incluso a las que os tengo lejos os siento muy cerca. Porque cuando estoy con vosotras quiero "retener todos los momentos en mis retinas".

A mis Madrileños favoritos: Cristina (Pichi) por superar conmigo crisis como la de "el tubo 4 está roto!", a Paloma por todo lo que hemos vivido juntas desde aquel cuarto compartido en Utrecht y a Andrés, madrileño de adopción, por ser un ejemplo de superarse a sí mismo y afrontar las cosas con valentía

A esa Tuna de Caminos (de la Universidad Politécnica de Madrid) que cuando por las calles pasa, hace vibrar a la masa y también a la Tomasa. Por hacerme reír tanto tras salir cansada del laboratorio y por haber conseguido dos cosas increíbles: que no me parezca ridículo ver a chicos con leotardos y que haya llegado al punto de saberme casi tantas de vuestras canciones como Pilar Frutos.

A los vallisoletanos que siguen contando conmigo aunque mi presencia por allí sea cada vez más escasa.

A mi familia, especialmente a mis abuelos porque sé que lo habrían disfrutado. A mis padres ellos son mi mejor ejemplo a seguir y mi mejor apoyo. Me han enseñado a trabajar duro, a superar todo tipo de obstáculos, a ver lo positivo de las cosas y a luchar por conseguir todo lo que me proponga. A mi hermano, por decirme las cosas que no quiero oír y dejarme siempre el listón muy alto. Me siento muy orgullosa de vosotros y por todo lo que significáis para mí os quiero dedicar esta tesis.

A Gabi, por su paciencia infinita, por aguantarme cada día, por ser capaz de sacar lo mejor de mí misma y hacerme superar retos que me parecían inalcanzables.

PRESENTACIÓN DE LA TESIS DOCTORAL COMO COMPENDIO DE PUBLICACIONES

Esta tesis doctoral se presenta como compendio de publicaciones originales, según la normativa aprobada por la Comisión de Dirección de Doctorado de la Universidad Autónoma de Madrid (UAM) / Comité de Dirección de la Escuela de Doctorado en el Consejo de Gobierno de 1 de junio de 2012 y modificación por Acuerdo de Comisión de Estudios de Posgrado de 24 de julio de 2013.

Este trabajo incluye, por orden, una introducción general a las publicaciones, un apartado de hipótesis y ojvetivos en el que se justifica la hipótesis de trabajo, se presentan los objetivos y se aclaran las aportaciones del doctorando a las publicaciones, un resumen de los resultados presentados en las publicaciones, un apartado de publicaciones en el que se insertan los artículos originales publicados o aceptados para su publicación, una discusión general de las mismas y un apartado con conclusiones.

Los cuatro artículos que se presentan son la producción científica de una línea de investigación centrada en el estudio de la implicación del sistema dopaminérgico en los mecanismos de neurotoxicidad de la metanfetamina:

1. Ares-Santos S*, Granado N*, Espadas I, Martinez-Murillo R, Moratalla R. (2013). Methamphetamine causes degeneration of dopamine cell bodies and terminals of the nigrostriatal pathway evidenced by silver staining. *Neuropsychopharmacology*. En prensa. doi: 10.1038/npp.2013.307
2. Ares-Santos S*, Granado N*, Oliva I, O'Shea E, Martin ED, Colado MI, Moratalla R (2012). Dopamine D(1) receptor deletion strongly reduces neurotoxic effects of methamphetamine. *Neurobiol Dis.* **45:**810-20.
3. Granado N, Ares-Santos S, Oliva I, O'Shea E, Martin ED, Colado MI, Moratalla R. (2011a). Dopamine D2-receptor knockout mice are protected against dopaminergic neurotoxicity induced by methamphetamine or MDMA. Neurobiol Dis. **42**:391-403.
4. Granado N*, Lastres-Becker I*, Ares-Santos S, Oliva I, Martin E, Cuadrado A, Moratalla R. (2011b). Nrf2 deficiency potentiates methamphetamine-induced dopaminergic axonal damage and gliosis in the striatum. *Glia*. **59**:1850-63.

ABREVIATURAS

1x30	protocolo de administración de 1 inyección i.p. de 30mg/Kg de salino o metanfetamina
3-NT	3-nitrotirosina
3x5	protocolo de administración de 3 inyecciones i.p. de 5mg/Kg de salino o metanfetamina ,separadas por 3 h
3x10	protocolo de administración de 3 Inyecciones i.p. de 10mg/Kg de metanfetamina, separadas por 3 h
5-HIAA	ácido 5-hidroxiindol acético
5-HT	serotonina
6-OHDA	6-hidroxidopamina
αMPT	alfa-metil-para-tirosina
A	amperios
Ab-I	anticuerpo primario
AC	enzima adenilato ciclasa
aCSF	fluido cerebroespinal artificial
A-Cu-Ag	tinción amino cúprico-argéntica o técnica de Olmos
ADN	ácido desoxirribonucleico
Ag	plata
AIS	estación de análisis de imagen
AMPA	alfa-amino-3-hidroxi-5-metil-4-Isoxazol
AMPc	adenosín monofosfato cíclico
ANOVA	análisis de varianza
ARNm	ácido ribonucleico mensajero
RNAm	
ATP	adenosín trifosfato
ATS	estimulantes de tipo anfetamínico
BAC	cromosome artificial bateriano
BER	reparación por escisión de base
cDNA	ácido desoxirribonucleico complementario
CFE	electrodo de fibra de carbono
CuZnSOD	superóxido dismutasa de Cobre-Zinc
ΔF/F0	incremento de fluorescencia
d	días
D1 o D1R	receptor dopaminérgico D1
$D1^{-/-}$, $D1R^{-/-}$	knockout del receptor dopaminérgico D1
D2 o D2R	receptor dopaminérgico D2
$D2^{-/-}$, $D2R^{-/-}$	knockout del receptor dopaminérgico D2
D3	receptor dopaminérgico D3
D4	receptor dopaminérgico D4
D5	receptor dopaminérgico D5
DA	dopamina
DAB	diaminobencidina
DAPI	4 ',6-diamino-2-fenilindol
DAT	transportador de dopamina
DOPAC	ácido 3,4-dihidroxifenilacético
EDTA	ácido etilendiaminotetraacético
EM	microscopía electrónica
ER	retículo endoplasmático
ERA	elementos de respuesta antioxidante
et al.	del latín, *et alii*, y otros
FDA	del inglés, *Food and Drug Administration*, Agencia de Alimentos y Medicamentos
Fig.	figura
FJ	Fluoro Jade
FSCV	del inglés *fast scan cyclic voltammetry*, voltametría cíclica
g	gramos
Gclc	subunidad catalítica de la enzima gamma cisteín ligasa
Gclm	subunidad moduladora de la enzima gamma cisteín ligasa
GFAP	proteína acídica fibrilar de la glía, marcador de astrocitos reactivos
GFP	proteína verde fluorescente
GPx	enzima glutation peroxidasa
Gsta2	glutation S-transferasa A2
h	horas
H&E	tinción hematoxilina-eosina
H_20_2	peróxido de hidrógeno
HO-1	enzima hemo-oxigenasa-1
HPLC	**c**romatografía líquida de alta resolución
HVA	ácido 4-hidroxi-3-metoxifenilacético / ácido homovanílico
i.p.	intraperitoneal
Iba-1	marcador de microglía reactiva
IL-15	interleuquina-15
IL-1β	interleuquina-1β
IL-6	interleuquina-6
iNOS	óxido nítrico sintasa inducible
ir	inmunoreactividad
ISCIII	Instituto de Salud Carlos III
JNK	quinasas N-terminal c-jun
L-DOPA	L-3,4-dihidroxifenil alanita
µ	micro
µm	micras
Mac-1	marcador de microglía reactiva CD11b
MAO	enzima monoaminoxidasa
MBF	*middle forebrain bundle*, haz prosencefálico medial
MDA	3,4-metilenodioxianfetamina

MDMA	3,4-metilenodioximetanfetamina, éxtasis
METH	metanfetamina
mg	miligramos
min	minutos
ml	mililitros
mm	milímetros
MnSOD	enzima superóxido dismutasa de manganeso
MOR-1	Receptor mu opioide 1
MPTP	1-metil-4-fenil-1,2,3,6-tetrahidropiridina
MSN	neuronas espinosas medianas, neuronas de proyección del estriado
NaCl	salino
NADPH	nicotinamida adenina dinucleótido fosfato
NIDA	*National Institute on Drug Addiction,* Instituto Americano de Adicción
NGS	suero de cabra normalizado
NMDA	N-metil-D-aspartato
nNOS	enzima óxido nítrico sintasa neural
NO	óxido nítrico
NOS	enzima óxido nítrico sintasa
NQO1	enzima NADPH quinona oxidoreductasa
Nrf2	factor 2 relacionado con el factor nuclear eritroide 2
Nrf2$^{-/-}$	knockout de Nrf2
ºC	grados Celsius
O_2-	anión superóxido
•OH	radical hidroxilo
ONOO-	peroxinitrito
PB	búfer fosfato
PBN	α-fenil-N-terbutil nitrona
PBS	solución salina tamponada con fosfato
PBS-Tx ,	PBS con tritón
PBST	
PCP	fenciclinidna
PCR	reacción en cadena de la polimerasa
PD	enfermedad de Parkinson
PET	tomografía de emisión de positrones
PNSD	Plan Nacional Sobre Drogas
qRTPCR	PCR cuantitativa en tiempo real
RedRTA	Red de Trastornos Adictivos
res	reserpina
RNA	ácido ribonucleico
RNS	especies reactivas de nitrógeno
ROS	especies reactivas de oxígeno
s	segundos
Sal	salino
SCH23390	R-(+)-7-cloro-8-hidroxi-3-metil-l fenil-2,3,4,5-tetrahidro-1H-3-benzapina
SEM	error estándar de la media
SN	sustancia negra
SNC	sistema nervioso central
SNpc	sustancia negra pars compacta
SOD	enzima superóxido dismutasa
TDAH	trastorno por déficit de atención con hiperactividad
TH	tirosina hidroxilasa
Tmt	proteína rojo tomate fluorescente
TNFα	factor de necrosis tumoral alfa
UNODC	*United Nations Office for Drug and Crime ,* Oficina de Drogas y Crimen de las Naciones Unidas
VMAT-2	transportador vesicular de monoaminas
V	Voltios
Vs	versus
WT	animals controles C57BL/6
w/v	peso/ volumen

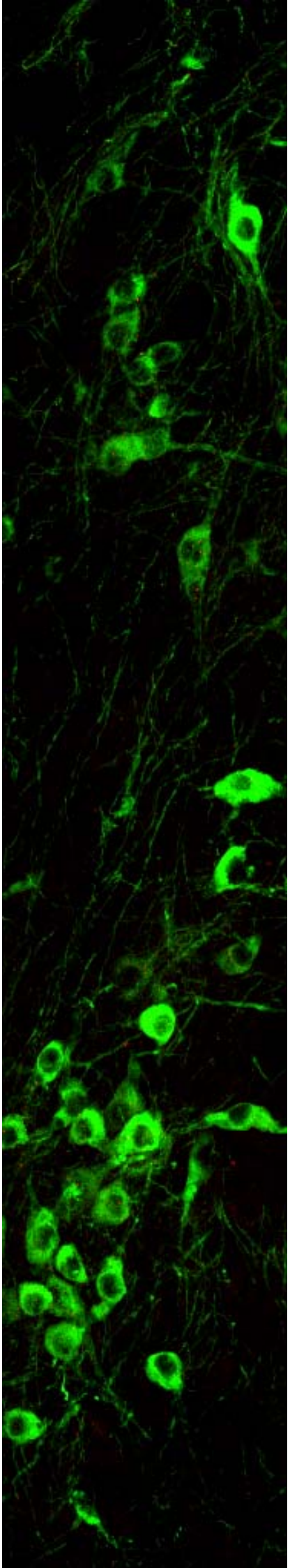

ÍNDICE

Foto de la página anterior: Neuronas dopaminérgicas de la SN de un ratón WT tratado con metanfetamina (3x5) 1d después del tratamiento, teñidas con inmunofluorescencia para TH (verde) .

RESUMEN

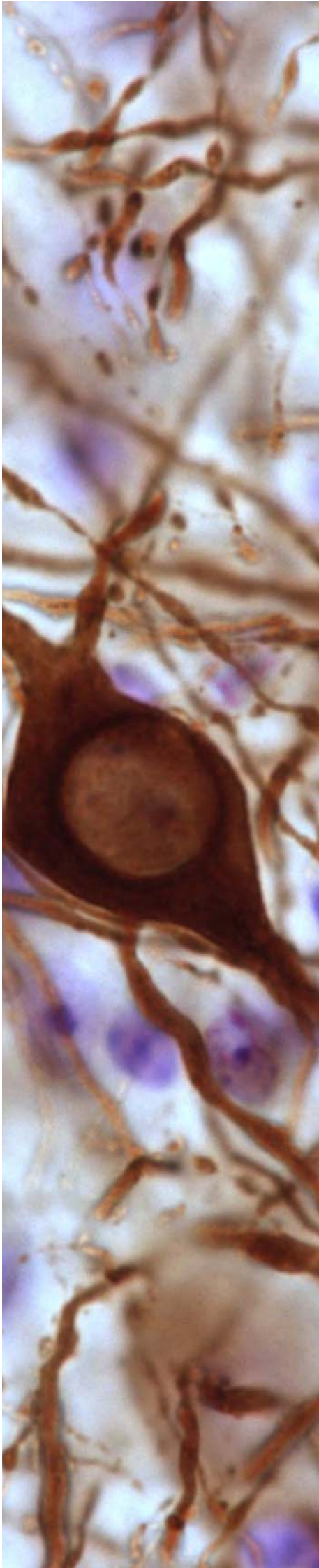

Foto de la página anterior: Cuerpo celular de una neurona dopaminérgica y fibras dopaminérgicas teñidas mediante inmunohistoquímica para TH (marrón) entre núcleos de otras células teñidos con Nissl con cresil violeta (violeta) en la SNpc de un ratón 1d después de ser tratado con salino (3x5).

La metanfetamina es un psicoestimulante muy adictivo y la segunda droga de abuso más consumida a nivel mundial, sólo superada por el cannabis. Estudios epidemiológicos recientes han demostrado que el consumo de metanfetamina aumenta el riesgo de desarrollar enfermedad de Parkinson, lo que está de acuerdo con estudios en animales de experimentación que muestran que esta droga produce neurotoxicidad sobre los terminales dopaminérgicos de la vía nigroestriatal, que se acompaña de gliosis. Los efectos neurotóxicos de la metanfetamina implican una liberación excesiva de dopamina, por lo que es probable que los receptores dopaminérgicos D1 y D2, los más abundantes en el estriado, estén implicados en la neurotoxicidad. Algunos estudios farmacológicos han mostrado previamente evidencias avalando esta idea, pero dado que los antagonistas farmacológicos existentes ejercen sus efectos sobre varios subtipos de receptores dopaminérgicos a la vez, aún no se ha determinado específicamente la implicación de los subtipos de receptores dopaminérgicos D1 y D2. Además, la metanfetamina induce estrés oxidativo, que se correlaciona con los efectos neurotóxicos de la droga sobre los terminales dopaminérgicos en el estriado. Por ello el factor de trascripción Nrf2, el guardián de la homeostasis redox, podría tener un papel importante en la protección contra la neurotoxicidad de la metanfetamina.

En el presente trabajo, hemos examinado el efecto de la administración de dosis bajas repetidas (que modelizan el consumo tipo compulsivo o "*binge*") y de una única dosis alta (que modeliza un consumo esporádico de una dosis alta) en la vía dopaminérgica nigroestriatal de ratones WT (C57BL/6). Evaluamos la integridad de las neuronas presinápticas en estriado y SNpc, y de las neuronas postsinápticas en el estriado, a diferentes tiempos tras la administración de metanfetamina mediante inmunohistoquímica para marcadores dopaminérgicos, tirosina hidroxilasa (TH) y transportador de dopamina (DAT) y tinción de plata (técnica de Olmos). Además, queríamos conocer el curso temporal de la degeneración en estriado y SN, y si los efectos neurotóxicos en la vía nigroestriatal se correlacionaban con deficiencias funcionales de tipo motor, para lo que evaluamos la actividad locomotora y la coordinación motora de los animales a diferentes tiempos tras el consumo de metanfetamina. Para definir el papel de los receptores dopaminérgicos D1 y D2, administramos un régimen neurotóxico de metanfetamina a ratones knock-out del receptor D1 ($D1^{-/-}$) ó del D2 ($D2^{-/-}$) y a ratones WT de su camada. Finalmente, evaluamos el papel del factor de trascripción Nrf2 en la neurotoxicidad de la metanfetamina mediante la administración de un régimen neurotóxico de esta droga a ratones knock-out de Nrf2 ($Nrf2^{-/-}$).

La administración de dosis bajas repetidas de metanfetamina produce más pérdida de terminales dopaminérgicos en el estriado que la de una única dosis alta. Además, se pueden apreciar algunos axones degenerando entre el estriado y la SNpc. Todos los protocolos inducen una degeneración similar de neuronas dopaminérgicas en la SNpc, evidenciada por la presencia de neuronas TH+ marcadas con plata. Estas neuronas mueren por necrosis o apoptosis. La metanfetamina también mata neuronas en el estriado. Empleando ratones transgénicos BAC D1-Tmt/D2-GFP, hemos observado que las neuronas que degeneran en el estriado se distribuyen por igual entre las neuronas de proyección de la vía directa, de la vía indirecta y el resto de las neuronas estriatales, probablemente interneuronas que serían especialmente vulnerables a la metanfetamina. Pese a que el número de neuronas dopaminérgicas en la SNpc se mantiene reducido incluso a los 30 días del tratamiento con la droga, hay una recuperación parcial de terminales dopaminérgicos del estriado a medida que pasa el

tiempo tras la administración de metanfetamina. La inactivación de los receptores dopaminérgicos D1 ó D2 previene la pérdida de terminales dopaminérgicos, la hipertermia y los aumentos en gliosis y de iNOS en el estriado. Además, la inactivación de cualquiera de estos receptores, D1 ó D2, evita la pérdida de neuronas dopaminérgicas en la SNpc. Para explorar la relación entre la hipertermia y la neurotoxicidad inducidas por la metanfetamina, se les administró a los ratones $D1^{-/-}$ y $D2^{-/-}$ un régimen de dosis bajas repetidas de metanfetamina en una sala a alta temperatura ambiente (29-30ºC). En estas condiciones, los animales $D1^{-/-}$ sí desarrollaron hipertermia tras el tratamiento con la droga y presentaron la misma pérdida de terminales dopaminérgicos en el estriado que los ratones WT tratados a 23ºC. Sin embargo, los animales $D2^{-/-}$ no presentaron hipertermia inducida por metanfetamina, ni tampoco efectos neurotóxicos, ni siquiera en estas condiciones. Aún así, estos efectos neuroprotectores no pueden explicarse sólo por el bloqueo de la hipertermia, ya que el pretratamiento con reserpina, que vacía las vesículas de dopamina liberándola al citosol, bloquea la hipertermia en todos los genotipos (WT, $D1^{-/-}$, $D2^{-/-}$, y potencia la pérdida de terminales dopaminérgicos en el estriado en los ratones WT y $D1^{-/-}$, pero no en los $D2^{-/-}$. Además, la liberación de dopamina estriatal medida por voltametría cíclica en presencia de metanfetamina fue significativamente mayor en los animales $D1^{-/-}$ que en los WT, pero significativamente menor en los animales $D2^{-/-}$, lo que sugiere que los animales $D1^{-/-}$ tienen un mayor contenido de dopamina vesicular que los WT, mientras que el de los $D2^{-/-}$ es menor que el de los WT. Por otra parte, la falta de Nrf2 impide la activación de las enzimas antioxidantes de fase 2 y aumenta el daño a los terminales dopaminérgicos, la degeneración de neuronas, la gliosis y la expresión de TNF-α e IL-15 en el estriado, pero no en la SN.

Estos datos muestran evidencias sólidas de que la metanfetamina produce una pérdida de larga duración/degeneración de cuerpos celulares de neuronas dopaminérgicas en la SNpc, junto con destrucción de terminales dopaminérgicas en el estriado. Tanto el receptor dopaminérgico D1 como el D2 están involucrados en los efectos neurotóxicos de la metanfetamina aunque de forma diferente. La protección conferida por la inactivación del receptor dopaminérgico D1 se debe en parte al bloqueo de la hipertermia inducida por la droga, pero también al menor contenido y reciclaje de dopamina y a la mayor acumulación de dopamina en vesículas que se da en los animales $D1^{-/-}$. Sin embargo, el efecto neuroprotector de la inactivación del receptor D2 depende en parte de su efecto sobre la temperatura corporal, pero también del bloqueo de la recaptación de dopamina por la menor actividad del DAT que se da cuando el receptor D2 no está activo, que resulta en menores niveles de dopamina citosólica en los animales $D2^{-/-}$. Además nuestros resultados conforman que el estrés oxidativo favorece la degeneración de terminales en el estriado y que el factor de transcripción Nrf2 tiene un papel importante en la protección frente a estrés oxidativo, la degeneración y la inflamación inducidos por la metanfetamina en el estriado.

INTRODUCCIÓN

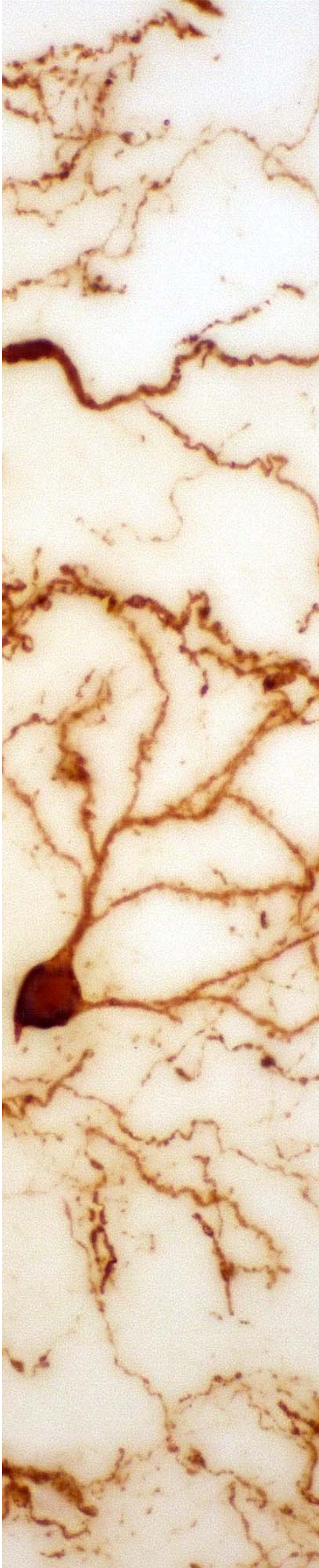

Foto de la página anterior: Neurona estriatal que expresa TH (marrón) teñida mediante inmunohistoquímica en el estriado de un ratón tratado con metanfetamina (3x5) que sufre una gran pérdida de terminales dopaminérgicos a los 3 días del tratamiento.

ANTECEDENTES Y ESTADO ACTUAL

Aspectos generales sobre la metanfetamina

La metanfetamina es un potente psicoestimulante, perteneciente al grupo de las llamadas drogas de síntesis o de diseño, usada en todo el mundo como droga de abuso o recreativa. Esta droga tiene un alto potencial de adicción y su abuso puede producir dependencia psicológica y física. Por ello, está clasificada dentro de la Lista II del Convenio sobre Sustancias Psicotrópicas. Otros fármacos de esta categoría son la cocaína y la fenciclidina (también conocido como polvo de ángel o PCP). La simplicidad de su síntesis, generalmente por reducción de la efedrina o pseudoefedrina, parece haber contribuido a su popularidad, y es que ha reemplazado a la cocaína, a la heroína y a la marihuana como droga recreativa de elección en muchos países. También se utiliza para perder peso y para mejorar el estado de alerta, la concentración, la motivación y la claridad mental durante largos periodos de tiempo.

Estructura química

La metanfetamina (N-metil-1-fenilpropan-2-amina), está relacionada estructuralmente con los neurotransmisores dopamina y feniletilamina y con otros psicoestimulantes del grupo de las anfetaminas (Figura 1). Existen bastantes derivados anfetamínicos, que reflejan las muchas variaciones químicas que se pueden hacer sobre la base de la sustancia natural feniletilamina. La anfetamina tiene un grupo metilo adicional (-CH3) y la adición de un segundo grupo metilo en el nitrógeno básico conduce a la metanfetamina. La 3,4-metilendioximetanfetamina (MDMA), más comúnmente conocida como "éxtasis", y la metilendioxianfetamina (MDA), también conocida como la “droga del amor” o “Eva” sólo se diferencian de la metanfetamina en los radicales sobre el anillo de benceno (Figura 1). Otro compuesto de origen natural, la catinona, es químicamente similar a la efedrina y el componente principal del khat, abundante en el este de África y en la Península Arábiga. Como la mayoría de estos compuestos, la metanfetamina contiene un átomo de carbono quiral, y por lo tanto existe como dos isómeros ópticos: la l-metanfetamina (levometanfetamina), que no tiene actividad estimulante, y la d-metanfetamina (dextrometanfetamina), que es biológicamente activa y tiene actividad psicoestimulante (Figura 1).

Historia

La metanfetamina fue sintetizada por primera vez en Japón en 1893, a partir de la efedrina, por el químico Nagai Nagayoshi. Es un polvo cristalino cuyos efectos estimulantes son mayores y más duraderos que los de otras anfetaminas (o fenilisopropilaminas). Las investigaciones farmacológicas preliminares se centraron en sus efectos periféricos y demostraron que se trataba de una amina simpaticomimética con propiedades broncodilatadoras. Se fabricó en Japón en la década de 1920 como un estimulante y como complemento para dietas. A partir de 1935 se empezó a usar para tratar la narcolepsia por su efecto estimulante, y fue en el año 1937 cuando la American Medical Association la aprobó para su uso en dicho trastorno. En 1938, la metanfetamina se introdujo en el mercado bajo el nombre comercial de Methedrina®. Fue muy consumida por los ejércitos durante la Segunda Guerra Mundial para eliminar la fatiga y mantener la resistencia física de los combatientes. Se distribuyó a las fuerzas de élite y personal de tanques y aeronaves. En 1941, los dirigentes nazis prohibieron su uso

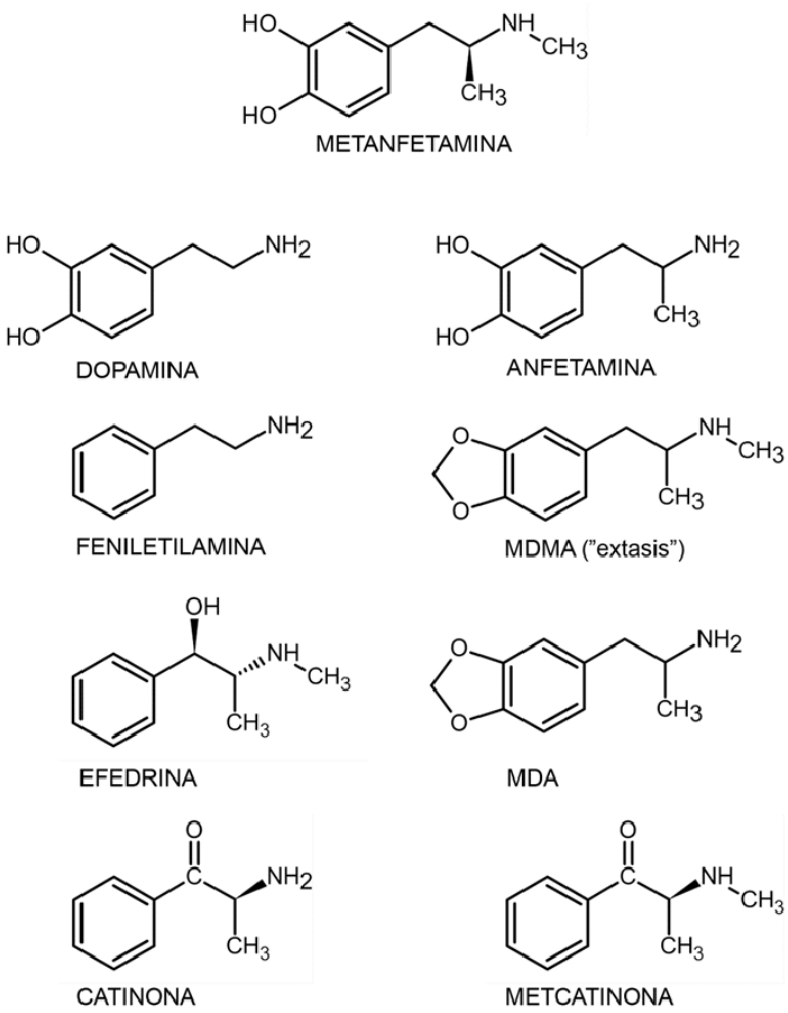

Figura 1. Estructura química de la dopamina, la metanfetamina y de otros derivados anfetamínicos. Todos estos compuestos comparten una estructura química similar y por ello tienen efecto sobre el sistema dopaminérgico. (Modificado de Ares-Santos *et al*. 2013a).

debido a los incidentes de psicosis y de muerte por agotamiento. Pilotos japoneses en misiones kamikazes tomaban metanfetamina antes de sus vuelos suicidas, lo que concuerda con el hecho de que la metanfetamina estimula los comportamientos agresivos, aumenta la autoconfianza y el comportamiento paranoide y produce una tendencia a perder las emociones humanas más básicas de compasión y piedad. En 1944, la *Food and Drug Administration* (FDA) de Estados Unidos aprobó el uso de la metanfetamina en el tratamiento de la narcolepsia, la depresión leve, el parkinsonismo postencefalítico, el alcoholismo crónico, la arteriosclerosis cerebral, la fiebre del heno y la obesidad. Estas indicaciones de uso de metanfetamina fueron incluidas en la edición 1954 de Farmacología y Terapéutica. En los años 1950 y 1960, se creía todavía que el consumo de metanfetamina tenía muy pocas consecuencias negativas. Se manufacturaba y comercializaba en Estados Unidos como Methedrina, vendiéndose a las amas de casa como un antídoto para la depresión y el aumento de peso, a los camioneros para ayudarles a conducir más tiempo sin dormir, y a estudiantes y atletas para mejorar el rendimiento físico e intelectual. Esta dispensación indiscriminada de metanfetamina, así como la percepción pública de que se trataba de un medicamento seguro, llevó a un uso recreativo masivo de metanfetamina durante los años 80 del siglo pasado en Estados Unidos, que resultó en abuso y adicción (Ares-Santos *et al*. 2013a).

Uso médico

Actualmente, las indicaciones médicas aceptadas para el uso de metanfetamina son muy

limitadas, debido a su alto potencial de adicción y toxicidad. Por tal razón está incluida en la lista II de sustancias psicotrópicas, aunque las dosis empleadas en usos médicos son más bajas que las que utilizan quienes la consumen como droga de abuso. Sólo en algunos países como Australia o Estados Unidos se mantienen aprobadas algunas indicaciones para el uso médico de la metanfetamina: el trastorno por déficit de atención con hiperactividad (TDAH), el tratamiento a corto plazo de la obesidad exógena, y la narcolepsia (Hart *et al*. 2012). Se comercializa bajo los nombres de Desoxyn®, Metedrina®, Desoxiefedrina®, Pervitin®, Anadrex®, Metilanfetamina® y Syndrox®.

Epidemiología

El uso indebido de estimulantes de tipo anfetamínico (ATS) (metanfetamina, anfetamina, metcatinona y éxtasis) y la metanfetamina, en particular, se reconoce cada vez más como un problema de salud global. El último Informe Mundial sobre las Drogas de la Oficina de Drogas y Crimen de las Naciones Unidas (UNODC) sugiere que la prevalencia mundial del uso de los ATS sólo es superada por la del cannabis (UNODC, 2013).

Dentro de los ATS, las anfetaminas (metanfetamina, anfetamina y metcatinona) siguen siendo los más destacados, habiendo sido consumidos por 33,8 millones de personas en 2010, lo que equivale a una prevalencia de 0,7% de la población mundial de 15-64 años (Figura 2). El uso de ATS (excluyendo el éxtasis) sigue siendo generalizado a nivel mundial, y parece ir en aumento; de momento continúa siendo el segundo tipo de droga más consumida en el mundo, sólo por detrás del cannabis y superando al número total de usuarios de cocaína (UNODC, 2013).

Si bien las estimaciones de prevalencia no están disponibles en Asia y África, los expertos mantienen que se perciben aumentos en el uso de ATS. Aunque el uso de ATS ya era un problema en el

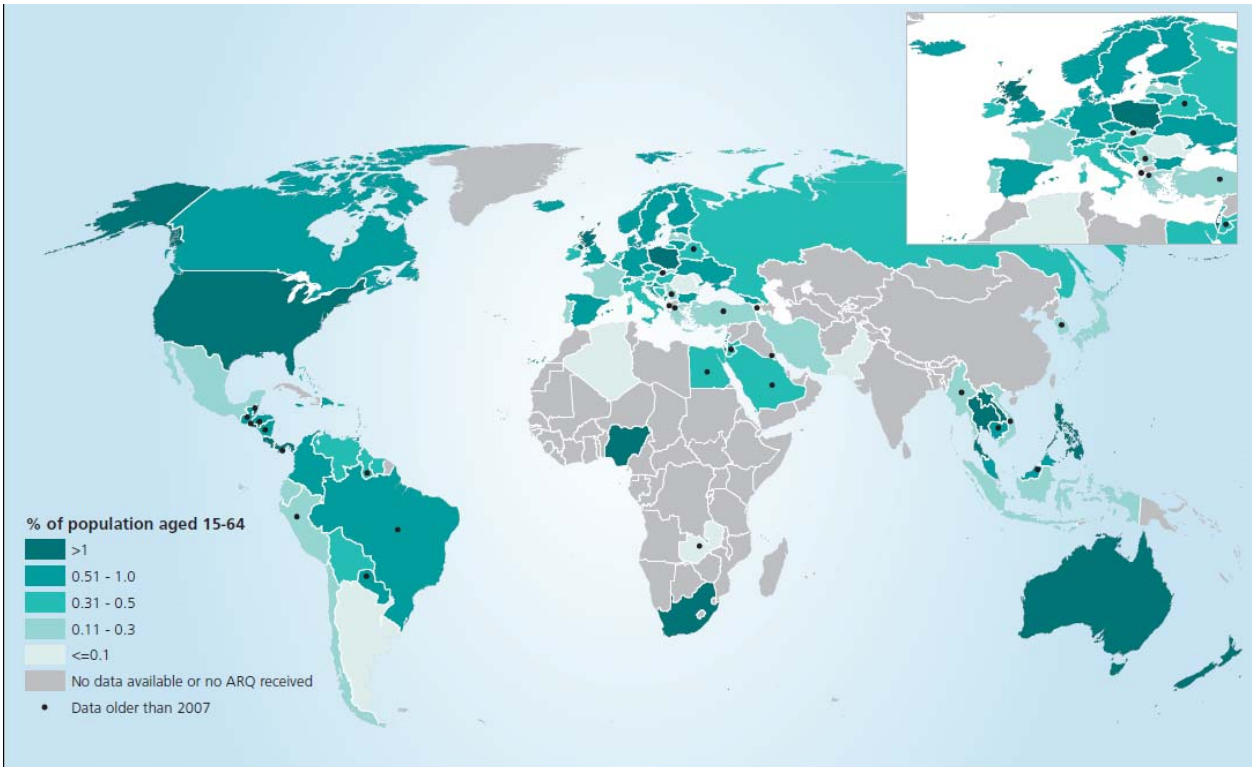

Figura 2. Prevalencia del consumo de estimulantes tipo anfetamina (excluyendo el "éxtasis") en 2011, según las estimaciones de la UNODC basadas en datos del cuestionario para los informes anuales y otras fuentes oficiales (UNODC, 2013).

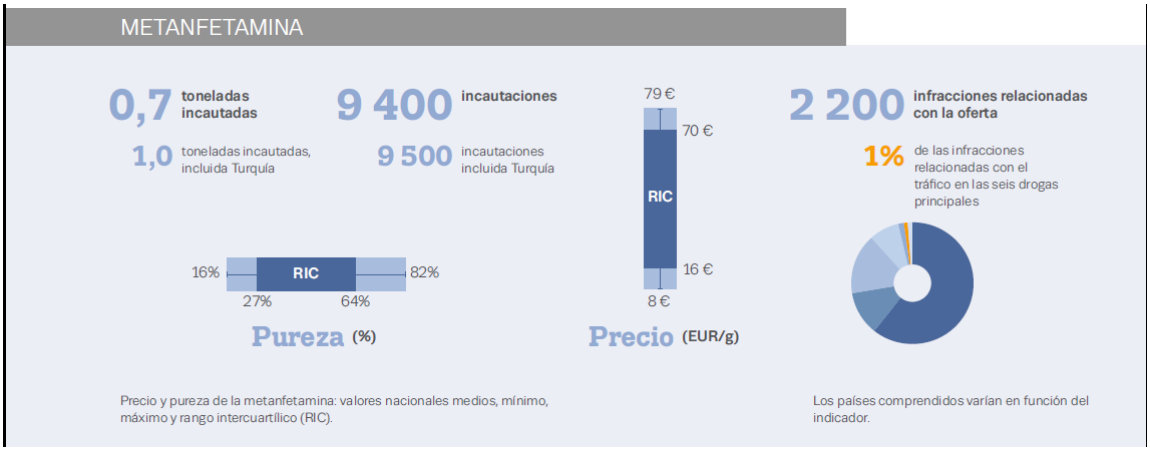

Figura 3. Datos sobre precio, pureza, incautaciones, e infracciones relacionadas con la metanfetamina en Europa. Fuente: Tomado de Informe Europeo sobre Drogas, Observatorio Europeo de las Drogas y Toxicomanías, 2013).

este y el sudeste de Asia, se ha informado de una creciente desviación de precursores químicos y de aumentos en las incautaciones y la fabricación de metanfetamina, junto con un aumento de su uso (UNODC, 2013). Los mayores niveles de consumo de ATS se presentan en Oceanía (2,1% de prevalencia en Australia y Nueva Zelanda), América Central y del Norte (1,3%) y África (0,9%), mientras que la prevalencia anual estimada en Asia (0,7%) es comparable con el promedio global.

En Europa, unos 13 millones de individuos han probado los ATS y unos 2-3 millones los consumieron durante el último año, lo que supone una prevalencia del 0,5-1,3% (UNODC, 2013; Observatorio Europeo de las Drogas y Toxicomanías, 2013). Aunque la disponibilidad de anfetamina es mayor que la de metanfetamina, cuyo consumo ha estado históricamente restringido a la República Checa y, en épocas más recientes a Eslovaquia, datos recientes indican un aumento de la disponibilidad de metanfetamina, que en determinados mercados está desplazando a la anfetamina (Observatorio Europeo de las Drogas y Toxicomanías, 2013).

Formas de presentación, administración y patrón de consumo

La metanfetamina se presenta de varias formas (Figura 4). La sal de clorhidrato de metanfetamina es un polvo blanco, cristalino, amargo e inodoro, soluble en agua y fuertemente higroscópico (absorbe agua rápidamente). Los nombres con los que comúnmente se le denomina en la calle son *"Speed"*, *"Meth"* o "tiza", que se refieren a la sal, mientras que "cristal", *"crystal meth"*, y *"ice"*, se refieren a la metanfetamina cristalina, una forma más pura que el polvo. La metanfetamina también se conoce por una variedad de otros nombres, incluyendo "shabu", "batu", "d-metanfetamina", "tina", y "vidrio". La metanfetamina como base libre es oleosa y es poco común en la calle. La que se vende en el mercado negro está adulterada con productos como cafeína, fenilpropanolamina o fenciclidina (también conocido como polvo de ángel o PCP), leche de magnesia o talco.

Puede tomarse por vía oral (en comprimidos o cápsulas de 10 a 15mg), por inyección intravenosa, fumada, inhalada (en polvo), o mediante la inserción anal o vaginal de un supositorio. Las formulaciones de metanfetamina contienen entre 5 y 90 mg. Una dosis superior a 90 mg en un consumidor sin tolerancia a esta droga podría ser letal. Después de su administración por cualquier vía se distribuye a la mayoría de los órganos, incluyendo los pulmones, el hígado y el estómago. Niveles

Figura 4.Formas de presentación de la metanfetamina. A. En cristales. B En polvo. C. En comprimidos. D. En cápsulas. Tomado de *Drug Enforcement Administration* (A, B, C), y de *National Anti Drug Strategy* (D).

moderados de la droga llegan al cerebro al atravesar la barrera hematoencefálica. También atraviesa la placenta y se excreta en la leche materna. Se metaboliza en el hígado, y algunos de los principales metabolitos son compuestos activos como la anfetamina, la 4-hidroxianfetamina, y norefedrina (Lin *et al*.1997). Los niveles máximos de concentración de metabolitos de metanfetamina se dan entre 10 y 24h después de su administración. Los efectos experimentados por el usuario duran unas 6-8h, según la velocidad con la que la metanfetamina llega a la sangre, que depende de la vía de administración. Por ejemplo, tras la administración oral la metanfetamina se absorbe fácilmente, dándose un pico de concentración de metanfetamina en sangre entre 3 y 6h después de la ingesta. Sin embargo, cuando la droga es inyectada o fumada llega inmediatamente al torrente sanguíneo y produce una sensación intensa, conocida como *"rush"* en inglés, que dura unos segundos y que los consumidores describen como extremadamente placentera, seguida de un estado de euforia que se mantiene hasta 12h. Cuanto más rápido llega a la sangre la droga, mayor es el *"rush"* y otros efectos experimentados por el usuario. Así, la administración por vía nasal u oral produce también una sensación de euforia, pero menos intensa.

El abuso de la metanfetamina tiene dos patrones de uso diferentes. El primero, que se caracteriza por un uso de baja intensidad, no confiere la dependencia psicológica. El segundo, conocido como uso *"binge"*, consiste en un consumo compulsivo (8-10 veces al día) de dosis altas (300 mg-1g), normalmente por inhalación o inyección, a diario durante un período de 3 a 10 días consecutivos (Davidson *et al*. 2001; Konuma 1994; Kramer *et al*.1967). La frecuencia de dosificación depende de si la intención es permanecer despierto o alcanzar los efectos eufóricos o el *"rush"*. La vida media mínima de la metanfetamina es 5-6 h, pudiendo llegar hasta 34h según el PH urinario. Los consumidores

compulsivos de metanfetamina (*"speed freaks"*) usan intervalos menores entre administraciones repetidas de la droga, por lo que se alcanzan de manera muy rápida concentraciones plasmáticas de la droga estables con pocas fluctuaciones. Las dosis se repiten cada 3-8h para mantenerse despierto o cada 0,5 a 4h para volver a alcanzar el *"rush"*, dado que los efectos placenteros desaparecen antes de que la concentración en sangre se reduzca significativamente. La redosificación a menudo consiste en tomar la misma dosis de la droga; sin embargo, cuando una redosificación continúa más allá de 48h, las dosis tienden a aumentar para conseguir el mismo efecto debido a la tolerancia que produce (Elkashef *et al.* 2008). Las dosis consumidas habitualmente varían entre 50 y 500 mg (Cruickshank y Dyer, 2009). Una vez estabilizado el consumo, el abandono brusco de la droga produce el síndrome de abstinencia, entre cuyos síntomas se incluyen disforia, fatiga, falta de energía mental, alteraciones del sueño y aumento del apetito (Davison *et al*. 2001; Newton *et al*. 2004).

Mecanismo de acción y efectos

Los efectos psicomotores de la metanfetamina se deben a su parecido estructural con el neurotransmisor dopamina (Figura 1). Las neuronas dopaminérgicas forman 4 importantes vías cerebrales: la mesolímbica, la mesocortical, la nigroestriatal y la tuberoinfundibular (Figura 5), las cuales influyen en las respuestas emocionales y motivacionales, en el sistema de recompensa y en el control de la actividad motora (Wise, 2009).

En condiciones fisiológicas, las catecolaminas (incluyendo la dopamina) se sintetizan en los terminales presinápticos y se encuentran tanto en el citoplasma como almacenadas en vesículas presinápticas. En respuesta a los potenciales de acción presinápticos, se liberan por exocitosis al espacio sináptico y actúan en los receptores postsinápticos para generar un potencial de acción postsináptico (Seiden *et al*. 1993). Las monoaminas liberadas actúan también sobre receptores presinápticos y/o se recaptan en los terminales y en las vesículas presinápticas mediante sistemas de transporte específicos (Venton *et al*. 2003).

Cuando se consume metanfetamina, ésta puede atravesar fácilmente la barrera hematoencefálica y alcanzar el cerebro, donde no puede activar directamente los receptores de

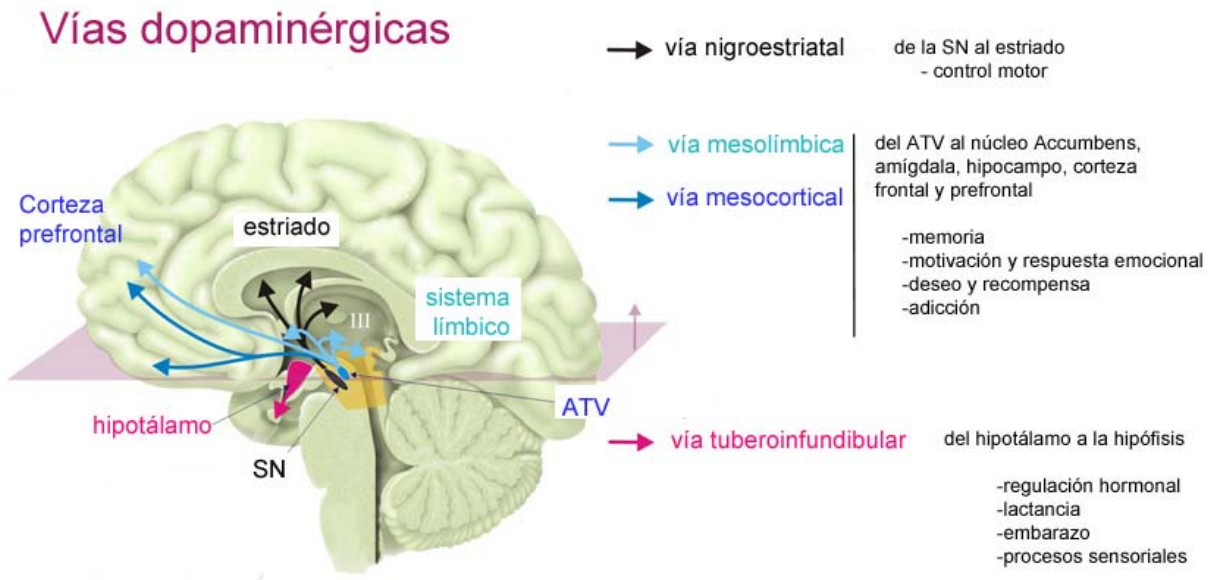

Figura 5. Esquema de las vías dopaminérgicas y sus funciones. (Modificado de *The DB-DRD4 Database Project* y de *Cell Biology Promotion*)

dopamina sino que actúa como un agonista indirecto de los receptores de dopamina. La metanfetamina se introduce en los axones de las neuronas dopaminérgicas a través del transportador de dopamina (DAT) y por difusión pasiva (Krasnova y Cadet 2009). Una vez dentro del axón altera el gradiente de protones de las vesículas provocando una liberación de dopamina desde las vesículas al citoplasma (Sulzer y Rayport, 1990). La metanfetamina también afecta a las concentraciones citoplasmáticas de dopamina porque altera la función del transportador vesicular de monoaminas (VMAT-2) (Brown *et al*. 2002) y bloquea la actividad de la monoamino oxidasa (MAO), que metaboliza la dopamina en el citoplasma, lo que favorece un aumento de su concentración (Kita *et al*. 2003; Schep *et al*. 2010). Tras este aumento de la dopamina citoplasmática, la inversión de la direccionalidad del DAT produce una liberación independiente del potencial de acción de dopamina a la sinapsis (Sulzer *et al*. 2005). Este hecho, junto con la disminución de la recaptación de dopamina, produce una concentración inusualmente elevada de dopamina en la sinapsis (Fleckenstein *et al*. 1997; Kita *et al*. 2003; Krasnova y Cadet 2009) La metanfetamina también libera noradrenalina y serotonina por un mecanismo similar (Kita *et al.* 2003; Schep *et al.*2010) .

Como consecuencia de este aumento de la liberación de monoaminas en varias áreas del cerebro, la metanfetamina produce una serie de efectos psicológicos agudos (como el ya descrito *"rush"*) que duran sólo unos minutos. Después de este corto periodo, pueden aparecer otras sensaciones y comportamientos, como un falso sentido de poder y confianza en uno mismo (delirios de grandeza), locuacidad, mal humor, irritabilidad, ansiedad, nerviosismo, agresividad y comportamiento violento. El consumo de metanfetamina tiene muchos efectos físicos adversos graves, incluyendo hipertermia (que puede llegar a ser letal), aumento de la presión arterial y de la frecuencia cardíaca,

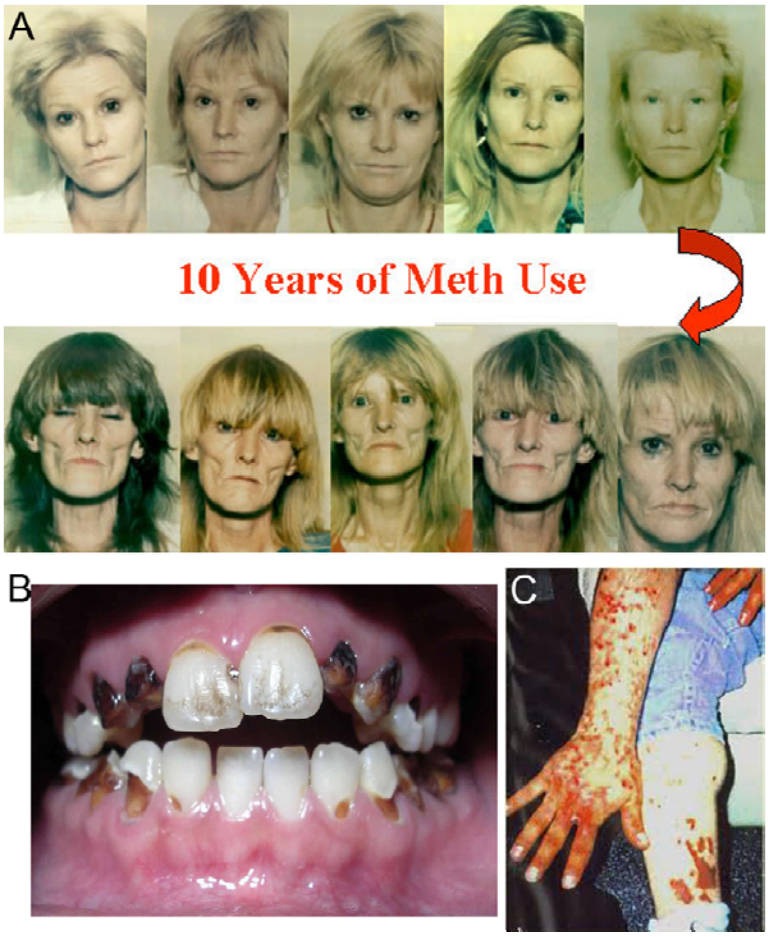

Figura 6. El abuso de metanfetamina puede producir envejecimiento acelerado, "boca de metanfetamina", y "ácaros de metanfetamina". A. Aspecto físico de una mujer en varios momentos a lo largo de 10 años de abuso de metanfetamina. B. Caso de "boca de metanfetamina". C. Las llagas en la piel conocida como "ácaros de metanfetamina" producidos por los consumidores al rascarse para aliviar el picor y la sensación de tener pequeños insectos caminando debajo de la piel. (Tomado de Drug Enforcement Administration, (A); Wikimedia Commons (foto tomada por Dozenist) (B); y de Photobucket (C).

midriasis (dilatación de la pupila), verborrea, rechinar de dientes (trismus y bruxismo), irritación gastrointestinal, pérdida del apetito, picazón, ronchas en la piel, hiperactividad, movimientos involuntarios del cuerpo, daño irreversible de los vasos sanguíneos en el cerebro que resulta en accidentes cerebrovasculares, arritmia, taquicardia, colapso cardiovascular e incluso muerte. Los síntomas más comunes de abuso crónico de la metanfetamina incluyen el síndrome de la articulación temporomandibular, erosión dental y dolor miofacial, todas ellas manifestaciones de trismus agudo y bruxismo. Otros síntomas a largo plazo son la pérdida de apetito, pérdida de peso, envejecimiento acelerado, sangrado por la nariz, y "boca de metanfetamina", una enfermedad oral caracterizada por la erosión dental, caries extensas, desgaste y pérdida de dientes, placa y sarro (Figura 6) (Ares-Santos *et al.* 2013a).

Neurotoxicidad inducida por la metanfetamina

La administración repetida de metanfetamina produce neurotoxicidad, tanto en humanos como en animales de experimentación. Esta neurotoxicidad afecta principalmente a las neuronas dopaminérgicas de la vía nigroestriatal, como se ve reflejado por las reducciones persistentes en los niveles de dopamina, sus metabolitos ácido 3,4-dihidroxifenilacético (DOPAC) y ácido homovanílico (HVA), y de marcadores dopaminérgicos como la tirosina hidroxilasa (TH), enzima limitante de la síntesis de dopamina, y el DAT en el estriado (Krasnova y Cadet 2009).

1. Neurotoxicidad en humanos

En consumidores de metanfetamina, estudios de tomografía de emisión de positrones (PET) realizados después de un corto periodo de abstinencia, demuestran una reducción en la densidad del DAT del 26% en el núcleo caudado y del 21% en el putamen (Volkow *et al.* 2001a). Otros autores han descrito pérdidas similares de DAT incluso 3 años después de haber dejado de consumir metanfetamina (Figura 7) (McCann *et al.* 1998). Los estudios postmortem realizados en el tejido estriatal de consumidores crónicos de metanfetamina, muestran una reducción significativa de los niveles de dopamina concomitantes con pérdida de inmunoreactividad de DAT y TH, indicativos de la pérdida de terminales dopaminérgicos. Estos efectos se han relacionado con déficits neurológicos, incluyendo pérdida de memoria y deficiencias de aprendizaje verbal y motor (Volkow *et al.* 2001b) así

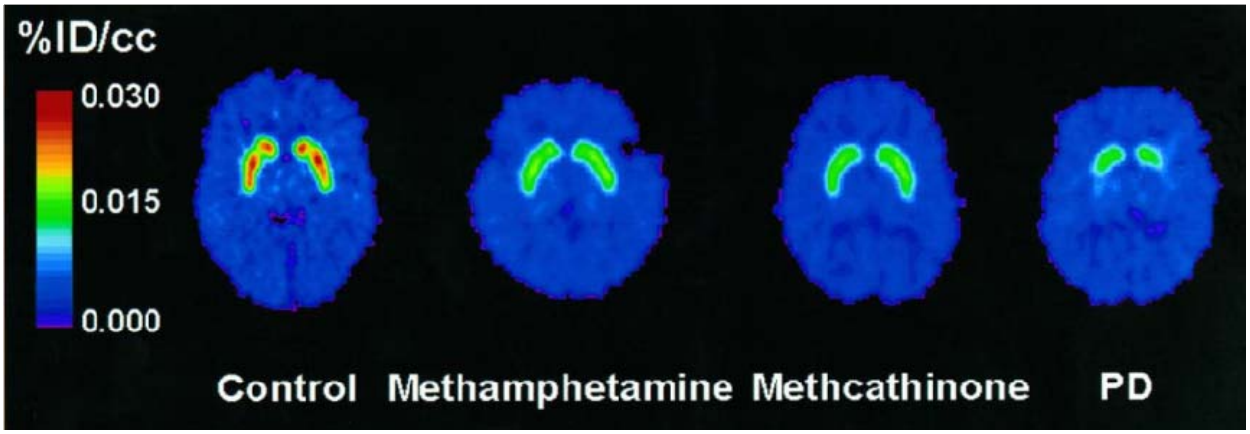

Figura 7. Reducción de la función del DAT en consumidores de metanfetamina. Imágenes de PET muestran la acumulación de [11C] WIN-35, 428 en el cuerpo estriado de un sujeto no consumidor (control), de sujetos que ha abandonado el consumo de metanfetamina o metcatinona y un enfermo de Parkinson, 70-90 min después de la inyección de [11C] WIN-35, 428 (Tomado de McCann *et al*. 1998).

como un mayor riesgo de padecer la enfermedad de Parkinson en el futuro (Callaghan *et al.* 2012). Un estudio reciente en humanos muestra, además, que la metanfetamina también provoca neurotoxicidad en otras áreas cerebrales, como se ha visto por los descensos del metabolismo de glucosa, no sólo en los núcleos caudado (-12%) y putamen (-6%), sino también en el tálamo (-17%), mientras que se ha observado un aumento del metabolismo de glucosa en la corteza parietal de usuarios de metanfetamina ya desintoxicados (Volkow *et al.* 2001c).

2. Neurotoxicidad en animales de experimentación

Existen estudios de toxicidad en animales de experimentación (ratón, rata, mono, etc.) que demuestran la pérdida de terminales dopaminérgicos en el núcleo estriado después del uso repetido de metanfetamina, evidenciada por la pérdida de inmunorreactividad de TH y DAT (Koda y Gibb 1973; Kogan *et al*. 1976; Wagner *et al.* 1980). Este efecto va acompañado por una disminución en el contenido de dopamina y sus metabolitos DOPAC y HVA en el estriado. También se han descrito aumentos concomitantes en la microglía y astrología reactivas en el estriado como marcadores indirectos de esta neurotoxicidad (Caligliuri y Buitenhuys 2005; O 'Callaghan y Miller 1994). Estudios con tinción de plata, el método de referencia para estudiar neurodegeneración (Switzer 2000), mostraron pruebas concluyentes de que la metanfetamina produce destrucción de terminales en el estriado (Ricaurte *et al.* 1982, 1984). Aunque existe una recuperación parcial de los niveles de expresión de TH y DAT a medida que pasa el tiempo, los efectos neurotóxicos en mono y ratón se mantienen incluso meses después de la administración de la droga (Kita *et al.* 2003; O' Dell *et al.* 1991; Seiden *et al*. 1988). Del mismo modo, los niveles de dopamina se mantienen reducidos en monos hasta 4 años después del consumo (Woolverton *et al.* 1989).

Resultados previos de nuestro laboratorio indican que, curiosamente, los diferentes compartimentos del núcleo estriado del ratón, los estriosomas y la matriz, difieren en su vulnerabilidad a la neurotoxicidad de la metanfetamina (Granado *et al*. 2010) (Figura 8).Los estriosomas, que están conectados con el sistema límbico y funcionalmente relacionados con conductas de recompensa y eventos emocionales (White e Hiroi 1998), son más vulnerables a la pérdida de terminales dopaminérgicos inducida por metanfetamina que la matriz, que está conectada a las regiones sensorimotoras del cerebro y está más estrechamente relacionada con las funciones motoras normales. El patrón de degeneración de la dopamina en el estriado es similar al observado en las primeras etapas de otras enfermedades neurodegenerativas como la enfermedad de Huntington, lesión isquémica-hipoxia y el tratamiento con MPTP, una neurotoxina selectiva de las neuronas dopaminérgicas utilizada como un modelo estándar de la enfermedad de Parkinson. El núcleo accumbens es más resistente a la pérdida de terminales dopaminérgicos (Granado *et al.* 2010), lo que también coincide con lo que ocurre en los enfermos de Parkinson (Granado *et al.* 2013a).

3. Mecanismos de neurotoxicidad inducida por la metanfetamina

Los mecanismos subyacentes a la neurotoxicidad dopaminérgica son objeto de estudio desde hace décadas y el conocimiento en este tema se ha expandido en los últimos años. Los resultados de los estudios de investigación señalan a la desregulación de la dopamina, el estrés oxidativo y nitrosativo, el daño en el ácido desoxirribonucleico (ADN) y la disfunción mitocondrial, como los principales responsables de los efectos neurotóxicos de esta droga (Krasnova y Cadet 2009).

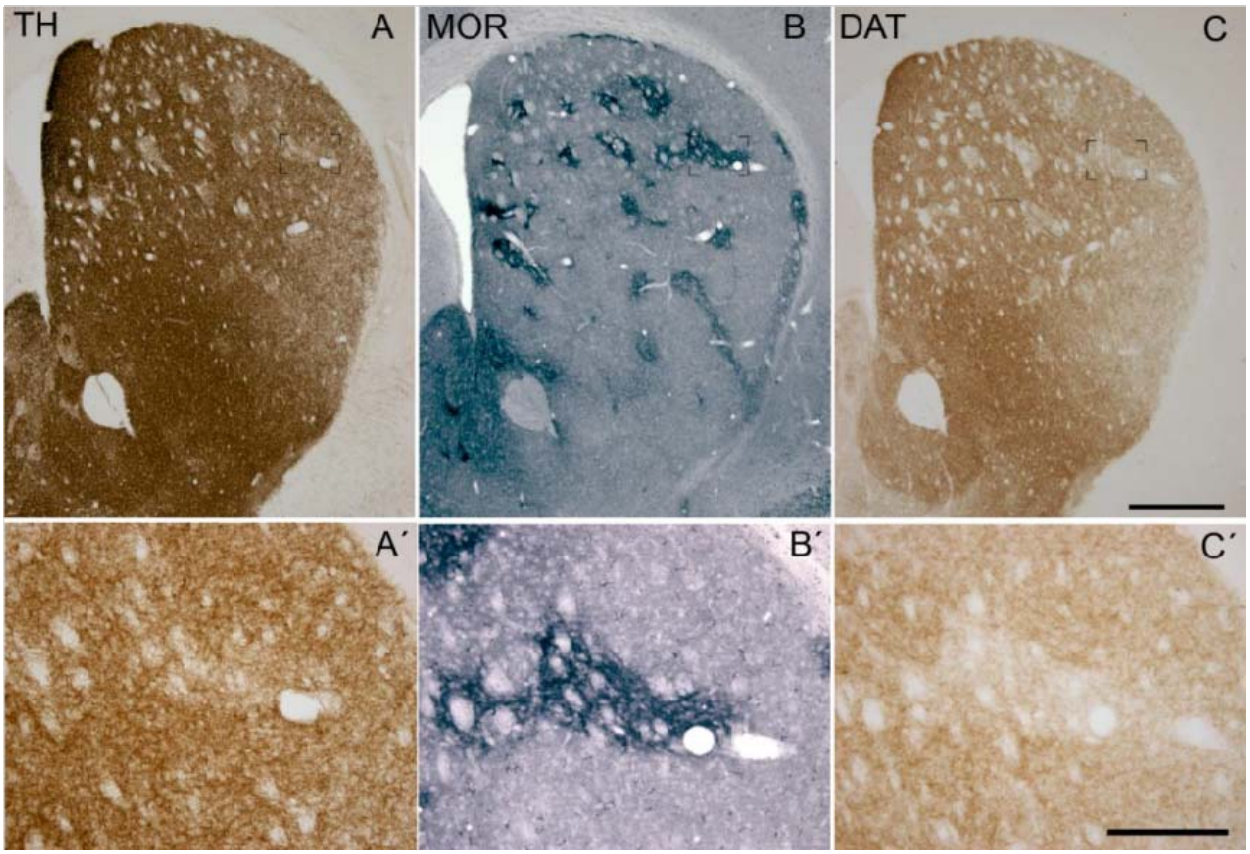

Figura 8. Los estriosomas son más vulnerables que la matriz a los efectos neurotóxicos de la metanfetamina. Fotomicrografías de secciones adyacentes de cerebro de ratón 7 días después del tratamiento con metanfetamina teñidas con TH y DAT para ver el daño y con MOR-1 para marcar los estriosomas. La metanfetamina produce mayor pérdida de TH y DAT en los estriosomas que en la matriz. La barra de escala indica 500 micras. (Tomado de Granado *et al.* 2010).

Papel de la dopamina

El consumo de metanfetamina aumenta en gran medida la concentración de dopamina en la sinapsis del cerebro. Como se ha explicado previamente, el exceso de dopamina en la hendidura sináptica es responsable de la mayor parte de los efectos físicos y psicológicos de esta droga, incluyendo los efectos estimulantes adictivos y psicomotores. Pero además, el desequilibrio en la distribución de la dopamina intracelular, en concreto el aumento de dopamina citosólica parece estar implicado en la neurotoxicidad, hecho que explica por qué la degeneración inducida por esta droga afecta principalmente a los terminales dopaminérgicos (Figura 9).

Tras su síntesis en las neuronas dopaminérgicas, la dopamina se almacena primero en vesículas, donde está protegida del metabolismo y la auto-oxidación, antes de ser liberada al citosol. La metanfetamina induce una redistribución de la dopamina dentro del terminal, produciendo la liberación de dopamina de las vesículas hacia el citosol, donde es sustrato de reacciones metabólicas y oxidativas, dando lugar a la producción de quinonas de dopamina, aniones superóxido y peróxido de hidrógeno y radicales hidroxilo. Esto promueve aún más la oxidación de la dopamina citosólica, favoreciendo el estrés oxidativo que conduce a la disfunción mitocondrial y al daño en el terminal dopaminérgico (Krasnova y Cadet 2009, Thomas *et al.* 2008b). La implicación del exceso de dopamina citosólica en los efectos neurotóxicos de la metanfetamina está apoyada por el hecho de que cuando se inhibe la síntesis de dopamina con alfa-metil-para-tirosina (αMPT), se atenúa la toxicidad de la

metanfetamina (Albers y Sonsalla 1995; Ares-Santos *et al.* 2012). Por el contrario, el pretratamiento con L-dopa (precursor de la dopamina) o con reserpina (que libera la dopamina de las vesículas al citoplasma) potencia la toxicidad inducida por la metanfetamina (Albers y Sonsalla 1995; Granado *et al.* 2011a). Del mismo modo, los ratones knock-out de VMAT-2, que tienen niveles más altos de dopamina citosólica, son más sensibles a la toxicidad dopaminérgica inducida por metanfetamina y muestran una mayor expresión de marcadores de estrés oxidativo que los animales WT (Larsen *et al.* 2002). (Larsen *et al.* 2002).

Implicaciones del estrés oxidativo

Las especies reactivas de nitrógeno (RNS) y las de oxígeno (ROS) son subproductos del metabolismo fisiológico normal en el cerebro, pero la producción excesiva de estas especies reactivas pueden dañar los componentes celulares, incluyendo los lípidos por peroxidación lipídica, las proteínas mediante la formación de la carbonilos, el ADN nuclear y mitocondrial por la peroxidación de estas macromoléculas. Estas especies reactivas dañan las enzimas de la cadena respiratoria mitocondrial e inhiben la ATPasa sodio-potasio, lo que genera estrés oxidativo y nitrosativo que conduce a un colapso metabólico y la muerte celular por necrosis o apoptosis (Davidson *et al*. 2001). lipídica, las proteínas mediante la formación de la carbonilos, el ADN nuclear y mitocondrial por la peroxidación de estas macromoléculas. Estas especies reactivas dañan las enzimas de la cadena respiratoria mitocondrial e inhiben la ATPasa sodio-potasio, lo que genera estrés oxidativo y nitrosativo que conduce a un colapso metabólico y la muerte celular por necrosis o apoptosis (Davidson *et al*. 2001).

La administración de metanfetamina aumenta los niveles de dopamina citosólica, donde puede ser metabolizada por la MAO o auto-oxidada en un proceso que genera quinonas de dopamina tóxicas. Estas quinonas de dopamina pueden dañar las proteínas celulares mediante su unión a los residuos de cisteína o mediante la generación de peróxido de hidrógeno (H_20_2) y anión superóxido (O_2•-) considerado el principal responsable de la toxicidad de la metanfetamina. El aumento inducido por la metanfetamina en la interacción de superóxidos y peróxido de hidrógeno con metales de transición como el hierro puede conducir a la formación de radicales hidroxilo (•OH), que provocan estrés oxidativo, disfunción mitocondrial y daño peroxidativo a las membranas de los terminales dopaminérgicos (Krasnova y Cadet 2009).

El aumento inducido por la metanfetamina del estrés oxidativo es probablemente el resultado de un desequilibrio entre la producción de ROS y la capacidad de los sistemas de enzimas antioxidantes para secuestrar ROS: la metanfetamina aumenta la producción de ROS y reduce los niveles de los eliminadores de ROS como superóxido dismutasa de Cobre-Zinc (CuZnSOD), catalasa, glutationina, y peroxirredoxinas en el cerebro (Jayanthi *et al.* 1998; Li *et al.* 2008). Esto podría explicar la mayor susceptibilidad del compartimento estriosomal, donde la superóxido dismutasa (SOD) es menos abundante que en la matriz (Medina *et al.* 1996), a la toxicidad dopaminérgica inducida por la metanfetamina (Granado *et al.* 2010). Esta idea concuerda con los estudios que muestran que los ratones transgénicos que sobreexpresan CuZnSOD son resistentes al daño estriatal inducido por la metanfetamina (Hirata *et al.* 1996). Además, los antioxidantes como el ácido ascórbico (vitamina C), vitamina E, bromocriptina (un eliminador de radicales hidroxilo), y la coenzima Q10 (antioxidante y potenciador de la energía mitocondrial) atenúan la toxicidad metanfetamina (Wagner *et al.* 1986). Los

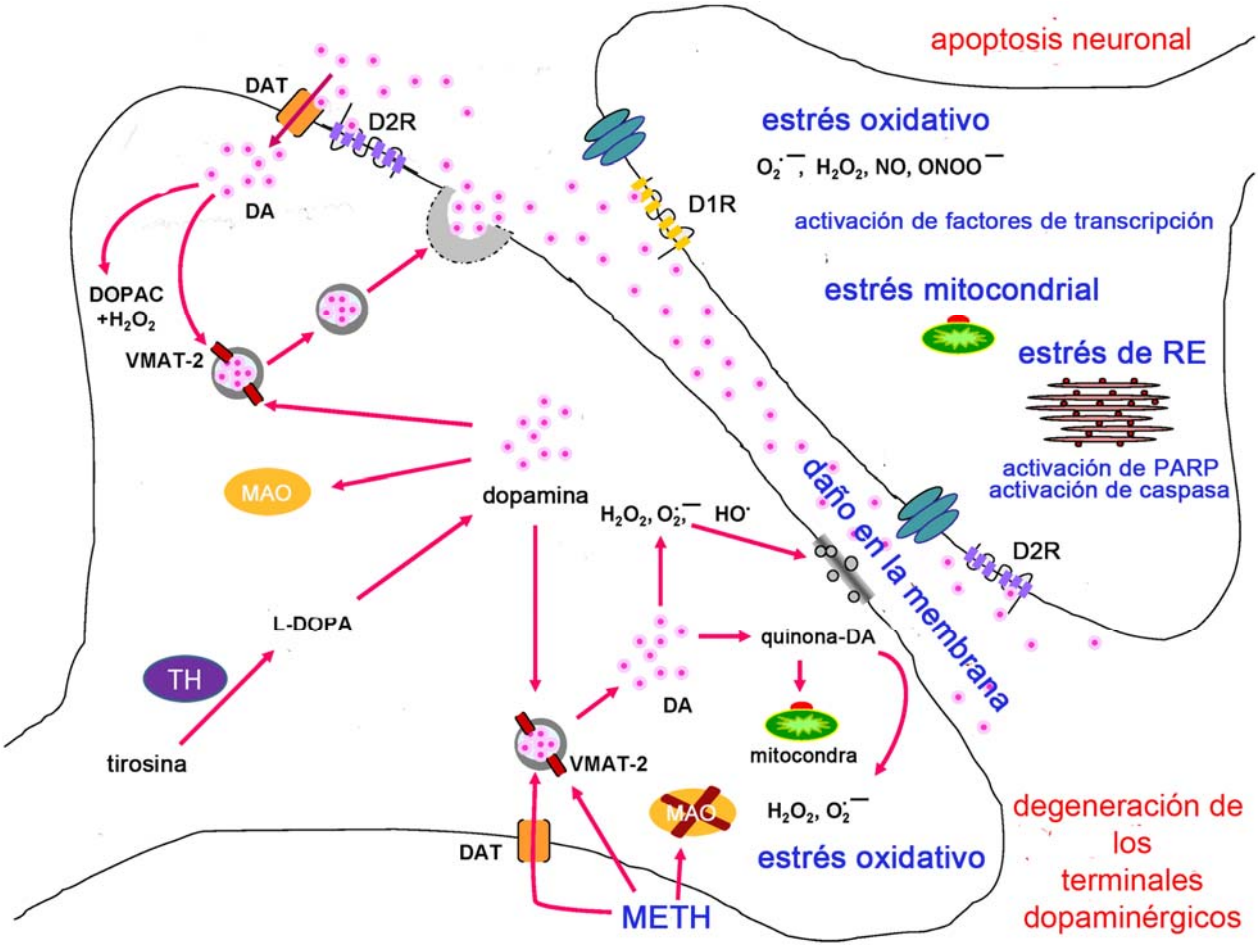

Figura 9. Acontecimientos celulares y moleculares implicados en la degeneración inducida por metanfetamina en los terminales dopaminérgicos del estriado. La metanfetamina (METH) entra en las neuronas dopaminérgicas a través del DAT y por difusión pasiva y provoca la liberación de dopamina (DA) vesicular al citoplasma a través de los cambios en el equilibrio del pH. En el citoplasma, la dopamina se auto-oxida formando quinonas de dopamina tóxicas, y generando radicales superóxido, peróxidos de hidrógeno y radicales hidroxilo que conducen a estrés oxidativo, disfunción mitocondrial y daño peroxidativo a las membranas presinápticas. (Modificado de Krasnova y Cadet 2009)

eliminadores de radicales libres como el PBN (α-fenil-N-terbutil nitrona) también reducen el daño neurotóxico (Yamamoto y Zhu 1998), sin alterar la respuesta hipertérmica que sigue a la administración de metanfetamina y que contribuye a la neurotoxicidad metanfetamina. ascórbico (vitamina C), vitamina E, bromocriptina (un eliminador de radicales hidroxilo), y la coenzima Q10 (antioxidante y potenciador de la energía mitocondrial) atenúan la toxicidad metanfetamina (Wagner *et al.* 1986). Los eliminadores de radicales libres como el PBN (α-fenil-N-terbutil nitrona) también reducen el daño neurotóxico (Yamamoto y Zhu 1998), sin alterar la respuesta hipertérmica que sigue a la administración de metanfetamina y que contribuye a la neurotoxicidad metanfetamina (ver papel de hipertermia a continuación).

Papel de hipertermia

La metanfetamina produce una respuesta hipertérmica, tanto en animales de experimentación como en consumidores humanos, que es proporcional a la dosis de la droga y a la temperatura ambiental. Esta hipertermia puede ser letal (es la primera causa de muerte inducida por la metanfetamina) y puede promover la neurotoxicidad a largo plazo, como se ha observado en una

relación entre la respuesta hipertérmica y la neurotoxicidad inducida por la droga (Ares-Santos *et al.* 2012; Bowyer *et al.* 1994; Granado *et al.* 2010, 2011a). Las estrategias que reducen o evitan esta respuesta hipertérmica después del tratamiento con metanfetamina, tales como su administración a bajas temperaturas (4 ºC) o el tratamiento previo con agentes farmacológicos que eviten la respuesta hipertérmica, como diclocipina o haloperidol, pueden prevenir o atenuar su neurotoxicidad (Albers y Sonsalla 1995; O 'Callaghan y Miller 1994). Por el contrario, la administración de metanfetamina a alta temperatura ambiental promueve la hipertermia y aumenta su neurotoxicidad (Ares-Santos *et al.* 2012; Bowyer *et al.* 1994; Granado *et al.* 2011a; Miller y O 'Callaghan 2003). Se cree que la correlación entre la hipertermia y la neurotoxicidad se debe a que la hipertermia puede potenciar la función del DAT (Xie *et al.* 2000), promover una mayor producción de radicales libres y una mayor oxidación de la dopamina en el cerebro (Krasnova y Cadet 2009; LaVoie y Hastings 1999). Por el contrario, la hipotermia tiene efectos inhibidores sobre el estrés oxidativo, ya que reduce la oxidación de la dopamina (LaVoie y Hastings 1999) y la formación de radicales hidroxilo (Fleckenstein *et al.* 1997; Krasnova y Cadet 2009). Por otra parte, las neuronas de animales mantenidos a temperaturas bajas reducen su demanda energética, lo que puede favorecer su protección ya que la administración de metanfetamina produce pérdida estriatal de adenosín trifosfato (ATP), posiblemente como consecuencia del estrés metabólico de las neuronas dopaminérgicas (Chan *et al.* 1994).

Discrepando con estos resultados, otros estudios farmacológicos y genéticos indican que la hipertermia puede contribuir a la neurotoxicidad dopaminérgica aunque no es absolutamente necesaria. Así la reserpina, un agente farmacológico que reduce drásticamente la temperatura corporal, potencia fuertemente la neurotoxicidad inducida por la metanfetamina, pese a impedir la respuesta hipertérmica (Albers y Sonsalla 1995; Ares-Santos *et al.* 2012; Granado *et al.* 2011a). Estos resultados indican que el bloqueo de la respuesta hipertérmica no es suficiente para proteger contra el daño neuronal. Por otra parte, la inactivación total o parcial del DAT, de la enzima óxido nítrico sintasa neuronal (nNOS), de la interleuquina 6 (IL-6), o c-jun protege contra la toxicidad inducida por la metanfetamina sin alterar la respuesta hipertérmica (Krasnova y Cadet 2009). Del mismo modo, la inyección intraestriatal de un antagonista de los receptores dopaminérgicos tipo D1, atenúa la neurotoxicidad dopaminérgica de la metanfetamina en el estriado manteniendo la hipertermia (Friend y Keefe 2013). Por lo tanto, la hipertermia inducida por la metanfetamina contribuye, pero no es necesaria para los efectos neurotóxicos de la droga.

Papel del glutamato y del óxido nítrico

La metanfetamina produce excitotoxicidad mediante el aumento de la liberación de glutamato en el estriado (Nash y Yamamoto, 1992) y la consiguiente activación de los receptores NMDA y AMPA. La estimulación de estos receptores aumenta los niveles intracelulares de Ca^{2+}, causando la activación de quinasas, lipasas y proteasas que dañan el citoesqueleto, favorecen la generación de radicales libres y causan daño en el ADN (Sattler y Tymianski 2000). Estudios farmacológicos muestran que MK801, un antagonista no competitivo del receptor NMDA, previene la toxicidad dopaminérgica inducida por la metanfetamina (Sonsalla *et al.* 1989). Por otra parte, la sobreactivación de los receptores NMDA produce radicales superóxido (O2 • -) y óxido nítrico (NO). Cuando estas dos especies reaccionan entre sí, se forma el peroxinitrito (ONOO-), una especie oxidativa todavía más potente, que parece ser una

de las principales responsables de la neurotoxicidad de la metanfetamina (Imam *et al.* 2001). La inactivación genética o farmacológica de nNOS reduce la neurotoxicidad de la metanfetamina sin afectar a la respuesta hipertérmica (Itzhak *et al.* 1998, 2000, 2002), probablemente debido a la pérdida de la producción de peroxinitrito.

Papel de la activación microglial y astroglial

El sistema nervioso central (SNC) es un área "inmunoprivilegiada" con un sistema inmune distinto del que existe en el resto del cuerpo. La microglía, un tipo de células gliales, son los macrófagos residentes en el sistema nervioso central, y actúan como su primera y principal defensa inmune. Normalmente se encuentran en estado de reposo, pero se activan tras ciertos tipos de daño en el SNC, como parte de la respuesta inmune innata. La microglía activada puede migrar rápidamente a los sitios de daño y secretar especies reactivas, incluyendo citoquinas proinflamatorias como interleuquina-1β (IL-1β), IL-6, TNF-α, quimioquinas, prostaglandinas, ROS, NO y superóxido para proteger el cerebro. Sin embargo, su excesiva activación puede producir efectos neurotóxicos (Krasnova y Cadet 2009). Las anfetaminas aumentan la activación microglial en las áreas en las que se produce neurotoxicidad dopaminérgica, con un pico de activación a las 24 h después de su administración, y la intensidad de la activación parece estar correlacionada con el nivel de daño dopaminérgico (Granado *et al*. 2008b, Thomas et al. 2004). La metanfetamina también induce activación de la microglía en otras áreas como cerebelo, hipocampo y corteza (Escubedo *et al.* 1998; Kelly *et al.* 2012). Además, la metanfetamina produce un aumento de los niveles de las tres principales citoquinas proinflamatorias: IL-1β, IL-6, TNF-α, que en gran parte son resultado de la activación microglial (Clark *et al.* 2013). Por lo tanto, la activación microglial representa una respuesta directa al daño inducido por anfetaminas y es parte de la cascada que conduce al daño neuronal (Thomas *et al.* 2008). Aunque muchas de las moléculas secretadas por la microglía activada están implicadas en la neurotoxicidad inducida por metanfetamina, y algunos fármacos anti-inflamatorios (ketoprofeno, indometacina, tetraciclina y minociclina) pueden proteger contra la activación microglial y la neurotoxicidad, el bloqueo de la activación microglial no es suficiente para impedir la neurotoxicidad inducida por metanfetamina (Sriram *et al.* 2006).

El daño en el SNC también conlleva la activación de los astrocitos, que son las células más abundantes en el cerebro humano y se ocupan de proporcionar nutrientes al tejido nervioso, mantener el equilibrio iónico extracelular y también desempeñan un papel importante en la formación y reparación de cicatriz en el SNC después de una lesión. Pueden proteger frente a la toxicidad, porque favorecen el aumento de los niveles de glutationina (un antioxidante), facilitando el crecimiento o "*sprouting*" de las fibras nerviosas y proporcionando factores de crecimiento, moléculas quimiotáxicas y de sostén para la regeneración axonal. Pero también pueden iniciar varias cascadas neuroinflamatorias y liberar citoquinas inflamatorias, algunas de las cuales son neurotóxicas. Sin embargo, parece probable que los astrocitos desempeñen un papel positivo en la limitación de la neuroinflamación y que sea el equilibrio entre la activación de la microglía y la astrología lo que conduzca a un resultado beneficioso o perjudicial (Clark *et al.* 2013). La astrogliosis reactiva se considera una reacción universal a la lesión del SNC y se utiliza como un marcador sensible de daño neuronal. La metanfetamina aumenta la activación de los astrocitos en las áreas más afectadas por la metanfetamina como el estriado, como se ve por el aumento de la expresión de la proteína marcadora

ácida fibrilar glial (GFAP) que alcanza niveles máximos entre 3 y 7 días después de la administración de la droga (O 'Callaghan y Miller 1994; Granado *et al.* 2011a).

Papel de la disfunción mitocondrial y el daño al ADN

Durante la exposición a la metanfetamina se produce una gran demanda de energía y aumentos agudos del metabolismo energético en las regiones cerebrales activadas (Halpin *et al.* 2013). Esto produce un compromiso del metabolismo energético y deja vacías las reservas de energía en zonas como el estriado (Chan *et al.* 1994; Huang *et al.* 1999), lo que resulta en una disfunción mitocondrial que aumenta la producción de ROS que contribuye a los efectos neurotóxicos de la metanfetamina (Krasnova y Cadet 2009). Estos déficits en el metabolismo energético se exacerban aún más con el daño mitocondrial y de los complejos II-III y IV de la cadena de trasporte de electrones (Burrows *et al.* 2000), que se dan incluso en ausencia de hipertermia y que parecen estar mediados por glutamato y NO (Brown *et al.* 2005; Burrows *et al.* 2000). La administración de sustratos de los complejos II-III tras la exposición a la metanfetamina previene el daño mitocondrial y el daño de las terminales dopaminérgicas (Halpin *et al.* 2013). Además, la elevada producción de ROS, RNS y productos no radicales relacionados, también puede dañar el ADN (Jeng *et al.* 2006), causando transversiones o mutaciones, alteraciones en la unión de factores de transcripción nuclear de ADN o bloqueo de la ARN polimerasa, que resultan en una transcripción alterada o retardada de las proteínas (Markkanen *et al.* 2012) que puede llevar a muerte celular apoptótica en animales de experimentación (Deng y Cadet 2000).

Uso de las tinciones de plata en histología

Las tinciones de plata se han utilizado mucho en histología para visualizar diversas estructuras en el SNC. La tinción de Golgi fue el primero de los llamados “métodos de plata reducida” y fue explotada por Cajal para estudiar la estructura del sistema nervioso y validar su doctrina de la neurona (Switzer 2000). Estas técnicas permitieron identificar los componentes del SNC y trazar las vías de los axones. Cada método de tinción fue desarrollado por ensayo-error y explotando la afinidad del sistema nervioso por la plata (argirofilia). Las tinciones de plata pueden ser "dirigidas" para teñir diferentes características del tejido nervioso según el tipo de fijación, el tratamiento previo ("mordiente"), la composición de la solución o soluciones que contienen plata, y la forma de revelado (reducción). Así, Bielschowsky introdujo una tinción con plata que, a diferencia de la de Golgi, teñía todos los tipos celulares y procesos neuronales, y podía emplearse para identificar características anormales entre los componentes normales observados con la tinción (Bielschowsky 1904). Este método se veía limitado por la dificultad de encontrar elementos degenerando entre los elementos normales también teñidos (poca señal con respecto al fondo o poco contraste). La solución a esta falta de contraste vino de utilizar el hecho de que los elementos neuronales degenerados tienen mayor afinidad por la plata que los normales, algo que Cajal ya describió (Leonard, 1981). Tratando previamente el tejido con diversas soluciones antes de la exposición a soluciones de plata (Glees 1946, Nauta y Gygax 1951), se conseguía una supresión de la impregnación de plata en los axones normales y una impregnación más intensa de los axones degenerados, alcanzando así un alto contraste. Fink y Heimer refinaron aún más el pretratamiento y desarrollaron una técnica que por primera vez fue capaz de detectar botones

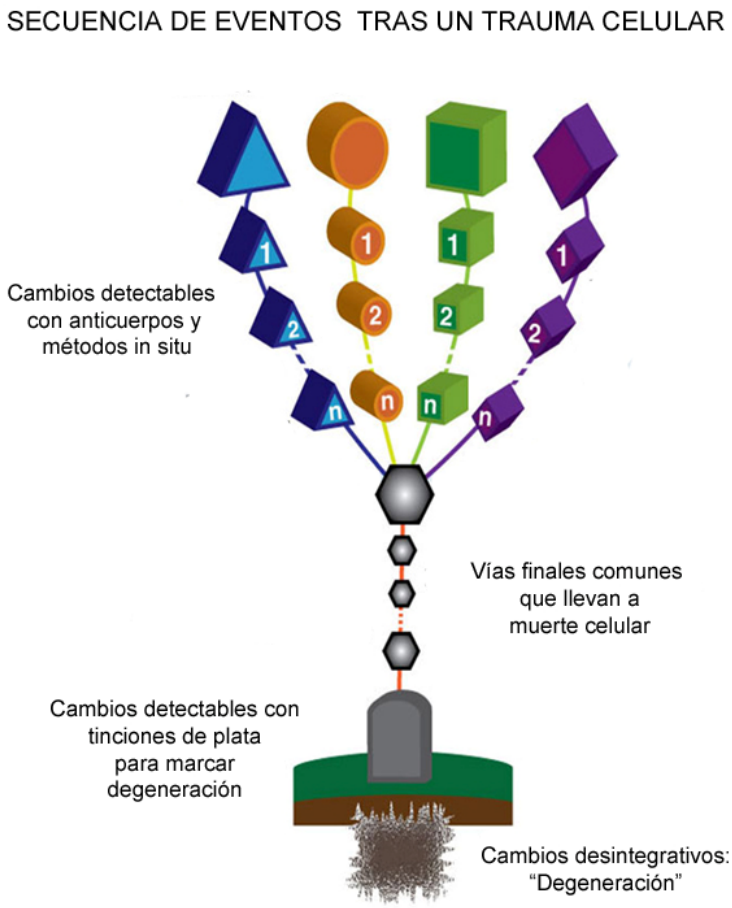

Figura 10. Etapas de la aplicabilidad de marcaje con anticuerpos y con las técnicas de plata para marcar degeneración. Cuando una célula sufre una agresión o trauma, comienza una secuencia de efectos (representado por las formas geométricas en la parte superior) diferente según la agresión recibida, que en un principio pueden ser reversibles y detectables con marcaje con anticuerpos. Al final, cualquier perturbación o trauma puede resultar en la muerte de la célula, que se puede producir por diferentes secuencias. Todas ellas, sin embargo, convergen para recorrer un camino final común ya irreversible (pequeños polígonos grises) que resulta en la muerte celular, pero que ya no puede ser detectado con anticuerpos. Las tinciones de plata para marcar degeneración siguen siendo los mejores métodos para marcar este punto final de la neurotoxicidad. (Modificado de Switzer 1993).

sinápticos degenerando, permitiendo el seguimiento completo de las vías axonales (Fink y Heimer 1967). Casi al mismo tiempo, de Olmos desarrolló la técnica amino-cúprico-argéntica (A-Cu-Ag) (de Olmos 1969) , que en su forma actual (de Olmos *et al*. 1994) es la que proporciona mayor sensibilidad y contraste ya que la degeneración se ve como elementos teñidos de negro sobre un fondo pálido sin teñir (de componentes normales no afectados). Además se puede combinar con técnicas de inmunohistoquímica, facilitando la identificación del fenotipo de las neuronas en degeneración (de Olmos *et al*. 2009).

Mecanismo de la tinción de Olmos (A-Cu-Ag)

La técnica de Olmos (de Olmos *et al*. 1994) se caracteriza por su alta sensibilidad y reproducibilidad para la detección de la degeneración del soma de las neuronas y también de sus axones, dendritas y terminales sinápticas (Bender *et al*. 2010; de Olmos *et al*. 1994; Jensen *et al*. 1993; Switzer 2000). Cuando una neurona se muere, se desintegra y son los restos celulares de esta desintegración que lo que registran las técnicas de plata que marcan degeneración. Se cree que la tinción resulta de la precipitación de plata iónica en torno a grupos químicos reductores presentes en las estructuras subcelulares, tales como proteínas dañadas desmanteladas por el mecanismo proteolítico (Beltramino *et al.* 1993; Eiland *et al.* 2002; Switzer 2000). Los iones de plata y de otros metales como el cobre, forman complejos con aminoácidos individuales o con secuencias de aminoácidos (péptidos) (Breslow 1973; Freeman 1973). Estos complejos o entidades de coordinación son asociaciones moleculares que involucran un grupo central, llamado núcleo de coordinación (generalmente un catión metálico) que posee orbitales de valencia no ocupados, rodeado por un cierto

número de moléculas o iones (ligandos) que poseen pares de electrones no compartidos. Estos electrones no compartidos pueden ser inyectados en los orbitales vacíos del grupo central para formar enlaces coordinados o covalentes dativos (Leigh 1990). Cada aminoácido tiene distinta afinidad por la plata: los aminoácidos con grupos sulfuro individuales son los que tienen la mayor afinidad por los iones de plata, pero éstos también puede formar complejos con los grupos amino y carboxilo terminales o con los grupos laterales de cualquier aminoácido (Black y Ansley 1966). Cuando una proteína está intacta, su conformación es más o menos globular, y muchos de estos grupos no están accesibles para los iones de plata. Sin embargo, en una célula que está degenerando, los mecanismos proteolíticos comienzan a desmantelar las proteínas y en el proceso, exponen más sitios sobre los que la plata puede formar complejos. (Switzer 2000). Curiosamente, la tinción con plata y cobre también se ha aplicado para detectar mezclas complejas de proteínas separadas en un gel de electroforesis en 2-dimensiones (Switzer *et al.* 1979). Las proteínas en esos geles no se están "desintegrando", es decir, no están fragmentadas, pero sí desdobladas y con los grupos laterales expuestos. Cada lugar en el que se forma un complejo se comporta como un punto de nucleación sobre el cual se agregan otros iones de plata (Liesegang 1911), comparable a lo que sucede en un proceso fotográfico, lo que supone una considerable amplificación de la señal.

Por las características de esta técnica, su alto sensibilidad y contraste para marcar degeneración y la posibilidad de combinarse con técnicas inmunohistoquímicas, esta técnica fue la que empleamos para estudiar la degeneración dopaminérgica en la vía nigroestriatal.

HIPÓTESIS

Y

OBJETIVOS

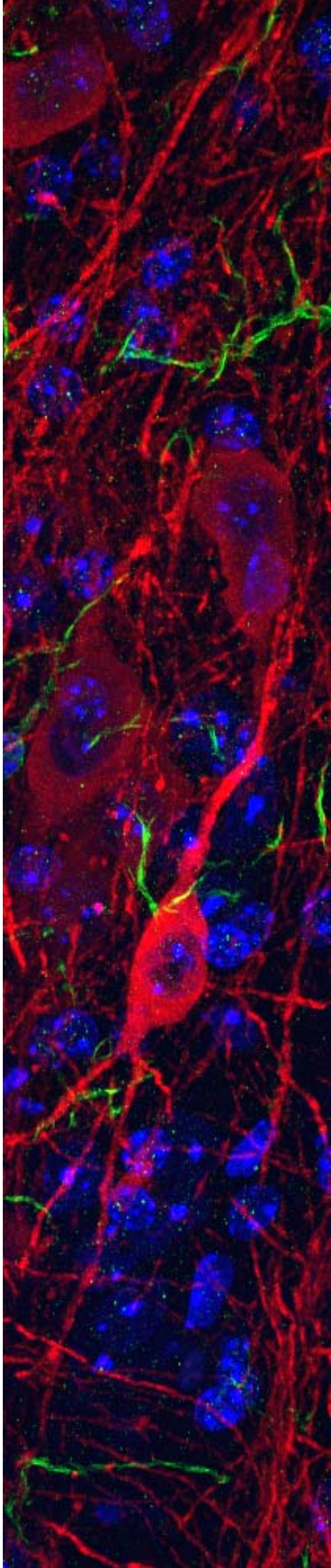

Foto de la página anterior: Cuerpo celular de una neurona dopaminérgica y fibras dopaminérgicas teñidas mediante inmunofluorescencia para TH (rojo) entre células de microglía teñidas con inmunofluorescencia para Iba-1 (verde) y núcleos de otras células teñidos con DAPI (azul) en la SNpc de un ratón 1d después de ser tratado con metanfetamina (3x5).

JUSTIFICACIÓN E HIPÓTESIS DE TRABAJO

HIPÓTESIS 1: La metanfetamina produce degeneración de los cuerpos celulares de las neuronas dopaminérgicas de la SNpc .

La neurotoxicidad que produce la metanfetamina sobre los terminales dopaminérgicos del estriado se ha estudiado desde hace décadas (Hotchkiss y Gibb 1980; Ricaurte *et al.* 1982,1984; Seiden *et al.* 1976; Wagner *et al.* 1980). Sin embargo, existe una controversia en cuanto a si la metanfetamina produce o no degeneración de los cuerpos de las neuronas dopaminérgicas en la sustancia negra pars compacta (SNpc). La mayoría de los estudios indican que la metanfetamina daña selectivamente los terminales de las neuronas dopaminérgicas, pero no los cuerpos celulares (Cadet *et al.* 2003; Krasnova y Cadet 2009; Ricaurte *et al.* 1982). No obstante, algunos estudios informan de la pérdida de neuronas dopaminérgicas (demostrada mediante inmunotinciones de TH) en la SNpc (Hall *et al.* 1996; Hirata y Cadet 1997; Kim *et al.* 2000; Sonsalla *et al.* 1996; Wang *et al.* 2012) aunque esto podría deberse sólo a una menor expresión de esta proteína. Hasta la fecha, no hay ninguna prueba directa que evidencie la degeneración de los cuerpos celulares de las neuronas dopaminérgicas. Dado que la disminución de neuronas TH+ en la SNpc tras la administración de metanfetamina y otras drogas como el MDMA, persiste con la misma intensidad durante al menos 1 mes (Granado *et al.* 2008b) ,a pesar de la recuperación parcial de los terminales, y que se ha descrito recientemente que los consumidores de metanfetamina tienen un mayor riesgo de desarrollar la enfermedad de Parkinson (Callaghan *et al.* 2012), nuestra hipótesis de partida es que la metanfetamina daña permanentemente no sólo los terminales de las neuronas dopaminérgicas de la vía nigroestriatal, sino también los cuerpos celulares de dichas neuronas en la SNpc, produciendo su degeneración.

Para evaluar esta hipótesis, hemos empleado una técnica de tinción de plata (tinción A-Cu-Ag o de Olmos) (de Olmos *et al.* 1994) combinada con inmunohistoquímica para TH en el estriado y la SNpc de ratones tratados con metanfetamina. Se han utilizado varios protocolos de administración de metanfetamina: una única dosis alta de metanfetamina, (30mg/Kg) -nos referiremos a este grupo como **1x30,** modelo de un consumo esporádico de una dosis elevada-, o varias dosis más bajas pero repetidas que modelizan un consumo compulsivo o tipo "*binge"* (tres inyecciones de 5 ó 10 mg/Kg, separadas por intervalos de 3h) -nos referiremos a ellas como **3x5** ó **3x10-**. Además, hemos evaluado el curso temporal de la neurotoxicidad inducida por metanfetamina (**3x5**) en el estriado y SNpc, junto con los cambios en la actividad y coordinación motora que se producen como consecuencia de la neurotoxicidad. Por último estudiamos la muerte de neuronas estriatales inducida por estos protocolos de administración de metanfetamina mediante el uso de la tinción A-Cu-Ag y ratones transgénicos BAC (cromosoma artificial bacteriano) D1-Tmt/D2-GFP, que expresan la proteína rojo tomate (tmt) bajo el promotor del receptor D1 y la proteína verde fluorescente (GFP) bajo el promotor del receptor D2.

HIPÓTESIS 2: Los receptores dopaminérgicos D1 y D2 están implicados en la neurotoxicidad dopaminérgica de la metanfetamina.

Dado que la metanfetamina actúa como un agonista indirecto de los receptores dopaminérgicos y produce sus efectos a través de la liberación de dopamina, estos receptores podrían tener un papel

mediador en la toxicidad. Los efectos de la dopamina se deben a su acción en las células diana a través de receptores metabotrópicos acoplados a proteínas G heterotriméricas. Hay cinco receptores dopaminérgicos diferentes (D1 a D5), divididos farmacológica y molecularmente en dos familias: los receptores tipo-D1 (D1 y D5) y los receptores tipo-D2 (D2, D3 y D4) (Beaulieu y Gainetdinov 2011). Ambas familias están involucradas en el comportamiento y la cognición, el movimiento voluntario, la motivación, el castigo y la recompensa, la atención, la memoria de trabajo y el aprendizaje, y en varias enfermedades neurodegenerativas como la enfermedad de Parkinson (Darmopil *et al.* 2009; Ortiz *et al.* 2010). Hay varios subtipos de receptores dopaminérgicos presentes en el estriado, pero los D1 y D2 son los más abundantes. En general se acepta que estos dos tipos de receptores están segregados, expresándose los receptores D1 en las neuronas estriatales de proyección que forman la vía directa y proyectan a la SN, mientras que los receptores D2 lo hacen en las neuronas de proyección que forman la vía indirecta, y proyectan al globo pálido (Beaulieu y Gainetdinov 2011; Callier *et al.* 2003). Además el subtipo D2 se localiza también presinápticamente en las terminales dopaminérgicas del estriado, donde funciona como autorreceptor regulando la liberación de dopamina y su recaptación (Beaulieu y Gainetdinov 2011; de Mei *et al.* 2009; Usiello *et al.* 2000).

Existen estudios farmacológicos centrados en dilucidar el papel de los receptores dopaminérgicos en la neurotoxicidad de la metanfetamina. Estudios con antagonistas de los receptores tipo-D2: sulpiride, eticlopride, y raclopride, han demostrado una prevención dosis-dependiente de la toxicidad inducida por metanfetamina en ratón (Albers y Sonsalla 1995; Eisch y Marshall 1998). Los antagonistas de los receptores de la familia D1, como SCH23390, también protegen frente a dicha neurotoxicidad (Sonsalla *et al.* 1986, Jayanthi *et al.* 2005; Krasnova y Cadet 2009). Sin embargo, estos compuestos generalmente bloquean también la respuesta hipertérmica inducida por la droga, lo que podría mediar la neuroprotección observada. Además, no diferencian entre los miembros de cada una de las familias de receptores por lo que no está claro qué subtipos de receptores median esta neurotoxicidad. Estudios previos de nuestro laboratorio han mostrado que los subtipos D1 y D2 median la neurotoxicidad inducida por MDMA, otro derivado anfetamínico (Granado *et al.* 2011a, 2013b) por lo que parece probable que también sean los implicados en el caso de la metanfetamina.

Nuestra hipótesis es que los receptores D1 y D2 están selectivamente implicados en mediar los efectos hipertérmicos y neurotóxicos de la metanfetamina. Para testar esta hipótesis, hemos evaluado la hipertermia y la neurotoxicidad dopaminérgica inducida por metanfetamina en ratones knock-out, para el receptor dopaminérgico D1 ($D1^{-/-}$) o para el receptor D2 ($D2^{-/-}$) mediante el uso de HPLC e inmunohistoquímica para marcadores dopaminérgicos y de gliosis.

HIPÓTESIS 3: El factor Nrf2 es importante en la protección frente a la neurotoxicidad dopaminérgica inducida por la metanfetamina.

El estrés oxidativo parece estar críticamente implicado en la neurotoxicidad y neuroinflamación producidas por la metanfetamina (Krasnova y Cadet 2009; Yamamoto y Zhu 1998; Thomas *et al.* 2004). Por ello, la identificación de dianas moleculares que refuercen las respuestas antioxidantes y antiinflamatorias frente a la metanfetamina en los ganglios basales, es importante para atenuar esta neurotoxicidad. El factor de transcripción Nrf2 (factor 2 nuclear relacionado con el factor eritroide 2)

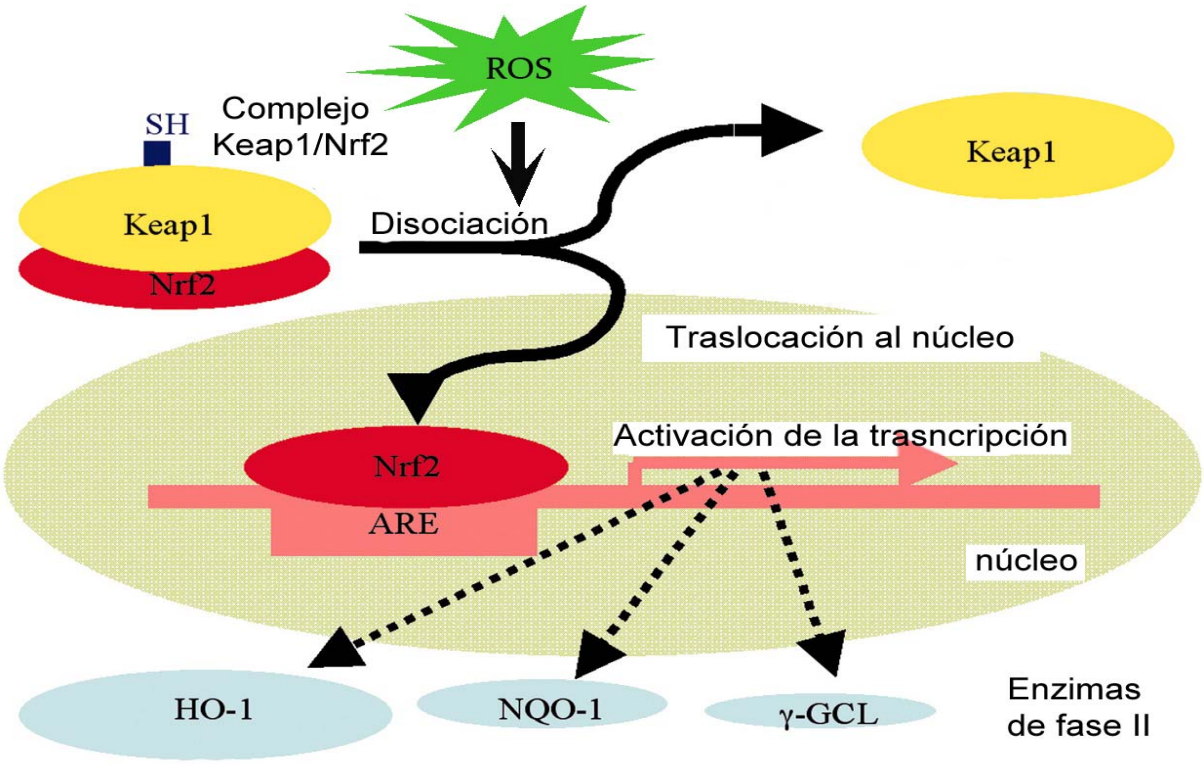

Figura 11. Mecanismo propuesto de neuroprotección por activación de Nrf2. Las ROS activan Nrf2 disociándolo de Keap1 y permitiendo su traslocación al núcleo celular, donde activa la transcripción de enzimas de fase 2 antioxidantes (Modificado de Satoh *et al.* 2006).

se considera el principal regulador de la homeostasis redox, ya que regula la expresión de un grupo de genes que codifican enzimas de desintoxicación de fase 2 antioxidante y antixenobiótica, y que son citoprotectores frente al estrés oxidativo e inflamatorio (Figura 9). Entre ellos se incluyen la hemo-oxigenasa-1 (HO-1), la NADPH quinona oxidorreductasa (NQO1), y las subunidades catalítica y moduladora de la γ-glutamilsintetasa (GCLC, GCLM) (Clark y Simon 2009; Johnson *et al.* 2008). En condiciones normales, el Nrf2 tiene una vida media muy corta debido a su interacción con la proteína Keap1, que promueve la degradación del Nrf2 por el proteasoma (Lo *et al.* 2006). Sin embargo, las moléculas oxidantes son capaces de disociar el complejo, permitiendo la entrada del Nrf2 al núcleo donde puede activar la transcripción de enzimas de fase 2 y la respuesta antioxidante. Estudios recientes han demostrado que la administración de metanfetamina activa Nrf2 (Jayanthi *et al.* 2009). Por ello, nuestra hipótesis es que el Nrf2 desempeña un papel importante en la protección de las neuronas dopaminérgicas contra el estrés oxidativo inducido por la metanfetamina.

Para evaluar esta hipótesis, hemos estudiado la hipertermia, la neurotoxicidad y la respuesta antioxidante inducidas por metanfetamina en la vía nigrostriatal en ratones knock-out para el factor Nrf2 ($Nrf2^{-/-}$) mediante técnicas inmunohistoquímicas , HPLC y qRTPCR (PCR cuantitativa en tiempo real).

,

OBJETIVOS

Los objetivos principales de la investigación son:

1. Determinar si la metanfetamina induce muerte de neuronas dopaminérgicas en la sustancia negra (SN).

2. Evaluar la implicación de los receptores dopaminérgicos D1 en la hipertermia y neurotoxicidad dopaminérgica inducida por metanfetamina en el estriado y SN y estudiar su mecanismo de acción.

3. Evaluar la implicación de los receptores dopaminérgicos D2 en la hipertermia y neurotoxicidad dopaminérgica inducida por metanfetamina en el estriado y SN y estudiar su mecanismo de acción

4. Evaluar la implicación del factor de transcripción Nrf2 en la neurotoxicidad dopaminérgica inducida por metanfetamina en estriado y SN.

APORTACIONES DE LA DOCTORANDA

La doctoranda Sara Ares Santos contribuyó activamente en el desarrollo de los trabajos presentados en esta Tesis Doctoral, en el marco de los proyectos financiados por el Plan Nacional Sobre Drogas (PNSD). La doctoranda contribuyó a la adquisición de los datos experimentales, su análisis e interpretación. Además participó en la escritura y revisión crítica de los artículos.

RESUMEN DE RESULTADOS

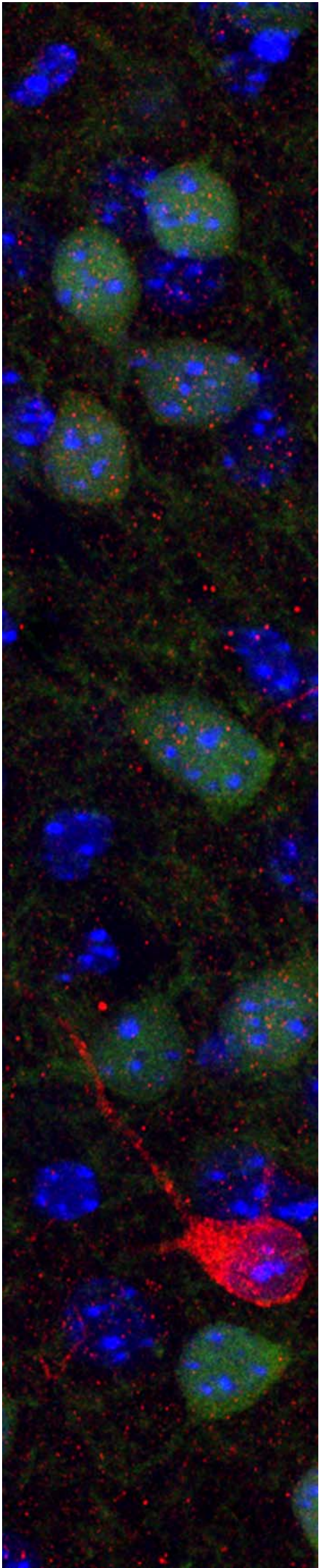

Foto de la página anterior: Sección de estriado de un ratón transgénico BAC D1-Tmt/D2-GFP en la que se ha hecho una tinción inmunofluorescente para las neuronas dopaminérgicas (TH, rojo) y para las neuronas de proyección de la vía indirecta (D2-GFP, verde) y se han teñido los núcleos celulares con DAPI (azul).

1. **La metanfetamina produce degeneración de los cuerpos celulares y de los terminales de las neuronas dopaminérgicas de la vía nigroestriatal.**

La administración i.p. de metanfetamina (**3x5, 3x10 ó 1x30)** indujo hipertermia y una pérdida de terminales dopaminérgicos en el estriado, lo que se evidenció por una pérdida de TH asociada temporal y espacialmente con un aumento de la tinción de plata en el estriado. El protocolo de **3x10**, fue el que produjo mayor degeneración de las terminales del estriado, seguido por el **3x5** y **1x30**. Se observaron algunos axones degenerando en su camino desde la SNpc al estriado. Además, la metanfetamina produjo degeneración de los cuerpos neuronales dopaminérgicos en la SNpc, que se puso de manifiesto por el aumento significativo del número de neuronas TH positivas (TH+) marcadas con plata, sin diferencias entre los 3 protocolos de administración. La muerte de estas neuronas se produce, al menos, por apoptosis y por necrosis.

La degeneración de los terminales dopaminérgicos del estriado tras la administración repetida de dosis bajas (**3x5**) comenzó entre 3 y 12h después de la última inyección, y llegó a su máximo a las 24h. Los estudios de ultraestructura confirmaron la presencia de terminales en degeneración y marcados con 3-nitrotirosina (3NT). Tras esta pérdida de terminales, se observó una recuperación progresiva detectada a los 3, 7 y 30 días del tratamiento. Esta recuperación no fue total y los déficits en la cantidad de fibras TH+ en el estriado persistieron al menos a los 30 días del tratamiento. A su vez, la degeneración de los cuerpos de las neuronas dopaminérgicas en la SNpc, (contabilizando neuronas TH+ teñidas con plata) empezó a observarse a las 12h y alcanzó su máximo (7%) a 1 y 3 días del tratamiento. El número de neuronas TH+ restantes en esta área se mantuvo reducido (-20-25%) en comparación con los controles salinos a los 7 y 30 días del tratamiento.

Además, la administración de múltiples dosis bajas de metanfetamina produjo déficits en la actividad locomotora y en la coordinación motora entre 1-3 días después del tratamiento, coincidiendo con el tiempo de máxima degeneración en estriado tras la droga. Estos déficits no se observaron ya a los 7 días de la exposición a metanfetamina.

Los protocolos de **3x10** y **1x30** también provocaron muerte de neuronas estriatales observada 1 y 3 días después del tratamiento. Mediante el uso de ratones transgénicos BAC D1-Tmt/D2-GFP, se observó que las neuronas estriatales en degeneración se distribuyen por igual entre las neuronas de proyección de la vía directa, de la vía indirecta y otras neuronas del estriado, probablemente interneuronas, lo que significaría que las interneuronas son más vulnerables a la neurotoxicidad de metanfetamina, ya que mueren en igual número pese a suponer una población menor en el estriado.

2. **La inactivación genética del receptor dopaminérgico D1 reduce fuertemente la neurotoxicidad dopaminérgica inducida por metanfetamina.**

La inactivación genética del receptor dopaminérgico D1 bloqueó la hipertermia inducida por la administración de metanfetamina (**3x5**) y previno el descenso de los marcadores de las fibras dopaminérgicas (TH y DAT) y de los niveles de dopamina y sus metabolitos (DOPAC y HVA), tanto 1 como 7 días después del tratamiento. Aunque a los 7 días del tratamiento con metanfetamina los animales WT habían recuperado parcialmente los niveles de dopamina y sus metabolitos, estos eran aún inferiores a los de los animales tratados con salino. La falta del receptor D1 también previno la

gliosis reactiva inducida por metanfetamina, tanto en el estriado como en la SN, en comparación con los animales WT. Estos datos se observaron mediante inmunohistoquímica para Mac-1 y GFAP a 1 y 7 días tras la droga. Además, la inactivación del receptor D1 previno el aumento de la expresión de la enzima óxido nítrico sintasa inducible (iNOS) en el estriado inducido por metanfetamina. Finalmente, la pérdida de neuronas dopaminérgicas en la SNpc inducida por la metanfetamina no se produjo en los ratones $D1^{-/-}$, en los que tampoco se observaron los cuerpos apoptóticos presentes en la SN de los animales WT tratados con metanfetamina.

En un experimento diseñado para estudiar la relación entre la hipertermia y la neurotoxicidad, la metanfetamina fue administrada en una sala a alta temperatura ambiente (29ºC). Los ratones $D1^{-/-}$ tratados en estas condiciones desarrollaron hipertermia, sin que se diera la neuroprotección que se había observado por la inactivación del receptor D1 a 23ºC. Sin embargo, el pretratamiento con αMPT en ratones WT bloqueó la respuesta hipertérmica a la metanfetamina sin bloquear completamente la pérdida de estriatal TH-ir, lo que indica que la prevención de la respuesta hipertérmica no es suficiente para prevenir la neurotoxicidad. Además, el pretratamiento con reserpina hizo que los animales $D1^{-/-}$ presentaran la misma neurotoxicidad dopaminérgica frente a metanfetamina que los WT. De este hecho, junto con los resultados de voltametría, que muestran que la inactivación del receptor D1 aumenta la liberación de dopamina estriatal inducida por metanfetamina, se deduce que los ratones $D1^{-/-}$ tienen mas dopamina vesicular, a pesar de que presentan menos dopamina total en estriado, lo que indica que sus niveles de dopamina citosólicos son inferiores.

3- La inactivación del receptor D2 protege frente a la neurotoxicidad dopaminérgica inducida por metanfetamina.

La falta del receptor dopaminérgico D2 evitó la hipertermia tras el tratamiento con metanfetamina (4mg/kg, i.p. 3 inyecciones separadas por intervalos de 3 horas) y atenuó el descenso en la inmunoreactividad de TH y DAT en el estriado y en los niveles de dopamina y sus metabolitos en la misma área, inducidos por la metanfetamina 1 ó 7 días después del tratamiento. La falta del receptor D2 también previno la gliosis reactiva, tanto en el estriado como en la SN, inducida por metanfetamina. Además, la inactivación del receptor D2 previno los aumentos de la expresión de iNOS e interleuquina 15 (IL-15) en el estriado inducidos por metanfetamina 1 día después del tratamiento. Por otra parte, la pérdida de neuronas dopaminérgicas de la SNpc inducida por metanfetamina no se produjo en los ratones $D2^{-/-}$, en los que tampoco se observaron neuronas Fluoro-Jade positivas como las presentes en la SN de los animales WT.

Cuando los ratones $D2^{-/-}$ fueron tratados con metanfetamina en una sala a 30ºC, tampoco desarrollaron hipertermia sino hipotermia y los niveles de TH y DAT presentados por estos animales fueron similares a los de los ratones tratados con salino. Sin embargo, el pretratamiento con reserpina indicó que el efecto neuroprotector de la inactivación del receptor D2 no puede ser explicado únicamente por su capacidad para prevenir la hipertermia inducida por metanfetamina, ya que la reserpina produce una marcada hipotermia en ambos genotipos, y pese a ello potencia la toxicidad de la metanfetamina en los animales WT, pero no en los $D2^{-/-}$. Los resultados de voltametría muestran que la metanfetamina indujo una liberación de dopamina significativamente menor en los animales $D2^{-/-}$ que en los ratones WT, lo que indica que los ratones $D2^{-/-}$ tienen menos dopamina vesicular. Además, aunque los niveles basales de dopamina estriatales son similares en ambos genotipos, los

$D2^{-/-}$ tienen mayores niveles de DOPAC y HVA, indicando que estos animales tienen mayor recambio de dopamina en el estriado.

4. La falta del Nrf2 potenció el daño de los terminales dopaminérgicos inducido por metanfetamina, pero no la pérdida de células TH en la SNpc

La inactivación genética del factor de transcripción Nrf2 exacerbó la pérdida de TH y DAT inducida por metanfetamina en el estriado 1 día después de su administración, de forma independiente de la hipertermia. La ausencia de Nrf2 no modificó el aumento inducido por metanfetamina en el Ca^{2+} intracelular en los astrocitos del estriado a los pocos minutos de su administración, indicando que la deficiencia de Nrf2 no altera la respuesta astrocítica primaria. Sin embargo, la falta de Nrf2 favoreció la activación glial inducida por metanfetamina 1 día después del tratamiento, con mayores aumentos en los niveles de ácido ribonucleico mensajero (RNAm) y proteínas de Mac-1 y Iba-1 y GFAP en el estriado tras la administración de la droga.

Al mismo tiempo, la falta de Nrf2 aumentó el estrés oxidativo y los efectos proinflamatorios inducidos por la metanfetamina en el estriado. El tratamiento con metanfetamina no indujo a las 24h cambios en la expresión de las enzimas de fase-2 NQO1 y Gsta2 (datos no mostrados) pero sí indujo cambios en la expresión de los genes antioxidantes que están regulados por Nrf2, incluyendo Gclc, (pero no Gclm), la superóxido dismutasa de manganeso (Mn SOD), la Cu/Zn SOD, y la glutation peroxidasa (GPx). Además, la inactivación de Nrf2 potenció un aumento drástico en el RNAm de TNF-α así como en la expresión de la proteína IL-15 en el estriado, que curiosamente colocalizaba con los astrocitos, inducidos por la metanfetamina.

Asimismo, la deficiencia de Nrf2 potenció la degeneración de neuronas estriatales inducida por metanfetamina. Sin embargo, contrastando con los resultados obtenidos en el estriado, la deficiencia de Nrf2 no alteró la pérdida de neuronas dopaminérgicas inducida por metanfetamina ni los marcadores gliales o las moléculas proinflamatorias en la SN.

COPIA DE LOS TRABAJOS PUBLICADOS

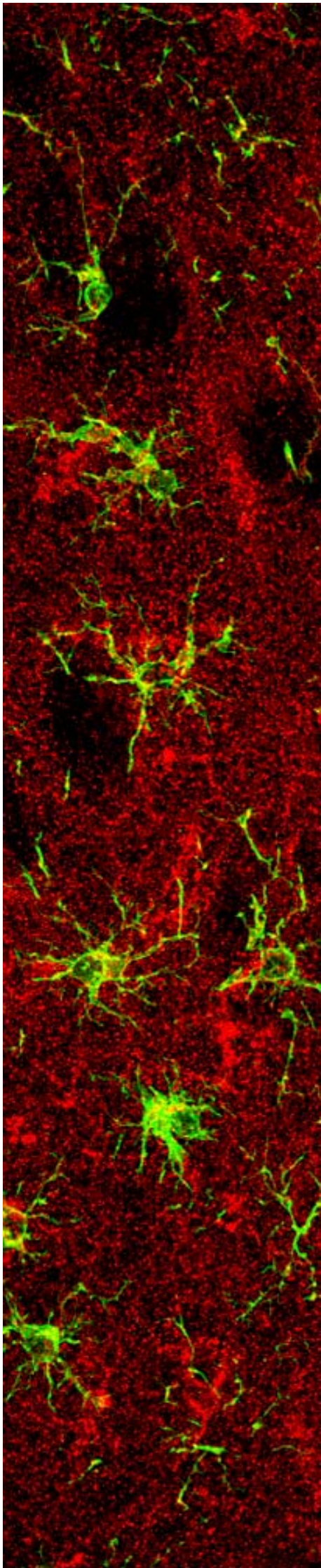

Foto de la página anterior: Sección de estriado de un ratón tratado con metanfetamina en la que se ha realizado una tinción inmunofluorescente para las IL-15 (rojo) y para las microglía reactiva (Iba-1, verde) .

1. Methamphetamine causes degeneration of dopamine cell bodies and terminals of the nigrostriatal pathway evidenced by silver staining.

Ares-Santos S*, Granado N*, Espadas I, Martínez-Murillo R, Moratalla R *Neuropsychopharmacology*. In press

* equal contribution

Neuropsychopharmacology (2013), 1–15

www.neuropsychopharmacology.org

Methamphetamine Causes Degeneration of Dopamine Cell Bodies and Terminals of the Nigrostriatal Pathway Evidenced by Silver Staining

Sara Ares-Santos[1,2,4], Noelia Granado[1,2,3,4], Isabel Espadas[1], Ricardo Martinez-Murillo[1] and Rosario Moratalla*[,1,2]

[1]Instituto Cajal, Consejo Superior de Investigaciones Científicas (CSIC), Madrid, Spain; [2]CIBERNED, ISCIII, Madrid, Spain; [3]Facultad de Medicina, Universidad Complutense de Madrid, Madrid, Spain

Methamphetamine is a widely abused illicit drug. Recent epidemiological studies showed that methamphetamine increases the risk for developing Parkinson's disease in agreement with animal studies showing dopaminergic neurotoxicity. We examined the effect of repeated low and medium doses *vs* single high dose of methamphetamine on degeneration of dopaminergic terminals and cell bodies. Mice were given methamphetamine in one of the following paradigms: three injections of 5 or 10 mg/kg at 3 h intervals or a single 30 mg/kg injection. The integrity of dopaminergic fibers and cell bodies was assessed at different time points after methamphetamine by tyrosine hydroxylase immunohistochemistry and silver staining. The 3 × 10 protocol yielded the highest loss of striatal dopaminergic terminals, followed by the 3 × 5 and 1 × 30. Some degenerating axons could be followed from the striatum to the substantia nigra pars compacta (SNpc). All protocols induced similar significant degeneration of dopaminergic neurons in the SNpc, evidenced by amino-cupric-silver-stained dopaminergic neurons. These neurons died by necrosis and apoptosis. Methamphetamine also killed striatal neurons. By using D1-Tmt/D2-GFP BAC transgenic mice, we observed that degenerating striatal neurons were equally distributed between direct and indirect medium spiny neurons. Despite the reduced number of dopaminergic neurons in the SNpc at 30 days after treatment, there was a partial time-dependent recovery of dopamine terminals beginning 3 days after treatment. Locomotor activity and motor coordination were robustly decreased 1–3 days after treatment, but recovered at later times along with dopaminergic terminals. These data provide direct evidence that methamphetamine causes long-lasting loss/degeneration of dopaminergic cell bodies in the SNpc, along with destruction of dopaminergic terminals in the striatum.

Neuropsychopharmacology accepted article preview 30 October 2013; doi:10.1038/npp.2013.307

Keywords: amphetamine derivatives; cell death; Parkinson's disease; psychostimulants; neurotoxicity; silver-degeneration stain

INTRODUCTION

Methamphetamine is an addictive illegal psychostimulant consumed by between 14.3 million and 53.1 million users worldwide, according to past estimations from the United Nations Office on Drugs and Crime (UNODC, 2013). Despite its high popularity, attributed to its wide availability, relative low cost, and long duration of psychoactive effects, methamphetamine is a neurotoxic drug that can produce long-lasting impairments in abusers (Krasnova and Cadet, 2009; McCann *et al*, 1998; Volkow *et al*, 2001a). Brain PET studies in human abusers showed dopamine transporter (DAT) reductions in the caudate nucleus and putamen that are associated with reduced motor skills (Volkow *et al*, 2001a,b; McCann *et al*, 1998). Furthermore, recent epidemiological studies provided evidence that the risk for developing Parkinson's disease is almost doubled in individuals with a history of methamphetamine use (Callaghan *et al*, 2012).

It is established that methamphetamine is a potent inducer of dopamine release and is toxic to dopamine neurons. Neurodegeneration of dopaminergic terminals in the striatum is evidenced by reductions in the immunoreactivity of tyrosine hydroxylase (TH), the rate-limiting enzyme for dopamine synthesis, and of DAT, accompanied by decreases in levels of dopamine and its metabolites (Ares-Santos *et al*, 2012, 2013a, b, 2014; Hotchkiss and Gibb, 1980; Granado *et al*, 2010, 2011a,b; Ricaurte *et al*, 1982,1984; Seiden *et al*, 1976; Wagner *et al*, 1980; Zhu *et al*, 2006a). Concomitant increases in reactive astrocytes and microglia in the striatum have also been described as indirect markers of this neurotoxicity.

However, a controversy exists regarding whether or not methamphetamine produces neurodegeneration of dopaminergic cell bodies in the substantia nigra pars compacta

*Correspondence: Dr R Moratalla, Instituto Cajal, Consejo Superior de Investigaciones Científicas (CSIC), Avda Dr Arce 37, Madrid 28002, Spain, Tel: +34 91 58 54 705, Fax: +34 91 58 54 754, E-mail: moratalla@cajal.csic.es
[4]The first two authors contributed equally to this work
Received 2 September 2013; revised 21 October 2013; accepted 22 October 2013

(SNpc); although most studies indicate that methamphetamine selectively injures dopamine terminals while dopaminergic cell bodies are spared (Krasnova and Cadet, 2009; Ricaurte *et al*, 1982), others report loss of dopaminergic neurons in the SNpc: TH-immunoreactive (TH-ir) revealed that methamphetamine causes a reduction in the number of TH neurons in the SNpc (Ares-Santos *et al*, 2012; Granado *et al*, 2011a, b, 2013; Hirata and Cadet, 1997; Sonsalla *et al*, 1996). Furthermore, recent reports from our laboratory have shown that methamphetamine not only reduces TH expression, which could be due to a reduction in its synthesis rather than neuronal loss, but also produces neuronal degeneration, evidenced by Nissl-stained apoptotic bodies, Fluorojade-stained neurons, and reduction in the total number of neurons in the SNpc (Ares-Santos *et al*, 2012; Granado *et al*, 2011a, b). However, to date, no direct proof of degeneration of nigral dopaminergic neurons has been reported.

The aim of this study was to test whether methamphetamine produces neurodegeneration of dopaminergic cell bodies in the SN by looking for direct evidence of degeneration of dopaminergic neurons. Moreover, we wanted to know if different regimens of methamphetamine delivery had different neurotoxic effects in the striatum and SNpc, and to test whether these effects were permanent or transient. We compared the effects of three different administration paradigms: a single high dose (bolus) (1×30 mg/kg), which models acute methamphetamine intoxication, *vs* repeated administration (binge) of lower doses (3×5 or 3×10 mg/kg), modeling methamphetamine use by humans (Bowyer *et al*, 2008). In addition, with the lowest dose protocol (3×5) we evaluated the time course of degeneration of dopamine terminals and cell bodies to determine the persistence of neurotoxic effects, and assessed locomotor activity and motor coordination at short (1 and 3 days) and long time points (7 and 30 days) after treatment to correlate neurotoxicity with functional behavioral changes.

We used the amino-cupric-silver (A-Cu-Ag) staining to identify damaged cell somas and processes. This technique, also known as de Olmos stain (de Olmos *et al*, 1994), specifically stains somatodendritic and terminal degeneration (Beltramino *et al*, 1993; de Olmos *et al*, 1981, 1994). We combined A-Cu-Ag staining with TH immunohistochemistry to determine if dopaminergic neurons in the SNpc degenerate after methamphetamine. In addition, we used it in D1R-tomato-D2R-eGFP BAC transgenic mice to identify specific neuronal populations sensitive to methamphetamine. We further evaluated the neurotoxic changes in the striatum by electron microscopy (EM).

MATERIALS AND METHODS

Animals

Male C57BL/6J mice (3–4 months old, weighing 20–33 g) ($n = 10$–14 per group) from the Instituto de Investigación Médica Mercedes y Martín Ferreyra or from the Instituto Cajal (Harlan Iberica, Barcelona, Spain) were housed in groups of 4–6 per cage in conditions of constant temperature at $21 \pm 2\,^{\circ}$C, in a 12 h light/dark cycle, with free access to food and water. All experimental procedures conformed to European Community guidelines (2003/65/CE) and were approved by Cajal Institute's Bioethics Committee (following DC86/609/EU).

Treatment and Measurement of Rectal Temperature

(+)-Methamphetamine hydrochloride was obtained from Sigma-Aldrich (Madrid, Spain), dissolved in 0.9% (w/v) NaCl (saline) and injected in a volume of 10 ml/kg. Doses refer to the base. A single high dose of (+)-methamphetamine (30 mg/kg) or multiple lower doses (3 doses of 5 or 10 mg/kg, at 3 h intervals) were injected intraperitoneally in a room at constant temperature of $23 \pm 2\,^{\circ}$C. Control mice received saline. Mice were housed in groups of 4–6 per cage during treatment. Rectal temperature was measured every 30 min immediately before and after each methamphetamine injection and 1, 2, and 3 h after each drug administration as described before (Ares-Santos *et al*, 2012; Granado *et al*, 2010, 2011a, b). Animals were killed 1 or 3 days after treatment. To examine the time course of methamphetamine (3×5) effects, mice were killed 3 or 12 h, and 1, 3, 7, or 30 days after treatment.

Tissue Collection and Detection of Neuronal Degeneration by the A-Cu-Ag Stain

Animals were anesthetized with 6% chloral hydrate or sodium pentobarbital (50 mg/kg), and perfused transcardially with 4% paraformaldehyde in 0.2 M borate buffer (pH 7.4). Brains were left overnight in the skull and afterwards removed and placed in 30% sucrose. Brain sections of 50 μm were obtained in a freezing microtome and stored in 4% paraformaldehyde for A-Cu-Ag technique or immunohistochemistry. One hemisphere of each brain was cut in sagital and the other in coronal sections to study the anatomical neurodegeneration. Neuronal degeneration was analyzed by the A-Cu-Ag stain, which stains degenerating perikarya, dendrites, stem axons, and their terminal ramifications (synaptic endings) (de Olmos *et al*, 1994; Switzer, 2000). The A-Cu-Ag technique was set up in the lab after the training in the Laboratory of Experimental Neuroanatomy and Histology, Instituto de Investigación Médica Mercedes y Martín Ferreyra (INIMEC-CONICET, Cordoba, Argentina).

Immunohistochemistry

Immunostaining was carried out on free-floating sections with standard avidin–biotin immunocytochemical protocols (Granado *et al*, 2008a; Ortiz *et al*, 2010). Endogenous peroxidase activity was removed by incubation in 3% H_2O_2 for 10 min. This step was avoided if immunostaining was performed in silver-stained tissue. The specific primary antibodies (Ab-I) used were as follows: rabbit anti-TH (1 : 1000; Chemicon International, Temecula, CA); rat anti-GFP (1 : 1000; Nacalai Tesque, Kyoto, Japan); and rabbit anti-Tmt (DsRed) (1 : 1000; Clontech). For immunofluorescence experiments, we used Alexa Fluor 488- and 594-conjugated secondary antibodies (1 : 400–500; Invitrogen, Eugene, OR).

Quantitative Assessment of Degeneration of Dopaminergic Terminals in the Striatum

Quantification of TH expression and silver staining in the striatum was carried out using pictures of the striatal sections taken with a $\times 4$ lens in an optic microscope equipped with a Leica DFC 290 HD videocamera. An image analysis system (Analytical Imaging Station; Imaging Research, Linton, UK) was used to convert color intensities into a gray scale and to quantify the area of staining in the striatum as a proportion of pixels in the striatum that show staining (stained area) in relation to total pixels in the striatum (scanned area). We refer to this as proportional stained area (Darmopil *et al*, 2008, 2009). The threshold was chosen in saline animals and applied to all animals.

Electron Microscopy

Degeneration of striatal fibers was confirmed at the ultrastructural level by EM following the protocol described previously (Rivera *et al*, 2002). Cryoprotected tissue was frozen with liquid nitrogen and thawed in cold 0.1 M PB. Sections (40 μm thick) were cut with a Vibratome (Leica Microsystems GmbH, Wetzlar, Germany) and immunostained for 3-nitrotyrosine (primary antibody from Dr Martinez-Murillo; diluted 1 : 2000) to mark protein nitration (Castro-Blanco *et al*, 2003), or for TH (1 : 1000). After DAB reaction, sections were washed with PBS, postfixed in 1% osmium tetroxide in 0.1 M PB, dehydrated in graded ethanols (1% uranyl acetate was included at the 70% ethanol), mounted on Durcupan ACM resin (Fluka) slides under a plastic coverslip, and cured for 3 days at 56 °C. Selected areas of the caudate–putamen were dissected out, re-embedded in Durcupan, and cut in ultrathin sections (1–0.5 μm thick) with Ultramicrotome (Leica Microsystems), mounted on Formvar-coated grids, stained with lead citrate, and examined in a Jeol 1200 EX electron microscope.

Stereological Quantification of Degenerating Neurons in the Striatum and in SNpc

The number of striatal A-Cu-Ag-stained neurons was counted unilaterally in every 4th sections of the striatum of saline- and methamphetamine-treated animals ($n = 4$–6) stained for A-Cu-Ag. The degeneration of neurons in the SNpc was assessed by counting TH-ir neurons, A-Cu-stained neurons, and TH/A-Cu-Ag doubled-stained neurons unilaterally in every 4th section of the SNpc of all experimental groups ($n = 4$–6) in which TH immunostaining was performed following the A-Cu-Ag technique (de Olmos *et al*, 2009). The optical fractionator, Stereoinvestigator program (Microbrightfield Bioscience, Colchester, VT), was used as described (Ares-Santos *et al*, 2012; Espadas *et al*, 2012) by an experienced observer unaware of treatment conditions. The outline of the striatum and SNpc (including SN pars lateralis) were drawn at low power ($\times 2$) using defined anatomic landmarks (Ares-Santos *et al*, 2012; Baquet *et al*, 2009; Granado *et al*, 2008c), and the number of cells was counted at higher power ($\times 20$ for the striatum and $\times 100$ for the SNpc). At these magnifications, A-Cu-Ag-stained cell bodies were easily identified among the terminal degeneration in the striatum and among TH-ir, TH/A-Cu-Ag-stained or A-Cu-Ag non-dopaminergic neurons in the SNpc. To avoid double counting, neurons were counted when their nuclei were optimally visualized, which occurred only in one focal plane. Only A-Cu-Ag-stained particles with the size and morphology of degenerating cells or apoptotic bodies were counted. Neurons that stained for both TH and A-Cu-Ag were only counted if there was a silver-stained cell body surrounded by TH staining. Although this criterion may have excluded some dopaminergic degenerating neurons, it should have reliably excluded all non-dopaminergic degenerating cells. Some neurons with extremely faint signs of TH expression were not counted as TH-expressing neurons (see Figure 4f). Results are expressed as bilateral estimations.

Identification of Striatal Degenerating Neurons

For these studies, we used D1R-tomato-D2R-eGFP BAC transgenic mice obtained by crossing D1R-tomato with D2R-eGFP BAC transgenic mice obtained from MMRRC, SC, and from Jackson Labs, ME. These mice were backcrossed for six generations to C57BL/6N mice using a speed congenic protocol, D1R-tomato-D2R-eGFP mice (Suárez *et al*, 2013) were administered a single high dose of methamphetamine (1×30 mg/kg), killed 1 day later, and processed for silver staining in combination with immunohistochemistry for GFP or tomato red (Tmt) proteins. The number of total striatal A-Cu-Ag-stained neurons positive for GFP or Tmt was quantified by stereology as described for striatal degenerating neurons ($n = 5$).

Histopathological Studies in SNpc

Coronal midbrain sections (30 μm) containing SNpc of animals treated with saline or methamphetamine (3×5 mg/kg) were mounted on slides and dried overnight, rehydrated, and stained for hematoxylin and eosin (H&E) or for Fluoro-Jade C as described before (Granado *et al*, 2008b, 2011a, b). Nissl staining was performed on SNpc sections after TH immunohistochemistry.

Locomotor Activity and Motor Coordination

Horizontal and vertical movements were recorded in the same animals in naive conditions and after 1, 3, 7, and 30 days of treatment with saline or methamphetamine (3×5) ($n = 10$) in 60 min sessions as described previously (Granado *et al*, 2008c). Motor coordination was measured at the same time points in the same animals, right after the locomotor activity evaluation, using an accelerating rotarod apparatus (Hugo Basile, Rome, Italy) as described previously (Rodrigues *et al*, 2007).

Statistics

Data are presented as mean ± standard error of the mean (SEM). Data were analyzed using Student's *t*-test and two-way ANOVA. Relevant differences were analyzed pair-wise by *post hoc* comparisons with Student–Newman–Keuls and Tukey's test, to determine specific group differences. All statistical analyses and graphical representations were performed using Sigma Plot 11.0 program and the threshold for statistical significance was set at $p < 0.05$.

RESULTS

Methamphetamine-Induced Hyperthermia Peaks at 30 min after Each Administration

Animals treated with methamphetamine in all three different administration protocols showed significant increases in rectal temperature compared with saline-treated animals (Figure 1a). The multiple dose regimens produced hyperthermia, peaking 30 min after each administration, compared with saline-treated animals ($p<0.001$). The 3×10 regimen induced greater hyperthermia than the 3×5, which induced a slight hypothermia 2 h after the first injection, in comparison with saline-treated animals ($p<0.05$). A single high dose (30 mg/kg) of methamphetamine induced a single peak of hyperthermia in the first 30–60 min after the injection that was similar to those

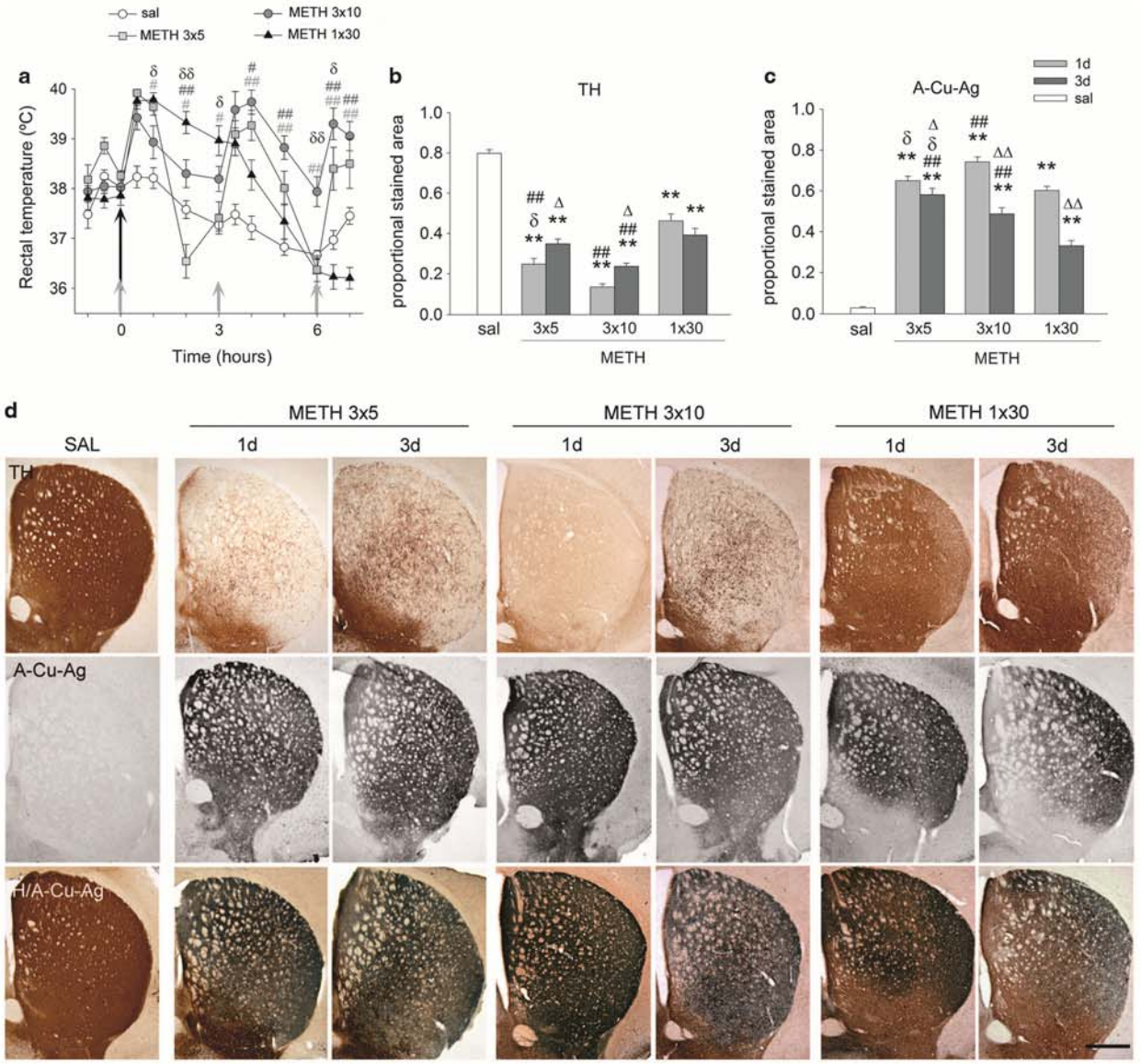

Figure 1 Single administration of methamphetamine (1×30) induced less dopaminergic terminal degeneration in the striatum than multiple administration treatments (3×5 or 3×10). (a) Methamphetamine produced hyperthermia after each injection, with three peaks in the multiple administration regimens, and a single and more sustained peak of hyperthermia after single administration of (1×30 mg/kg). Data represent mean ± SEM, $n=10$–14 per group. Arrows indicate drug injection. (b and c) Histograms show the proportional stained area of tyrosine hydroxylase (TH) and amino-cupric-silver staining in the striatum. Data represent mean ± SEM, $n=4$–6 per group. (d) Photomicrographs of striatal sections from mice 1 and 3 days after treatment with saline (sal) or methamphetamine (3×5), (3×10), or (1×30), stained for TH (top), A-Cu-Ag (middle), or TH/A-Cu-Ag (bottom). $^{*}p<0.05$, $^{**}p<0.001$ *vs* sal, $^{\#}p<0.05$, $^{\#\#}p<0.001$ *vs* (1×30), $^{\delta}p<0.05$, $^{\delta\delta}p<0.001$ *vs* (3×10), $^{\Delta}p<0.05$, $^{\Delta\Delta}p<0.001$ *vs* 1 day. Statistical analysis was performed by two-way analysis of variance and *post hoc* Newman–Keuls analysis. Bar indicates 500 μm (d).

produced by multiple lower dose regimens. However, in the single high-dose protocol, hyperthermia was sustained, and significantly higher than following multiple lower doses for 3 h ($p<0.05$), and gradually decreased until reaching control levels at 5 h after administration ($p<0.05$ *vs* saline). Body temperature in these animals continued decreasing and resulted in slight hypothermia (Figure 1a) 7 h after the injection ($p<0.05$).

A Single High Dose of Methamphetamine Induced Less Degeneration of TH-ir Terminals than Multiple Lower Doses

One day after methamphetamine administration, a marked overall decrease in the density of TH-ir terminals in the striatum was evident compared with the intense TH staining in saline-treated animals (Figure 1b and d). At this time point, quantitative image analysis revealed significant decreases in TH-ir in all treatment paradigms compared with saline ($p<0.001$): 69% in the 3×5 group, 83% in the 3×10 group, and 42% in the 1×30 group. As expected, multiple dose regimens induced a dose-dependent TH terminal loss in the striatum ($p<0.001$). The multiple lower dose protocols produced greater reductions in TH-ir in the striatum than the single high dose ($p<0.001$), with only some scattered TH fibers visible throughout the whole striatum. In the single high-dose regimen, striosomes of the dorsolateral part of the caudoputamen were the most affected areas, with severe TH-ir loss compared with the rest of the striatum. Three days after treatment, the levels of striatal TH-ir were still reduced in methamphetamine-treated animals compared with saline animals ($p<0.001$). However, a slight increase in the density of TH terminals was seen in the multiple dose regimens ($p<0.05$). This tendency to recover TH-ir levels was not observed in the single high-dose group (Figure 1b and d).

In parallel with changes observed in striatal TH-ir, a marked overall increase in the density of A-Cu-Ag-stained terminals in the striatum (Figure 1c and d), with a widespread punctuate silver deposition (see Figure 2a), was evident in methamphetamine-treated animals one day after the treatment compared with saline-treated animals ($p<0.001$), indicating that methamphetamine produces strong terminal degeneration in the striatum (Figure 1). TH-ir was performed on A-Cu-Ag-stained striatal sections to see if the signals of the two techniques were inversely associated. The increase in A-Cu-Ag-stained degenerating terminals in the striatum was complementary to the loss of TH-ir, strongly suggesting that dopaminergic fibers are the ones that degenerate after methamphetamine.

The multiple dose regimens induced a dose-dependent effect on A-Cu-Ag staining levels in the striatum, as the 3×10 protocol had greater effect than the 3×5 protocol ($p<0.05$). The single high-dose administration (1×30) had less effect on the integrity of dopaminergic terminals than multiple lower dose protocols ($p<0.001$). This high dose produced a stronger silver deposition in the striosomes and in the dorsolateral part of the caudoputamen than in the rest of the striatal areas (Figure 1c and d). Silver deposits in striatal dopaminergic fibers were still detected 3 days after the treatment with methamphetamine in comparison with saline animals ($p<0.001$). However, the intensity of A-Cu-Ag signal in the striatum was reduced compared with 1 day after treatment (Figure 1c and d). This degeneration was accompanied by microgliosis (assessed by Iba-1-ir) and astrogliosis (GFAP-ir), peaking 1 and 3 days after treatment, respectively (data not shown), in agreement with previous reports (Ares-Santos *et al*, 2012; O'Callaghan and Miller, 1994; LaVoie *et al*, 2004).

Methamphetamine Induces Striatal Cell Death

A-Cu-Ag-stained neurons were observed in the striatum of methamphetamine-treated animals (Figure 2). The lowest dose (3×5) did not cause a significant increase in striatal A-Cu-Ag-stained neurons compared with saline, but higher doses (3×10 and 1×30) did. The 3×10 dose increased stained neurons in the striatum by five- to sevenfold at 1 and 3 days after treatment and the 1×30 dose increased stained neurons by ~9-fold at 1 and 3 days. There was no significant difference between numbers of stained neurons at 1 and 3 days for either dosing paradigm (Figure 2b). Degenerating striatal cells were generally more abundant in the ventromedial part of the striatum, although at 1 day after treatment with the 1×30 protocol, they were also observed frequently in dorsolateral parts of the striatum (Figure 2c).

Degenerating Neurons were Equally Distributed between Direct Pathway MSNs, Indirect Pathway MSNs and Other Striatal Neurons

No colocalization of Tmt and GFP proteins was found in the striatal neurons of D1R-Tmt-D2R-eGFP BAC transgenic mice (Figure 2d). In these mice, Tmt fluorescence identifies

Figure 2 Methamphetamine produced degeneration of striatal neurons. (a) Photomicrographs of tyrosine hydroxylase/amino-cupric-silver (TH/A-Cu-Ag)-stained sections of the striatum of mice treated with saline (sal) or methamphetamine (3×5), (3×10), or (1×30) 1 day or 3 days after the treatment, at high magnification. (b) Histogram showing the number of A-Cu-Ag-positive cells in the striatum counted by stereology in sections of mice treated with saline or methamphetamine (3×5), (3×10), or (1×30) 1 day or 3 days after the treatment (mean ± SEM, $n=4$–6 per group). Treatment with methamphetamine (3×10) or (1×30) induced the appearance of A-Cu-Ag-stained neurons in the striatum. Data represent mean ± SEM, $n=4$–6 per group, $^*p<0.05$ *vs* sal. (c) Stereoinvestigator drawings of the striatum of mice treated with saline or methamphetamine (3×5), (3×10), or (1×30), showing the distribution of A-Cu-Ag-stained neurons at different rostrocaudal levels at 1 day (stars) and 3 days (dots) after treatment. (d) Striatal neurons in D1-Tmt/D2-GFP BAC transgenic mice did not coexpress GFP and Tmt proteins. (e) Among the degenerating striatal cells, about one-third were direct pathway medium spiny neurons (MSNs), another third indirect pathway MSN, and the remaining third were other types of striatal neurons ($n=5$). (f) Photomicrographs of Tmt/A-Cu-Ag-, GFP/A-Cu-Ag-, or A-Cu-Ag-positive neurons in the striatum of D1-Tmt/D2-GFP BAC transgenic mice 1 day after treatment with methamphetamine (1×30). Statistical analysis was performed by two-way analysis of variance and *post hoc* Newman–Keuls analysis. Bar indicates 30 μm (a), 25 μm (d), 500 μm (c), or 10 μm (f). BAC, bacterial artificial chromosome; GFP, green fluorescent protein; Tmt, tomato red.

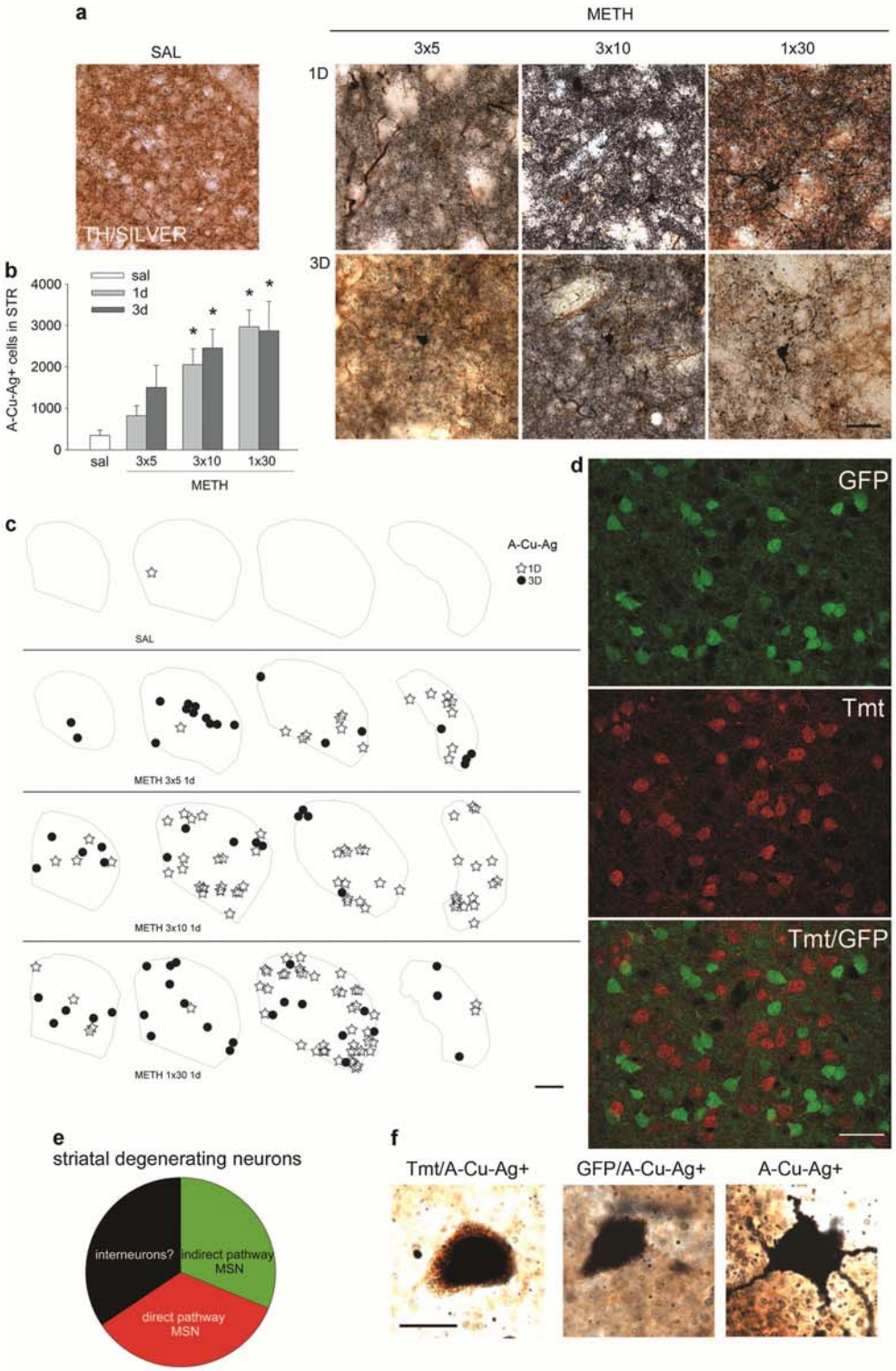
a
METH
SAL
3x5
3x10
1x30
1D
3D
TH/SILVER
b
A-Cu-Ag+ cells in STR
sal
1d
3d
4000
3000
2000
1000
0
sal
3x5
3x10
1x30
METH
c
A-Cu-Ag
1D
3D
SAL
METH 3x5 1d
METH 3x10 1d
METH 1x30 1d
d
GFP
Tmt
Tmt/GFP
e
striatal degenerating neurons
interneurons?
indirect pathway MSN
direct pathway MSN
f
Tmt/A-Cu-Ag+
GFP/A-Cu-Ag+
A-Cu-Ag+

medium spiny neurons (MSNs) of the direct pathway and GFP fluorescence identifies MSNs of the indirect pathway. A third (34%) of the A-Cu-Ag-stained striatal cells observed 1 day after the treatment with the single high dose (1 × 30) colocalized with Tmt-positive neurons (D1R, direct pathway MSN), and another third (31%) colocalized with GFP-positive neurons (D2R, indirect pathway MSN). The remaining third (35%) of degenerating neurons did not colocalize with either red or green fluorescence, suggesting that other populations of striatal neurons are affected as well (Figure 2e and f).

Degenerating Axons were Observed in the Nigrostriatal Pathway

In sagital brain sections from animals treated with methamphetamine, but not in saline animals, some A-Cu-Ag-stained axons were observed in the nigrostriatal pathway leading from the SNpc, via medial forebrain bundle (MFB), to the striatum (Figure 3). However, A-Cu-Ag staining was not as abundant as in the striatum. No appreciable loss of TH axons in the MFB was revealed by visualization of sagital sections of methamphetamine-treated animals at low magnification (× 2.5), despite the significant loss of dopaminergic terminals in the striatum.

Methamphetamine Administration Induced Degeneration of Dopaminergic Neurons in the SNpc

As reported previously (Ares-Santos *et al*, 2012; Granado *et al*, 2011a, b), methamphetamine administration resulted in significant loss of TH-expressing neurons in the SNpc. One day after methamphetamine administration, the number of TH-ir cell bodies in the SNpc was reduced by 22% in the 3 × 5 paradigm, 34% in the 3 × 10, and 21% in the 1 × 30 group. The number of TH-expressing neurons in this area remained stable 3 days after treatment with each of the different regimens of the drug (Figure 4a and b).

This reduction in the number of TH neurons was at least partially due to degeneration of dopamine neurons, as TH soma colocalized with A-Cu-Ag deposits (TH/A-Cu-Ag) in the SNpc (Figure 4c and g). The percentage of double-stained neurons at 1 day after treatment with methamphetamine represented 7.1% of the total number of dopaminergic neurons in the 3 × 5 group, 14.8% in the 3 × 10 group, and 13% in the 1 × 30 group. The percentage of double-stained neurons remained similar 3 days after treatment in all the protocols (Figure 4c). The estimated percentage of double-stained neurons was lower than the percentage of TH-ir neuron loss, which could indicate that some neurons do lose TH expression before degenerating or without degeneration (see Figure 4f).

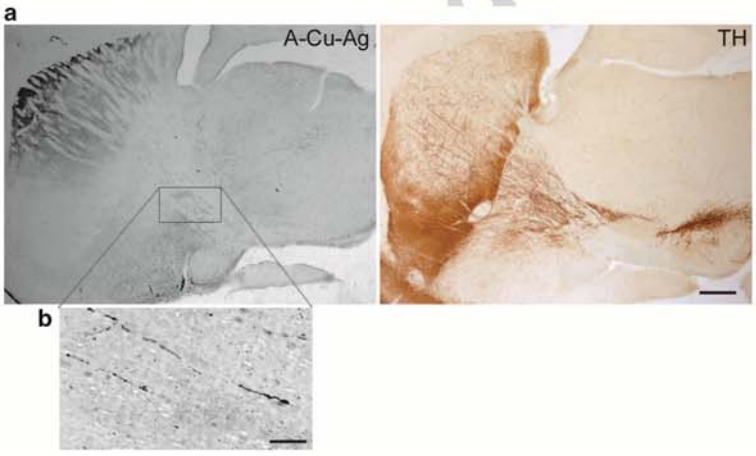

Figure 3 Some degenerating nigrostriatal axons are observed in sagital sections of methamphetamine-treated animals. (a) Representative photomicrographs of sagital sections of the brain of a mouse that received methamphetamine (3 × 5) stained for amino-cupric-silver (A-Cu-Ag) or tyrosine hydroxylase (TH) 1 day after drug delivery. (b) Note that some degenerating A-Cu-Ag axons can be observed in the nigrostriatal pathway among many intact TH-stained axons. Bar indicates 500 μm (a) and 30 μm (b).

Figure 4 Methamphetamine induces degeneration of dopaminergic neurons in substantia nigra pars compacta (SNpc). (a–d) Left, histograms show the number of tyrosine hydroxylase (TH)- (b), TH/amino-cupric-silver (A-Cu-Ag)- (c), A-Cu-Ag-positive cells (d), and the accumulated mean of each of them (a) in the SNpc, counted by stereology in sections of mice treated with saline (sal) or methamphetamine (3 × 5), (3 × 10), or (1 × 30) 1 day or 3 days after the treatment (mean ± SEM, $n = 4$–6 per group). $^{*,**}p < 0.05$, 0.001 *vs* sal. Statistical analysis was performed by Student's *t*-test. Right, high magnification photomicrographs of nigral sections stained for TH/A-Cu-Ag illustrating TH-stained neurons in saline animals (e), and neurons seen in animals treated with methamphetamine 3 × 5, 3 × 10, or 1 × 30 (f–i). (f) Neurons that have only faint remaining TH staining. (g) Degenerating dopaminergic neurons stained with TH and A-Cu-Ag. (h) Degenerating neurons that do not express TH. (i) A-Cu-Ag-stained apoptotic bodies. Bars indicate 10 μm. (j) Degeneration of nigrostriatal neurons may be caused by different death pathways. Photomicrographs of neurons in the SNpc of mice show normal neurons in a saline control (upper row), and degenerating neurons 1 day after treatment with methamphetamine (lower row). Positive FluoroJade staining, eosinophilic necrotic red neurons stained with hematoxylin and eosin (H&E), and Nissl-stained apoptotic bodies were observed in mice after methamphetamine (3 × 5) treatment but not in saline animals. Bar indicates 10 μm.

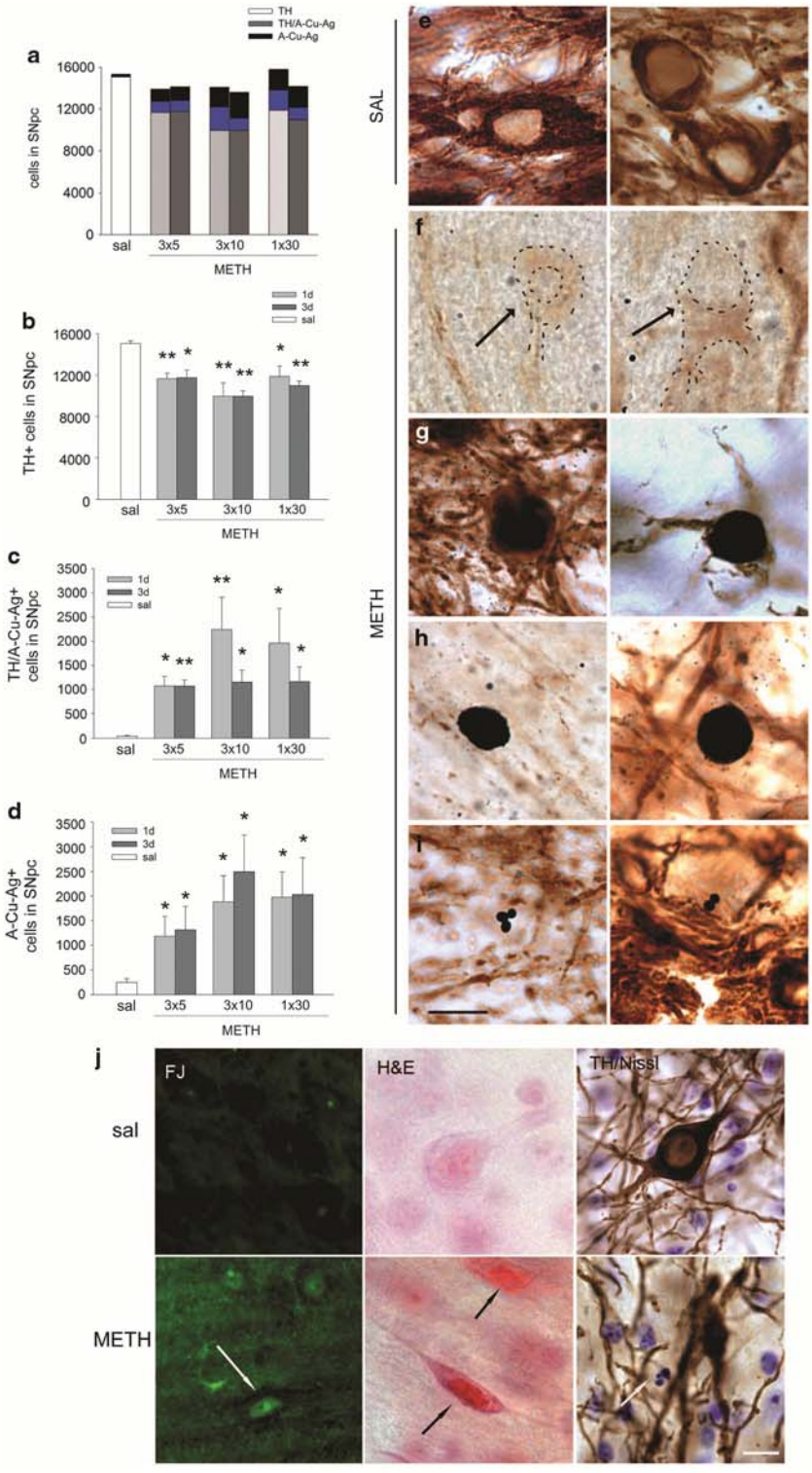
a
TH
TH/A-Cu-Ag
A-Cu-Ag
cells in SNpc
16000
12000
8000
4000
0
sal
3x5
3x10
1x30
METH
b
1d
3d
sal
TH+ cells in SNpc
c
TH/A-Cu-Ag+ cells in SNpc
3500
3000
2500
2000
1500
1000
500
d
A-Cu-Ag+ cells in SNpc
SAL
METH
e
f
g
h
i
j
FJ
H&E
TH/Nissl
sal
METH

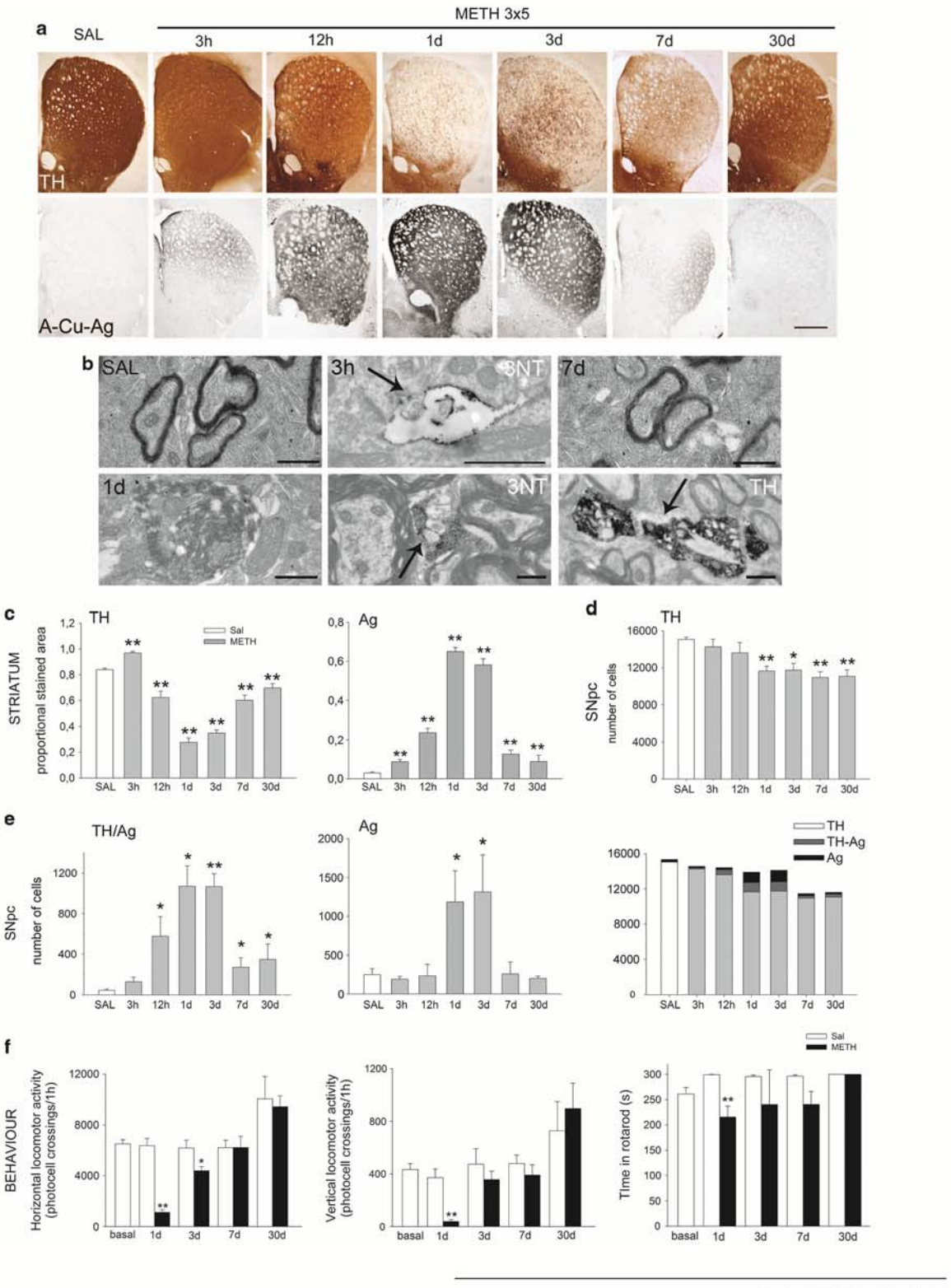
a
SAL
METH 3x5
3h
12h
1d
3d
7d
30d
TH
A-Cu-Ag
b
SAL
3h
3NT
7d
1d
3NT
TH
c
STRIATUM
proportional stained area
TH
Sal
METH
Ag
d
SNpc
number of cells
TH
e
SNpc
number of cells
TH/Ag
Ag
TH
TH-Ag
Ag
f
BEHAVIOUR
Horizontal locomotor activity (photocell crossings/1h)
Vertical locomotor activity (photocell crossings/1h)
TIme in rotarod (s)
Sal
METH
basal
1d
3d
7d
30d

Some degenerating or apoptotic cell bodies stained for A-Cu-Ag but not for TH were seen in this area (Figure 4d, h, and i). These could be dopaminergic neurons that degenerate after the loss of TH expression or non-dopaminergic degenerating neurons. The number of these TH-negative but A-Cu-Ag-positive soma was significantly greater 1 and 3 days after treatment with any of methamphetamine regimens ($p<0.05$) than saline. No significant changes in the estimate of non-dopaminergic-A-Cu-Ag-positive neurons (A-Cu-Ag) were observed at 3 days *vs* 1 day after reatment (Figure 4d).

Dopaminergic Neurons in the SNpc Degenerate by Necrosis or Apoptosis

Degeneration of neurons in the SNpc 1 day after treatment with methamphetamine (3×5) was also detected by FluoroJade staining (Figure 5). As evidenced by H&E, some degenerating neurons in this area after methamphetamine (3×5) were necrotic (eosinophilic necrotic neurons) (Fujikawa *et al*, 2010), whereas there were no eosinophilic neurons in the SNpc following saline treatment (Figure 4j). In addition, as described previously (Ares-Santos *et al*, 2012), Nissl-stained apoptotic bodies were observed in mice with methamphetamine (3×5) but not in saline animals, indicating that apoptosis mediates degeneration of some of these neurons (Figure 4j).

Time Course of Methamphetamine-Induced Loss of TH-ir Terminals in the Striatum

Three hours after methamphetamine (3×5) administration, TH-ir in the striatum was more intense ($p<0.001$) and the signal was more diffuse, appearing to extend into cortical areas, compared with the TH staining in saline-treated animals (Figure 5a and c). Silver staining was already slightly increased ($p<0.01$). At 12 h after treatment, TH-ir was decreased (by 25%, $p<0.001$), whereas silver staining was further increased compared with saline ($p<0.001$). As indicated by TH-ir, dopamine terminal loss was greatest at 1 day after treatment, with a 70% reduction compared with saline levels ($p<0.001$). Afterwards, there was a progressive recovery of dopamine terminals at 3, 7, and 30 days after treatment: striatal TH-ir levels were 58%, 28%, and 16% below saline controls, respectively ($p<0.001$). The persistence of reduced TH-ir at 30 days indicates that recovery was not complete, at this time point. Striatal A-Cu-Ag staining also peaked at 1 day after treatment and decreased over time (7 and 30 days), but was still slightly increased over saline control at 30 days ($p<0.001$) (Figure 5a amd c).

EM Confirmed Terminal Degeneration

To confirm that increases in A-Cu-Ag staining in the striatum after methamphetamine were due to fiber degeneration, evidence for neurodegeneration was obtained by EM. Striatal sections from saline- and methamphetamine (3×5)-treated animals were processed for EM (Figure 5b). Normal looking neuropil with typical dendritic and axonal striatal profiles were observed in saline-treated animals (Figure 5b, SAL). Striatal terminals looked normal 3 h after methamphetamine (3×5), although nitration of intrinsic striatal dendrites was observed (Figures 5b and 3h). At 1 day after treatment, several fibers had a characteristic degenerating morphology, similar to that reported after MPTP treatment (Cochiolo *et al*, 2000). These fibers exhibited an abnormal collection of altered membranous structures (Figure 5b, bottom row, left). Some nitrated terminals were observed at this time point (Figure 5b, bottom row, middle). In addition, vacuolated TH-ir fibers with characteristic degenerating morphology were observed 1 day after the treatment. Seven days after drug injection, the morphology of most striatal axons and synaptic terminals was similar to that seen in saline-treated animals. At this time, terminals containing densely packed small synaptic vesicles and establishing typical synaptic contacts were observed (Figure 5b).

Time Course of Methamphetamine-Induced Loss of Dopamine Neurons in the SNpc

The number of TH-ir cell bodies in the SNpc showed a tendency to decrease at 3 and 12 h (4% and 8%, respectively) after methamphetamine (3×5). A significant reduction (22%, $p<0.001$) was observed 1 day after treatment and persisted at 3, 7, and 30 days, (Figure 5d and e). Degenerating dopamine neurons were first detected by TH/Ag staining at 12 h after methamphetamine ($p<0.05$), comprising about 4% of total dopamine neurons in the SNpc (Figure 5e). The number of TH/Ag double-stained neurons peaked at 1 day and 3 days after methamphetamine, representing 7% of the total number of dopaminergic neurons. The percentage of TH/Ag neurons decreased significantly at 7 and 30 days (2%) after treatment but remained elevated

Figure 5 Time course of methamphetamine (3×5) effects: neurotoxicity in the striatum, substantia nigra pars compacta (SNpc), and motor behavior. (a) Photomicrographs of tyrosine hydroxylase- (TH) or amino-cupric-silver- (A-Cu-Ag) stained sections of the striatum of mice treated with saline (sal) or methamphetamine (3×5) 3 h, 12 h, 1 day, 3 days, 7 days, and 30 days after the treatment. Bar indicates 500 μm. (b) Ultrastrutural evidence of nitration of a striatal dendrite at 3 h after methamphetamine (3 h, upper middle) and, at 1 day after methamphetamine, nitration (lower middle), a degenerating terminal (lower left), and degenerating TH-immunoreactive (TH-ir) axon (lower right) in the striatum. Bar indicates 0.5 μm. (c) Histograms show the proportional stained area of TH and amino-cupric-silver staining in the striatum. Data represent mean ± SEM, $n=4$–6 per group. (d and e) Histograms show the number of TH- (d), TH/A-Cu-Ag- (e, left), A-Cu-Ag-positive cells (e, middle), and the accumulated mean of each (e, right) in the SNpc, counted by stereology in sections of mice treated with saline or methamphetamine (3×5), 3 h, 12 h, 1 day, 3 days, 7 days and 1 month after the treatment (mean ± SEM, $n=4$–6 per group). (f) Methamphetamine induced a decrease in horizontal locomotor activity 1 and 3 days after treatment with methamphetamine (3×5), with return to control levels at 7 days after treatment. Methamphetamine (3×5) also induced a decrease in the vertical motor activity of the animals at 1 day after treatment, returning to control levels at 3 days, and remaining stable 7 days after the treatment. (j) Methamphetamine (3×5) impaired motor coordination, as animals showed reduced latency time on an accelerating rotarod 1 day after treatment with the drug. Motor coordination returned to normal at 3 and 7 days after treatment with methamphetamine. $^{*}p<0.05$, $^{**}p<0.001$ *vs* sal. Statistical analysis was performed by Student's *t*-test.

compared with control levels ($p<0.05$) (Figure 5e). These results indicate that the degeneration wave peaks 1–3 days after methamphetamine, although a small number of dopaminergic neurons degenerate at later times (Figure 5e). By contrast, the number of A-Cu-Ag-positive, TH-ir-negative neurons in the SNpc was significantly increased 1 and 3 days after methamphetamine 3×5 ($p<0.05$), but no significant differences *vs* control animals were observed before or after these time points (see Figure 5e).

Methamphetamine Temporarily Decreases Motor Activity and Motor Coordination

Mice treated with methamphetamine (3×5) showed drastic reductions in horizontal and vertical locomotor activity 1 day after treatment, scoring an average of 1115 and 38 photocell crossings in a 60-min period, respectively, compared with saline animals (an average of 6364 horizontal and 370 vertical crossings, $p<0.001$; Figure 5f). At 3 days after treatment, vertical locomotor activity returned to normal levels (365 crossings) but horizontal locomotor activity remained reduced (4393 crossings, $p<0.05$) despite partial TH-terminal recovery. At 7 days after treatment with methamphetamine, both horizontal (6219 crossings) and vertical (391 crossings) locomotor activity had returned to normal levels. In the rotarod test of motor coordination, naive mice quickly adapted to the accelerating rod, reaching the cutoff time (300 s) in the acquisition day (Figure 5f). However, 1 day after methamphetamine mice were unable to reach the cutoff timer, and achieved an average latency time of just 215 s ($p<0.001$ *vs* saline animals). At 3 and 7 days after methamphetamine, the latency time increased to 240 s, not significantly different from saline animals. These results indicate that motor behavior is drastically impaired at 1 and 3 days after methamphetamine and then recovers, consistent with the time course of TH loss in the striatum.

DISCUSSION

We found that multiple low doses of methamphetamine produced a greater, but still dose-dependent, loss of dopaminergic terminals than a single higher dose. There was also degeneration of striatal neurons after treatment with methamphetamine, with degenerating neurons equally divided between direct pathway MSNs, indirect pathway MSNs, and other striatal neurons. We show for the first time that methamphetamine kills dopaminergic neurons in the SNpc of mice, which can be detected 1 day after the treatment. Despite the significant differences between the effects of the three regimens on the striatum, similar toxicity was observed in the SNpc following all three delivery paradigms. With the multiple low dose (3×5) paradigm, loss of dopamine terminals started as soon as 3–12 h after the last injection, peaked at 1 day and was followed by partial reinervation of the striatum, although dopamine terminal deficits persisted for more than 30 days after the last dose. EM confirmed fiber degeneration, first showing degenerating dopamine fibers and nitrated terminals 1 day after the treatment with the drug. In parallel, the loss of dopamine neurons in the SNpc started by 12 h after the last injection, peaking by 1 day. The number of TH-ir neurons did not change at 3, 7, or 30 days after drug administration, indicating long-lasting loss of TH-ir neurons. These neurotoxic changes had functional consequences: animals showed deficits in locomotor activity and motor coordination with a time course consistent with the observed dopaminergic terminal degeneration, peaking at 1–3 days after methamphetamine and returning to normal levels by 7 days after the treatment.

The A-Cu-Ag technique is highly sensitive detecting degenerating neurons soma, dendrites, axons, and synaptic terminals (de Olmos *et al*, 2009; de Olmos *et al*, 1994; Switzer 2000). Degeneration is seen as black stained objects against a pale unstained background (of normal unaffected components). Staining is thought to result from the precipitation of ionic silver around chemical reducing groups present in damaged subcellular structures, like proteins dismantled by proteolitic mechanism (Beltramino *et al*, 1993; Switzer, 2000). This technique has the advantage of selectively identifying degenerating nerve cell components while producing a high contrast image that is relatively easy to observe and can be combined with immunohistochemistry, facilitating identification of the phenotype of degenerating neurons (de Olmos *et al*, 2009). Results from this study agree with previous reports with other suppressive silver methods that indicated that methamphetamine produces destruction and loss of dopaminergic terminals in the striatum (Ricaurte *et al*, 1982, 1984). The concomitant reductions of TH-ir fibers along with the presence of A-Cu-Ag-stained terminals (Figures 1–3) reveal the selective degeneration of dopaminergic terminals in the striatum 1 day after methamphetamine. This is also evidenced by the presence of degenerating striatal terminals detected by EM.

Multiple doses of methamphetamine (3×5 or 3×10) were clearly more toxic to the dopaminergic terminals in the striatum than single administration (1×30) (Figure 1b–d). This difference could be due to the different effects of these regimens on blockade of DAT or VMAT2, resulting in cytosolic accumulation of dopamine, which have been shown to be greater and longer lasting for multiple administrations of methamphetamine than for a single injection (Fleckenstein *et al*, 1999; Metzger *et al*, 2000). In addition, the hyperthermic response was greater and had more peaks for multiple administration regimens than for single administration (Figure 1a), which may potentiate the neurotoxic effects of methamphetamine although hyperthermia is not solely responsible for methamphetamine-induced neuropathology (Albers and Sonsalla, 1995; Ares-Santos *et al*, 2012, 2013b; Granado *et al*, 2011a; Urrutia *et al*, 2013).

Consistent with previous reports, methamphetamine induced degeneration of striatal cells 1 day after treatment (Zhu *et al*, 2006a, b) and degenerating neurons were still visible 3 days later (Figure 2a and b). Surprisingly, no differences were observed in the number of degenerating striatal neurons between the (3×10) and (1×30) protocols despite the significant difference they present in neurotoxic effects on dopaminergic terminals in the striatum (Figure 1). Previous reports showed that striatal apoptosis is independent of the hyperthermic response and that multiple administration of methamphetamine (4×10 mg/kg)

was less effective in inducing apoptotic cell death assessed by TUNEL staining 24 h after treatment than single bolus administration of 1×30 mg/kg (Zhu *et al*, 2006a), in line with our results.

Notably, this is the first study to report that the degenerating neurons that appear in the striatum following methamphetamine treatment are equally distributed between direct and indirect projection pathways neurons. A third of the degenerating Ag-stained striatal neurons did not colocalize with either Tmt/D1R or GFP/D2R (Figure 2e and f). This could mean that some striatal projection neurons have lost the expression of Tmt/GFP proteins before degenerating, or that they are interneurons. As interneurons comprise a much smaller cell population in the striatum (5–10%) relative to projection neurons (90–95%) (Kawaguchi *et al*, 1995), the equal absolute numbers of degenerating cell populations (direct and indirect pathway projection neurons and putative interneurons) suggest that interneurons are selectively more vulnerable to methamphetamine toxicity. In line with this, previous work showed that projection neurons are less vulnerable to methamphetamine neurotoxicity than parvalbumin interneurons or cholinergic interneurons, although somatostatin interneurons are refractory to methamphetamine neurotoxicity (Zhu *et al*, 2006b). Alternatively, it is possible that the loss of striatal projection neurons is due to systemic rather than specific toxicity as opposed to that of the interneurons.

This is also the first study to provide direct evidence of degeneration of dopaminergic neurons in the SN (pars compacta and pars lateralis) after exposure to methamphetamine (Figure 4), confirming previous studies that reported a decrease of TH-ir neurons, (Ares-Santos *et al*, 2012; Granado *et al*, 2011a, b; Sonsalla *et al*, 1996). Although it has been proposed that axonal degeneration, rather than neuronal loss, has the dominant causative role in the clinical manifestations of Parkinson's disease (Burke and O'Malley, 2012), the permanent loss of a small fraction of the dopaminergic cells in the SNpc significantly diminishes the capacity for protective compensation following future insults. Ricaurte *et al* (1982) previously used a silver technique and found no evidence of TH-soma loss after methamphetamine. The discrepancy between our studies is likely the result of timing: they looked at 6 weeks after methamphetamine and our time-course experiment showed the biggest cell body degeneration at 1–3 days after methamphetamine. This is consistent with silver-suppressive studies with other neurotoxic agents (Switzer, 2000) that indicate that degenerating cell bodies can only be detected shortly after the injury. Several nigrostriatal degenerating axons stained for A-Cu-Ag could be followed from SNpc to the striatum via the MFB (Figure 3). However, degenerating axons and dopaminergic neurons in the SNpc after methamphetamine exposure represent a small percentage compared with the massive terminal damage observed in the striatum.

The mechanisms mediating methamphetamine-induced degeneration of dopaminergic neurons in the SNpc seem to include more than one known death pathway. We have reported previously the appearance of Nissl-stained apoptotic cell bodies in the SNpc 1 day after treatment with methamphetamine (Ares-Santos *et al*, 2012). On the other hand, we have also observed necrotic eosinophilic neurons following methamphetamine. Necrosis and apoptosis can occur either as distinct conditions, in combination, or as sequential events (Davidson *et al*, 2001). Results from *in vitro* research with dopaminergic cell culture models point to activation of the apoptotic cascade involving caspase-3 and DNA fragmentation in neurodegeneration of these cells and suggest that other factors may contribute to cell death, including ER stress, ubiquitin dysfunction, and autophagic impairment (Kanthasamy *et al*, 2011; Larsen *et al*, 2002).

Our time-course experiment with the lowest multiple-dose regimen of methamphetamine (3×5) showed that dopamine terminal and cell body loss had already started at 3–12 h and peaked at one day for the terminals and between 1 and 3 days after treatment for the cell bodies (Figure 5a–e). From this time onwards, the number of silver-stained cell bodies decreased, but remained significant 7 and 30 days after treatment compared with saline-treated animals. As the A-Cu-Ag staining only labels cells actively undergoing degeneration, these later appearing silver-stained cells may be damaged neurons that initially survive methamphetamine, but eventually degenerate and die (Figure 5e). In line with this, there was no recovery of TH-ir neuron numbers in the SNpc even 30 days after the treatment, confirming the idea that, unlike the partial recovery of terminals in the striatum, the loss of striatal neurons is permanent. It is likely that the major source of TH terminal regrowth is the spared dopaminergic neurons in the SNpc. Neurodegeneration in the striatum and SNpc were accompanied by strong glial activation, in agreement with previous results (Ares-Santos *et al*, 2012; O'Callaghan and Miller, 1994; LaVoie *et al*, 2004).

Although non-selective systemic methamphetamine toxicity might contribute to the selective loss of dopamine (Halpin and Yamamoto, 2012), the motor impairment we observed is due to the loss of dopamine terminals in the striatum as has been shown in drug abusers (Volkow *et al*, 2001a,b; McCann *et al*, 1998). Thus, the loss of dopamine markers after methamphetamine neurotoxicity may be the cause of the motor impairment we observed: a drastic, but transient, decrease in horizontal and vertical movement and motor coordination. The timing of these changes paralleled the degeneration and partial recovery of dopamine terminals, and complete recovery of these motor indicators suggested they were not related to the permanent loss of nigral neurons. Our results with methamphetamine further confirm the requirement for certain dopamine levels in the striatum for motor activity and motor coordination (Rodrigues *et al*, 2007). Once dopamine terminals have recovered to at least 78%, they produce sufficient dopamine for the neurotoxicity to be subsymptomatic. The finding that the persistent 25% loss of nigral neurons produces no motor symptoms mirrors previous findings in animal models of PD, in which motor impairment appears only after an 80% loss of striatal dopamine and 30–60% loss of nigral dopamine neurons (Burke and O'Malley, 2012; Fearnley and Lees, 1991), indicating that methamphetamine could destroy many dopamine neurons with no PD symptomatology (Davidson *et al*, 2001).

The dying-back axonopathy hypothesis in Parkinson's disease suggest that degeneration begins in the distal axon

and proceeds toward the cell body (Burke and O'Malley, 2012). In contrast, our finding that degenerative processes in the terminal and neuronal body occurred simultaneously suggest a direct effect of methamphetamine administration on SNpc neurons and terminals, as opposed to retrograde degeneration. A large body of evidence indicates that the molecular mechanisms of terminal degeneration are separate and distinct from those of neuron somatic degeneration (Burke and O'Malley, 2012; Coleman, 2005; Raff *et al*, 2002; Ries *et al*, 2008). This idea is further supported by the fact that genetic inactivation of Nrf2 potentiates dopamine terminal loss without affecting survival of dopamine neurons in the SNpc (Granado *et al*, 2011b). In line with this, we observe no significant differences between the effects of single high dose and multiple lower doses on methamphetamine-induced dopaminergic neuronal loss, despite the clear dose dependence of dopamine terminal loss in the striatum. Further investigation is required to characterize the process leading to neurodegeneration and to define the distinct mechanisms that may mediate terminal and somatic neurodegeneration.

Our results are consistent with the recent report that methamphetamine abusers have higher risk for future development of Parkinson's disease (Callaghan *et al*, 2012) and with other reports of neurotoxic effects of methamphetamine in human abusers that indicate poor motor performance associated with DAT loss in the caudate nucleus and putamen (Volkow *et al*, 2001a,b; McCann *et al*, 1998). Similar partial recovery of dopaminergic markers in the striatum has been reported in human methamphetamine abusers after periods of abstinence (Volkow *et al*, 2001a). Persistent dopamine terminal loss has been also documented after 11 months (Volkow *et al*, 2001a) or 3 years of abstinence (McCann *et al*, 1998) in line with the loss we see at 30 days. However, to date, there are no published reports of anatomical evidence of dopamine neuronal destruction in SNpc of human methamphetamine abusers. Some evidence of neurodegenerative changes exists: for example, a specific decrease in pigmented neurons in SN of human abusers, similar to that seen in PD patients (Büttner and Weis, 2006; Büttner, 2011). Moreover, the morphology of the SN (as measured by transcranial sonography) in individuals with a history of stimulant abuse, including methamphetamine, is abnormal, and is associated with reduced dopamine uptake in the striatum and increased risk for development of Parkinson's disease (Todd *et al*, 2013). Our results indicating very low, but significant, rates, around 0.17%, considering 1.72×10^6 total neuronal population (Rosen and Williams, 2001), of striatal cell death after methamphetamine are also consistent with the small decrease (5%) in the neuronal marker *N*-acetylaspartate described in the striatum of abstinent methamphetamine abusers (Ernst *et al*, 2000).

In summary, the data presented here provide anatomical evidence of dopamine cell body degeneration and a persistent loss of dopaminergic cell soma after exposure to methamphetamine in mice, making it clear that some neurotoxic effects of this drug are long-lasting despite partial regeneration of dopaminergic terminals in the striatum. The lower neuronal content and/or the priming and damage of the spared neurons represent a likely vulnerability factor for further neurotoxic insults (like other neurotoxins, age, or genetic risk factors for PD). As it is true for other susceptibility factors for PD, the methamphetamine-increased susceptibility does not mean that all methamphetamine users will develop PD. The low disease concordance in relatives and the low penetrance of some genetic mutations described as risk factors for PD suggests that a combination of insults or interaction between multiple predisposing factors, 'multiple hits', is required for developing PD (Sulzer, 2007). Our data indicate that methamphetamine abuse is highly likely to represent one such hit, predisposing abusers to PD.

FUNDING AND DISCLOSURE

The authors declare that, except for income received from my primary employer, no financial support or compensation has been received from any individual or corporate entity over the past 3 years for research or professional service and there are no personal financial holdings that could be perceived as constituting a potential conflict of interest.

ACKNOWLEDGEMENTS

This work was supported by grants from the Spanish Ministry of Sanidad, Servicios Sociales e Igualdad, PNSD No. 2012/071, Spanish Ministry of Economía y Competitividad Grant No. BFU2010-20664, CIBERNED No. CB06/05/0055 and Comunidad de Madrid ref S2010/BMD-2336 to RM and SAF2010-15173 to RMM. NG received a Juan de la Cierva postdoctoral fellowship and a research contract NEUROSTEM-CM S2010/BMD-2336; SAS a JAE predoctoral fellowship and a JAE short-stay fellowship in 2012 to learn the de Olmos technique at the Laboratory of Experimental Neuroanatomy and Histology of the Instituto de Investigación Médica Mercedes y Martín Ferreyra. We thank Dr Soledad de Olmos for her teaching of de Olmos technique, and Mr Martin Ian Maher and Andrea Pozo-Rodrigálvarez for their help with electron microscopy, Dr Eduardo Martín for his help with H&E staining and Mrs Emilia Rubio, Mr Marco de Mesa, Mr Florian Giuglaris, Ms Lorena Orgaz, Ms Ana Carmena, Ms María Azazu, and Mr Jose María Caramés for their excellent technical assistance.

REFERENCES

Albers DS, Sonsalla PK (1995). Methamphetamine-induced hyperthermia and dopaminergic neurotoxicity in mice: pharmacological profile of protective and nonprotective agents. *J Pharmacol Exp Ther* **275**: 1104–1114.

Ares-Santos S, Granado N, Moratalla R (2014). Neurotoxicity of methamphetamine. In: Kostrzewa RM (ed) *Handbook of Neurotoxicity*. Springer: New York, NY, USA, ISBN: 978-1-4614-7458-6 (in press).

Ares-Santos S, Granado N, Moratalla R (2013a). Neurobiology of methamphetamine. In: Miller PM (ed) *Biological Research on Addiction: Comprehensive Addictive Behaviors and Disorders* Chapter 57. (Elsevier, Academic Press: San Diego, CA, USA, pp 579–591, ISBN: 9780123983350).

Ares-Santos S, Granado N, Moratalla R (2013b). Role of dopamine receptors in the neurotoxicity of methamphetamine. *J Intern Med* **273**: 437–453 (review).

Ares-Santos S, Granado N, Oliva I, O'Shea E, Martin ED, Colado MI *et al* (2012). Dopamine D(1) receptor deletion strongly reduces neurotoxic effects of methamphetamine. *Neurobiol Dis* **45**: 810–820.

Baquet ZC, Williams D, Brody J, Smeyne RJ (2009). A comparison of model-based (2D) and design-based (3D) stereological methods for estimating cell number in the substantia nigra pars compacta (SNpc) of the C57BL/6J mouse. *Neuroscience* **161**: 1082–1090.

Beltramino CA, de Olmos JS, Gallyas F, Heimer L, Záborszky L (1993). Silver staining as a tool for neurotoxic assessment. *NIDA Res Monogr* **136**: 101–126 discussion 126–132 (review).

Bowyer JF, Thomas M, Schmued LC, Ali SF (2008). Brain region-specific neurodegenerative profiles showing the relative importance of amphetamine dose, hyperthermia, seizures, and the blood–brain barrier. *Ann N Y Acad Sci* **1139**: 127–139.

Burke RE, O'Malley K (2012). Axon degeneration in Parkinson's disease. *Exp Neurol* **246**: 72–83.

Büttner A, Weis S (2006). Neuropathological alterations in drug abusers: the involvement of neurons, glial, and vascular systems. *Forensic Sci Med Pathol* **2**: 115–126.

Büttner A (2011). The neuropathology of drug abuse. *Neuropathol Appl Neurobiol* **37**: 118–134 (review).

Callaghan RC, Cunningham JK, Sykes J, Kish SJ (2012). Increased risk of Parkinson's disease in individuals hospitalized with conditions related to the use of methamphetamine or other amphetamine-type drugs. *Drug Alcohol Depend* **120**: 35–40.

Castro-Blanco S, Encinas JM, Serrano J, Alonso D, Gómez MB, Sánchez J *et al* (2003). Expression of nitrergic system and protein nitration in adult rat brains submitted to acute hypobaric hypoxia. *Nitric Oxide* **8**: 182–201.

Cochiolo JA, Ehsanian R, Bruck DK (2000). Acute ultrastructural effects of MPTP on the nigrostriatal pathway of the C57BL/6 adult mouse: evidence of compensatory plasticity in nigrostriatal neurons. *J Neurosci Res* **59**: 126–135.

Coleman M (2005). Axon degeneration mechanisms: commonality amid diversity. *Nat Rev Neurosci* **6**: 889–898 (review).

Darmopil S, Martín AB, De Diego IR, Ares S, Moratalla R (2009). Genetic inactivation of dopamine D1 but not D2 receptors inhibits L-DOPA-induced dyskinesia and histone activation. *Biol Psychiatry* **66**: 603–613.

Darmopil S, Muñetón-Gómez VC, de Ceballos ML, Bernson M, Moratalla R (2008). Tyrosine hydroxylase cells appearing in the mouse striatum after dopamine denervation are likely to be projection neurones regulated by L-DOPA. *Eur J Neurosci* **27**: 580–592.

Davidson C, Gow AJ, Lee TH, Ellinwood EH (2001). Methamphetamine neurotoxicity: necrotic and apoptotic mechanisms and relevance to human abuse and treatment. *Brain Res Brain Res Rev* **36**: 1–22 (review).

de Olmos JS, Beltramino CA, de Olmos de Lorenzo S (1994). Use of an amino-cupric-silver technique for the detection of early and semiacute neuronal degeneration caused by neurotoxicants, hypoxia, and physical trauma. *Neurotoxicol Teratol* **16**: 545–561.

de Olmos JS, Ebbesson SOE, Heimer L (1981). Silver methods for the impregnation of degenerating axoplasm. In: Heimer L, RoBards MJ (ed). *Neuroanatomical Tract-Tracing Methods*. Plenum Press: New York, NY, USA, pp 117–170.

de Olmos S, Bender C, De Olmos JS, Lorenzo A (2009). Neurodegeneration and prolonged immediate early gene expression throughout cortical areas of the rat brain following acute administration of dizocilpine. *Neuroscience* **164**: 1347–1359.

Ernst T, Chang L, Leonido-Yee M, Speck O (2000). Evidence for long-term neurotoxicity associated with methamphetamine abuse: a ^{1}H MRS study. *Neurology* **54**: 1344–1349.

Espadas I, Darmopil S, Vergaño-Vera E, Ortiz O, Oliva I, Vicario-Abejón C *et al* (2012). L-DOPA-induced increase in TH-immunoreactive striatal neurons in parkinsonian mice: insights into regulation and function. *Neurobiol Dis* **48**: 271–281.

Fearnley JM, Lees AJ (1991). Ageing and Parkinson's disease: substantia nigra regional selectivity. *Brain* **114**: 2283–2301.

Fleckenstein AE, Haughey HM, Metzger RR, Kokoshka JM, Riddle EL, Hanson JE *et al* (1999). Differential effects of psychostimulants and related agents on dopaminergic and serotonergic transporter function. *Eur J Pharmacol* **382**: 45–49.

Fujikawa DG, Zhao S, Ke X, Shinmei SS, Allen SG (2010). Mild as well as severe insults produce necrotic, not apoptotic, cells: evidence from 60-min seizures. *Neurosci Lett* **469**: 333–337.

Granado N, Ares-Santos S, Moratalla R (2013). Methamphetamine and Parkinson's disease. *Parkinsons Dis* **2013**: 308052.

Granado N, Ares-Santos S, O'Shea E, Vicario-Abejón C, Colado MI, Moratalla R (2010). Selective vulnerability in striosomes and in the nigrostriatal dopaminergic pathway after methamphetamine administration: early loss of TH in striosomes after methamphetamine. *Neurotoxicol Res* **18**: 48–58.

Granado N, Ares-Santos S, Oliva I, O'Shea E, Martin ED, Colado MI *et al* (2011a). Dopamine D2-receptor knockout mice are protected against dopaminergic neurotoxicity induced by methamphetamine or MDMA. *Neurobiol Dis* **42**: 391–403.

Granado N, Escobedo I, O'Shea E, Colado I, Moratalla R (2008a). Early loss of dopaminergic terminals in striosomes after MDMA administration to mice. *Synapse* **62**: 80–84.

Granado N, Lastres-Becker I, Ares-Santos S, Oliva I, Martin E, Cuadrado A *et al* (2011b). Nrf2 deficiency potentiates methamphetamine-induced dopaminergic axonal damage and gliosis in the striatum. *Glia* **59**: 1850–1863.

Granado N, Ortiz O, Suárez LM, Martín ED, Ceña V, Solís JM *et al* (2008c). D1 but not D5 dopamine receptors are critical for LTP, spatial learning, and LTP-Induced arc and zif268 expression in the hippocampus. *Cereb Cortex* **18**: 1–12.

Granado N, O'Shea E, Bove J, Vila M, Colado MI, Moratalla R (2008b). Persistent MDMA-induced dopaminergic neurotoxicity in the striatum and substantia nigra of mice. *J Neurochem* **107**: 1102–1112.

Halpin LE, Yamamoto BK (2012). Peripheral ammonia as a mediator of methamphetamine neurotoxicity. *J Neurosci* **32**: 13155–13163.

Hirata H, Cadet JL (1997). P53-knockout mice are protected against the long-term effects of methamphetamine on dopaminergic terminals and cell bodies. *J Neurochem* **69**: 780–790.

Hotchkiss AJ, Gibb JW (1980). Long-term effects of multiple doses of methamphetamine on tryptophan hydroxylase and tyrosine hydroxylase activity in rat brain. *J Pharmacol Exp Ther* **214**: 257–262.

Kanthasamy K, Gordon R, Jin H, Anantharam V, Ali S, Kanthasamy AG *et al* (2011). Neuroprotective effect of resveratrol against methamphetamine-induced dopaminergic apoptotic cell death in a cell culture model of neurotoxicity. *Curr Neuropharmacol* **9**: 49–53.

Kawaguchi Y, Wilson CJ, Augood SJ, Emson PC (1995). Striatal interneurones: chemical, physiological and morphological characterization. *Trends Neurosci* **18**: 527–535 (Review. Erratum in: *Trends Neurosci* 1996;**19**:143).

Krasnova IN, Cadet JL (2009). Methamphetamine toxicity and messengers of death. *Brain Res Rev* **60**: 379–407. Review.

Larsen KE, Fon EA, Hastings TG, Edwards RH, Sulzer D (2002). Methamphetamine-induced degeneration of dopaminergic neurons involves autophagy and upregulation of dopamine synthesis. *J Neurosci* **22**: 8951–8960.

LaVoie MJ, Card JP, Hastings TG (2004). Microglial activation precedes dopamine terminal pathology in methamphetamine-induced neurotoxicity. *Exp Neurol* **187**: 47–57.

McCann UD, Wong DF, Yokoi F, Villemagne V, Dannals RF, Ricaurte GA (1998). Reduced striatal dopamine transporter density in abstinent methamphetamine and methcathinone users: evidence from positron emission tomography studies with [^{11}C]WIN-35,428. *J Neurosci* **18**: 8417–8422.

Metzger RR, Haughey HM, Wilkins DG, Gibb JW, Hanson GR, Fleckenstein AE (2000). Methamphetamine-induced rapid decrease in dopamine transporter function: role of dopamine and hyperthermia. *J Pharmacol Exp Ther* **295**: 1077–1085.

Ortiz O, Delgado-García JM, Espadas I, Bahí A, Trullas R, Dreyer JL *et al* (2010). Associative learning and CA3-CA1 synaptic plasticity are impaired in D1R null, Drd1a−/− mice and in hippocampal siRNA silenced Drd1a mice. *J Neurosci* **30**: 12288–12300.

O'Callaghan JP, Miller DB (1994). Neurotoxicity profiles of substituted amphetamines in the C57BL/6J mouse. *J Pharmacol Exp Ther* **270**: 741–751.

Raff MC, Whitmore AV, Finn JT (2002). Axonal self-destruction and neurodegeneration. *Science* **296**: 868–871.

Ricaurte GA, Guillery RW, Seiden LS, Schuster CR, Moore RY (1982). Dopamine nerve terminal degeneration produced by high doses of methylamphetamine in the rat brain. *Brain Res* **235**: 93–103.

Ricaurte GA, Seiden LS, Schuster CR (1984). Further evidence that amphetamines produce long-lasting dopamine neurochemical deficits by destroying dopamine nerve fibers. *Brain Res* **303**: 359–364.

Ries V, Silva RM, Oo TF, Cheng HC, Rzhetskaya M, Kholodilov N *et al* (2008). JNK2 and JNK3 combined are essential for apoptosis in dopamine neurons of the substantia nigra, but are not required for axon degeneration. *J Neurochem* **107**: 1578–1588.

Rivera A, Cuéllar B, Girón FJ, Grandy DK, de la Calle A, Moratalla R (2002). Dopamine D4 receptors are heterogeneously distributed in the striosomes/matrix compartments of the striatum. *J Neurochem* **80**: 219–229.

Rodrigues TB, Granado N, Ortiz O, Cerdán S, Moratalla R (2007). Metabolic interactions between glutamatergic and dopaminergic neurotransmitter systems are mediated through D(1) dopamine receptors. *J Neurosci Res* **85**: 3284–3293.

Rosen GD, Williams RW (2001). Complex trait analysis of the mouse striatum: independent QTLs modulate volume and neuron number. *BMC Neurosci* **2**: 5.

Seiden LS, Fischman MW, Schuster CR (1976). Long-term methamphetamine induced changes in brain catecholamines in tolerant rhesus monkeys. *Drug Alcohol Depend* **1**: 215–219.

Sonsalla PK, Jochnowitz ND, Zeevalk GD, Oostveen JA, Hall ED (1996). Treatment of mice with methamphetamine produces cell loss in the substantia nigra. *Brain Res* **738**: 172–175.

Sulzer D (2007). Multiple hit hypotheses for dopamine neuron loss in Parkinson's disease. *Trends Neurosci* **30**: 244–250.

Suárez LM, Solís O, Caramés JM, Taravini IR, Solís JM, Murer MG *et al* (2013). L-DOPA treatment selectively restores spine density in dopamine receptor D2-expressing projection neurons in dyskinetic mice. *Biol Psychiatry* (pii: S0006-3223(13)00416-2) doi:10.1016/j.biopsych.2013.05.006.

Switzer RC III (2000). Application of silver degeneration stains for neurotoxicity testing. *Toxicol Pathol* **28**: 70–83 (review).

Todd G, Noyes C, Flavel SC, Della Vedova CB, Spyropoulos P, Chatterton B *et al* (2013). Illicit stimulant use is associated with abnormal substantia nigra morphology in humans. *PLoS One* **8**: e56438.

UNODC (2013): *World Drug Report 2013* (United Nations publication, Sales No. E.13.XI.6)Available at: http://www.unodc.org/unodc/secured/wdr/wdr2013/World_Drug_Report_2013.pdf.

Urrutia A, Rubio-Araiz A, Gutierrez-Lopez MD, ElAli A, Hermann DM, O'Shea E *et al* (2013). A study on the effect of JNK inhibitor, SP600125, on the disruption of blood–brain barrier induced by methamphetamine. *Neurobiol Dis* **50**: 49–58.

Volkow ND, Chang L, Wang GJ, Fowler JS, Franceschi D, Sedler M *et al* (2001a). Loss of dopamine transporters in methamphetamine abusers recovers with protracted abstinence. *J Neurosci* **21**: 9414–9418.

Volkow ND, Chang L, Wang GJ, Fowler JS, Leonido-Yee M, Franceschi D *et al* (2001b). Association of dopamine transporter reduction with psychomotor impairment in methamphetamineabusers. *Am J Psychiatry* **158**: 377–382.

Wagner GC, Ricaurte GA, Seiden LS, Schuster CR, Miller RJ, Westley J (1980). Long-lasting depletions of striatal dopamine and loss of dopamine uptake sites following repeated administration of methamphetamine. *Brain Res* **181**: 151–160.

Wilson JM, Kalasinsky KS, Levey AI, Bergeron C, Reiber G, Anthony RM *et al* (1996). Striatal dopamine nerve terminal markers in human, chronic methamphetamine users. *Nat Med* **2**: 699–703.

Zhu JP, Xu W, Angulo JA (2006b). Methamphetamine-induced cell death: selective vulnerability in neuronal subpopulations of the striatum in mice. *Neuroscience* **140**: 607–622.

Zhu JP, Xu W, Angulo N, Angulo JA (2006a). Methamphetamine-induced striatal apoptosis in the mouse brain: comparison of a binge to an acute bolus drug administration. *Neurotoxicology* **7**: 131–136.

2. Dopamine D1 receptor deletion strongly reduces neurotoxic effects of methamphetamine.

Ares-Santos S*, Granado N*, Oliva I, O'Shea E, Martin ED, Colado MI, Moratalla R (2012). *Neurobiol Dis.* 45:810-20. doi: 10.1016/j.nbd.2011.11.005.

* equal contribution

Neurobiology of Disease 45 (2012) 810–820

Contents lists available at SciVerse ScienceDirect

Neurobiology of Disease

journal homepage: www.elsevier.com/locate/ynbdi

Dopamine D_1 receptor deletion strongly reduces neurotoxic effects of methamphetamine

S. Ares-Santos [a,b,1], N. Granado [a,c,1], I. Oliva [d], E. O'Shea [c], E.D. Martin [d], M.I. Colado [c], R. Moratalla [a,b,*]

[a] Instituto Cajal, Consejo Superior de Investigaciones Científicas, CSIC, 28002, Madrid, Spain
[b] CIBERNED, Instituto de Salud Carlos III, Madrid, Spain
[c] Departamento de Farmacología, Facultad de Medicina, Universidad Complutense de Madrid, 28040 Madrid, Spain
[d] Laboratorio de Neurofisiología y Plasticidad Sináptica, Instituto de Investigación en Discapacidades Neurológicas (IDINE), Universidad de Castilla-La Mancha, Albacete, Spain

ARTICLE INFO

Article history:
Received 5 September 2011
Revised 31 October 2011
Accepted 7 November 2011
Available online 13 November 2011

Keywords:
Dopamine toxicity
TH
DAT
Glia
Amphetamine derivatives
Striatum
Substantia nigra
Drug-addiction
Parkinson's disease
Dopamine overflow

ABSTRACT

Methamphetamine (METH) is a potent, highly addictive psychostimulant consumed worldwide. In humans and experimental animals, repeated exposure to this drug induces persistent neurodegenerative changes. Damage occurs primarily to dopaminergic neurons, accompanied by gliosis. The toxic effects of METH involve excessive dopamine (DA) release, thus DA receptors are highly likely to play a role in this process. To define the role of D_1 receptors in the neurotoxic effects of METH we used D_1 receptor knock-out mice ($D_1R^{-/-}$) and their WT littermates. Inactivation of D_1R prevented METH-induced dopamine fibre loss and hyperthermia, and increases in gliosis and pro-inflammatory molecules such as iNOS in the striatum. In addition, D_1R inactivation prevented METH-induced loss of dopaminergic neurons in the substantia nigra. To explore the relationship between hyperthermia and neurotoxicity, METH was given at high ambient temperature (29 °C). In this condition, $D_1R^{-/-}$ mice developed hyperthermia following drug delivery and the neuroprotection provided by D_1R inactivation at 23 °C was no longer observed. However, reserpine, which empties vesicular dopamine stores, blocked hyperthermia and strongly potentiated dopamine toxicity in $D_1R^{-/-}$ mice, suggesting that the protection afforded by D_1R inactivation is due to both hypothermia and higher stored vesicular dopamine. Moreover, electrical stimulation evoked higher DA overflow in $D_1R^{-/-}$ mice as demonstrated by fast scan cyclic voltammetry despite their lower basal DA content, suggesting higher vesicular DA content in $D_1R^{-/-}$ than in WT mice. Altogether, these results indicate that the D_1R plays a significant role in METH-induced neurotoxicity by mediating drug-induced hyperthermia and increasing the releasable cytosolic DA pool.

Introduction

Methamphetamine (METH), a synthetic derivative of amphetamine, is a psychostimulant with high addictive potential used by between 13.7 and 52.9 million people world-wide (UNODC, World Drug Report, 2010). METH is a known neurotoxin, causing damage primarily to the dopaminergic system in all species studied: monkeys (Seiden et al., 1976), rodents (Granado et al., 2010, 2011a,b; Krasnova et al., 2011) and humans (McCann et al., 1998; Volkow et al., 2001). In mice, repeated exposure to METH causes persistent neurotoxicity to dopaminergic terminals and neurons, evidenced by reduced tyrosine hydroxylase (TH) (Bowyer et al., 2008; Deng et al., 1999; O'Callaghan and Miller, 1994; Xu et al., 2005; Zhu et al., 2005) and dopamine transporter (DAT) levels (Achat-Mendes et al., 2005; Deng et al., 1999; Fumagalli et al., 1999) in the striatum. In addition, this drug induces neuronal death in the striatum, which occurs by a process resembling neuronal apoptosis (Cadet and Krasnova, 2009; Cadet et al., 2005, 2007).

METH also causes cell body loss in the substantia nigra (Granado et al., 2011a,b; Sonsalla et al., 1996), affecting the same nigrostriatal dopaminergic neurons that undergo selective degeneration in Parkinson's disease (Granado et al., 2010). We have recently shown that METH selectively damages the nigrostriatal pathway, sparing the mesolimbic dopaminergic pathway, and that the striosomes are more sensitive than the striatal matrix, as indicated by greater TH/DAT-immunoreactivity loss (Granado et al., 2010). METH also causes reactive astrocytosis and microgliosis (Cadet and Krasnova, 2009; Fantegrossi et al., 2008; O'Callaghan and Miller, 1994; Thomas et al., 2004, 2008a), providing additional evidence for neuronal injury.

Although the exact molecular mechanisms of METH-induced dopaminergic neurotoxicity are not established, dopamine itself appears to play a significant role (Albers and Sonsalla, 1995; Thomas et al., 2008b). Specifically, it has been suggested that newly synthesized DA in the cytoplasmic pool (Thomas et al., 2008b) can be metabolized via auto-oxidation to produce DA quinones, superoxide anions and hydrogen oxygen species, with subsequent generation of oxidative stress, mitochondrial dysfunction, and damage within dopaminergic

* Corresponding author at: Instituto Cajal, CSIC, Avd. Dr. Arce 37, 28002, Madrid, Spain. Fax: +34 91 585 4754.
E-mail address: moratalla@cajal.csic.es (R. Moratalla).
[1] Contributed equally in this work.
Available online on ScienceDirect (www.sciencedirect.com).

0969-9961/$ – see front matter © 2011 Published by Elsevier Inc.
doi:10.1016/j.nbd.2011.11.005

terminals (Albers and Sonsalla, 1995; Cadet and Krasnova, 2009; LaVoie and Hastings, 1999). Alternatively, neurotoxicity may result from the increase in extracellular DA induced by METH. Excessive release of DA following METH administration has been shown to activate stress pathways in the ER (endoplasmic reticulum) in a D_1R-dependent manner (Jayanthi et al., 2009).

Pharmacological studies with dopamine receptor antagonists also implicate dopamine receptors in the neurotoxicity induced by METH. We recently demonstrated that genetic inactivation of dopamine D_2R reduced the damage to nigrostriatal terminals and cell bodies induced by METH (Granado et al., 2011a). However, the protective effect provided by inactivation of D_2R is incomplete, suggesting that D_1R may be also involved since SCH23390, a D_1/D_5R antagonist, can also prevent neurotoxicity induced by METH (Angulo et al., 2004; Broening et al., 2005; Bronstein and Hong, 1995; Metzger et al., 2000; Sonsalla et al., 1986; Xu et al., 2005).

To determine the role of D_1R in neurotoxicity induced by METH, we examined the effect of this drug on loss of dopaminergic fibres and nigrostriatal dopamine neurons in D_1R knockout mice ($D_1R^{-/-}$), revealing a protective effect of D_1R inactivation. D_1R inactivation also blocked METH-induced hyperthermia, a hallmark of the response to amphetamine derivatives. To further explore the role of the D_1R and the relationship between hyperthermia and neuronal damage, we compared the effects of this drug given at normal (23 °C) or elevated (29 °C) ambient temperature by examining dopaminergic parameters and the glial response in the striatum and substantia nigra in D_1R knock-out animals. In addition, we did fast scan cyclic voltammetry (FSCV) and pretreatment with αMPT or reserpine to study how inactivation of D_1R might protect against neurotoxicity induced by this drug.

Methods

Animals and treatment

Experiments were carried out in male and female dopamine D_1 receptor knockout ($D_1R^{-/-}$) mice generated by homologous recombination as described previously (Granado et al., 2008c; Moratalla et al., 1996; Xu et al., 1994) and in their wild type (WT) littermates. Mice used in this study were derived from mating heterozygous mice. We used adult males and females initially weighing 20–25 g whose genotype was determined by PCR analysis. Mice were housed in groups of 4–6 per cage, in conditions of constant room temperature (21–22 °C) and a 12 h light/dark cycle (lights on at 7:00 h) and given free access to food and water. Animals were treated in accordance with European Community guidelines (2003/65/CE), and all experimental procedures were approved by the Bioethics Committee of the Instituto Cajal.

Mice received three injections of either (+)-METH (5 mg/kg i.p.) or saline (control) at 3 h intervals, a neurotoxic regimen previously shown to produce marked depletion of mouse striatal DA. METH was dissolved in 0.9% w/v NaCl (saline) and injected in a volume of 10 ml/kg. METH hydrochloride was obtained from Sigma-Aldrich (Madrid, Spain). Doses are quoted in terms of the base. Reserpine (3 mg/kg, i.p. Sigma-Aldrich, Madrid, Spain) was dissolved in 0.1% acetic acid and administered 18 h before METH (3 injections of 3 mg/kg i.p). This lower dose of METH was used in order to better see the potentiation of METH toxicity induced by reserpine. Animals in this experiment were sacrificed 5 days after treatment with METH or saline.

For the elevated ambient temperature experiment, $D_1R^{-/-}$ mice receiving METH were maintained at a room temperature of 29 ± 2 °C for 2 h prior to treatment, during the injection paradigm, and for 1 h following the last injection. The α-methyl-p-tyrosine (αMPT) was obtained from Sigma-Aldrich (Madrid, Spain). αMPT was dissolved in 0.9% w/v NaCl and administered i.p. (100 mg/kg × 4) at 24, 16, 2 and 1 h before treatment with METH (5 mg/kg, i.p. 3 injections at 3 hour intervals). Animals were sacrificed 1 or 7 days after drugs administration.

Measurement of rectal temperature

Rectal temperature was measured using a digital readout thermocouple (BAT-12 thermometer, Physitemp Instruments, Clifton, NJ, USA) with a resolution of 0.1 °C and accuracy of +/−0.1 °C attached to a RET-3 Rodent Sensor. The sensor was inserted 2 cm into the mouse rectum, while the mouse was lightly restrained by holding in the hand. A steady readout was obtained within 10 s of probe insertion. Temperature readings were taken every 30 min immediately before and after each METH injection and then 1, 2 and 3 h after drug administration.

Measurement of monoamines and their metabolites in the striatum

One or seven days after the treatment, mice were killed by cervical dislocation and decapitation (n = 4–6 per group). The brains were rapidly removed and the striatum dissected out on ice. Dopamine, serotonin, and their metabolites 3,4-dihydroxyphenylacetic acid (DOPAC), homovanillic acid (HVA) and 5-hydroxyindolacetic acid (5-HIAA) were measured by high-performance liquid chromatography and electrochemical detection as described previously (Granado et al., 2010; Gutierrez-Lopez et al., 2010). The mobile phase consisted of KH_2PO_4 (0.05 M), octanesulfonic acid (0.4 mM), EDTA (0.1 mM), and methanol (16%) and was adjusted to pH 3.7 with phosphoric acid, filtered, and degassed. The flow rate was 1 ml/min. The high-performance liquid chromatography system consisted of a pump (Waters 510) linked to an automatic sample injector (Loop 200 μl, Waters 717 plus Autosampler) and a stainless steel reversed-phase column (Spherisorb ODS2, 5 μm, 150 × 4.6 mm^2; Waters, Milford, MA, USA) with a precolumn and a coulometric detector (Coulochem II; Esa, Chelmsford, M, USA). The working electrode potential was set at 400 mV with a gain of 2 μA. The current produced was monitored by means of integration software (Clarity Software, DataApex, Prague, Czech Republic).

Immunohistochemistry

One or seven days after the treatment, animals (n = 3–6 per group) were deeply anaesthetized with sodium pentobarbital (50 mg/kg, i.p.) and then transcardially perfused with 4% paraformaldehyde dissolved in PB (Buffer phosphate, pH 7.4). After perfusion, brains were removed and immersed overnight in the same fixative solution. Coronal brain sections (30 μm) were obtained on a slicing vibratome (Leica, Madrid, Spain) and kept in PB solution at 4 °C until use. Immunostaining was carried out on free-floating sections with standard avidin–biotin immunocytochemical protocols (Darmopil et al., 2008, 2009; Ortiz et al., 2010; Pavon et al., 2006). Endogenous peroxidase activity was removed by incubation in 3% H_2O_2 for 10 min. Sections were preblocked for 1 h with normal goat serum (NGS) (Vector Laboratories, Burlingame, CA, USA). Sections were incubated overnight with specific primary antibodies (Ab-I): rabbit tyrosine hydroxylase antiserum (TH, used at 1:1000 Chemicon International, Temecula, CA, USA); rat monoclonal antibody against dopamine transporter (DAT, used at 1:1000, Chemicon International); rabbit anti-glial fibrillary acidic protein antibody (GFAP, used at 1:1000, DakoCytomation, Denmark); rat monoclonal anti-Mac1 or CD11b (1:500, Serotec, Kinlington, Oxford, UK); and a polyclonal antiserum against iNOS (1:4000, gift from Dr. R Martínez, Instituto Cajal, CSIC, Madrid, Spain). All primary antibodies were prepared in Buffer phosphate with triton (PBST) solutions containing NGS. After careful washing, sections were incubated with the appropriate secondary biotinylated antiserum (Vector) at room temperature and developed using diaminobenzidine (DAB). The reaction was monitored every 5 min using an optical microscope (Leica). After washing, sections were mounted on gelatin-coated slides, air-dried and dehydrated in ascending concentrations of ethanol, cleared with xylene and coverslipped under Permount.

Quantification of TH and DAT expression was carried out using an image analysis system (Analytical Imaging Station (AIS), Imaging

Research Inc., Linton, UK) with a 5× lens, converting color intensities into a gray scale and quantifying the area of staining in the striatum of treated animals as a proportion of that in untreated animals (Darmopil et al., 2008, 2009; Granado et al., 2008a).

Stereological quantification of Nissl-stained neurons and TH positive neurons in SNpc

The total number of TH-positive (SNpc) Substantia Nigra pars compacta neurons was counted in the different groups of animals (n = 4–6 per group) using the optical fractionator (Granado et al., 2008b). This unbiased method of cell counting is not affected by the volume of reference (SNpc) or the size of the counted element (neurons). Immunostaining was performed with a polyclonal antibody to TH (1:1000, Chemicon International), followed by counterstaining with Nissl. TH- and Nissl-stained neurons were counted in the left SNpc of every fourth section throughout the entire extent of the SNpc, yielding 9–12 sections per animal (Jackson-Lewis et al., 2000). Each midbrain section was viewed at low power (10x objective) and the SNpc was outlined using the set of anatomic landmarks defined previously (Granado et al., 2008b; Jackson-Lewis et al., 2000). Then, starting at a random microscope visual field, the number of TH-stained cells was counted at high power (100×). To avoid double counting of neurons with unusual shapes, TH-stained and Nissl-stained neurons were counted only when their nuclei were optimally visualized which occurred only in one focal plane. In addition, neurons were differentiated from non-neuronal cells, including glia, on the Nissl stain by excluding cells that did not have a clearly defined nucleus, cytoplasm and a prominent nucleolus. Although these criteria may have excluded some small neurons, it should have reliably excluded all non-neuronal cells.

Fast scan cyclic voltammetry in brain striatal slices

Transverse brain slices (450 μm thickness) were prepared from mice using conventional methods (Martín and Buño, 2005), and incubated for >1 h at room temperature (21–24 °C) in artificial cerebrospinal fluid (aCSF). The aCSF contained (in mM): NaCl 124, KCl 2.69, KH_2PO_4 1.25, $MgSO_4$ 2, $NaHCO_3$ 26, $CaCl_2$ 2 and glucose 10, and was gassed with 95% O_2 and 5% CO_2. Slices were transferred to an immersion recording chamber and superfused (2.5 ml/min) with gassed aCSF warmed to 32–34 °C. Following 1 h of equilibration, a bipolar tungsten stimulating electrode with a tip separation of 200 μM (A-M Systems, Inc., Carlsborg, WA, USA) was placed in the dorsolateral striatum (Fig. 9A). A carbon fibre electrode (CFE; 10 μm diameter; 50 μm exposed length) was placed 100–200 μm from stimulating electrode. Fast scan cyclic voltammetry (FSCV) at the CFE was used to detect changes in extracellular concentrations of dopamine following electrical stimulation of the brain slice. Stimuli were single biphasic pulses (20 V, 500 μs) delivered via a 2100 isolated pulse stimulator (A-M Systems). Stimulus intervals between pulses were not less than 5 min. FSCV was carried out using a three electrode voltage-clamp amplifier (VAMP-1, Registim LLC, Coral Gables, FL, USA). The working electrode was connected to active CFE, an Ag/AgCl was used as reference electrode, and a platinum wire was used as auxiliary electrode. Using the common reference and auxiliary electrodes, a brief sawtooth voltage waveform with a voltage scan rate of 400 V/s was applied consecutively every 200 ms to working CFE electrode. The sawtooth had four phases: 0 to −1 V, to +1.4 V, to −1 V to 0 V (Fig. 9A). Changes in extracellular dopamine were determined by monitoring the current at the peak oxidation potential for dopamine. Subtracting the current obtained before stimulation from the current obtained in the presence of dopamine created background-subtracted cyclic voltammograms. Current was digitized at 10 kHz using PowerLab 4/25T (AD Instruments, Bella Vista, Australia) acquisition system. Data were acquired and analyzed with Scope software (AD Instruments). Electrodes were calibrated with DA standards of known concentration in the recording chamber before and after each use. The average of the pre- and post-calibration measurements was used as the calibration factor.

Statistics

Data are presented as mean ± standard error of the mean (S.E.M.). The results of rectal temperature measurements were analysed using two-way analysis of variance (ANOVA) for repeated measures. Data obtained from image analysis of striatal TH and DAT immunostaining were analysed using two-way ANOVA. Relevant differences were analyzed pair-wise by post-hoc comparisons with Newman-Keuls and Tukey's test, to determine specific group differences. All statistical analyses were performed using Sigma Stat 2.03 program and the threshold for statistical significance was set at $p<0.05$. Graphical representations were obtained using Sigma Plot 9.0 software.

Results

Genetic inactivation of D_1R blocked hyperthermia induced by METH

In agreement with previous reports (Granado et al., 2011a,b), METH (5 mg/kg, i.p., 3 injections given at 3-hour intervals) administration to WT mice induced significant increases in rectal temperatures that were not seen following saline treatment. The highest temperatures were recorded 30 min after the second and third injections of METH (Fig. 1A, $p<0.001$). In contrast, there was no significant hyperthermic response in $D_1R^{-/-}$ animals after any of the drug injections (Fig. 1A). In fact, the first METH injection in $D_1R^{-/-}$ animals induced a hypothermic response, with rectal temperatures decreasing from 37.5 to 35.7 °C ($p<0.001$). This hypothermic response was not observed after the second and third injections. The rectal temperatures of the saline-treated $D_1R^{-/-}$ animals were slightly, but significantly, lower than those of saline-treated WT mice (Fig. 1A).

Genetic inactivation of D_1R attenuated METH-induced loss of monoamines in the striatum

Basal levels of dopamine and its metabolites, DOPAC and HVA, were lower in $D_1R^{-/-}$ animals than in their WT littermates (Fig. 1B). The METH-induced reduction in striatal dopamine content was significantly smaller in $D_1R^{-/-}$ than in WT mice 1 day post-drug (Fig. 1C, $p<0.001$, two-way ANOVA and post-hoc Newman–Keuls analysis). Although DA levels recovered to some extent in WT mice 7 days after METH treatment, they remained lower in WT than in $D_1R^{-/-}$ animals (Fig. 1C, $p<0.001$). Similar results were obtained for the dopamine metabolites, DOPAC and HVA, whose depletions induced by METH (1 or 7 days) were attenuated in $D_1R^{-/-}$ animals (Table 1, $p<0.001$). There were no differences in levels of striatal serotonin (5-HT) or its metabolite, 5-HIAA (data not shown) indicating that the serotonergic system was not affected by METH treatment in these mice.

Genetic inactivation of D_1R attenuated METH-induced loss of TH expression in the striatum

Previous studies have shown that treatment with METH induced a decrease in the density of TH-immunoreactive fibres in the striatum of WT animals 1 and 7 days after its administration (Granado et al., 2010, 2011a,b). Loss of striatal TH-ir was almost completely blocked in $D_1R^{-/-}$ mice 1 and 7 days following METH administration (Fig. 2). Quantitative image analysis confirmed these observations, revealing a 62% decrease in TH-ir fibres in WT animals 1 day after METH administration ($p<0.001$, two-way ANOVA followed by Tukey's test). At 7 days post-METH treatment, the density of TH-ir fibres had partially recovered ($p<0.05$), but remained 38% lower than levels measured in saline-treated WT mice (Fig. 2, $p<0.001$).

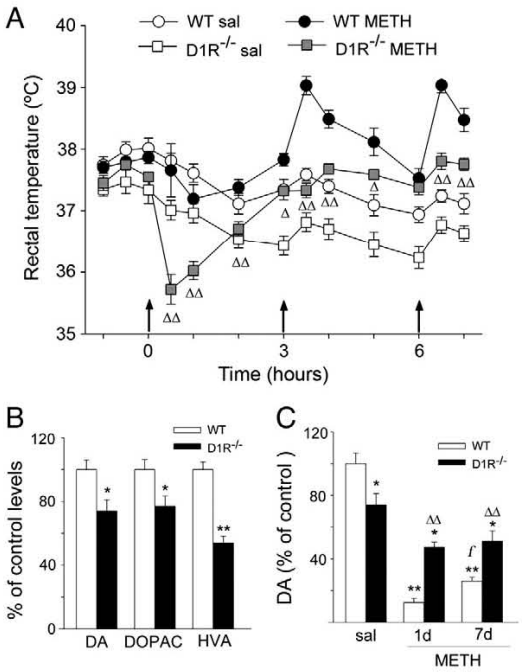

Fig. 1. Genetic inactivation of D_1R blocked METH-induced hyperthermia and attenuated the loss of DA induced by this drug. A. METH (5 mg/kg) (i.p., every 3 h, ×3) failed to produce hyperthermia in $D_1R^{-/-}$ mice but produced hypothermia after the first injection. Arrows indicate drug injections. Data represent mean ± S.E.M., n = 9–21 per group. For simplicity, only statistical differences between WT METH and $D_1R^{-/-}$ METH treated animals are indicated. Δ, ΔΔ $p<0.05$, 0.001 vs. WT METH, respectively. B. $D_1R^{-/-}$ mice have lower basal content of DA, DOPAC and HVA than WT mice. C. The reduction in DA levels was smaller in $D_1R^{-/-}$ mice 1 or 7 days after METH injections. Results shown as mean ± S.E.M.; n = 5–10 mice per group, *,** $p<0.05$, 0.001 vs. sal, Δ, ΔΔ $p<0.05$, 0.001 vs. WT, *f* $p<0.05$ vs 1 day. Statistical analysis was performed by two-way ANOVA and post-hoc Newman–Keuls analysis.

In contrast, $D_1R^{-/-}$ mice showed only a slight, although significant ($p<0.05$), reduction in TH-ir fibres at 1 or 7 days after METH treatment, even in the absence of hyperthermia. The damage was mainly observed in the dorsolateral part of the striatum in agreement with our previous observations that this is the most vulnerable area in the striatum (Granado et al., 2010), compared with saline-treated $D_1R^{-/-}$ mice (Fig. 2). There was no difference in the extent of TH-ir in saline-treated $D_1R^{-/-}$ and WT mice.

Genetic inactivation of D_1R attenuated METH-induced loss of DAT expression in the striatum

We also evaluated DAT by immunohistochemistry to confirm that TH fibre loss reflected terminal damage and not just a reduction in TH synthesis. As we have shown previously (Granado et al., 2010, 2011a), METH treatment induced significant decreases in DAT-ir in WT animals 1 or 7 days after drug delivery ($p<0.001$). At both time points, METH-induced changes in DAT-ir were significantly smaller in $D_1R^{-/-}$ mice than in WT mice ($p<0.001$). There was no difference in baseline DAT-ir between saline-treated WT and $D_1R^{-/-}$ mice (Fig. 2).

Table 1
Genetic inactivation of D_1R attenuated METH-induced loss of monoamines in the striatum.

	DA		DOPAC		HVA	
	WT	$D_1R^{-/-}$	WT	$D_1R^{-/-}$	WT	$D_1R^{-/-}$
SAL	100	74*	100	77*	100	54**
METH 1 d	12**	47* ΔΔ	33**	59 Δ	35**	45
METH 7 d	26**	73 ΔΔ	35**	60 Δ	40 **	45

Values are expressed as percent of control levels for dopamine and its metabolites in WT and $D_1R^{-/-}$ mice before and after METH treatment. * $p<0.05$ vs. sal ** $p<0.005$ vs. sal, Δ $p<0.05$ vs. WT METH, ΔΔ $p<0.001$ vs. WT METH. Statistical analysis was performed by two-way ANOVA and post-hoc Newman–Keuls analysis.

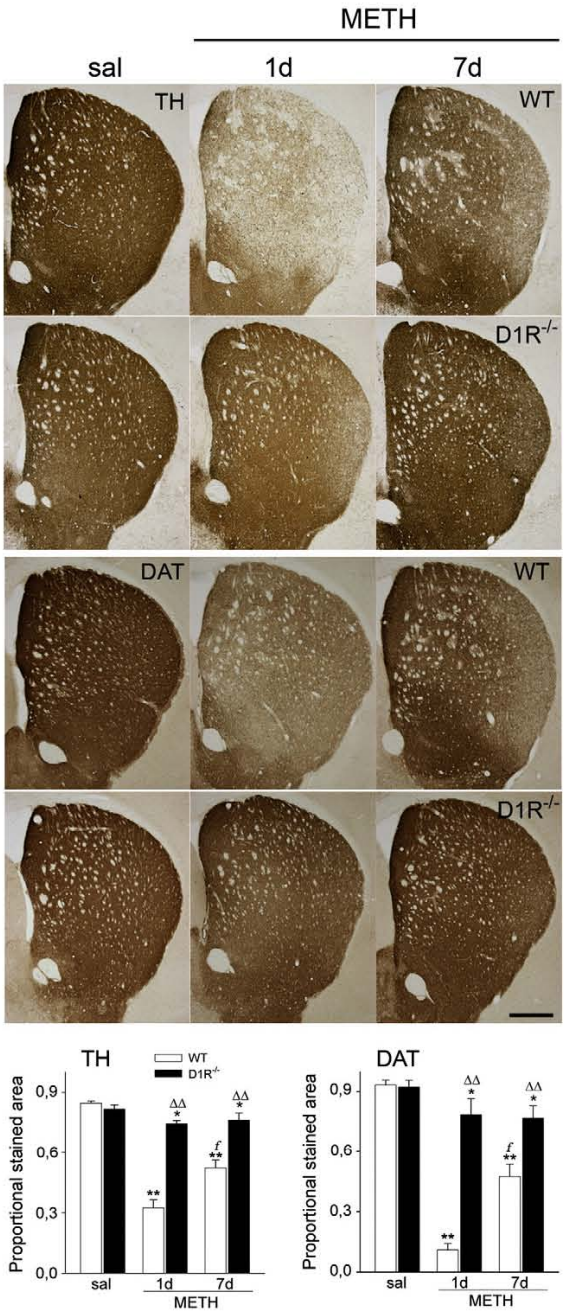

Fig. 2. Inactivation of D_1R attenuated METH-induced decreases in TH and DAT expression in the striatum. Photomicrographs of striatal sections from mice 1 and 7 days after treatment with saline or METH, stained for TH and DAT. Histograms show the proportional stained area of TH- and DAT-immunoreactivity staining in the striatum. Data represent mean ± S.E.M, n = 6–8 per group * $p<0.05$ vs saline, ** $p<0.001$ vs saline, ΔΔ $p<0.001$ vs WT METH, *f* $p<0.05$ vs 1 day; two-way ANOVA followed by Tukey's test. Bar indicates 500 μm.

METH-induced microgliosis and astrogliosis in the striatum were inhibited in $D_1R^{-/-}$ mice

Augmented microglial activation is a hallmark of amphetamine derivative-induced neurotoxicity (Boyle and Connor, 2010). Immunohistochemistry for Mac-1 (CD11b), a marker of microglia, revealed a significant increase in activated microglia in WT mice 1 day after METH treatment. However, there was no increase in Mac-1-ir following METH delivery to $D_1R^{-/-}$ mice (Fig. 3).

In addition to their effects on microglial cells, amphetamine derivatives like METH typically cause an increase in expression of GFAP, a marker of astrocyte activation, in the striatum (Thomas et al., 2004, 2008a). As expected, in WT METH-treated animals, we observed a homogeneous increase in GFAP-ir throughout the caudoputamen 1 day after METH treatment, which became more pronounced by 7 days after treatment. Interestingly, the increase in GFAP seen after METH administration was partially prevented in $D_1R^{-/-}$ mice (Fig. 3).

METH-induced increase in iNOS expression is prevented in $D_1R^{-/-}$ mice

The cytokine-inducible nitric oxide synthase, iNOS, produces large amounts of NO that can have neurotoxic effects (Dawson, 2006). High levels of NO can react with superoxide leading to peroxynitrite formation and subsequent neurotoxicity (Anderson and Itzhak, 2006). iNOS overexpression often follows METH treatment (Granado et al., 2011a). In our experiment, WT, but not $D_1R^{-/-}$, mice had increased striatal levels of iNOS 1 day after METH delivery (Fig. 4). These results indicate a role for D_1R in the induction of iNOS expression following administration of METH.

METH-induced dopaminergic neuronal loss in the substantia nigra is prevented in $D_1R^{-/-}$ mice

To see if the protection against axonal loss seen in $D_1R^{-/-}$ mice corresponded to prevention of cell body loss, we quantified dopaminergic neurons in the SN, by stereological counting of TH-positive cells. As previously reported (Granado et al., 2011a, 2011b), in WT mice treated with METH, there was a decrease in TH-ir in the SN pars compacta (SNpc), which contains dopaminergic cell bodies, and in the pars reticulata (dopaminergic neuropil) (Fig. 5D). The number of TH-ir neurons in SN of WT mice was decreased by 25% compared to saline-treated WT mice ($p<0.05$, two-way ANOVA followed by Tukey's test) at 1 day following METH injection and by 20% ($p<0.05$) at 7 days after injection (Fig. 5A). In contrast, there was no loss of TH-ir neurons in SN of $D_1R^{-/-}$ mice, indicating that inactivation of D_1R prevents dopaminergic cell loss in the SN (Fig. 5A). Similarly, the number of Nissl-stained SNpc neurons was significantly decreased in WT animals at both time points ($p<0.001$), but not in $D1R^{-/-}$ animals compared to saline-treated animals (Fig. 5B). Apoptotic cell profiles were identified by Nissl staining in the SN of METH-treated WT mice, further demonstrating that some dopaminergic neurons undergo cell death by apoptosis after METH treatment (Fig. 5C). No apoptotic bodies were seen in $D1R^{-/-}$ animals after METH treatment. In addition, following METH treatment, there was less astrogliosis and microgliosis in the SNpc in $D_1R^{-/-}$ mice than in WT mice (Figs. 5E and F).

High ambient temperature reverses the effects of genetic inactivation of D_1R on METH-induced hyperthermia and loss of striatal TH

To evaluate whether blockade of hyperthermia is important for protection against METH-induced loss of dopaminergic terminals in $D_1R^{-/-}$ animals, we exposed $D_1R^{-/-}$ animals to a higher environmental temperature during METH treatment in an attempt to facilitate hyperthermia in this group of animals. Thus, $D_1R^{-/-}$ mice were kept at the high ambient temperature of 29 ± 2 °C for 2 h before,

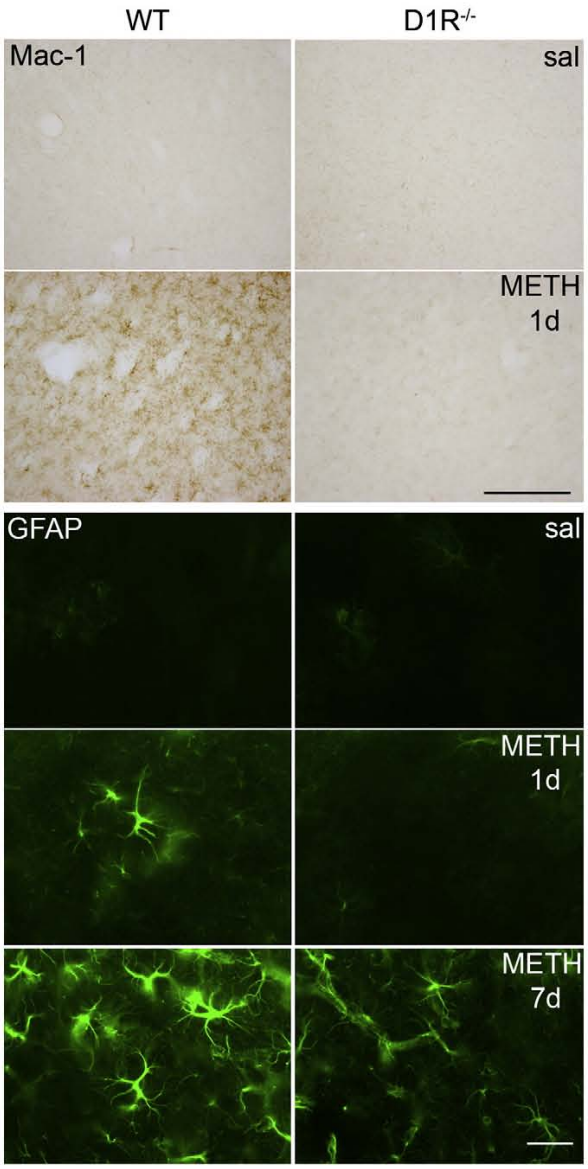

Fig. 3. Inactivation of D_1R partially prevented METH-induced astrogliosis and microgliosis in mouse striatum. Photomicrographs of striatal sections from mice treated with saline or METH stained for GFAP or Mac-1 (CD-11b) in WT and $D_1R^{-/-}$ mice. Animals were killed 1 and 7 days after treatment. METH induced the expression of GFAP and Mac-1 in WT animals, but $D_1R^{-/-}$ mice showed smaller increases in GFAP and no increases in Mac-1. Bar indicates 200 μm (Mac-1) and 50 μm (GFAP).

during, and for 1 h after the drug treatment, whereas WT animals were treated in another room at 23 °C, in order to avoid excessive animal death induced by high hyperthermia.

At 29 °C, $D_1R^{-/-}$ mice exhibited a hyperthermic response to METH treatment, similar to that seen in WT animals treated with METH at 23 °C. Average rectal temperatures in the $D_1R^{-/-}$ mice rose from 38.2 to 39.4 °C and 39.5 °C after the second and third METH injections, which translates to significant increases of 1.9 °C and 2.1 °C in comparison to $D_1R^{-/-}$ mice treated with saline at 29 °C (Fig. 6A, $p<0.001$). There were no significant differences between rectal temperatures in WT mice treated with saline at 23 °C and $D_1R^{-/-}$ mice treated with saline at 29 °C (Fig. 6A). Interestingly, the protection

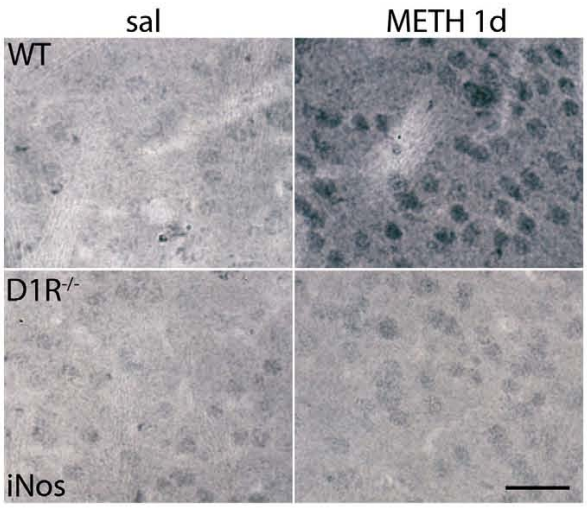

Fig. 4. Inactivation of D_1R prevented METH-induced iNOS striatal expression in mice. Photomicrographs of striatal sections from mice treated with saline or METH stained for iNOS in WT and $D_1R^{-/-}$ mice. Animals were killed 1 day (iNOS) after treatment with METH. METH induced the expression of iNOS in WT animals and to a lesser extend in $D_1R^{-/-}$ mice. Bar indicates 100 μm.

against METH-induced TH-ir loss afforded by D_1R inactivation at normal ambient temperature disappeared at 29 °C. Specifically, TH-ir levels were significantly more reduced in $D_1R^{-/-}$ mice (88%) treated at 29 °C than in WT mice (45%) treated at 23 °C in spite of reaching similar hyperthermia levels (Figs. 6B and C, $p<0.05$, two-way ANOVA and post-hoc Newman–Keuls analysis).

Pretreatment with α-methyl-p-tyrosine blocks METH toxicity in WT and $D_1R^{-/-}$ mice

α-Methyl-p-tyrosine (αMPT), an inhibitor of TH that affords protection against the neurotoxic effects of METH (Albers and Sonsalla, 1995; Thomas et al., 2008b), completely prevented the loss of striatal TH-ir in $D_1R^{-/-}$ mice treated at 23 °C room temperature, but only attenuated this loss in WT mice (Figs. 7B and C, $p<0.05$ two-way ANOVA followed by Tukey's test). Interestingly, following pretreatment with αMPT, both genotypes had a marked hypothermic response after the first injection with METH that reached lower levels in $D_1R^{-/-}$ mice (Fig. 7A, $p<0.05$). Moreover, WT mice still suffered a small loss of TH-ir (6%) without exhibiting any hyperthermic response during the treatment.

Pretreatment with reserpine abolishes the neuroprotective effect of D_1R inactivation against METH toxicity

To further dissociate the effect of D_1R inactivation on hypothermia from its effects on METH toxicity, we treated animals with reserpine, a monoamine depleting compound that induces hypothermia in rodents. METH administration (3 mg/kg, 3 times) in reserpinized mice raised body temperature to the same levels seen in saline-treated animals in both genotypes without causing hyperthermia at any time after drug delivery (Fig. 8A). Nevertheless, there was a substantial loss of TH-ir in spite of the lack of hyperthermia (45% for WT and 46% for $D1R^{-/-}$ mice) (Figs. 8B, C, $p<0.001$, two-way ANOVA followed by Tukey's test). Interestingly, METH alone produced no effects on TH expression in $D_1R^{-/-}$ mice, but induced a great TH-ir loss in reserpinized $D_1R^{-/-}$ animals, even though these animals were hypothermic. This suggests that releasing dopamine vesicle stores into the cytosol abolished the protection conferred by D_1R deletion by rendering D_1R-mediated METH toxicity temperature-independent. Together,

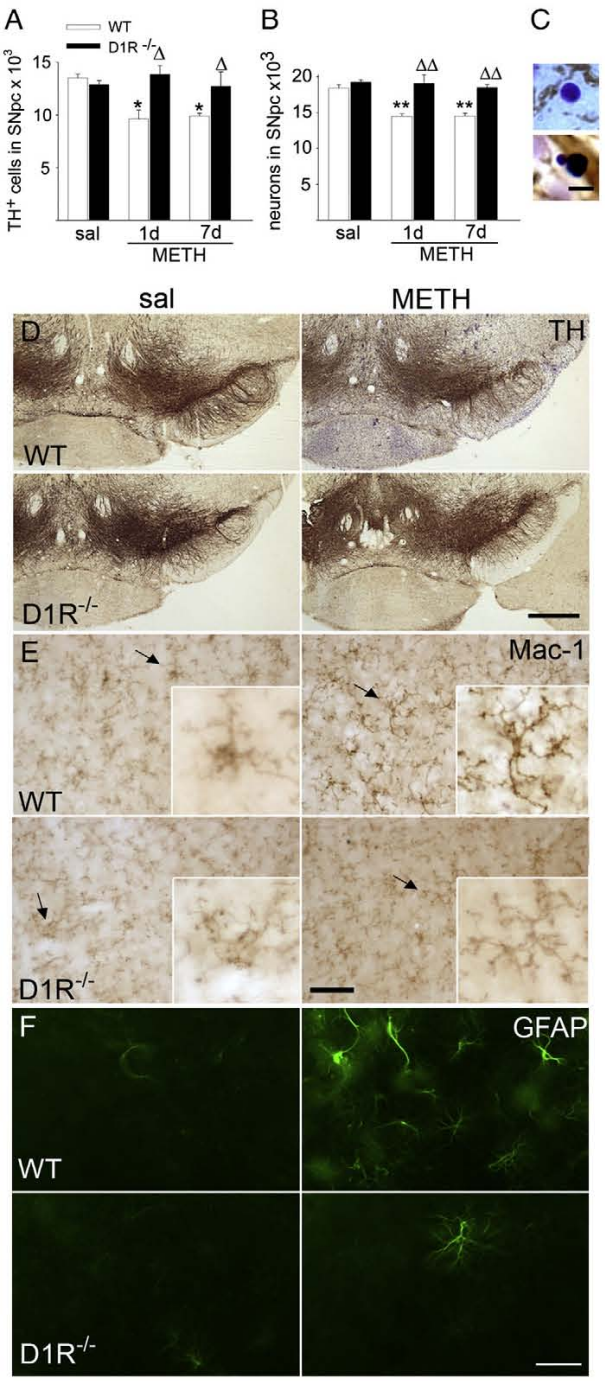

Fig. 5. Dopamine D_1R inactivation prevent METH-induced loss of TH-ir neurons and gliosis in the substantia nigra. A,B. Histograms show numbers of TH positive cells (A) and Nissl-stained neurons (B) in the SNpc of WT and $D1R^{-/-}$ mice (mean ± S.E.M, n = 4–6 per group) counted by stereology in midbrain sections from animals obtained 1 or 7 days after METH treatment. * $p<0.05$,** $p<0.001$ vs sal, Δ $p<0.05$, ΔΔ $p<0.001$ vs WT METH two-way ANOVA, followed by Tukey's test. C. Photomicrographs of Nissl-stained apoptotic bodies observed in the SN of WT mice 1 day after METH. D. Photomicrographs of sections of SN from mice treated with saline or METH stained for TH, 1 day after treatment. E. Photomicrographs of sections stained with Mac-1, indicating microgliosis. F. Sections stained with GFAP, a marker for astrogliosis. Bar indicates 5 μm (C) 500 μm (D) and 50 μm (E and F).

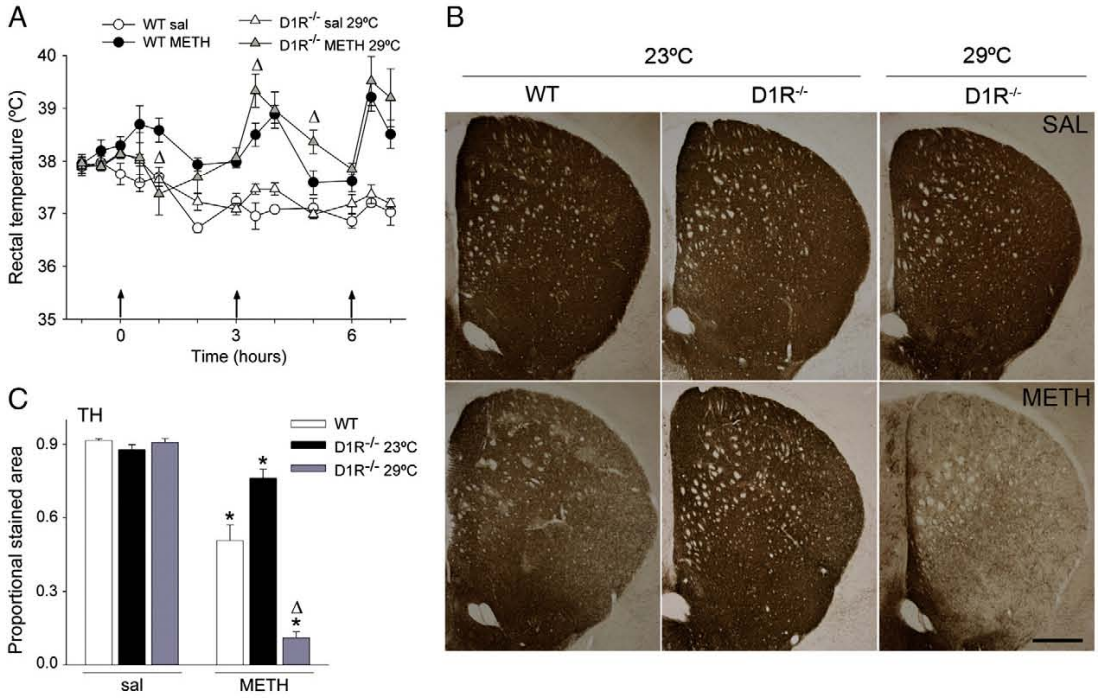

Fig. 6. METH induced hyperthermia and decreases in striatal TH expression in $D_1R^{-/-}$ mice when administered at 29 °C. A. METH produced similar increases in the rectal temperature in WT mice housed in a room at 23 °C and $D_1R^{-/-}$ METH-treated mice, housed at 29 °C. The arrows indicate drug injections. Data represent mean ± SEM, n = 6–8 per group, two-way ANOVA, Δ $p<0.05$ vs. WT METH. B and C. METH produced a decrease in TH expression in the striatum of $D_1R^{-/-}$ mice when treated in a room at 29 °C. Histograms show the proportional stained area of TH-ir staining in the striatum. Data represent mean ± SEM, n = 6–8 per group. * $p<0.05$ vs sal, Δ $p<0.05$ vs WT METH. Statistical analysis was performed by two-way ANOVA and post-hoc Newman-Keuls analysis. Bar indicates 500 μm.

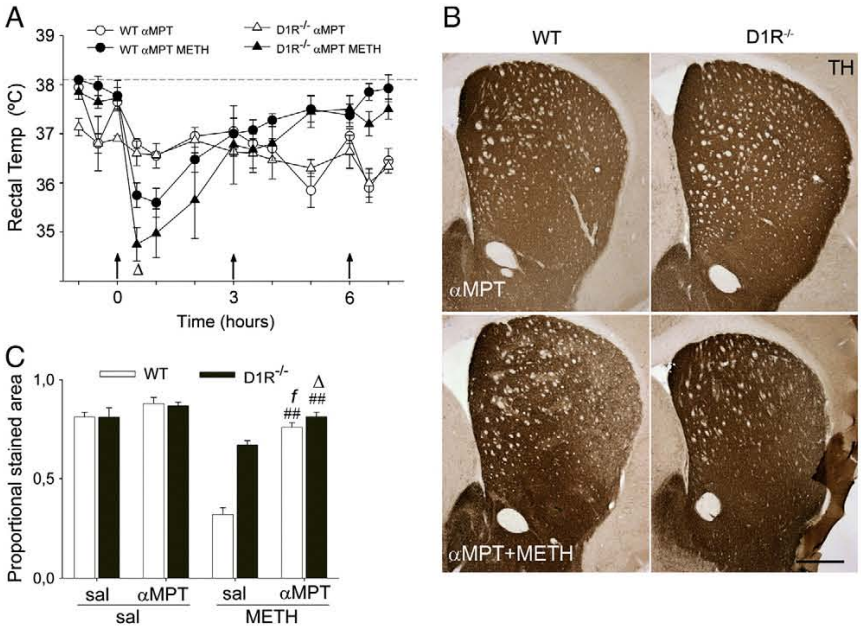

Fig. 7. Pretreatment with αMPT blocks METH toxicity in WT and $D_1R^{-/-}$ mice. A. Pretreatment with αMPT (100 mg/kg x4) before METH produced a decrease in the rectal temperature of WT and $D_1R^{-/-}$ animals that was more pronounced in $D_1R^{-/-}$ mice, peaking 30 min after the first injection of METH. The arrows indicate drug injection. Data represent mean ± SEM, n = 3–4 per group. For simplicity, only statistical differences between WT and $D_1R^{-/-}$ mice treated with αMPT plus METH are indicated. Δ $p<0.05$. B and C. Photomicrographs and histograms showing striatal TH stained area. Δ $p<0.05$ vs WT, ## $p<0.001$ vs METH, $f<0.05$ vs αMPT, two-way ANOVA followed by Tukey's test. Bar indicates 500 μm.

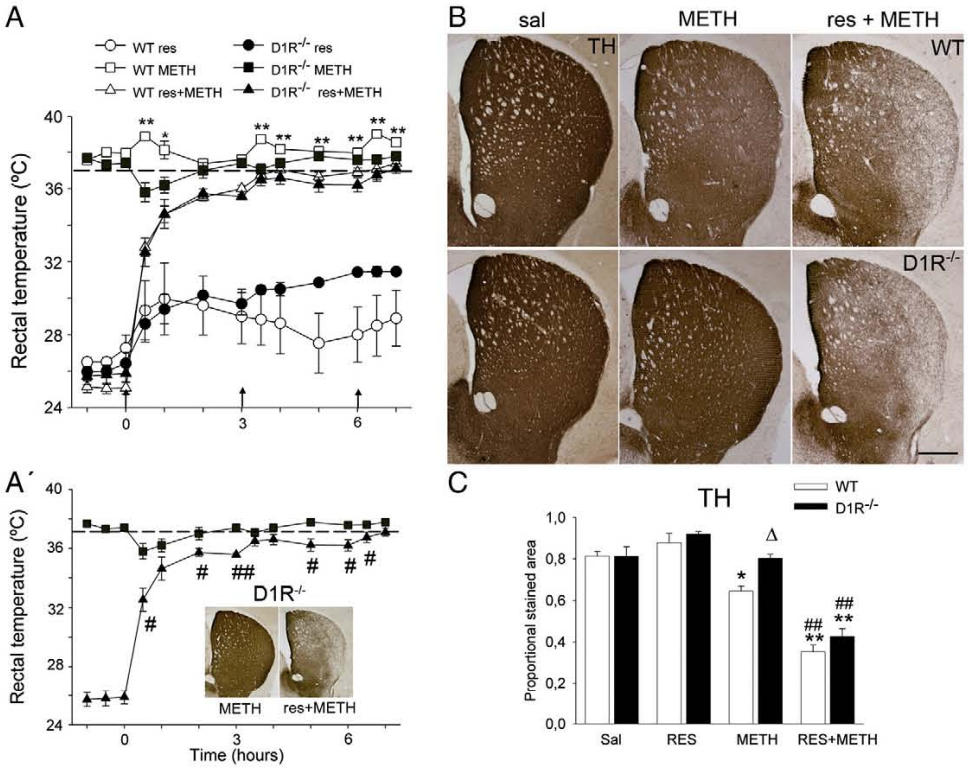

Fig. 8. Reserpine produced hypothermia and increased METH-induced neurotoxicity in D1R$^{-/-}$ mice. Reserpine (3 mg/kg) and Methamphetamine (3 mg/kg ×3, 3 h). A) Reserpine blocked METH-induced increases in rectal temperature in WT and D1R$^{-/-}$ mice. Arrows indicate drug injections. A') D1R$^{-/-}$ mice reserpinized mice treated with METH have lower rectal temperatures but greater TH-ir loss that D1R$^{-/-}$ mice treated with METH alone. B) Photomicrographs of striatal sections from WT and D1R$^{-/-}$ mice treated with sal or METH or reserpine and METH stained for TH. C) Histograms show the proportional stained area for TH-ir in the striatum. Data represent mean ± S.E.M., n = 4–6 per group. * p<0.05 **, p<0.001 vs. saline; # p<0.05, ## p<0.001 vs. METH-treated mice and Δ p<0.05 vs. WT; two-way ANOVA, followed by Tukey's test. Bar indicates 500 μm.

these results suggest that the neuroprotection afforded by D_1R inactivation is not solely due to its ability to block hyperthermia, but also to the redistribution of dopamine inside the terminal.

Inactivation of D_1R results in increased striatal DA overflow induced by METH

Since inactivation of D_1R prevented METH-induced striatal loss of dopaminergic fibre, we examined whether METH would alter extrasynaptic DA overflow in WT and $D_1R^{-/-}$ mice in corticostriatal slices. DA overflow is determined by the balance between DA release and reuptake and was recorded with a carbon fibre electrode in the dorsal striatum of corticostriatal slices using FSCV (see Materials and Methods; Fig. 9A). In control conditions, we found that, compared to WT mice, $D_1R^{-/-}$ mice showed a significant increase in DA overflow in response to a single biphasic pulse (20 V, 500 μs) (Fig. 9B) indicating that $D_1R^{-/-}$ mice have a higher vesicular DA release and lower DA reuptake capacity than WT. In the presence of 30 μM METH, after 30 min of voltammogram stabilization, similar pulse stimulation induced a significant increase in DA overflow for both genotypes compared with control conditions (Fig. 9C). This increase was greater in $D_1R^{-/-}$ than in WT mice (Fig. 9C) suggesting that the protective effect of inactivating D_1R is in part due to higher vesicular dopamine content and to higher DA release from presynaptic terminals.

Discussion

This study showed that genetic inactivation of dopamine D_1 receptor provides protection against the neurotoxic effects of METH. The neuroprotective effect of D_1R deletion was evident in the striatum, where METH-induced decreases in TH- and DAT-immunoreactivity were almost completely blocked. In the SN, METH-induced dopaminergic neuronal loss and gliosis were also prevented. The increase in gliosis in the striatum observed following METH administration in WT mice was also significantly attenuated in $D_1R^{-/-}$ mice. In addition, D_1R inactivation attenuated induction of striatal iNOS expression by METH. However, when $D_1R^{-/-}$ mice were treated with METH at high ambient temperature or after pretreatment with reserpine, the protection conferred by D_1R deletion was abolished. We also determined that dopamine overflow (measured by FSCV) was higher in $D_1R^{-/-}$ than in WT mice, an increase that was potentiated in the presence of METH. These findings indicate a role for the dopamine D_1R subtype in the neurotoxic effects of this amphetamine derivative.

Our results are consistent with the previous reports that a D_1/D_5R antagonist inhibits METH-induced hyperthermia (Broening et al., 2005). Indeed, in $D_1R^{-/-}$ mice, the first injection of the drug induced pronounced hypothermia. Subsequent doses did not significantly raise body temperature. Therefore, it appears possible that the protective effects observed in $D_1R^{-/-}$ mice were due to the hypothermic effect of the first dose, or to the absence of hyperthermia following subsequent doses. Interestingly, administration of METH to $D_1R^{-/-}$ mice kept at 29 °C did induce hyperthermia: rectal temperatures were similar to those observed in WT METH-treated mice maintained at standard ambient temperature, as previously reported using a D_1/D_5R antagonist, SCH23390, in rats (Broening et al., 2005). Because this antagonist blocked both D_1 and D_5 receptors, our results in $D_1R^{-/-}$ animals conclusively demonstrate that the D_1R subtype is required for the hyperthermic response induced by METH at normal

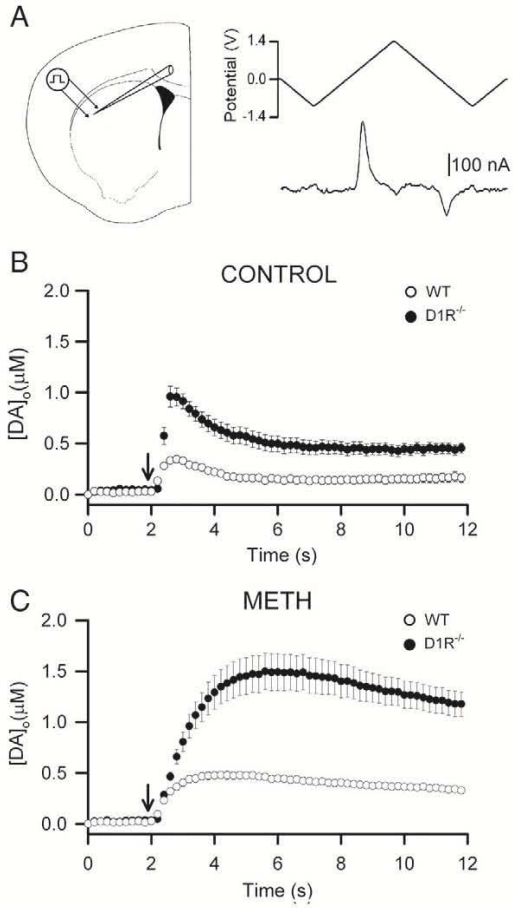

Fig. 9. DA overflow in response to single-pulse stimulation in striatal slices from $D_1R^{-/-}$ and WT mice in control conditions and after perfusion with METH. A. Left, schematic diagram illustrating the placement of the carbon fibre microelectrode (recording electrode) and the bipolar stimulating electrode in the dorsolateral striatum. Right, fast-scan cyclic voltammetry voltage waveform at 400 V/s scan rate (upper trace), and subtracted voltammograms for 1 μM of dopamine (lower trace). B. Time course of dopamine overflow evoked by a single intrastriatal stimulus (arrow; 20 V, 0.5 ms) in WT (n = 11 slices from 3 mice) and $D_1R^{-/-}$ (n = 10 slices from 3 mice) slices. C. Time course of dopamine overflow evoked by a single intrastriatal stimulus (arrow) in the presence of 30 μM METH in WT (n = 10 slices from 3 mice) and $D_1R^{-/-}$ (n = 10 slices from 3 mice) slices. Data represent mean ± S.E.M.

ambient room temperature (23 °C), but not at 29 °C. Taken together with previous studies from our laboratory that demonstrated that the hyperthermic response to METH is secondary to D_2R stimulation at ambient temperatures of 23 or 30 °C (Granado et al., 2011a), the current study indicates that, at 23 °C, the D_1R is also required.

The neuroprotection provided by D_1R inactivation was no longer observed when the $D_1R^{-/-}$ animals were treated at a high ambient temperature (29 °C) and developed hyperthermia after METH administration, further supporting the possibility that the protective effects of D_1R inactivation are due, at least in part, to the hypothermic response. Body temperature is an important factor in the toxic responses to METH (Krasnova and Cadet, 2009; Tata et al., 2007; Yamamoto et al., 2010) and has been shown to potentiate DAT function (Xie et al., 2000), increasing free radicals and DA oxidation in the brain (Kil et al., 1996; LaVoie and Hastings, 1999; Spencer et al., 2002). However, other pharmacological and genetic studies indicate that hyperthermia may contribute to, but is not required for, METH-induced dopaminergic neurotoxicity (Albers and Sonsalla, 1995; Fumagalli et al., 1998; Granado et al., 2011a; Thomas et al., 2008b). In line with this, our results showed that pretreatment with reserpine, which blocked METH-induced hyperthermia, potentiated its neurotoxic effects, abolishing the protection induced by D_1R inactivation, indicating that the protective effects of D_1R inactivation are not solely the result of blocking hyperthermia.

Reduced dopamine content and turnover in $D_1R^{-/-}$ mice may also be a factor in their resistance to METH-induced neurotoxicity. Dopamine has been proposed to play a crucial role in METH-induced neurotoxicity. METH produces an increase in cytosolic DA, which is metabolized by auto-oxidation, with subsequent generation of reactive oxygen species (ROS) such as hydrogen peroxide, hydroxyl radicals, DA quinones and superoxide anions (Cadet and Brannock, 1998; Krasnova and Cadet, 2009; LaVoie and Hastings, 1999). Thus, the lower content and turnover of DA in $D_1R^{-/-}$ mice might significantly decrease the production of ROS compared to WT mice.

This hypothesis is also supported by our experiments with α-methyl-p-tyrosine (αMPT). Pretreatment with αMPT, which decreases cytosolic dopamine by blocking TH activity and has been shown to protect against METH toxicity (Albers and Sonsalla, 1995; Thomas et al., 2008b), induces more pronounced protective effects in $D_1R^{-/-}$ mice than in their WT controls. This data indicates that αMPT is more effective in $D_1R^{-/-}$ than in WT, possibly due to their lower TH activity, since dopamine turnover is also lower in $D_1R^{-/-}$ mice than in WT, as shown in our experiments by HPLC. This is in agreement with previous reports showing that αMPT is more effective in blocking TH activity in $DAT^{-/-}$ mice with lower dopamine content (Jones et al., 1998). The lower DA content and turnover observed in $D_1R^{-/-}$ could reflect feedback regulation of dopamine synthesis: lack of D_1R could change the rate of dopamine synthesis, as has been demonstrated following manipulation of other components of the dopaminergic system such as inactivation of D_2R (Granado et al., 2011a; Tinsley et al., 2009) or DAT (Jaber et al., 1999; Jones et al., 1998).

Another possible mechanism underlying the protective effects seen in $D_1R^{-/-}$ mice could be related to the different distribution of DA within the terminal, as cytosolic dopamine is directly implicated in the neurotoxic effects of METH while vesicular dopamine is not involved (Fumagalli et al., 1999; Granado et al., 2011a; Thomas et al., 2008b). In our experiments, FSCV revealed significantly higher striatal extracellular DA overflow in $D_1R^{-/-}$ mice than in WT after a single electric pulse. The enhancement of this overflow induced by the presence of METH in the media was also bigger in $D_1R^{-/-}$ than in control mice. The peak DA overflow is a function of competing mechanisms of synaptic release and reuptake, whereas the time course of the subsequent DA decrement reflects the rates of DA reuptake and diffusion (Bull et al., 1990; Wightman and Zimmerman, 1990). Thus, our experiments indicate that $D_1R^{-/-}$ mice show a higher vesicular DA release and lower DA reuptake capacity than WT, despite their lower basal dopamine content, suggesting that $D_1R^{-/-}$ animals store more DA in vesicles and therefore have a reduced cytosolic dopamine pool compared to WT mice, providing a plausible reason as to why METH induces less dopaminergic damage in $D_1R^{-/-}$ mice.

The higher vesicular dopamine content in $D_1R^{-/-}$ mice is also evidenced by our reserpine experiment, in which reserpine-induced release of dopamine from the vesicles to the cytosol caused $D_1R^{-/-}$ mice to have the same neurotoxic damage induced by METH than WT animals. This argument is consistent with a higher DA overflow induced by SCH23395, a D_1/D_5 receptor antagonist (O'Dell et al., 1993) when given alone in in vivo microdialysis studies. This idea is also supported by the data obtained when METH was administered at high ambient temperature, 29 °C. In this condition, $D_1R^{-/-}$ animals exhibited hyperthermia after the second and third METH injections, that was very similar to that observed in WT animals treated with METH at 23 °C. However, there is a dramatic potentiation of METH-induced neurotoxicity in $D1R^{-/-}$ animals compared to WT, despite very similar hyperthermic responses to the three METH administrations. The higher DA overflow we observed in $D_1R^{-/-}$ mice combined

with the fact that DA uptake increases with temperature (Volz et al., 2006) would result in higher cytosolic DA levels, thus producing a potentiation of METH-induced dopaminergic neurotoxicity in $D_1R^{-/-}$ mice at 29°.

Ultimately, inactivation of D_1R located postsynaptically to the DA terminals in striatal neurons could be directly implicated in the observed neuroprotection. Previous studies have demonstrated that pretreatment with SCH23390, a dopamine D_1/D_5R antagonist, reduces METH-induced striatal expression of various genes related to endoplasmic reticulum stress, such as ATF4, ATF6, along with heat shock proteins involved in apoptosis and cell death (Jayanthi et al., 2009). D_1/D_5R blockade also decreases dopamine-induced oxidation and cytotoxicity mediated by ERK and JNK activation (Chen et al., 2004). Moreover, blockade of D_1/D_5R can prevent striatal neurotoxicity by suppressing activation of caspases 3 and 8, mediators of the calcineurin/NFAT/FasL-dependent apoptotic cell death pathway (Jayanthi et al., 2005; Krasnova and Cadet, 2009). At least one study described striatal apoptosis preceding the depletion of DA terminal markers in the striatum, perhaps due to the loss of nigrostriatal dopaminergic afferents (Zhu et al., 2005). Thus, attenuation of striatal apoptosis in the absence of D_1R could also contribute to the presynaptic neuroprotection observed in $D_1R^{-/-}$ mice.

Astroglial and microglial activation may also play a role in the neuroprotection afforded by inactivation of D_1R. GFAP activation is a hallmark of amphetamine derivative-induced neurodegeneration (Deng et al., 1999; O'Callaghan and Miller, 1994). Astrocytes can protect against dopamine neuron loss and MPTP-induced oxidative stress directly by scavenging free radicals and indirectly by increasing glutathionine, which has antioxidant activity (Jia et al., 2009). Activated microglia can release a variety of reactants that damage neurons (Block and Hong, 2007) and could be the source of virtually all reactant species that have been implicated in amphetamine derivative-induced neurotoxicity, including reactive oxygen (Cadet et al., 1994, 2007) and reactive nitrogen species (Imam et al., 2001). Anti-inflammatory drugs like ketoprofen, indometacin and minocycline afford protection against METH-induced microgliosis and neurotoxicity (Zhang et al., 2006). Nevertheless, attenuation of microglial activation by itself is not sufficient to protect against METH neurotoxicity (Sriram et al., 2006). Our results are consistent with these previous findings, since we found that METH-exposed $D_1R^{-/-}$ mice not only exhibit reduced neurotoxicity, but also have attenuated astroglial and microglial responses in both striatum and the SN.

Our findings support a role for the dopamine D_1R subtype in the neurotoxic effects of amphetamine derivatives, identifying it as an important target for therapeutic interventions related to METH neurotoxicity. The D_1R knockout mouse provides an important model for further analysis of the role of dopamine and dopamine receptors in brain neurotoxicity induced by drugs or disease.

Statement of conflicts of interest

The authors state no conflict of interest.

Acknowledgments

This work was supported by grants from the Spanish Ministries de Ciencia e Innovación and Sanidad y Política Social, ISCIII: BFU2010-20664, PNSD, RedRTA (RD06/0001/1011) and CIBERNED to RM and SAF2007-65175, FIS PI070892, PNSD 2006/1018, 2008/074; RTA06/0001/0006 to MIC. Spanish Ministerio de Ciencia e Innovación (BFU2008-04196), Consejería de Educación Ciencia y Cultura, JCCM (PEII10-0095-872) and INCRECyT project from European Social Fund and JCCM to EDM. SAS is a recipient of a JAE predoctoral fellowship from the CSIC. NG is a recipient of Juan de la Cierva contract. The authors would like to thank Mrs Emilia Rubio and Mr Marco de Mesa for their excellent technical assistance.

References

Achat-Mendes, C., Ali, S.F., Itzhak, Y., 2005. Differential effects of amphetamines-induced neurotoxicity on appetitive and aversive Pavlovian conditioning in mice. Neuropsychopharmacology 30, 1128–1137.
Albers, D.S., Sonsalla, P.K., 1995. Methamphetamine-induced hyperthermia and dopaminergic neurotoxicity in mice: pharmacological profile of protective and nonprotective agents. J. Pharmacol. Exp. Ther. 275, 1104–1114.
Anderson, K.L., Itzhak, Y., 2006. Methamphetamine-induced selective dopaminergic neurotoxicity is accompanied by an increase in striatal nitrate in the mouse. Ann. N. Y. Acad. Sci. 1074, 225–233.
Angulo, J.A., Angulo, N., Yu, J., 2004. Antagonists of the neurokinin-1 or dopamine D1 receptors confer protection from methamphetamine on dopamine terminals of the mouse striatum. Ann. N. Y. Acad. Sci. 1025, 171–180.
Block, M.L., Hong, J.S., 2007. Chronic microglial activation and progressive dopaminergic neurotoxicity. Biochem. Soc. Trans. 35, 1127–1132.
Bowyer, J.F., Robinson, B., Ali, S., Schmued, L.C., 2008. Neurotoxic-related changes in tyrosine hydroxylase, microglia, myelin, and the blood–brain barrier in the caudate-putamen from acute methamphetamine exposure. Synapse 62, 193–204.
Boyle, N.T., Connor, T.J., 2010. Methylenedioxymethamphetamine ('Ecstasy')-induced immunosuppression: a cause for concern? Br. J. Pharmacol. 161, 17–32 Review..
Broening, H.W., Morford, L.L., Vorhees, C.V., 2005. Interactions of dopamine D1 and D2 receptor antagonists with D-methamphetamine-induced hyperthermia and striatal dopamine and serotonin reductions. Synapse 56, 84–93.
Bronstein, D.M., Hong, J.S., 1995. Effects of sulpiride and SCH 23390 on methamphetamine-induced changes in body temperature and lethality. J. Pharmacol. Exp. Ther. 274, 943–950.
Bull, D.R., Palij, P., Sheehan, M.J., Millar, J., Stamford, J.Á., Kruk, Z.L., et al., 1990. Application of fast cyclic voltammetry to measurement of electrically dopamine overflow from brain slices in vitro. J. Neurosci. Meth. 32, 37–44.
Cadet, J.L., Brannock, C., 1998. Free radicals and the pathobiology of brain dopamine systems. Neurochem. Int. 32, 117–131.
Cadet, J.L., Krasnova, I.N., 2009. Molecular bases of methamphetamine-induced neurodegeneration. Int. Rev. Neurobiol. 88, 101–119.
Cadet, J.L., Ali, S., Epstein, C., 1994. Involvement of oxygen-based radicals in methamphetamine-induced neurotoxicity: evidence from the use of CuZnSOD transgenic mice. Ann. N. Y. Acad. Sci. 738, 388–391.
Cadet, J.L., Jayanthi, S., Deng, X., 2005. Methamphetamine-induced neuronal apoptosis involves the activation of multiple death pathways. Neurotox. Res. 8, 199–206.
Cadet, J.L., Krasnova, I.N., Jayanthi, S., Lyles, J., 2007. Neurotoxicity of substituted amphetamines: molecular and cellular mechanisms. Neurotox. Res. 11, 183–202.
Chen, J., Rusnak, M., Luedtke, R.R., Sidhu, A., 2004. D1 dopamine receptor mediates dopamine-induced cytotoxicity via the ERK signal cascade. J. Biol. Chem. 279, 39317–39330.
Darmopil, S., Muñetón-Gómez, V.C., de Ceballos, M.L., Bernson, M., Moratalla, R., 2008. Tyrosine hydroxylase cells appearing in the mouse striatum after dopamine denervation are likely to be projection neurones regulated by L-DOPA. Eur. J. Neurosci. 27, 580–592.
Darmopil, S., Martín, A.B., De Diego, I.R., Ares, S., Moratalla, R., 2009. Genetic inactivation of dopamine D1 but not D2 receptors inhibits L-DOPA-induced dyskinesia and histone activation. Biol. Psychiatry 66, 603–613.
Dawson, T.M., 2006. Parkin and defective ubiquitination in Parkinson's disease. J. Neural Transm. Suppl. 209–213.
Deng, X., Ladenheim, B., Tsao, L.I., Cadet, J.L., 1999. Null mutation of c-fos causes exacerbation of methamphetamine-induced neurotoxicity. J. Neurosci. 15 (19), 10107–10115.
Fantegrossi, W.E., Ciullo, J.R., Wakabayashi, K.T., De La, G.R., Traynor, J.R., Woods, J.H., 2008. A comparison of the physiological, behavioral, neurochemical and microglial effects of methamphetamine and 3,4-methylenedioxymethamphetamine in the mouse. Neuroscience 151, 533–543.
Fumagalli, F., Gainetdinov, R.R., Valenzano, K.J., Caron, M.G., 1998. Role of dopamine transporter in methamphetamine-induced neurotoxicity: evidence from mice lacking the transporter. J. Neurosci. 1 (18), 4861–4869.
Fumagalli, F., Gainetdinov, R.R., Wang, Y.M., Valenzano, K.J., Miller, G.W., Caron, M.G., 1999. Increased methamphetamine neurotoxicity in heterozygous vesicular monoamine transporter 2 knock-out mice. J. Neurosci. 19, 2424–2431.
Granado, N., Escobedo, I., O'Shea, E., Colado, M.I., Moratalla, R., 2008a. Early loss of dopaminergic terminals in striosomes after MDMA administration to mice. Synapse 62, 80–84.
Granado, N., Ortiz, O., Suarez, L.M., Martin, E.D., Cena, V., Solis, J.M., et al., 2008b. D1 but not D5 dopamine receptors are critical for LTP, spatial learning, and LTP-induced arc and zif268 expression in the hippocampus. Cereb. Cortex 18, 1–12.
Granado, N., O'Shea, E., Bove, J., Vila, M., Colado, M.I., Moratalla, R., 2008c. Persistent MDMA-induced dopaminergic neurotoxicity in the striatum and substantia nigra of mice. J. Neurochem. 107, 1102–1112.
Granado, N., Ares-Santos, S., O'Shea, E., Vicario-Abejon, C., Colado, M.I., Moratalla, R., 2010. Selective vulnerability in striosomes and in the nigrostriatal dopaminergic pathway after methamphetamine administration: early loss of TH in striosomes after methamphetamine. Neurotox. Res. 18, 48–58.
Granado, N., Lastres-Becker, I., Ares-Santos, S., Oliva, I., Martin, E.D., Cuadrado, A., Moratalla, R., 2011a. Nrf2 deficiency potentiates methamphetamine-induced dopaminergic axonal damage and gliosis in the striatum. Glia. doi:10.1002/glia.21229.
Granado, N., Ares-Santos, S., Oliva, I., O'Shea, E., Martin, E.D., Colado, M.I., et al., 2011b. Dopamine D2R knockout mice are protected against dopaminergic neurotoxicity induced by methamphetamine or MDMA. Neurobiol. Dis. 42, 391–403.
Gutierrez-Lopez, M.D., Llopis, N., Feng, S., Barret, D.A., O'Shea, E., Colado, M.I., 2010. Involvement of 2-arachidonoyl glycerol in the increases consumption of and

preference for ethanol of mice treated with neurotoxic doses of methamphetamine. Br. J. Pharmacol. 160, 772–783 2010 Jun.
Imam, S.Z., el-Yazal, J., Newport, G.D., Itzhak, Y., Cadet, J.L., Slikker Jr., W., et al., 2001. Methamphetamine-induced dopaminergic neurotoxicity: role of peroxynitrite and neuroprotective role of antioxidants and peroxynitrite decomposition catalysts. Ann. N. Y. Acad. Sci. 939, 366–380 Review.
Jaber, M., Dumartin, B., Sagné, C., Haycock, J.W., Roubert, C., Giros, B., et al., 1999. Differential regulation of tyrosine hydroxylase in the basal ganglia of mice lacking the dopamine transporter. Eur. J. Neurosci. 11, 3499–34511.
Jackson-Lewis, V., Vila, M., Djaldetti, R., Guegan, C., Liberatore, G., Liu, J., et al., 2000. J. Comp. Neurol. 424, 476–488.
Jayanthi, S., Deng, X., Ladenheim, B., McCoy, M.T., Cluster, A., Cai, N.S., et al., 2005. Calcineurin/NFAT-induced up-regulation of the Fas ligand/Fas death pathway is involved in methamphetamine-induced neuronal apoptosis. Proc. Natl. Acad. Sci. U. S. A. 102, 868–873.
Jayanthi, S., McCoy, M.T., Beauvais, G., Ladenheim, B., Gilmore, K., Wood III, W., et al., 2009. Methamphetamine induces dopamine D1 receptor-dependent endoplasmic reticulum stress-related molecular events in the rat striatum. PLoS One 4, e6092.
Jia, Z., Zhu, H., Li, Y., Misra, H.P., 2009. Cruciferous nutraceutical 3H-1,2-dithiole-3-thione protects human primary astrocytes against neurocytotoxicity elicited by MPTP, MPP(+), 6-OHDA, HNE and acrolein. Neurochem. Res. 34, 1924–1934.
Jones, S.R., Gainetdinov, R.R., Jaber, M., Giros, B., Wightman, R.M., Caron, M.G., 1998. Profound neuronal plasticity in response to inactivation of the dopamine transporter. Proc. Natl. Acad. Sci. U. S. A. 95, 4029–4034.
Kil, H.Y., Zhang, J., Piantadosi, C.A., 1996. Brain temperature alters hydroxyl radical production during cerebral ischemia/reperfusion in rats. J. Cereb. Blood Flow Metab. 16, 100–106.
Krasnova, I.N., Cadet, J.L., 2009. Methamphetamine toxicity and messengers of death. Brain Res. Rev. 60, 379–407.
Krasnova, I.N., Ladenheim, B., Hodges, A.B., Volkow, N.D., Cadet, J.L., 2011. Chronic methamphetamine administration causes differential regulation of transcription factors in the rat midbrain. PLoS One 25 (6), e19179.
LaVoie, M.J., Hastings, T.G., 1999. Dopamine quinone formation and protein modification associated with the striatal neurotoxicity of methamphetamine: evidence against a role for extracellular dopamine. J. Neurosci. 19, 1484–1491.
Martín, E.D., Buño, W., 2005. Stabilizing effects of extracellular ATP on synaptic efficacy and plasticity in hippocampal pyramidal neurons. Eur. J. Neurosci. 21, 936–944.
McCann, U.D., Wong, D.F., Yokoi, F., Villemagne, V., Dannals, R.F., Ricaurte, G.A., 1998. Reduced striatal dopamine transporter density in abstinent methamphetamine and methcathinone users: evidence from positron emission tomography studies with [11C]WIN-35,428. J. Neurosci. 18, 8417–8422.
Metzger, R.R., Haughey, H.M., Wilkins, D.G., Gibb, J.W., Hanson, G.R., Fleckenstein, A.E., 2000. Methamphetamine-induced rapid decrease in dopamine transporter function: role of dopamine and hyperthermia. J. Pharmacol. Exp. Ther. 295, 1077–1085.
Moratalla, R., Xu, M., Tonegawa, S., Graybiel, A.M., 1996. Cellular responses to psychomotor stimulant and neuroleptic drugs are abnormal in mice lacking the D1 dopamine receptor. Proc. Natl. Acad. Sci. U. S. A. 93, 14928–14933.
O'Callaghan, J.P., Miller, D.B., 1994. Neurotoxicity profiles of substituted amphetamines in the C57BL/6J mouse. J. Pharmacol. Exp. Ther. 270, 741–751.
O'Dell, S.J., Weihmuller, F.B., Marshall, J.F., 1993. Methamphetamine-induced dopamine overflow and injury to striatal dopamine terminals: attenuation by dopamine D1 or D2 antagonists. J. Neurochem. 60, 1792–1799.
Ortiz, O., Delgado-García, J.M., Espadas, I., Bahí, A., Trullas, R., Dreyer, J.L., et al., 2010. Associative learning and CA3-CA1 synaptic plasticity are impaired in D1R null, Drd1a$^{-/-}$ mice and in hippocampal siRNA silenced Drd1a mice. J. Neurosci. 30, 12288–12300.
Pavon, N., Martin, A.B., Mendialdua, A., Moratalla, R., 2006. ERK phosphorylation and FosB expression are associated with L-DOPA-induced dyskinesia in hemiparkinsonian mice. Biol. Psychiatry 59, 64–74.
Seiden, L.S., Fischman, M.W., Schuster, C.R., 1976. Long-term methamphetamine induced changes in brain catecholamines in tolerant rhesus monkeys. Drug Alcohol Depend. 1, 215–219.
Sonsalla, P.K., Gibb, J.W., Hanson, G.R., 1986. Roles of D1 and D2 dopamine receptor subtypes in mediating the methamphetamine-induced changes in monoamine systems. J. Pharmacol. Exp. Ther. 238, 932–937.
Sonsalla, P.K., Jochnowitz, N.D., Zeevalk, G.D., Oostveen, J.A., Hall, E.D., 1996. Treatment of mice with methamphetamine produces cell loss in the substantia nigra. Brain Res. 738, 172–175.
Spencer, J.P., Whiteman, M., Jenner, P., Halliwell, B., 2002. 5-s-Cysteinyl-conjugates of catecholamines induce cell damage, extensive DNA base modification and increases in caspase-3 activity in neurons. J. Neurochem. 81, 122–129.
Sriram, K., Miller, D.B., O'Callaghan, J.P., 2006. Minocycline attenuates microglial activation but fails to mitigate striatal dopaminergic neurotoxicity: role of tumor necrosis factor-alpha. J. Neurochem. 96, 706–718.
Tata, D.A., Raudensky, J., Yamamoto, B.K., 2007. Augmentation of methamphetamine induced toxicity in the rat striatum by unpredictable stress: contribution of enhanced hyperthermia. Eur. J. Neurosci. 26, 739–748.
Thomas, D.M., Dowgiert, J., Geddes, T.J., Francescutti-Verbeem, D., Liu, X., Kuhn, D.M., 2004. Microglial activation is a pharmacologically specific marker for the neurotoxic amphetamines. Neurosci. Lett. 367, 349–354.
Thomas, D.M., Francescutti-Verbeem, D.M., Kuhn, D.M., 2008a. Methamphetamine-induced neurotoxicity and microglial activation are not mediated by fractalkine receptor signaling. J. Neurochem. 106, 696–705.
Thomas, D.M., Francescutti-Verbeem, D.M., Kuhn, D.M., 2008b. The newly synthesized pool of dopamine determines the severity of methamphetamine-induced neurotoxicity. J. Neurochem. 105, 605–616.
Tinsley, R.B., Bye, C.R., Parish, C.L., Tziotis-Vais, A., George, S., Culvenor, J.G., et al., 2009. Dopamine D2 receptor knockout mice develop features of Parkinson disease. Ann. Neurol. 66, 472–484.
UNODC, World Drug Report, 2010. United Nations Publication, Sales No.E.10.XI.13.
Volkow, N.D., Chang, L., Wang, G.J., Fowler, J.S., Franceschi, D., Sedler, M., et al., 2001. Loss of dopamine transporters in methamphetamine abusers recovers with protracted abstinence. J. Neurosci. 21, 9414–9418.
Volz, T.J., Hanson, G.R., Fleckenstein, A.E., 2006. Measurement of kinetically resolved vesicular dopamine uptake and efflux using rotating disk electrode voltammetry. J. Neurosci. Methods 155, 109–115.
Wightman, R.M., Zimmerman, J.B., 1990. Control of dopamine extracellular concentration in rat striatum by impulse flow and uptake. Brain Res. Rev. 15, 135–144.
Xie, T., McCann, U.D., Kim, S., Yuan, J., Ricaurte, G.A., 2000. Effect of temperature on dopamine transporter function and intracellular accumulation of methamphetamine: implications for methamphetamine-induced dopaminergic neurotoxicity. J. Neurosci. 20, 7838–7845.
Xu, M., Moratalla, R., Gold, L.H., Hiroi, N., Koob, G.F., Graybiel, A.M., et al., 1994. Dopamine D1 receptor mutant mice are deficient in striatal expression of dynorphin and in dopamine-mediated behavioral responses. Cell 79, 729–742.
Xu, W., Zhu, J.P., Angulo, J.A., 2005. Induction of striatal pre- and postsynaptic damage by methamphetamine requires the dopamine receptors. Synapse 58, 110–121.
Yamamoto, B.K., Moszczynska, A., Gudelsky, G.A., 2010. Amphetamine toxicities: classical and emerging mechanisms. Ann. N. Y. Acad. Sci. 1187, 101–121.
Zhang, L., Shirayama, Y., Shimizu, E., Iyo, M., Hashimoto, K., 2006. Protective effects of minocycline on 3,4-methylenedioxymethamphetamine-induced neurotoxicity in serotonergic and dopaminergic neurons of mouse brain. Eur. J. Pharmacol. 44, 1–3.
Zhu, J.P., Xu, W., Angulo, J.A., 2005. Disparity in the temporal appearance of methamphetamine-induced apoptosis and depletion of dopamine terminal markers in the striatum of mice. Brain Res. 1049, 171–181.

3. Dopamine D2-receptor knockout mice are protected against dopaminergic neurotoxicity induced by methamphetamine or MDMA.

Granado N, Ares-Santos S, Oliva I, O'Shea E, Martin ED, Colado MI, Moratalla R (2011a). *Neurobiol Dis.* **42**:391-403.. doi: 10.1016/j.nbd.2011.01.033.

Neurobiology of Disease 42 (2011) 391–403

Contents lists available at ScienceDirect

Neurobiology of Disease

journal homepage: www.elsevier.com/locate/ynbdi

Dopamine D2-receptor knockout mice are protected against dopaminergic neurotoxicity induced by methamphetamine or MDMA

Noelia Granado [a,c], Sara Ares-Santos [a,b], Idaira Oliva [d], Esther O´Shea [c], Eduardo D. Martin [d], M. Isabel Colado [c], Rosario Moratalla [a,b,*]

[a] Instituto Cajal, Consejo Superior de Investigaciones Científicas, CSIC, 28002 Madrid, Spain
[b] CIBERNED, Instituto de Salud Carlos III, Madrid, Spain
[c] Departamento de Farmacología, Facultad de Medicina, Universidad Complutense de Madrid, 28040 Madrid, Spain
[d] Laboratorio de Neurofisiología y Plasticidad Sináptica, Parque Científico y Tecnológico de Albacete (PCYTA). Instituto de Investigación en Discapacidades Neurológicas (IDINE), Universidad de Castilla-La Mancha, Albacete, Spain

ARTICLE INFO

Article history:
Received 30 December 2010
Accepted 28 January 2011
Available online 15 February 2011

Keywords:
Ecstasy
TH
DAT
Dopamine
Neurotoxicity
Neurodegeneration

ABSTRACT

Methamphetamine (METH) and 3,4-methylenedioxymethamphetamine (MDMA), amphetamine derivatives widely used as recreational drugs, induce similar neurotoxic effects in mice, including a marked loss of tyrosine hydroxylase (TH) and dopamine transporter (DAT) in the striatum. Although the role of dopamine in these neurotoxic effects is well established and pharmacological studies suggest involvement of a dopamine D2-like receptor, the specific dopamine receptor subtype involved has not been determined. In this study, we used dopamine D2 receptor knock-out mice (D2R $^{-/-}$) to determine whether D2R is involved in METH- and MDMA-induced hyperthermia and neurotoxicity. In wild type animals, both drugs induced marked hyperthermia, decreased striatal dopamine content and TH- and DAT-immunoreactivity and increased striatal GFAP and Mac-1 expression as well as iNOS and interleukin 15 at 1 and 7 days after drug exposure. They also caused dopaminergic cell loss in the SNpc. Inactivation of D2R blocked all these effects. Remarkably, D2R inactivation prevented METH-induced loss of dopaminergic neurons in the SNpc. In addition, striatal dopamine overflow, measured by fast scan cyclic voltammetry in the presence of METH, was significantly reduced in D2R $^{-/-}$ mice. Pre-treatment with reserpine indicated that the neuroprotective effect of D2R inactivation cannot be explained solely by its ability to prevent METH-induced hyperthermia: reserpine lowered body temperature in both genotypes, and potentiated METH toxicity in WT, but not D2R $^{-/-}$ mice. Our results demonstrate that the D2R is necessary for METH and MDMA neurotoxicity and that the neuroprotective effect of D2R inactivation is independent of its effect on body temperature.

Introduction

Methamphetamine (METH) and 3,4-methylenedioxymethamphetamine (MDMA) are powerful psychostimulants widely used as recreational drugs despite having been shown to be potent neurotoxins in the brains of rodents and non-human primates. In mice, repeated administration of either of the two drugs produces neurodegeneration of dopamine axon terminals in the striatum (Granado et al., 2008a,b; Krasnova and Cadet, 2009) and cell body loss in the substantia nigra (Granado et al., 2010). Damage has been demonstrated both histologically (Granado et al., 2008a, 2010; O'Callaghan and Miller, 1994; Sonsalla et al., 1996) and biochemically (Colado et al., 2001; Escobedo et al., 2005; Mann et al., 1997; O'Shea et al., 2003) and is reflected as a substantial decrease in the concentration of dopamine and its metabolites, a loss in the density of plasmalemmal (DAT) and vesicular dopamine transporters, and a decrease in tyrosine hydroxylase (TH) activity. Recent evidence demonstrates that striatal striosomes are more vulnerable than the matrix to both METH- and MDMA-induced TH/DAT-immunoreactivity loss while the mesolimbic dopaminergic pathway is not altered significantly by either of the two drugs (Granado et al. 2008a,b; 2010). Both drugs also cause reactive astrocytosis and microgliosis (Fantegrosi et al., 2008; Krasnova and Cadet, 2009; Thomas et al., 2004, 2008).

The mechanisms underlying this neurodegeneration are not fully understood at present, but a considerable body of data indicates that oxidative stress, excitotoxicity, hyperthermia, neuroinflammatory responses, microglial activation, mitochondrial dysfunction, and endoplasmic reticulum stress are involved. Several lines of evidence implicate dopamine in methamphetamine-induced neurotoxicity. First, α-methyl-p-tyrosine, which reduces dopamine synthesis,

* Corresponding author at: Instituto Cajal, CSIC, Avd. Dr. Arce 37, 28002 Madrid, Spain. Fax: +34 91 585 4754.
E-mail address: moratalla@cajal.csic.es (R. Moratalla).
Available online on ScienceDirect (www.sciencedirect.com).

0969-9961/$ – see front matter © 2011 Elsevier Inc. All rights reserved.
doi:10.1016/j.nbd.2011.01.033

decreases METH's toxic effects while L-DOPA, which restores cytoplasmic DA levels, enhances METH-induced toxicity (Thomas et al., 2008). Dopamine's role in METH toxicity is also supported by studies showing that dopamine induces production of reactive oxygen species (ROS) and oxidative stress. After displacement to the cytoplasm by METH, DA rapidly auto-oxidizes to form potentially toxic substances including superoxide radicals, hydroxyl radicals, hydrogen peroxide, and DA quinones (Cubells et al., 1994; LaVoie and Hastings, 1999; Larsen et al., 2002; Miyazaki et al., 2006). In addition, METH alters the balance between ROS production and the capacity of antioxidant enzyme systems to scavenge ROS, further amplifying the state of oxidative stress (Chen et al., 2007; Gluck et al., 2001; Jayanthi et al., 1998).

Pharmacological studies implicate the D2-like receptor family in METH neurotoxicity. Sulpiride dose-dependently blocked METH toxicity in mice, and eticlopride and raclopride prevented striatal dopamine loss induced by METH (Albers and Sonsalla, 1995; Eisch and Marshall, 1998; Metzger et al., 2000; but see also Hadlock et al., 2010). However, these compounds cannot differentiate between D2, D3 and D4 receptors, thus the possible contribution of each dopamine receptor subtype has not been demonstrated definitively. Due to its presynaptic location and its role in regulating dopamine release, the D2R is a particularly good candidate for involvement in METH-induced dopamine terminal loss.

To provide conclusive evidence that the dopamine D2R subtype is involved in METH toxicity, we examined the hyperthermic response and the loss of dopamine fibers and neurons following repeated administration of METH or MDMA in dopamine D2 receptor knockout ($D2R^{-/-}$) and WT mice. We assessed striatal density of TH/DAT positive terminals, expression of pro-inflammatory molecules and dopamine concentration in the striatum. We also quantified TH-positive neurons in the substantia nigra (SN) and striatal dopamine overflow in the presence of METH or MDMA.

Materials and methods

Animals and treatment

Experiments were carried out in 3- to 6-month-old female dopamine D2 receptor knockout ($D2R^{-/-}$) mice generated by homologous recombination as previously described (Kelly et al., 1997) and in female wild-type (WT) littermates. The mice used in this study were derived from mating heterozygous mice. Genotype was determined by polymerase chain reaction analysis. Mice were housed in groups of 4–6 per cage, in conditions of constant temperature (21–22 °C) and a 12 h light/dark cycle (lights on 7:00 am) and given free access to food and water. Animals were treated in accordance with European Community guidelines (86/609/ECC), and all procedures were approved by the Bioethical Committee at the Instituto Cajal.

Mice received a neurotoxic regimen of three injections of either (+)-METH (4 mg/kg, i.p.) or (±)-MDMA (30 mg/kg, i.p.) at 3 h intervals (O'Shea et al., 2003). Animals were sacrificed 1 or 7 days after drug administration. The doses and protocol of administration were previously shown to produce marked depletion of mouse striatal dopamine (Colado et al., 2001; Granado et al., 2008a). Both drugs were dissolved in 0.9% w/v NaCl (saline) and injected in a volume of 10 ml/kg. METH hydrochloride was obtained from Sigma-Aldrich (St. Louis, MO, USA) and MDMA hydrochloride from National Institute of Drug Abuse (NIH, USA). Doses are quoted in terms of the base. Reserpine (3 mg/kg, i.p. Sigma) was administered 18 h before METH and was dissolved in 0.1% acetic acid.

For the elevated ambient temperature experiment, $D2R^{-/-}$ mice receiving METH were maintained at a room temperature of 29±2 °C for 2 h prior to treatment, during the injection paradigm, and for 1 h following the last injection.

Measurement of rectal temperature

Rectal temperature was measured using a digital readout thermocouple (BAT-12 thermometer, Physitemp Instruments, Clifton, NJ, USA) with a resolution of 0.1 °C and accuracy of ±0.1 °C attached to a RET-3 Rodent Sensor. The sensor was inserted 2 cm into the mouse rectum, while the mouse was lightly restrained by holding the hand. A steady readout was obtained within 10 s of probe insertion. Temperature readings were taken every 30 min immediately before and after MDMA and METH injections and hourly thereafter.

Measurement of dopamine and its metabolites in the striatum

One and 7 days after METH treatment and 7 days after MDMA, mice were killed by cervical dislocation and decapitation, the brains were rapidly removed, and the striatum dissected out on ice. Dopamine and the metabolites, 3,4-dihydroxyphenylacetic acid (DOPAC) and homovanillic acid (HVA), were measured by high-performance liquid chromatography and electrochemical detection. The mobile phase consisted of KH_2PO_4 (0.05 M), octanesulfonic acid (0.4 mM), EDTA (0.1 mM), and methanol (16%) and was adjusted to pH 3 with phosphoric acid, filtered, and degassed. The flow rate was 1 ml/min. The high-performance liquid chromatography system consisted of a pump (Waters 510) linked to an automatic sample injector (Loop 200 µl, Waters 717 plus Autosampler) and a stainless steel reversed-phase column (Spherisorb ODS2, 5 µm, 150×4.6 mm; Waters, Milford, MA) with a precolumn and a coulometric detector (Coulochem II; Esa, Chelmsford, MA). The working electrode potential was set at 400 mV with a gain of 1 µA (for dopamine) and 500 nA (for the remaining compounds). The current produced was monitored by means of integration software (Clarity Software, DataApex, Prague, Czech Republic).

Immunohistochemistry

Animals were anaesthetized with pentobarbital (50 mg/kg, i.p.) and then perfused with 4% paraformaldehyde dissolved in PB (phosphate buffer, pH 7.4). After perfusion, brains were dissected and immersed overnight in the same fixative solution. Coronal brain sections (30 µm) were obtained on a slicing vibratome (Leica, Madrid, Spain) and kept in PB solution at 4 °C until use. Immunostaining was carried out on free-floating sections with a standard avidin-biotin immunohistochemical protocol previously described (Darmopil et al., 2008, 2009; Granado et al., 2008c; Pavon et al., 2006). Endogenous peroxidase activity was removed by incubation in 3% H_2O_2 for 10 min. Sections were preblocked with normal goat serum (NGS; Vector Laboratories, Burlingame, CA, USA) for 1 h. The sections were incubated overnight with specific primary antisera (Ab-I): rabbit tyrosine hydroxylase antiserum (TH) (1:1000, Chemicon International, Temecula, CA, USA); rat monoclonal antibody against dopamine transporter (DAT) (1:1000, Chemicon International); rabbit anti-glial fibrillary acidic protein antibody (GFAP) (1:1000, DakoCytomation, Denmark) or antibody directed against Mac-1 (or CD-11b) (1:500, Serotec, UK); goat anti-mouse interleukin 15 (IL-15, used at 1:200, Santa Cruz Biotechnologies, Santa Cruz, CA, USA) and a polyclonal antiserum against iNOS (1:4000, gift from Dr. R Martínez, Instituto Cajal, CSIC, Madrid, Spain). All primary antibodies were prepared in PBST solutions containing NGS. After careful washing, the sections were incubated with the secondary biotinylated secondary antisera (Vector) at room temperature and developed using diaminobenzidine (DAB). The reaction was monitored every 5 min using an optical microscope (Leica). After washing, the sections were mounted on gelatin-coated slides, air-dried, dehydrated in ascending concentrations of ethanol, cleared with xylene and coverslipped under Permount. Quantification of expression of TH and DAT was performed with the aid of an image analysis system (Analytical Imaging Station, Imaging Research Inc., Linton, UK) using a 5× lens,

converting color intensities into a gray scale and quantifying area of staining in treated animals as a proportion of that in untreated animals (Granado et al., 2010).

Stereological quantification of TH positive neurons in SNpc

The total number of TH-positive SNpc neurons was counted in the different groups of animals using the optical fractionator (Granado et al., 2008b). This unbiased method of cell counting is not affected by either the volume of reference (SNpc) or the size of the counted element (neurons). Immunostaining was performed with a polyclonal antibody to TH (1:1000, Chemicon International). TH-stained neurons were counted in the left SNpc of every fourth section throughout the entire extent of the SNpc (Granado et al., 2008b). Each midbrain section was viewed at low power (10× objective) and the SNpc was outlined using the set of anatomic landmarks defined previously (Granado et al., 2008b). Starting at a random microscope visual field, the number of TH-stained cells was counted at high power (100×). To avoid double counting of neurons with unusual shapes, TH-stained cells were counted only when their nuclei were optimally visualized which occurred only in one focal plane. In addition, neurons were differentiated from nonneuronal cells, including glia, on the Nissl stain by excluding cells that did not have a clearly defined nucleus, cytoplasm and a prominent nucleolus; although these criteria may have excluded some small neurons, it should have reliably excluded all nonneuronal cells.

Fluoro-Jade C staining

Coronal brain sections (30 μm) were obtained on a slicing vibratome as described above. The sections were mounted on gelatin-coated slides and allowed to dry fully for 20 min after which they were immersed in 100% ethyl alcohol for 3 min followed by a 1 min soak in 70% alcohol and a 1 min soak in distilled water. The slides were then transferred to a solution of 0.06% potassium permanganate for 15 min. The slides were rinsed for 1 min in distilled water and were then transferred to the Fluoro-Jade staining solution where they were gently agitated for 30 min. The 0.001% working solution of Fluoro-Jade was prepared by adding 10 ml of the stock Fluoro-Jade solution (0.01%) to 90 ml of 0.1% acetic acid in distilled water (Granado et al., 2008b; Schmued et al., 1997). After staining, sections were rinsed 3 times for 1 min each with fresh changes of distilled water. Excess water was drained off. When dry, the slides were immersed in xylene and coverslipped with D.P.X. mounting media. Sections were examined with a fluorescence microscope using a filter system suitable for visualizing fluorescein or FITC.

Electrochemical recordings in brain slices

Transverse brain slices (450 μm thickness) were prepared from mice using conventional methods (Martín and Buño, 2005), and incubated for >1 h at room temperature (21–24 °C) in artificial cerebrospinal fluid (aCSF). The aCSF contained (in mM): NaCl 124, KCl 2.69, KH_2PO_4 1.25, $MgSO_4$ 2, $NaHCO_3$ 26, $CaCl_2$ 2 and glucose 10, and was gassed with 95% O_2 and 5% CO_2. Slices were transferred to an immersion recording chamber and superfused (2.5 ml/min) with gassed aCSF warmed to 32–34 °C. Following 1 h of equilibration, a bipolar tungsten stimulating electrode with a tip separation of 200 μM (A-M Systems, Inc., Carlsborg, WA, USA) was placed in the dorsolateral striatum (Fig. 9A). A carbon fibre electrode (CFE; 10 μm diameter; 50 μm exposed length) was placed 100–200 μm from stimulating electrode. Fast scan cyclic voltammetry (FSCV) at the CFE was used to detect changes in extracellular concentrations of dopamine following electrical stimulation of the brain slice. Stimuli were single biphasic pulses (20 V, 500 μs) delivered via a 2100 isolated pulse stimulator (A-M Systems). Stimulus intervals between pulses were not less than 5 min. FSCV was carried out using a three electrode voltage-clamp amplifier (VAMP-1, Registim LLC, Coral Gables, FL, USA). The working electrode was connected to active CFE, an Ag/AgCl was used as reference electrode, and a platinum wire was used as auxiliary electrode. Using the common reference and auxiliary electrodes, a brief sawtooth voltage waveform with a voltage scan rate of 400 V/s was applied consecutively every 200 ms to working CFE electrode. The sawtooth had four phases: 0 to −1 V, to +1.4 V, to −1 V to 0 V (Fig. 8A). Changes in extracellular dopamine were determined by monitoring the current at the peak oxidation potential for dopamine. Subtracting the current obtained before stimulation from the current obtained in the presence of dopamine created background-subtracted cyclic voltammograms. Current was digitized at 10 kHz using PowerLab 4/25T (AD Instruments, Bella Vista, Australia) acquisition system. Data were acquired and analyzed with Scope software (AD Instruments). Electrodes were calibrated with DA standards of known concentration in the recording chamber before and after each use. The average of the pre- and post-calibration measurements was used as the calibration factor.

Statistics

Data are presented as mean ± standard error of the mean (S.E.M.). The results of rectal temperature measurements were analyzed using two-way analysis of variance (ANOVA) for repeated measures.

Data obtained from image analysis of striatal TH and DAT immunostaining were analyzed using two-way ANOVA. Relevant differences were analyzed pair-wise by post-hoc comparisons with Newman Keuls and Tukey test, to determine specific group differences. All statistical analyses were performed using SigmaStat 2.03 program and the threshold for statistical significance was set at $p<0.05$. Graphical representations were obtained using SigmaPlot 9.0 software.

Results

Inactivation of D2R blocks METH- and MDMA-induced hyperthermia

In WT animals, administration of METH (4 mg/kg, i.p., 3 injections given at 3 h intervals) or MDMA (30 mg/kg, i.p., 3 injections given at 3 h intervals) resulted in significantly higher rectal temperatures after each injection compared with saline-treated animals. In contrast, we observed a decrease in rectal temperature after METH or MDMA administration in $D2R^{-/-}$ animals, which was especially pronounced following the first injection, with a significant decrease of 2.0 and 2.2 °C after METH or MDMA, respectively (Fig. 1A, C). Following the second injection, the decrease was moderate but significant (0.5 and 0.9 °C after METH and MDMA, respectively) and with the third injection, the temperature did not differ from that observed in the same genotype animals, $D2R^{-/-}$ mice, treated with saline.

Inactivation of D2R prevents the striatal dopamine loss induced by METH and MDMA

In basal conditions, dopamine levels were similar in WT and $D2R^{-/-}$ mice (Fig 1) although DOPAC and HVA levels were increased in $D2R^{-/-}$ mice compared to WT animals as previously shown (Tinsley et al., 2009). Administration of METH (4 mg/kg, i.p., 3 times at 3 h intervals) to WT mice reduced the striatal dopamine concentration at both 1 (83.5%; $p<0.001$) and 7 (50.0 %; $p<0.01$) days after injection compared with saline-treated animals. In $D2R^{-/-}$ mice this effect was smaller at 1 day after METH injection (34.1%; $p<0.01$) and by 7 days after treatment there was no significant difference in striatal dopamine content between METH- and saline-treated mice (Fig. 1B). At both 1 and 7 days after METH administration, striatal dopamine levels were significantly different in WT and $D2R^{-/-}$ mice ($p<0.001$ and $p<0.05$, respectively). Striatal concentrations of DOPAC and HVA were similarly affected by METH in WT and $D2R^{-/-}$ mice (data not shown).

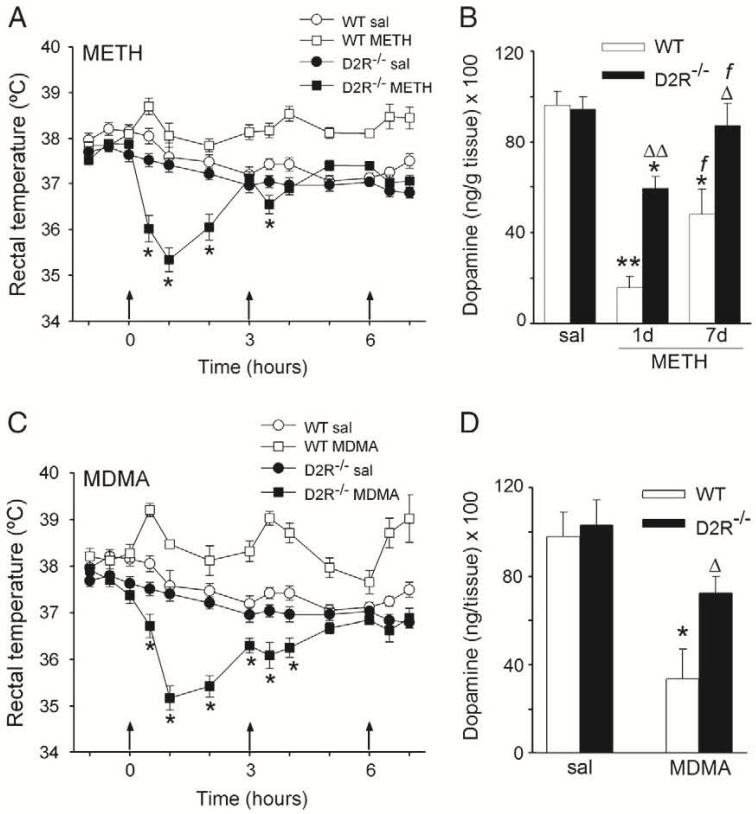

Fig. 1. Inactivation of D2R prevents hyperthermia and loss of striatal dopamine following administration of METH or MDMA. Methamphetamine (A; 4 mg/kg, i.p., every 3 h, ×3) and MDMA (C; 30 mg/kg, i.p., every 3 h, ×3) increased rectal temperature in WT animals, peaking 30 min after each injection. In D2R$^{-/-}$ mice, neither drug induced an increase in rectal temperature, instead producing pronounced hypothermia (A, C). Arrows indicate drug injections. Histograms in B and D show concentrations of dopamine (mean ± SEM, $n = 6–8$) in the striatum of mice 1 or 7 days after METH and 7 days after MDMA. *$p<0.01$, **$p<0.001$ vs. saline group; $^{\Delta}p<0.01$, $^{\Delta\Delta}p<0.001$ vs. WT and *f* indicates $p<0.05$ vs. day 1. Statistical analysis was by two-way ANOVA followed by Bonferroni's test.

Seven days after MDMA administration (30 mg/kg, i.p., 3 times at 3 h intervals) there was a significant reduction (65.7 %) in the striatal dopamine content in WT mice compared with saline-treated mice ($p<0.01$). No significant decrease in dopamine concentration was seen in D2R$^{-/-}$ mice (13.3% lower compared to saline-treated mice, $p = 0.3$). As observed with METH, there was a significant difference in striatal dopamine concentration in WT and D2R$^{-/-}$ mice 7 days after treatment with MDMA ($p<0.01$) (Fig. 1D). Striatal 5-HT and 5-HIAA concentrations were not altered by METH or MDMA in WT or D2R$^{-/-}$ mice (data not shown).

Inactivation of D2R prevents METH- or MDMA-induced loss of dopaminergic fibers in mouse striatum

Consistent with previous reports (Granado et al., 2010; Krasnova and Cadet, 2009) we observed a decrease in the density of TH-immunoreactive (TH-ir) fibers in striatum of WT animals 1 and 7 days after METH and 7 days following MDMA administration. Although TH fiber loss was homogeneous along the rostro-caudal axis (Fig. 2, first row), we observed a slightly greater loss in the lateral part of the striatum, as we reported previously (Granado et al., 2008b, 2010). This loss of striatal TH-ir appeared to be greatly inhibited in D2R$^{-/-}$ mice at 1 day following METH injection and completely reversed in D2R$^{-/-}$ mice 7 days following MDMA or METH injection (Fig. 2, second row).

Quantitative image analysis verified these findings, revealing significant decreases in TH-ir fibers in WT animals treated with METH compared with saline-treated mice: 75.8% at 1 day post-METH administration and 43.5% at 7 days ($p<0.001$ for both). In contrast, in D2R$^{-/-}$ mice, there was a significant but smaller reduction in TH-ir fibers at 1 (30.4%; $p<0.001$) and 7 (16.4%; $p<0.05$) days after METH treatment compared with saline-treated mice. MDMA administration induced loss of TH-ir fibers at 7 days after injection in WT mice (68.0%; $p<0.001$) but not in D2R$^{-/-}$ mice, $p = 0.7$, (Fig. 2, histograms).

As expected, the pattern of DAT-ir loss was very similar to the pattern of TH-ir loss, with a homogeneous decrease in DAT-ir fibers along the rostro-caudal axis, and a greater loss of DAT-ir fibers in the lateral parts of the striatum (Fig. 2, third row). Quantification of DAT-ir revealed significant decreases in striatum of METH-treated WT mice 1 (50.9%; $p<0.001$) and 7 (31.2%; $p<0.01$) days after drug administration whereas METH treatment did not alter DAT-ir in striatum of D2R$^{-/-}$ mice at any time point studied, $p = 0.15$ and $p = 0.7$ at 1 and 7 days, respectively, after treatment (Fig. 2, fourth row and histograms). Similarly, WT mice treated with MDMA showed a significant decrease in DAT-ir (Fig. 2 third row; 74.9%; $p<0.001$) compared with saline-treated animals. This effect was not observed in D2R$^{-/-}$ mice, $p = 0.9$ (Fig. 2, bottom row and histograms).

Inactivation of D2R prevents hyperthermia and striatal dopaminergic fiber loss induced by METH, even at high (29–30 °C) ambient temperature

Since METH administration does not produce a hyperthermic response in D2R$^{-/-}$ mice maintained at normal ambient temperature, we exposed D2R$^{-/-}$ mice to a high ambient temperature during METH treatment in an attempt to induce hyperthermia. WT mice were kept at 23 °C because of death risk. D2R$^{-/-}$ were placed at an

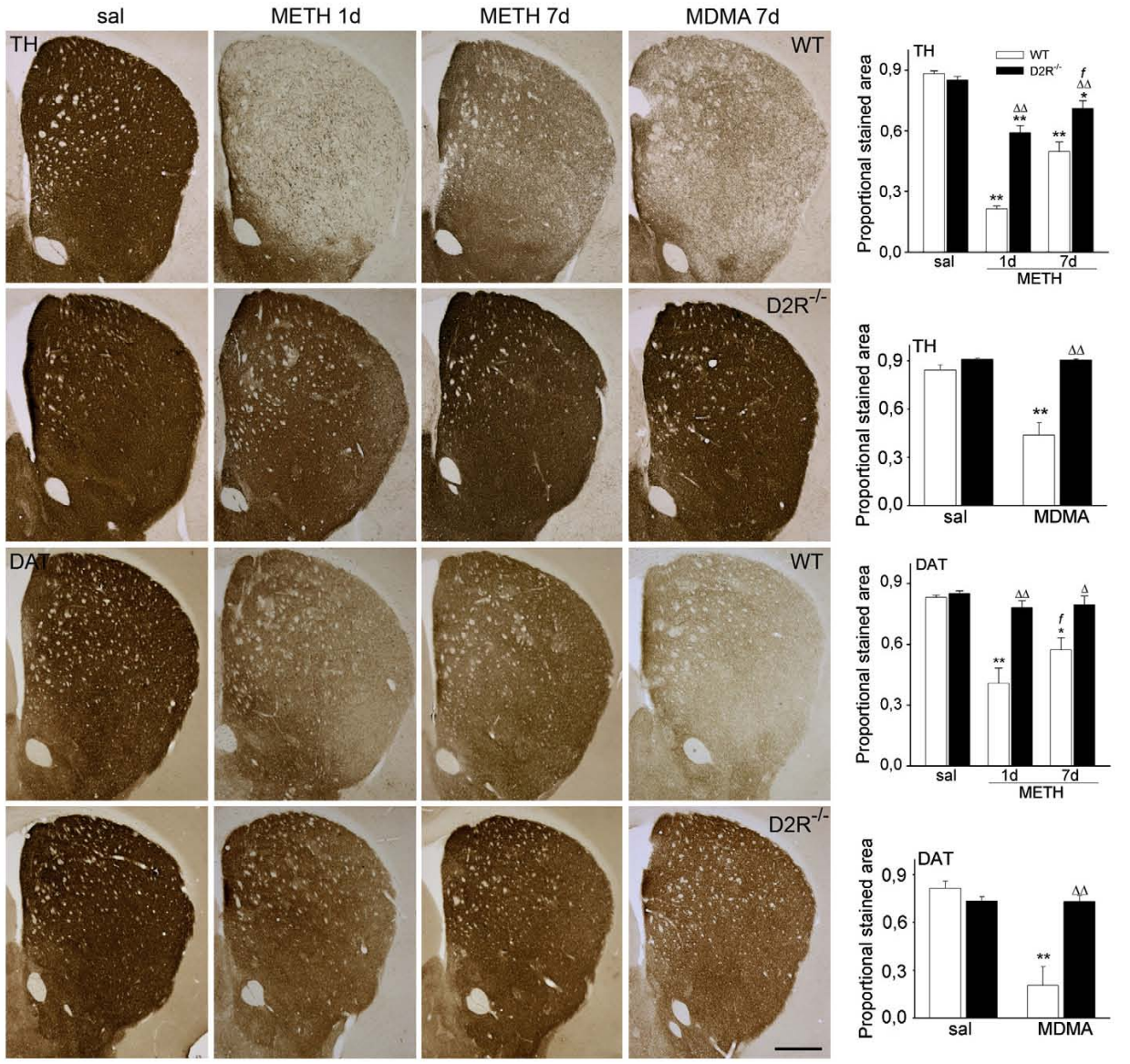

Fig. 2. Genetic inactivation of D2R prevents decreases in striatal TH- and DAT-immunoreactivity after METH or MDMA administration. Photomicrographs of striatal sections stained for TH (top two rows) and DAT (bottom two rows) from mice 1 and 7 days after treatment with METH or 7 days after MDMA. Histograms show the proportional stained area of TH- or DAT-ir in the striatum. Data represent mean ± S.E.M., $n = 6–8$ per group. $^{*}p<0.01$, $^{**}p<0.001$ vs. saline; $^{\Delta}p<0.01$ and $^{\Delta\Delta}p<0.001$ vs. WT and *f* indicates $p<0.05$ vs. day 1; two-way ANOVA followed by Bonferroni's test. Bar indicates 500 μm.

ambient temperature of 29–30 °C for 2 h before, during, and for 1 h following the last METH injection. Even with elevated ambient temperature, there was no hyperthermic response to any of the METH injections administered to D2R$^{-/-}$ mice. Instead, we observed a hypothermic response nearly identical to that observed in D2R$^{-/-}$ mice maintained at standard ambient temperature (Fig. 3A).

We also examined dopaminergic fibers in D2R$^{-/-}$ mice treated with METH at 29–30 °C. Seven days after METH administration at the elevated temperature, there was no difference in TH-ir compared with the saline group (Fig. 3B, E). In fact, TH-ir was similar to what we observed in these animals (D2R$^{-/-}$) treated with METH at 23 °C shown here again for better comparisons (Fig. 3B, E). Similar results were obtained for DAT-ir, thus, DAT-ir was similar in D2R$^{-/-}$ treated with METH at 23 or 30 °C ambient temperature (Fig. 3C, F).

Pre-treatment with reserpine does not reduce the neuroprotective effect of D2R inactivation against METH toxicity

In an attempt to dissociate the effect of D2R inactivation on hypothermia from its effect on METH toxicity, we treated animals with reserpine, a monoamine depleting compound that induces hypothermia in rodents. Reserpine treatment caused a potent hypothermia at 18 h after treatment in both genotypes, which was more pronounced in WT (24 °C) than in D2R$^{-/-}$ (26 °C) animals (Fig. 4A). METH administration in reserpinized mice caused a significant increase in rectal temperature in both genotypes (37.2 °C for WT and 35.4 °C for D2R$^{-/-}$, Fig. 4A). Although the magnitude of the METH-induced increase in body temperature was greater in reserpinized animals, the temperature attained in both

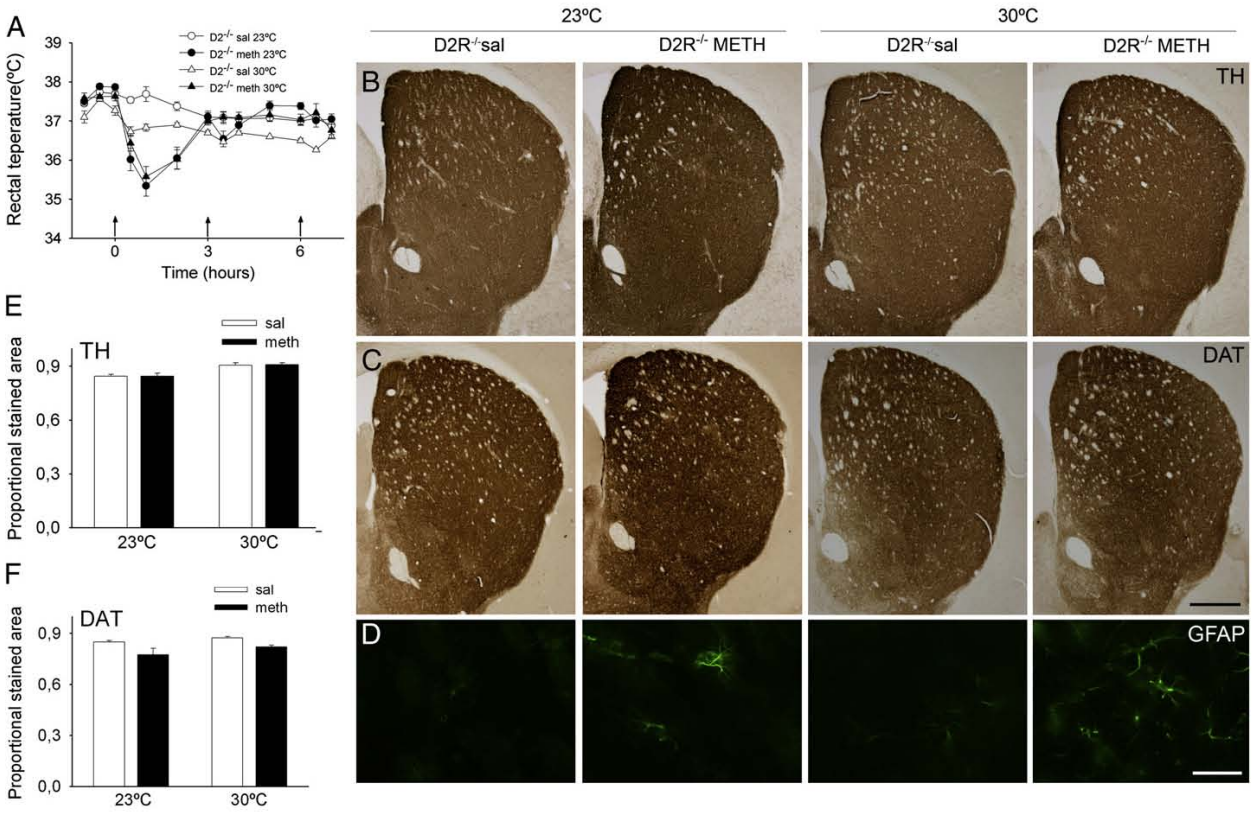

Fig. 3. Inactivation of D2R prevents the hyperthermia and striatal dopaminergic fiber loss induced by METH, even at high ambient temperature (30 °C). METH was unable to increase rectal temperature in $D2R^{-/-}$ mice (A). Arrows indicate drug injections. B–D. Striatal sections from $D2R^{-/-}$ mice 7 days after treatment with METH or saline at 23 or 30 °C, stained for TH (B), DAT (C) or GFAP (D). There is no loss of TH- or DAT-ir and no increase in GFAP-ir in $D2R^{-/-}$ mice at either temperature. Histograms show the proportional stained area of TH-ir (E) and DAT-ir (F) in the striatum of sections shown in B and C. Data represent the mean ± S.E.M., $n = 6–8$ per group. Bar indicates 500 μm (B, C) and 50 μm (D).

genotypes after METH treatment was significantly lower than in non-reserpinized WT animals after METH ($p<0.01$, Fig. 4A) and remained slightly below normal rectal temperature for at least 7 h after METH treatment. We measured TH and DAT immunoreactivity 7 days after METH or vehicle treatment. While reserpine slightly increased TH levels in both genotypes, METH induced a dramatic further reduction in TH and DAT levels in reserpinized WT mice (Fig. 4B, C). Thus, despite its hypothermic effect, reserpine strongly potentiated the neurotoxic effect of METH in WT animals, reducing TH-ir staining by 70% compared to WT animals treated with METH alone. The combined reserpine/METH treatment also reduced TH and DAT levels in $D2R^{-/-}$ animals. However, this effect was significantly smaller: there was only an 11% decrease in TH-ir levels compared to animals treated with METH alone. Similar data was obtained with DAT-ir quantification (Fig. 4B, C). Interestingly, METH treatment in $D2R^{-/-}$ mice and in reserpinized WT mice produced similar rectal temperatures (see Fig. 4A′); however, the extent of TH- and DAT-ir loss was very different in these two groups (2% for $D2R^{-/-}$ and 87% for WT for TH, with similar data for DAT), indicating that in these cases dopamine damage does not correlate with rectal temperature. Together, these results suggest that the neuroprotection afforded by D2R inactivation is not solely due to its ability to block hyperthermia.

Inactivation of D2R prevents MDMA- or METH-induced striatal gliosis in mice

Following METH or MDMA injection, astroglia and microglia were examined with antibodies against glial fibrillar acidic protein (GFAP) and Mac-1, respectively, to assess gliosis in the striatum. At 1 and 7 days after METH injections and 7 days after MDMA administration, there was an increase in GFAP immunoflourescence in the caudoputamen of WT mice compared with saline-treated animals, as seen previously (Granado et al., 2008b, 2010) but little or no increase in caudoputamen of $D2R^{-/-}$ mice (Fig. 5). In addition, following drug treatment, the stained astrocytes in WT mice displayed a characteristic reactive cell morphology which was not as evident in the $D2R^{-/-}$ mice (Fig. 5). Moreover, this little increase in GFAP expression observed following METH treatment in $D2R^{-/-}$ maintained at 23 °C was similar to that observed in mice treated with METH at the high ambient temperature, 30 °C, shown in Fig. 3D.

An increase in Mac-1 (CD11b) staining was observed in the striatum one day after METH administration to WT mice (Fig. 6). Inactivation of D2R completely inhibited this METH-induced increase in Mac-1 staining (Fig. 6). Seven days after METH or MDMA treatment, there was no change in Mac-1 staining in striatum of WT or $D2R^{-/-}$ animals compared to saline-treated animals.

Inactivation of D2R prevents METH-induced increases in pro-inflammatory molecules in the striatum

One day after METH administration, we observed a marked increase in iNOS-ir in the striatum of WT mice, similar to that induced by MDMA (Granado et al., 2008b). The morphology of the iNOS-ir cells suggests that iNOS is increased in neurons and glia. This increase was completely abolished in $D2R^{-/-}$ animals (Fig. 7, upper part). Immunohistochemistry for interleukin 15 (IL-15), a pro-inflammatory

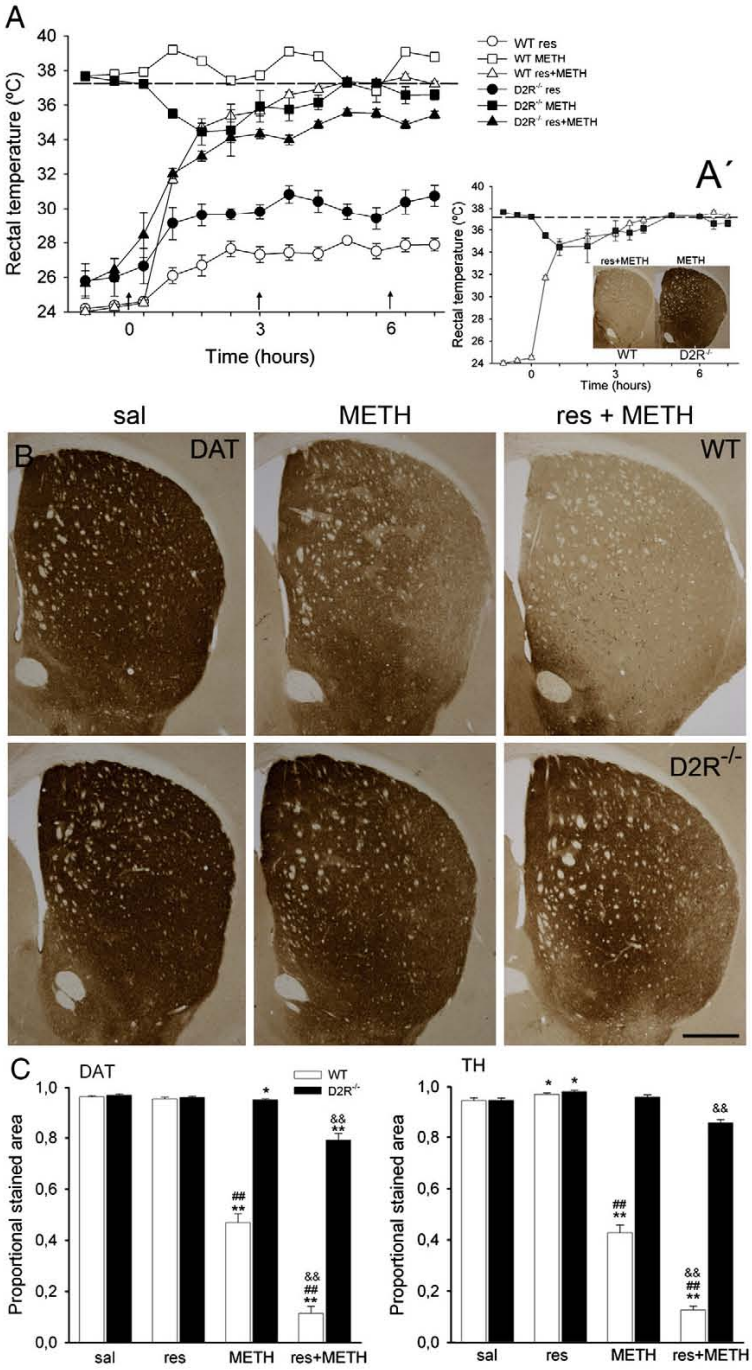

Fig. 4. Reserpine produced hypothermia and increased METH-induced neurotoxicity. Reserpine (3 mg/kg) and Methamphetamine (4 mg/kg × 3, 3 h), (A) Reserpine blocked METH-induced increases in rectal temperature in WT and D2R$^{-/-}$ mice. Arrows indicate drug injections. (A´) WT reserpinized mice treated with METH and D2R$^{-/-}$ mice treated with METH alone have similar rectal temperatures although they show great differences in DAT-ir content. (B) Photomicrographs of striatal sections from WT and D2R$^{-/-}$ mice treated with sal or METH or reserpine and METH stained for DAT. (C) Histograms show the proportional stained area for DAT or TH-ir in the striatum. Data represent mean ± S.E.M., $n = 6$ per group. $^{*}p<0.05$, $^{**}p<0.001$ vs. saline; and $^{\#\#}p<0.001$ vs. D2R$^{-/-}$ mice and $^{\&\&}p<0.001$ vs. METH-treated mice; two-way ANOVA followed by Tukey's test. Bar indicates 500 μm.

cytokine involved in regulating early inflammatory events after brain injury, showed similar results. One day after METH administration to WT mice, IL-15 was highly expressed in the striatum compared to saline-treated mice (Fig. 7, bottom part). Although there were some basal expressions of IL-15 in saline treated mice, more cell bodies and primary and secondary processes were IL-15-ir following METH treatment and staining intensity increased. IL-15 activation by METH administration was almost completely abolished in D2R$^{-/-}$ animals (Fig. 7). This data indicates a role for D2R in induction of iNOS and IL15 following METH administration.

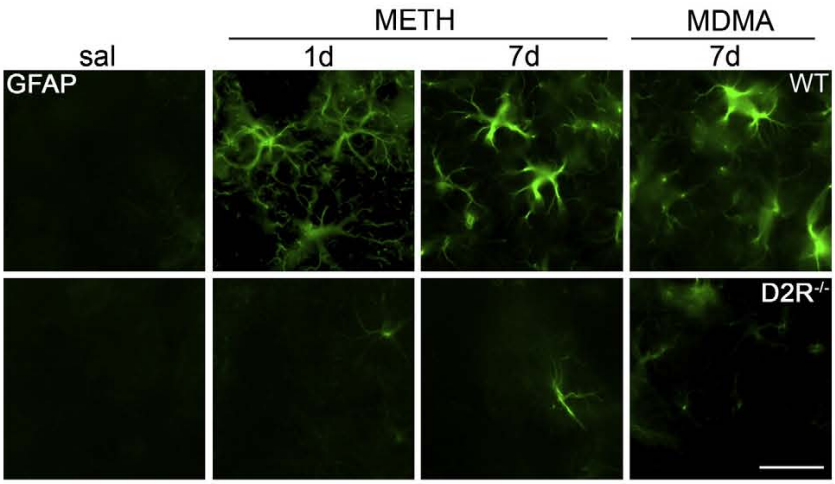

Fig. 5. Inactivation of D2R reduces astrogliosis induced by METH and MDMA in mouse striatum. Photomicrographs of striatal sections stained with GFAP from WT and D2R$^{-/-}$ mice 1 and 7 days after treatment with METH or 7 days after MDMA, compared to saline. MDMA and METH induced the expression of GFAP in WT animals (top row) and these increases were almost completely prevented in D2R$^{-/-}$ mice (bottom row). Bar indicates 50 μm.

Inactivation of D2R prevents dopaminergic neuronal loss in the substantia nigra

To see whether the dopaminergic fiber loss induced by METH corresponds to dopaminergic cell body loss in the SN, we quantified dopaminergic neurons in the SN using stereological analysis. SNpc dopaminergic neurons were identified by TH immunoreactivity. We observed a decrease in TH-ir in the SN pars compacta (SNpc; dopaminergic cell bodies) and in the pars reticulata (dopaminergic neuropil) of WT mice injected with METH (4 mg/kg, 3 injections) compared with the saline group. The number of TH-ir neurons in SN of WT METH-treated animals was significantly lower than saline-treated animals 1 (25.9%, $p<0.05$) and 7 days (19.9%, $p<0.05$) after injection (Fig. 8A, B). Similarly, the number of Nissl-stained neurons was significantly reduced at these two time points compared with saline treated mice (data not shown), indicating that the majority of lost cells were dopaminergic neurons. Strikingly, inactivation of D2R completely prevents this neuronal loss, and also prevents METH-induced increases in Mac-1 and GFAP expression in the SN (Fig. 8C, D). Moreover, 1 day after METH treatment, Fluoro-Jade C fluorescence identified degenerating neurons in the SN of WT animals but not D2R$^{-/-}$ mice (Fig. 8E). Together, our Flouro-Jade C and neuronal counting results indicate that the absence of the D2R protects dopaminergic neurons in the SN from neurotoxicity induced by METH or MDMA.

Inactivation of D2R counteracts striatal DA overflow induced by METH

Since inactivation of D2R prevents striatal dopaminergic fiber loss induced by METH, we examined whether METH modifies extrasynaptic DA overflow in WT and D2R$^{-/-}$ mice in corticostriatal slices. DA overflow is determined by the balance between DA release and reuptake and was recorded with a carbon fibre electrode in the dorsal striatum of corticostriatal slices using fast scan cyclic voltammetry (FSCV, see Materials and methods). In controlled conditions, we found that, compared to WT mice, D2R$^{-/-}$ mice showed a significant reduction of DA overflow in response to a single biphasic pulse (20 V,

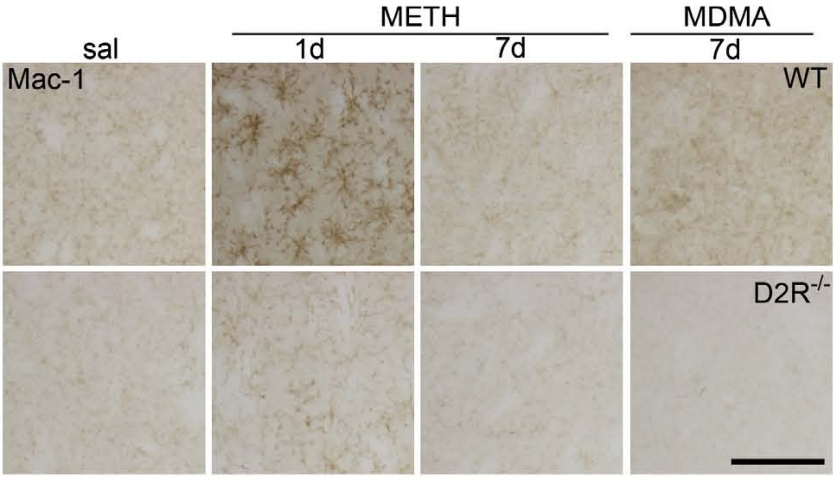

Fig. 6. D2R is required for striatal microgliosis induced by METH or MDMA administration in mouse. Photomicrographs of striatal sections stained for Mac-1 (CD-11b) from WT (top row) and D2R$^{-/-}$ (bottom row) mice 1 and 7 days after treatment with METH or 7 days after MDMA, compared to saline. MDMA and METH induce the expression of Mac-1 1 day after drug treatment in WT animals but not in D2R$^{-/-}$ mice. Bar indicates 100 μm.

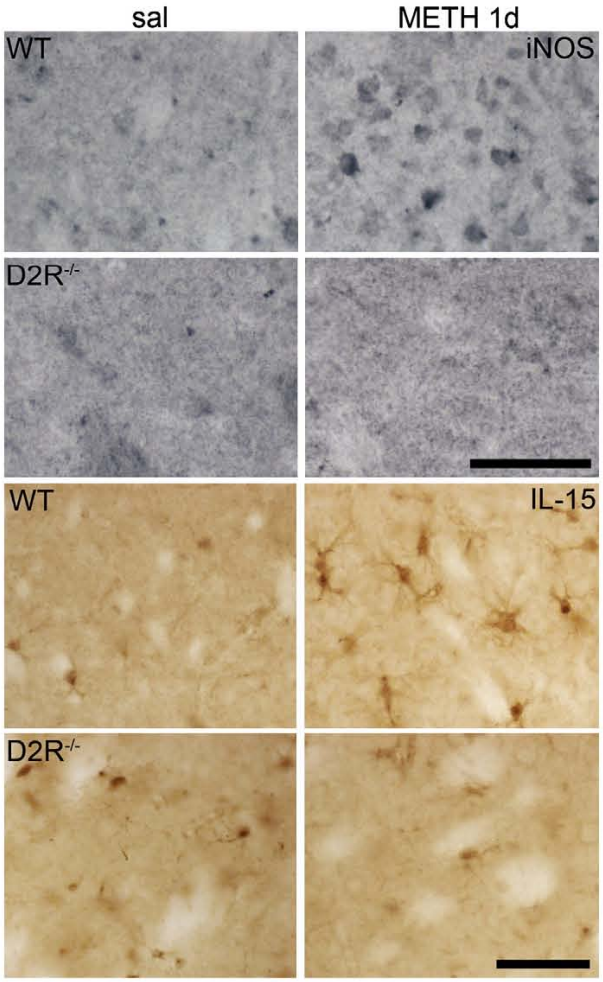

Fig. 7. Inactivation of D2R prevents METH-induced iNOS and IL-15 in the striatum. Photomicrographs of striatal sections stained for iNOS and for IL-15 from WT and D2R$^{-/-}$ mice 1 day after treatment with METH (right column) compared to saline (left column). METH increases iNOS and IL-15 expression 1 day after drug treatment in WT animals but not in D2R$^{-/-}$ mice. Bar indicates 100 μm.

500 μs) (Fig. 9B), in agreement with previous findings (Schmitz et al., 2002). In the presence of 30 μM METH, after 30 min of voltamogram stabilization, FSCV showed a significant increase in DA overflow for both genotypes compared with control conditions (Fig. 9C). The magnitude of this increase in DA overflow was significantly smaller in D2R$^{-/-}$ mice than in WT mice (Fig. 9C). In both genotypes, DA overflow reached a plateau before 15 min and did not return to baseline during the recording period (Fig. 9C). Taken together, these results indicate that METH inhibits uptake and/or increases release of DA from presynaptic terminals. Interestingly, DA overflow was significantly smaller in mice lacking D2 receptors suggesting that the protective effect of inactivating D2R is due in part to down regulation of METH-induced increases in extracellular DA.

Discussion

This is the first study showing that D2R$^{-/-}$ mice are resistant to the neurotoxic effects of METH and MDMA. The absence of the specific D2 receptor subtype provides complete protection against the loss of dopamine content, TH- and DAT-ir in the striatum 7 days after amphetamine administration. The METH-induced loss of TH-ir neurons in the SN observed in WT mice was also absent in D2R$^{-/-}$ mice. Dopamine overflow in the presence of METH was significantly reduced in D2R$^{-/-}$ mice. The pro-inflammatory cytokine, IL-15, was also reduced in the striatum. In addition, there is no increase in the expression of Mac-1 and GFAP immunoreactivity is less pronounced in striatum and SN of D2R$^{-/-}$ mice following METH administration, clearly indicating a role for the D2R subtype in the astroglial and microglial activation associated with neuronal damage and death induced by this neurotoxin.

As expected, both METH and MDMA induce hyperthermia in WT mice immediately after each of the three injections. We did not observe a hyperthermic response in D2R$^{-/-}$ mice, in agreement with previous results using nonspecific D2-like receptor antagonists such as sulpiride, raclopride or eticlopride (Albers and Sonsalla, 1995; Eisch and Marshall, 1998; Metzger et al., 2000). However, in the earlier studies, the effect could not be attributed definitively to loss of D2R function. In addition, both dopamine D2-like receptor agonists and antagonists dose-dependently induced hypothermia (Boulay et al., 1999; Oerther and Ahlenius, 2000; Sanchez and Arnt., 1992). Our data conclusively demonstrate that METH-induced hyperthermia requires functional D2R, indicating that other members of this receptor family, D3 and D4, are not involved (or at least not sufficient). This suggested that the protection observed in D2R$^{-/-}$ mice might be due to the absence of hyperthermia since hyperthermia has been correlated with neurotoxicity (Ali et al., 1996; Tata et al., 2007). Previous studies have shown that when MDMA is administered to rats housed at high ambient temperature (30 °C) the hyperthermic response induced is greater than that in rats treated at normal room temperature (Green et al., 2004). We therefore repeated the experiment with D2R$^{-/-}$ mice exposed to high ambient temperature before, during, and after METH treatment in order to elevate rectal temperature to that seen in WT mice treated with METH. However, even D2R$^{-/-}$ mice injected at high ambient temperature did not have elevated rectal temperatures; instead, they exhibited a hypothermic response nearly identical to that seen in D2R$^{-/-}$ animals injected at normal room temperature. In addition, there was no evidence of neuronal damage in D2R$^{-/-}$ mice treated at high ambient temperature.

By contrast, in reserpinized animals, we were able to dissociate neurotoxicity from body temperature in both genotypes. Reserpine strongly potentiated METH neurotoxicity in WT mice in spite of blocking hyperthermia, as previously reported (Albers and Sonsalla, 1995; Thomas et al., 2008). Similarly, in D2R$^{-/-}$ mice, reserpine slightly increased METH toxicity in spite of lowering rectal temperature. Thus, these results enabled us to substantiate the neuroprotective effect of D2R inactivation independent of its effect on body temperature. Previous work also showed that hyperthermia does not always correlate with METH-induced neurotoxicity, including studies showing that pretreatment with α-methyl-p-tyrosine and total or partial inactivation of DAT, nNOS, interleukin-6 or c-jun protect against METH-induced toxicity without altering the hyperthermic response (Deng et al., 2002; Fumagalli et al., 1998; Itzhak et al., 2000; Ladenheim et al., 2000; Thomas et al., 2008). Moreover, adrenalectomy blocks the hyperthermic response but not the neurotoxic effect of METH (Herring et al., 2010), further indicating that hyperthermia contributes to METH-induced neuropathology, but is not required.

The ability of dopamine antagonists to prevent the long-term effects of amphetamine derivatives has been evaluated by several groups aiming to determine the specific role of D1 and D2 receptors (Albers and Sonsalla, 1995; Eisch and Marshall, 1998; Metzger et al., 2000, Xu et al., 2005). However, these pharmacological studies used D1- or D2-like receptor antagonists that cannot differentiate between dopamine receptor subtypes. In addition, in most studies it was not possible to separate neuroprotection from body temperature; therefore, these experiments were not conclusive regarding the receptor subtype or the role of hyperthermia in METH neurotoxicity. Our current results using reserpine in D2R$^{-/-}$ animals clearly establish that the protective effect of D2R inactivation is independent of the hyperthermic response and that inactivation of D2R alone is sufficient for neuroprotection.

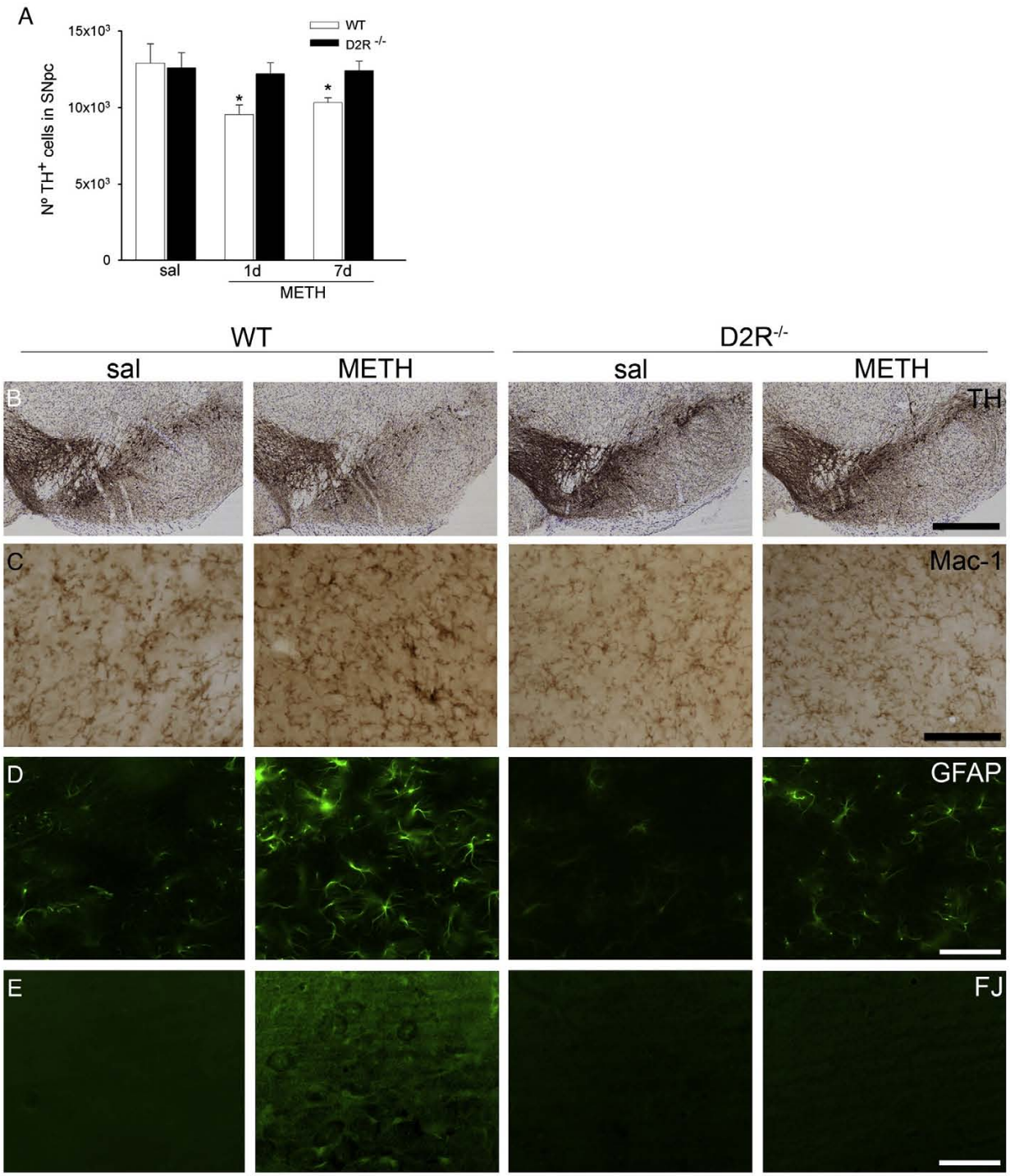

Fig. 8. Inactivation of D2R prevents METH-induced dopaminergic neuron loss and increased gliosis in the SN. (A) Histogram shows number of TH-positive neurons in the SN of WT or D2R$^{-/-}$ mice (mean ± S.E.M., $n = 6$–8 per group) counted by stereology in midbrain sections 1 and 7 days after METH treatment. *$p < 0.05$ vs. saline, two way ANOVA. B–E. Sections of SN from WT and D2R$^{-/-}$ mice stained for TH (B), Mac-1 (C), GFAP (D) and Fluoro-Jade (E) 1 day after treatment with METH or saline. Note that sections of D2R$^{-/-}$ mice show no TH-ir cell loss and no increase in Mac-1, GFAP or Fluoro-Jade signal staining. Bars indicate 500 μm (B), 100 μm (C) and 50 μm (D, E).

Furthermore, our results suggest that the dopamine D3 and D4 receptor subtypes are not critically involved in METH-induced toxicity.

In our experiments, basal striatal DA levels are similar in D2R$^{-/-}$ and WT mice, although D2R$^{-/-}$ exhibit higher DOPAC and HVA indicating higher DA turnover, as previously reported (Tinsley et al., 2009). It is not clear why D2R$^{-/-}$ mice are protected against the long-lasting neurotoxic effects of METH and MDMA; however, there are several plausible mechanisms. It has been demonstrated that the lack

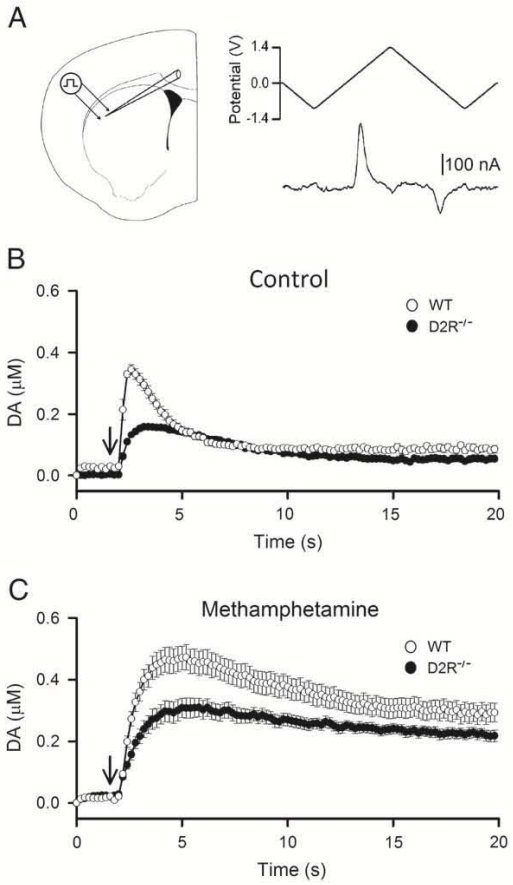

Fig. 9. DA overflow in response to single-pulse stimulation in striatal slices from $D2R^{-/-}$ and WT mice in control conditions and after perfusion with METH. (A) Left, schematic diagram illustrating the placement of the carbon fibre microelectrode (recording electrode) and the bipolar stimulating electrode in the dorsolateral striatum. Right, fast-scan cyclic voltammetry voltage waveform at 400 V/s scan rate (upper trace), and subtracted voltammograms for 1 μM of dopamine (lower trace). (B) Time course of dopamine overflow evoked by a single intrastriatal stimulus (arrow; 20 V, 0.5 ms) in WT ($n = 11$ slices from 3 mice) and $D2R^{-/-}$ ($n = 10$ slices from 3 mice) slices. (C) Time course of dopamine overflow evoked by a single intrastriatal stimulus (arrow) in the presence of 30 μM METH in WT ($n = 10$ slices from 3 mice) and $D2R^{-/-}$ ($n = 10$ slices from 3 mice) slices. Data represent mean ± S.E.M.

of D2R decreases striatal DAT activity (Dickinson et al., 1999). DAT is required for METH-induced striatal dopamine neurotoxicity since amfonelic acid, a DA uptake inhibitor, can antagonize the neurochemical response to METH (Pu et al., 1994). In addition, mice lacking DAT are protected against METH neurotoxicity (Fumagalli et al, 1998) while increased DAT activity exacerbated dopamine vulnerability (Afonso-Oramas et al., 2009; Manning-Boğ et al., 2007). These results indicate that inactivation of D2R blocks DA re-uptake by decreasing DAT activity, which results in lower intracytosolic DA levels. This could explain the neuroprotective effect of D2R inactivation, since cytosolic dopamine levels determine the severity of METH toxicity (Thomas et al., 2008).

Another mechanism that might underlie neuroprotection by D2R inactivation is a decrease in vesicular DA content and release. Our data, using fast scan cyclic voltammetry, demonstrate that METH induces a significantly smaller increase in vesicular DA overflow in $D2R^{-/-}$ than in WT mice. These data are consistent with the smaller increase in METH toxicity (as demonstrated by TH-ir loss) observed in reserpinized $D2R^{-/-}$ mice (11%) compared to reserpinized WT mice (70%), since reserpine increases METH toxicity by releasing DA from the vesicles to the cytosolic pool. In line with this, mice heterozygous for the vesicular monoamine transporter 2 exhibited increased METH toxicity (Fumagalli et al., 1999). Thus, our result measuring dopamine overflow, along with the results obtained in reserpinized animals, demonstrates that $D2R^{-/-}$ mice have lower vesicular DA release than WT mice. This may also contribute to the protection against METH toxicity observed in these mice.

Astrogliosis was observed in the striatum of WT mice at 1 and 7 days after METH injection. Microglial activation was also observed but only at 1 day post-drug administration. A similar gliosis profile was observed following MDMA treatment: 1 day after drug administration, both GFAP and Mac-1 staining were increased (Granado et al., 2008a,b,c) but 7 days later only GFAP staining remained elevated. Elevated GFAP expression reaches a peak 3 days after amphetamine administration, declining thereafter and remaining elevated until 1 week after treatment (Granado et al., 2008b; O'Callaghan and Miller, 1994). GFAP staining is considered to be a hallmark of neurotoxicity and has been closely associated with amphetamine-induced striatal dopaminergic neurotoxicity (Busceti et al., 2008; Fornai et al., 2004; Johnson et al., 2004; O'Callaghan and Miller, 1994). The increase in GFAP closely parallels the loss of dopamine content and tyrosine hydroxylase activity. Furthermore, nonneurotoxic l-stereoisomers of both METH and MDMA do not produce increases in striatal GFAP, supporting the close association between increased GFAP expression and dopaminergic neurotoxicity (O'Callaghan and Miller, 1994). More recently, the significance of microglial activation in amphetamine toxicity has been studied in greater depth. Microglial activation has been described as a marker of early neuronal damage caused by neurotoxic regimens of substituted amphetamines in mice (Thomas et al., 2004). Supporting evidence arises from studies demonstrating that METH provokes a dose- and time-dependent microglial response that is closely associated with the emergence of its neurotoxic effects (O'Callaghan and Miller, 1994; Thomas et al., 2004). More recent evidence implicates this reactive gliosis as a participant in the neurotoxic effects of METH and MDMA since minocycline inhibits microglial activation induced by these drugs and also protects against their dopamine depleting effects (Boger et al., 2009). In addition, minocycline protects against METH-induced DAT loss in monkey or rodent striatum (Boger et al., 2009; Hashimoto et al., 2007) and MDMA-induced 5-HT transporter loss in rats (Orio et al., 2010).

Activation of microglia is by no means limited to the neurotoxic amphetamines. Similar microglial activation patterns have been observed with the selective dopamine neurotoxins MPTP (Czlonkowska et al., 1996; Wu et al., 2002), rotenone (Gao et al., 2002) and 6-OHDA (Depino et al., 2003) and inhibition of this inflammatory response protects against the neurotoxic effects (Gao et al., 2002; He et al., 2001; Wu et al., 2002). Microglia, which contain dopamine receptors (Färber et al, 2005), produce a number of different proinflammatory cytokines, prostaglandins, and reactive oxygen species in response to a variety of stimuli. Reactive oxygen species in particular have been shown to play an important role in both METH- and MDMA-induced dopaminergic damage (Colado et al., 2001; Granado et al., 2008b, 2010). Thus, microglial activation may contribute to or amplify neurotoxic processes. Our finding that METH-or MDMA-induced increases in GFAP and Mac-1 staining are markedly reduced in $D2R^{-/-}$ mice concomitant with reduced dopaminergic toxicity confirms the role of the D2R in microglial activation as well as the association between microglial activation and neurotoxicity suggested by previous studies.

Moreover, the increased IL-15 expression in the striatum after METH was nearly completely abolished in $D2R^{-/-}$ mice. It has been shown that IL-15 expression regulates early inflammatory events after brain injury and that blockade of IL-15 activity inhibits activation of glial cells induced by lipopolysaccharide administration (Gomez-Nicola et al., 2008). These results are in agreement with our data showing that the inactivation of D2R severely decreases the METH-induced increases in GFAP and IL-15.

In conclusion, in $D2R^{-/-}$ mice, the neurotoxic effects of METH or MDMA were eliminated. In the absence of the D2R, there was no

decrease in striatal dopamine or loss of striatal TH and DAT inmunoreactivity after injections of MDMA or METH. In addition, D2 receptor ablation attenuated the increases in GFAP and Mac-1 expressions, reflecting a decrease in the glial activation produced by amphetamine derivatives. However, the absence of the D2R also resulted in the loss of the hyperthermic response, which plays an important role in METH or MDMA toxicity. These results suggest that the neuroprotection observed in the absence of the D2 dopamine receptor might depend, in part, on the inhibition of the hyperthermic response and also on the reduced intracytosolic DA levels. In addition, dopamine release and activation of dopamine receptors are strongly implicated as critical for METH-induced neurotoxic effects and hyperthermia because these responses are attenuated by both pharmacological blockade and genetic inactivation of the D2 receptor.

Acknowledgments

This research was supported by grants from the Spanish Ministerios de Ciencia e Innovación y de Sanidad y Política Social, ISCIII: BFU2010-20664, PNSD, RedRTA (RD06/0001/1011) and CIBERNED to RM and SAF2007-65175, FIS PI070892, PNSD 2006/1018, 2008/074; RTA06/0001/0006 to MIC and INCRECyT project from JCCM and PCYTA to EDM. NG is a recipient of Juan de la Cierva contract and SAS is funded with a JAE predoctoral fellowship from the CSIC. The authors would like to thank Dr. Diego Gomez-Nicola for the gift of IL-15 antiserum, Emilia Rubio and Marco de Mesa for their excellent technical assistance. (±)MDMA hydrochloride was obtained from NIDA (Research Triangle Park, North Carolina, USA).

References

Afonso-Oramas, D., Cruz-Muros, I., Alvarez de la Rosa, D., Abreu, P., Giráldez, T., Castro-Hernández, J., Salas-Hernández, J., Lanciego, J.L., Rodríguez, M., González-Hernández, T., 2009. Dopamine transporter glycosylation correlates with the vulnerability of midbrain dopaminergic cells in Parkinson's disease. Neurobiol. Dis. 36, 494–508.

Albers, D.S., Sonsalla, P.K., 1995. Methamphetamine-induced hyperthermia and dopaminergic neurotoxicity in mice: pharmacological profile of protective and nonprotective agents. J. Pharmacol. Exp. Ther. 275, 1104–1114.

Ali, S.F., Newport, G.D., Slikker Jr., W., 1996. Methamphetamine-induced dopaminergic toxicity in mice. Role of environmental temperature and pharmacological agents. Ann. NY Acad. Sci. 801, 187–198.

Boger, H.A., Middaugh, L.D., Granholm, A.C., McGinty, J.F., 2009. Minocycline restores striatal tyrosine hydroxylase in GDNF heterozygous mice but not in methamphetamine-treated mice. Neurobiol. Dis. 33, 459–466.

Boulay, D., Depoortere, R., Perrault, G., Borrelli, E., Sanger, D.J., 1999. Dopamine D2 receptor knock-out mice are insensitive to the hypolocomotor and hypothermic effects of dopamine D2/D3 receptor agonists. Neuropharmacology 38, 1389–1396.

Busceti, C.L., Biagioni, F., Riozzi, B., Battaglia, G., Storto, M., Cinque, C., Molinaro, G., Gradini, R., Caricasole, A., Canudas, A.M., Bruno, V., Nicoletti, F., Fornai, F., 2008. Enhanced tau phosphorylation in the hippocampus of mice treated with 3,4-methylenedioxymethamphetamine ("Ecstasy"). J. Neurosci. 28, 3234–3245.

Chen, H.M., Lee, Y.C., Huang, C.L., Liu, H.K., Liao, W.C., Lai, W.L., Lin, Y.R., Huang, N.K., 2007. Methamphetamine downregulates peroxiredoxins in rat pheochromocytoma cells. Biochem. Biophys. Res. Commun. 354, 96–101.

Colado, M.I., Camarero, J., Mechan, A.O., Sanchez, V., Esteban, B., Elliott, J.M., Green, A.R., 2001. A study of the mechanisms involved in the neurotoxic action of 3,4-methylenedioxymethamphetamine (MDMA, 'ecstasy') on dopamine neurones in mouse brain. Br. J. Pharmacol. 134, 1711–1723.

Cubells, J.F., Rayport, S., Rajendran, G., Sulzer, D., 1994. Methamphetamine neurotoxicity involves vacuolation of endocytic organelles and dopamine-dependent intracellular oxidative stress. J. Neurosci. 14, 2260–2271.

Czlonkowska, A., Kohutnicka, M., Kurkowska-Jastrzebska, I., Czlonkowski, A., 1996. Microglial reaction in MPTP (1-methyl-4-phenyl-1, 2, 3, 6-tetrahydropyridine) induced Parkinson's disease mice model. Neurodegeneration 5, 137–143.

Darmopil, S., Martín, A.B., De Diego, I.R., Ares, S., Moratalla, R., 2009. Genetic inactivation of dopamine D1 but not D2 receptors inhibits L-DOPA-induced dyskinesia and histone activation. Biol. Psychiatry 66, 603–663.

Darmopil, S., Muñetón-Gómez, V.C., de Ceballos, M.L., Bernson, M., Moratalla, R., 2008. Tyrosine hydroxylase cells appearing in the mouse striatum after dopamine denervation are likely to be projection neurones regulated by L-DOPA. Eur. J. Neurosci. 27, 580–592.

Deng, X., Jayanthi, S., Ladenheim, B., Krasnova, I.N., Cadet, J.L., 2002. Mice with partial deficiency of c-Jun show attenuation of methamphetamine-induced neuronal apoptosis. Mol. Pharmacol. 62, 993–1000.

Depino, A.M., Earl, C., Kaczmarczyk, E., Ferrari, C., Besedovsky, H., del, R.A., Pitossi, F.J., Oertel, W.H., 2003. Microglial activation with atypical proinflammatory cytokine expression in a rat model of Parkinson's disease. Eur. J. Neurosci. 18, 2731–2742.

Dickinson, S.D., Sabeti, J., Larson, G.A., Giardina, K., Rubinstein, M., Kelly, M.A., Grandy, D.K., Low, M.J., Gerhardt, G.A., Zahniser, N.R., 1999. Dopamine D2 receptor-deficient mice exhibit decreased dopamine transporter function but no changes in dopamine release in dorsal striatum. J. Neurochem. 72, 148–156.

Eisch, A.J., Marshall, J.F., 1998. Methamphetamine neurotoxicity: dissociation of striatal dopamine terminal damage from parietal cortical cell body injury. Synapse 30, 433–445 1998.

Escobedo, I., O'Shea, E., Orio, L., Sanchez, V., Segura, M., de la, T.R., Farre, M., Green, A.R., Colado, M.I., 2005. A comparative study on the acute and long-term effects of MDMA and 3,4-dihydroxymethamphetamine (HHMA) on brain monoamine levels after i.p. or striatal administration in mice. Br. J. Pharmacol. 144, 231–241.

Fantegrossi, W.E., Ciullo, J.R., Wakabayashi, K.T., De La, G.R., Traynor, J.R., Woods, J.H., 2008. A comparison of the physiological, behavioral, neurochemical and microglial effects of methamphetamine and 3,4-methylenedioxymethamphetamine in the mouse. Neuroscience 151, 533–543.

Färber, K., Pannasch, U., Kettenmann, H., 2005. Dopamine and noradrenaline control distinct functions in rodent microglial cells. Mol. Cell. Neurosci. 29, 128–138.

Fornai, F., Lenzi, P., Frenzilli, G., Gesi, M., Ferrucci, M., Lazzeri, G., Biagioni, F., Nigro, M., Falleni, A., Giusiani, M., Pellegrini, A., Blandini, F., Ruggieri, S., Paparelli, A., 2004. DNA damage and ubiquitinated neuronal inclusions in the substantia nigra and striatum of mice following MDMA (ecstasy). Psychopharmacology 173, 353–363.

Fumagalli, F., Gainetdinov, R.R., Valenzano, K.J., Caron, M.G., 1998. Role of dopamine transporter in methamphetamine-induced neurotoxicity: evidence from mice lacking the transporter. J. Neurosci. 18, 4861–4869.

Fumagalli, F., Gainetdinov, R.R., Wang, Y.M., Valenzano, K.J., Miller, G.W., Caron, M.G., 1999. Increased methamphetamine neurotoxicity in heterozygous vesicular monoamine transporter 2 knock-out mice. J. Neurosci. 19, 2424–2431.

Gao, H.M., Hong, J.S., Zhang, W., Liu, B., 2002. Distinct role for microglia in rotenone-induced degeneration of dopaminergic neurons. J. Neurosci. 22, 782–790.

Gluck, M.R., Moy, L.Y., Jayatilleke, E., Hogan, K.A., Manzino, L., Sonsalla, P.K., 2001. Parallel increases in lipid and protein oxidative markers in several mouse brain regions after methamphetamine treatment. J. Neurochem. 79, 152–160.

Gómez-Nicola, D., Valle-Argos, B., Suardíaz, M., Taylor, J.S., Nieto-Sampedro, M., 2008. Role of IL-15 in spinal cord and sciatic nerve after chronic constriction injury: regulation of macrophage and T-cell infiltration. J. Neurochem. 107, 1741–1752.

Granado, N., Escobedo, I., O'Shea, E., Colado, M.I., Moratalla, R., 2008a. Early loss of dopaminergic terminals in striosomes after MDMA administration to mice. Synapse 62, 80–84.

Granado, N., O'Shea, E., Bove, J., Vila, M., Colado, M.I., Moratalla, R., 2008b. Persistent MDMA-induced dopaminergic neurotoxicity in the striatum and substantia nigra of mice. J. Neurochem. 107, 1102–1112.

Granado, N., Ortiz, O., Suarez, L.M., Martin, E.D., Cena, V., Solis, J.M., Moratalla, R., 2008c. D1 but not D5 dopamine receptors are critical for LTP, spatial learning, and LTP-induced arc and zif268 expression in the hippocampus. Cereb. Cortex 18, 1–12.

Granado, N., Ares-Santos, S., O'Shea, E., Vicario-Abejon, C., Colado, M.I., Moratalla, R., 2010. Selective vulnerability in striosomes and in the nigrostriatal dopaminergic pathway after methamphetamine administration: early loss of TH in striosomes after methamphetamine. Neurotox. Res. 18, 48–58.

Green, A.R., Sanchez, V., O'Shea, E., Saadat, K.S., Elliott, J.M., Colado, M.I., 2004. Effect of ambient temperature and a prior neurotoxic dose of 3,4-methylenedioxymethamphetamine (MDMA) on the hyperthermic response of rats to a single or repeated ('binge' ingestion) low dose of MDMA. Psychopharmacology 173, 264–269.

Hadlock, G.C., Chu, P.W., Walters, E.T., Hanson, G.R., Fleckenstein, A.E., 2010. Methamphetamine-induced dopamine transporter complex formation and dopaminergic deficits: the role of D2 receptor activation. J. Pharmacol. Exp. Ther. 335, 207–212.

Hashimoto, K., Tsukada, H., Nishiyama, S., Fukumoto, D., Kakiuchi, T., Iyo, M., 2007. Protective effects of minocycline on the reduction of dopamine transporters in the striatum after administration of methamphetamine: a positron emission tomography study in conscious monkeys. Biol. Psychiatry 61, 577–581.

He, Y., Appel, S., Le, W., 2001. Minocycline inhibits microglial activation and protects nigral cells after 6-hydroxydopamine injection into mouse striatum. Brain Res. 909, 187–193.

Herring, N.R., Gudelsky, G.A., Vorhees, C.V., Williams, M.T., 2010. (+)-Methamphetamine-induced monoamine reductions and impaired egocentric learning in adrenalectomized rats is independent of hyperthermia. Synapse 64, 773–785.

Itzhak, Y., Martin, J.L., Ail, S.F., 2000. nNOS inhibitors attenuate methamphetamine-induced dopaminergic neurotoxicity but not hyperthermia in mice. NeuroReport 11, 2943–2946.

Jayanthi, S., Ladenheim, B., Cadet, J.L., 1998. Methamphetamine-induced changes in antioxidant enzymes and lipid peroxidation in copper/zinc-superoxide dismutase transgenic mice. Ann. NY Acad. Sci. 844, 92–102.

Johnson, E.A., O'Callaghan, J.P., Miller, D.B., 2004. Brain concentrations of d-MDMA are increased after stress. Psychopharmacology 173, 278–286.

Kelly, M.A., Rubinstein, M., Asa, S.L., Zhang, G., Saez, C., Bunzow, J.R., Allen, R.G., Hnasko, R., Ben-Jonathan, N., Grandy, D.K., Low, M.J., 1997. Pituitary lactotroph hyperplasia and chronic hyperprolactinemia in dopamine D2 receptor-deficient mice. Neuron 19, 103–113.

Krasnova, I.N., Cadet, J.L., 2009. Methamphetamine toxicity and messengers of death. Brain Res. Rev. 60, 379–407.

Ladenheim, B., Krasnova, I.N., Deng, X., Oyler, J.M., Polettini, A., Moran, T.H., Huestis, M. A., Cadet, J.L., 2000. Methamphetamine-induced neurotoxicity is attenuated in transgenic mice with a null mutation for interleukin-6. Mol. Pharmacol. 58, 1247–1256.

Larsen, K.E., Fon, E.A., Hastings, T.G., Edwards, R.H., Sulzer, D., 2002. Methamphetamine-induced degeneration of dopaminergic neurons involves autophagy and upregulation of dopamine synthesis. J. Neurosci. 22, 8951–8960.

LaVoie, M.J., Hastings, T.G., 1999. Dopamine quinone formation and protein modification associated with the striatal neurotoxicity of methamphetamine: evidence against a role for extracellular dopamine. J. Neurosci. 19, 1484–1491.
Mann, H., Ladenheim, B., Hirata, H., Moran, T.H., Cadet, J.L., 1997. Differential toxic effects of methamphetamine (METH) and methylenedioxymethamphetamine (MDMA) in multidrug-resistant (mdr1a) knockout mice. Brain Res. 769, 340–346.
Manning-Bog, A.B., Caudle, W.M., Perez, X.A., Reaney, S.H., Paletzki, R., Isla, M.Z., Chou, V.P., McCormack, A.L., Miller, G.W., Langston, J.W., Gerfen, C.R., Dimonte, D.A., 2007. Increased vulnerability of nigrostriatal terminals in DJ-1-deficient mice is mediated by the dopamine transporter. Neurobiol. Dis. 31, 334–341.
Martín, E.D., Buño, W., 2005. Stabilizing effects of extracellular ATP on synaptic efficacy and plasticity in hippocampal pyramidal neurons. Eur. J. Neurosci. 21, 936–944.
Metzger, R.R., Haughey, H.M., Wilkins, D.G., Gibb, J.W., Hanson, G.R., Fleckenstein, A.E., 2000. Methamphetamine-induced rapid decrease in dopamine transporter function: role of dopamine and hyperthermia. J. Pharmacol. Exp. Ther. 295, 1077–1085.
Miyazaki, I., Asanuma, M., Diaz-Corrales, F.J., Fukuda, M., Kitaichi, K., Miyoshi, K., Ogawa, N., 2006. Methamphetamine-induced dopaminergic neurotoxicity is regulated by quinone-formation-related molecules. FASEB J. 20, 571–573.
O'Callaghan, J.P., Miller, D.B., 1994. Neurotoxicity profiles of substituted amphetamines in the C57BL/6J mouse. J. Pharmacol. Exp. Ther. 270, 741–751.
Oerther, S., Ahlenius, S., 2000. Atypical antipsychotics and dopamine D(1) receptor-agonism: an in vivo experimental study using core temperature measurements in therat. J. Pharmacol. Exp. Ther. 292, 731–736.
O'Shea, E., Sanchez, V., Camarero, J., Green, A.R., Colado, M.I., 2003. On the protection against methamphetamine-induced neurotoxicity by benzamide, a PARP inhibitor. Psychopharmacology 165, 317–319.
Orio, L., Llopis, N., Torres, E., Izco, M., O'shea, E., Colado, M.I., 2010. A study on the mechanisms by which minocycline protects against MDMA ('ecstasy')-induced neurotoxicity of 5-HT cortical neurons. Neurotox. Res. 18, 187–199.
Pavon, N., Martin, A.B., Mendialdua, A., Moratalla, R., 2006. ERK phosphorylation and FosB expression are associated with L-DOPA-induced dyskinesia in hemiparkinsonian mice. Biol. Psychiatry 59, 64–74.
Pu, C., Fisher, J.E., Cappon, G.D., Vorhees, C.V., 1994. The effects of amfonelic acid, a dopamine uptake inhibitor, on methamphetamine-induced dopaminergic terminal degeneration and astrocytic response in rat striatum. Brain Res. 649, 217–224.
Sánchez, C., Arnt, J., 1992. Effects on body temperature in mice differentiate between dopamine D2 receptor agonists with high and low efficacies. Eur. J. Pharmacol. 211, 9–14.
Schmitz, Y., Schmauss, C., Sulzer, D., 2002. Altered dopamine release and uptake kinetics in mice lacking D2 receptors. J. Neurosci. 22, 8002–8009.
Schmued, L.C., Albertson, C., Slikker Jr., W., 1997. Fluoro-Jade: a novel fluorochrome for the sensitive and reliable histochemical localization of neuronal degeneration. Brain Res. 751, 37–46.
Sonsalla, P.K., Jochnowitz, N.D., Zeevalk, G.D., Oostveen, J.A., Hall, E.D., 1996. Treatment of mice with methamphetamine produces cell loss in the substantia nigra. Brain Res. 738, 172–175.
Tata, D.A., Raudensky, J., Yamamoto, B.K., 2007. Augmentation of methamphetamine-induced toxicity in the rat striatum by unpredictable stress: contribution of enhanced hyperthermia. Eur. J. Neurosci. 26, 739–748.
Thomas, D.M., Dowgiert, J., Geddes, T.J., Francescutti-Verbeem, D., Liu, X., Kuhn, D.M., 2004. Microglial activation is a pharmacologically specific marker for the neurotoxic amphetamines. Neurosci. Lett. 367, 349–354.
Thomas, D.M., Francescutti-Verbeem, D.M., Kuhn, D.M., 2008. Methamphetamine-induced neurotoxicity and microglial activation are not mediated by fractalkine receptor signaling. J. Neurochem. 106, 696–705.
Tinsley, R.B., Bye, C.R., Parish, C.L., Tziotis-Vais, A., George, S., Culvenor, J.G., Li, Q.X., Masters, C.L., Finkelstein, D.I., Horne, M.K., 2009. Dopamine D2 receptor knockout mice develop features of Parkinson's disease. Ann. Neurol. 66, 472–484.
Wu, D.C., Jackson-Lewis, V., Vila, M., Tieu, K., Teismann, P., Vadseth, C., Choi, D.K., Ischiropoulos, H., Przedborski, S., 2002. Blockade of microglial activation is neuroprotective in the 1-methyl-4-phenyl-1, 2, 3, 6-tetrahydropyridine mouse model of Parkinson's disease. J. Neurosci. 22, 1763–1771.
Xu, W., Zhu, J.P., Angulo, J.A., 2005. Induction of striatal pre- and postsynaptic damage bymethamphetamine requires the dopamine receptors. Synapse 58, 110–121.

4. Nrf2 deficiency potentiates methamphetamine-induced dopaminergic axonal damage and gliosis in the striatum.

Granado N*, Lastres-Becker I,* Ares-Santos S, Oliva I, O'Shea E, Martin ED, Cuadrado A, Moratalla R (2011b). *Glia.* **59**:1850-63. doi: 10.1002/glia.21229.

* equal contribution

GLIA

GLIA 59:1850–1863 (2011)

Nrf2 Deficiency Potentiates Methamphetamine-Induced Dopaminergic Axonal Damage and Gliosis in the Striatum

NOELIA GRANADO,[1,2,3] ISABEL LASTRES-BECKER,[2,4] SARA ARES-SANTOS,[1,2] IDAIRA OLIVA,[5] EDUARDO MARTIN,[5] ANTONIO CUADRADO,[2,4] AND ROSARIO MORATALLA[1,2]*

[1]*Instituto Cajal, CSIC, Madrid, Spain*
[2]*Centro de Investigaciones en Red sobre Enfermedades Neurodegenerativas (CIBERNED), Instituto de Salud Carlos III, Madrid, Spain*
[3]*Departamento de Farmacia, Facultad de Medicina, Universidad Complutense de Madrid, Madrid, Spain*
[4]*Departamento de Bioquímica and Instituto de Investigaciones Biomédicas "Alberto Sols" UAM-CSIC, Facultad de Medicina, Universidad Autónoma de Madrid, and Instituto de Investigación Sanitaria La Paz (IDIPAZ), Madrid, Spain*
[5]*Laboratorio de Neurofisiología y Plasticidad Sináptica, Parque Científico y Tecnológico de Albacete (PCYTA), Instituto de Investigación en Discapacidades Neurológicas (IDINE), Universidad de Castilla-La Mancha, Albacete, Spain*

KEY WORDS
neurodegeneration; Nrf2; amphetamine derivatives; inflammation

ABSTRACT
Oxidative stress that correlates with damage to nigrostriatal dopaminergic neurons and reactive gliosis in the basal ganglia is a hallmark of methamphetamine (METH) toxicity. In this study, we analyzed the protective role of the transcription factor Nrf2 (nuclear factor-erythroid 2-related factor 2), a master regulator of redox homeostasis, in METH-induced neurotoxicity. We found that Nrf2 deficiency exacerbated METH-induced damage to dopamine neurons, shown by an increase in loss of tyrosine hydroxylase (TH)- and dopamine transporter (DAT)-containing fibers in striatum. Consistent with these effects, Nrf2 deficiency potentiated glial activation, indicated by increased striatal expression of markers for microglia (Mac-1 and Iba-1) and astroglia (GFAP) one day after METH administration. At the same time, Nrf2 inactivation dramatically potentiated the increase in TNFα mRNA and IL-15 protein expression in GFAP+ cells in the striatum. In sharp contrast to the potentiation of striatal damage, Nrf2 deficiency did not affect METH-induced dopaminergic neuron death or expression of glial markers or proinflammatory molecules in the substantia nigra. This study uncovers a new role for Nrf2 in protection against METH-induced inflammatory and oxidative stress and striatal degeneration.

INTRODUCTION

Amphetamine-like drugs exert their powerful psychostimulant effects by promoting the release of monoamine neurotransmitters (carrier-mediated efflux) and inhibiting their uptake. These compounds have been used widely in clinical practice as anorectic agents to reduce body weight. However, chronic administration of amphetamine to rats leads to dopaminergic neurotoxicity rising important concerns about the use of these compounds in clinical practice and in drug abuse (Eisch et al., 1992). We have reported that methamphetamine (METH) alters the integrity of striosomes and the nigral dopaminergic tract in mice (Granado et al., 2010, 2011) and high doses of METH harm striatal monoaminergic terminals and transporters in humans (Volkow et al., 2001) and experimental animals (Ricaurte et al., 1982, Granado et al., 2011). METH induces hyperthermia (O'Callaghan and Miller, 1994), causes significant depletion of dopamine (DA) and its metabolites (Fantegrossi et al., 2008; O'Callaghan and Miller, 1994), inhibits tyrosine hydroxylase activity, reduces dopamine transporter protein levels (Sonsalla et al., 1986; Xu et al., 2005; Granado et al., 2011), and induces apoptosis (Cadet et al., 2005, 2007). Very relevant to this study, oxidative stress may be critically involved in METH neurotoxicity and neuroinflammation. Thus, METH increases the production of reactive oxygen species (Yamamoto and Zhu, 1998) as well as reactive astrocytosis (Zhu et al., 2005; Granado et al., 2011) and microglial activation (Thomas et al., 2004; Granado et al., 2011). Therefore, it is important to identify molecular targets to reinforce the antioxidant and anti-inflammatory defenses in the basal ganglia against METH.

Inducible adaptation to oxidative stress is controlled by the transcription factor Nrf2 (nuclear factor-erythroid 2-related factor 2), master regulator of redox homeostasis. Nrf2 regulates the expression of a group of genes that are cytoprotective against oxidative and inflammatory stress. Together, these genes constitute the phase 2 antioxidant and antixenobiotic response and include heme oxygenase-1 (HO-1), NADPH quinone oxidoreductase (NQO1), and the catalytic and modulatory subunits

Additional Supporting Information may be found in the online version of this article.

Noelia Granado and Isabel LastresBecker contributed equally to this work.

Grant sponsor: Spanish MSPS; Grant number PI071073; PI-2007/49; Grant sponsor: Spanish MICINN; Grant number: BFU2010-20664; SAF2010-17822, BFU2008-04196/BFI; Grant sponsor: JCCM INCRECyT project, PCYTA.

*Correspondence to: Rosario Moratalla, Instituto Cajal, CSIC, Avda Dr. Arce 37, 28002, Madrid, Spain. E-mail: moratalla@cajal.csic.es

Received 22 February 2011; Accepted 20 July 2011

DOI 10.1002/glia.21229

Published online 31 August 2011 in Wiley Online Library (wileyonlinelibrary.com).

of γ-glutamyl synthase (GCLM, GCLC), among others (Clark and Simon, 2009; Johnson et al., 2008). Nrf2 has a very short half-life because of its interaction with the BTB-Kelch protein Keap1, which promotes Nrf2 degradation by the proteasome (Lo et al., 2006). Oxidant molecules disrupt the Keap1/Nrf2 complex thereby rescuing Nrf2 from proteasomal degradation and allowing its entry into the nucleus and carrying out its transcriptional activity.

Nrf2 plays a crucial role in protection of dopaminergic neurons against oxidative stress, detoxification of mitochondrial complex I inhibitors, and downregulation of genes involved in the brain innate immune response. Thus, we and others have demonstrated that Nrf2-null ($Nrf2^{-/-}$) mice are more sensitive to 1-methyl-4-phenyl-1,2,3,6-tetrahydropyridine intoxication (Chen et al., 2009; Rojo et al., 2010). Moreover, $Nrf2^{-/-}$ mice exhibit exacerbated inflammation compared with wild-type littermates as determined by the release of proinflammatory cytokines in the basal ganglia (Rojo et al., 2010). Constitutive deletion of Nrf2 gene reduces the induction of glutathione-dependent enzymes in liver and augments cortical and striatal lesions induced by the mitochondrial complex II inhibitor 3-nitropropionic acid (Calkins et al., 2005; Shih et al., 2005). The relevance of Nrf2 in the modulation of the innate immune system has been also suggested in models of acute inflammation induced by lipolysaccharide (Innamorato et al., 2008; Rangasamy et al., 2004, 2005; Thimmulappa et al., 2006a,b).

Based on these prior studies, we explored the role of Nrf2 in METH-induced neurotoxicity in striatum and substantia nigra of $Nrf2^{-/-}$ mice and wild type littermates. Nrf2 deficiency resulted in exacerbated hyperthermia, enhanced striatal TH and DAT-fiber loss, as well as a bigger decrease in DA levels with increased DA and nigrostriatal dopaminergic alterations and gliosis following administration of METH. This report demonstrates a very relevant role of Nrf2 in protection of the basal ganglia against neurotoxicity induced by METH.

MATERIALS AND METHODS

Animals and Treatment

Experiments were carried out in male Nrf2 knockout ($Nrf2^{-/-}$) mice as well as wildtype (WT) littermates. We used adult male mice initially weighing 20–25 g, and the genotype of each mouse was determined by PCR analysis as described previously (Itoh et al., 1997). Mice were housed in groups of four to six per cage, in a 12-h-light/dark cycle (lights on 7:00 h), and given free access to food and water. Animals were cared for according to a protocol approved by the Ethical Committee for Research of the Universidad Autónoma de Madrid following institutional, Spanish, and European guidelines (Boletín Oficial del Estado (BOE) of 18 March 1988 and 86/609/EEC, 2003/65/EC European Council Directives).

Mice were exposed to a METH neurotoxicity regimen comprised of three injections of 5 mg/kg i.p. with a 3-h-interval between injections. During treatment, animals were housed in a temperature controlled room, maintained at 23°C, unless detailed otherwise. METH was dissolved in 0.9% w/v NaCl (saline) and injected in a volume of 10 mL/kg. Animals were sacrificed one day after drug administration. METH was obtained from Sigma-Aldrich.

Abbreviations

aCSF	artificial cerebrospinal fluid
DA	dopamine
DAB	diaminobenzidine
DAT	dopamine transporter
DOPAC	3,4-dihydroxyphenylacetic acid
GFAP	glial fibrillary acidic protein
GPx	glutathione peroxidase
HO-1	heme oxygenase-1
METH	methamphetamine
NQO1	NADPH quinone oxidoreductase
SNpc	SN pars compacta
SOD	superoxide dismutase
TH	tyrosine hydroxylase
WT	wildtype.

Measurement of Rectal Temperature

Rectal temperature was measured using a digital readout thermocouple (BAT-12 thermometer, Physitemp Instruments, Clifton, NJ, USA) with a resolution of 0.1°C and accuracy of ±0.1°C attached to a RET-3 Rodent Sensor. The sensor was inserted 2 cm into the mouse rectum, while the mouse was lightly restrained by holding in the hand. A steady readout was obtained within 10 s of probe insertion. Temperature readings were taken every 30 min immediately before and after METH injections and hourly thereafter.

Measurement of Dopamine in the Striatum

One day after treatment, mice were killed by cervical dislocation and decapitation, brains were rapidly removed, and the striatum was dissected out on ice. Dopamine and the metabolite, 3,4-dihydroxyphenylacetic acid (DOPAC) were measured by high-performance liquid chromatography and electrochemical detection. The mobile phase consisted of KH_2PO_4 (0.05 M), octanesulfonic acid (0.4 mM), EDTA (0.1 mM), and methanol (16%) and was adjusted to pH 3 with phosphoric acid, filtered, and degassed. The flow rate was 1 mL/min. The high-performance liquid chromatography system consisted of a pump (Waters 510) linked to an automatic sample injector (Loop 200 μL, Waters 717 plus Autosampler) and a stainless steel reversed-phase column (Spherisorb ODS2, 5 μm, 150 × 4.6 mm^2; Waters, Milford, MA) with a precolumn and a coulometric detector (Coulochem II; Esa, Chelmsford, MA). The working electrode potential was set at 400 mV with a gain of 1 μA (for dopamine) and 500 nA (for the remaining compounds). The current produced was monitored by means of integration software (Unipoint; Gilson, Villier Le Bel, France).

TABLE 1. Genes and Primers for Quantitative PCR Amplification

Gene Product	Forward Primer	Reverse Primer
BiP	5′ CATGGTTCTCACTAAAATGAAGG 3′	5′ GCTGGTACAGTAACAACTG 3′
CHOP/Gaddl53	5′ GGAAGTGCATCTTCATACACCACC 3′	5′ TGACTGGAATCTGGAGAGCGAGGGC 3′
Cu/ZnSOD	5′ AACCATCCACTTCGAGCAGA 3′	5′ CCCAGCATTTCCAGTCTTTG 3′
GCLC	5′ TTACCGAGGCTACGTGTCAGAC 3′	5′ TATCGATGGTCAGGTCGATGTC 3′
GCLM	5′ AATCAGCCCCGATTTAGTCAGG 3′	5′ CCAGCTGTGCAACTCCAAGGAC 3′
GFAP	5′ TCCTGGAACAGCAAAACAA 3′	5′ CAGCCTCAGGTTGGTTTCAT 3′
GPx	5′ GGACTACACCGAGATGAACG 3′	5′ GATGTACTTGGGGTCGGTCA 3′
GSTA2	5′ CGCCACCAAATATGACCTCT 3′	5′ CCTGTTGCCCACAAGGTAGT 3′
Iba-1	5′ GTCCTTGAAGCGAATGCTGG 3′	5′ CATTCTCAAGATGGCAGATC 3′
IL-1β	5′ CTGGTGTGTGACGTTCCCATTA 3′	5′ CCGACAGCACGAGGCTTT 3′
Mac-1	5′ TCGATTAACCCGTCAAAGTACAAA 3′	5′ TTTTTTCTTTGCCTTGGTTTT 3′
MnSOD	5′ AACAATCTCAACGCCACCGA 3′	5′ GATTAGAGCAGGCAGCAATC 3′
NQO1	5′ GGTAGCGGCTCCATGTACTC 3′	5′ CATCCTTCCAGGATCTGCAT 3′
TNF-α	5′ CATCTTCTCAAAATTCGAGTGACAA 3′	5′ TGGGAGTAGACAAGGTACAACCC 3′
β-actin	5′ TCCTTCCTGGGCATGGAG 3′	5′ AGGAGGAGCAATGATCTTGATCTT 3′

Immunohistochemistry

Animals were anaesthetized with 8 mg/kg ketamine and 1.2 mg/kg xylazine and then perfused with 4% paraformaldehyde dissolved in PB (Buffer phosphate, pH 7.4). After perfusion, brains were dissected and immersed overnight in the same fixative solution. Coronal brain sections (30 μm) were obtained on a slicing vibratome (Leica, Madrid, Spain) and kept in PB solution at 4°C until use. Immunostaining was carried out on free-floating sections with a standard avidin-biotin immunocytochemical protocol previously described (Granado et al., 2008c; Martin et al., 2008; Pavón et al., 2006; Rodrigues et al., 2007). Endogenous peroxidase activity was removed by incubation in 3% H_2O_2 for 10 min. Sections were preblocked with normal goat serum (Vector Laboratories, Burlingame, CA, USA) for 1 h. The sections were incubated overnight with specific primary antisera (Ab-I), a rabbit tyrosine hydroxylase antiserum (TH; Chemicon International, Temecula, CA, USA) diluted 1:1,000; rat monoclonal antibody against dopamine transporter (DAT; Chemicon International), diluted 1:1,000; a rabbit anti glial fibrillary acidic protein antibody (GFAP; DakoCytomation, Denmark), diluted 1:1,000; and rat monoclonal anti-Mac1 or CD11b (1:500, Serotec, Kinlington, Oxford, UK), or rabbit polyclonal anti Iba-1 (1:1000, Wako Pure Chemical Industries, Ltd Osaka, Japan) and goat anti-mouse interleukin 15 (IL-15, used at 1:200, Santa Cruz Biotechnologies, Santa Cruz, CA, USA) in PBST solutions containing normal goat serum. After careful washing, the sections were incubated with the secondary biotinylated secondary antisera (Vector) at room temperature and developed using diaminobenzidine (DAB). The reaction was monitored every 5 min using an optical microscope (Leica). After washing, the sections were mounted on gelatin-coated slides, air-dried, and dehydrated in ascending concentrations of ethanol, cleared with xylene, and coverslipped under Permount. For double immunofluorescence experiments, we used Alexa fluor 488 and 594 conjugated secondary antibodies (1:400–500; Invitrogen, Eugene, OR) and the sections were mounted in Mowiol solution (Calbiochem, San Diego, CA). Controls were performed to confirm the specificity of the primary and secondary antibodies.

Quantification of expression of TH and DAT was performed with the aid of an image analysis system [Analytical Imaging Station (AIS), Imaging Research Inc., Linton, UK] using a 5× lens, converting color intensities into a gray scale, and quantifying area of staining in treated animals as a proportion of that in untreated animals (Darmopil et al., 2008, 2009; Ortiz et al., 2010).

Analysis of mRNA Levels by Quantitative Real-Time PCR

Total RNA from striatum and ventral midbrain was extracted using TRIzol reagent according to the manufacturer's instructions (Invitrogen). One microgram of RNA from the different treatments were treated with DNase (Invitrogen) and reverse-transcribed for 30 min at 42°C using 4 μL of high capacity RNA-to-cDNA Master Mix (Applied Biosystem, Foster City, CA). For Real-Time PCR analysis, the reaction was performed in 25 μL using the fluorescent dye Power SYBER Green PCR Master Mix (Applied Biosystem, Foster City, CA) and a mixture of 5 pmol of reverse and forward primers. Primer sequences are shown in Table 1. Quantification was performed on a StepOne detection system (Applied Biosystem, Foster City, CA). PCR cycles proceeded as follows: initial denaturation for 10 min at 95°C, then 40 cycles of denaturation (15 s, 95°C), annealing (30 s, 60°C), and extension (30 s, 60°C). The melting-curve analysis showed the specificity of the amplications. Threshold cycle, which inversely correlates with the target mRNA level, was measured as the cycle number at which the reporter fluorescent emission appears above the background threshold (data not shown). To ensure that equal amounts of cDNA were added to the PCR, the β-actin housekeeping gene was amplified. Data analysis is based on the ΔΔCt method with normalization of the raw data to housekeeping genes as described in the manusfacturer's manual (Applied Biosystem, Foster City, CA). All PCRs were performed in triplicates.

Ca^{2+} Imaging in Striatal Brain Slices

Coronal brain slices (450 μm thickness) were prepared from mice using conventional methods (Martín and Buño, 2005) and incubated for >1 h at room temperature (21°C–24°C) in artificial cerebrospinal fluid (aCSF). The aCSF contained (in mM): NaCl 124, KCl 2.69, KH_2PO_4 1.25, $MgSO_4$ 2, $NaHCO_3$ 26, $CaCl_2$ 2, and glucose 10 and was gassed with 95% O_2 and 5% CO_2. Ca^{2+} levels in astrocytes located in dorsolateral striatum were monitored by fluorescence microscopy using the Ca^{2+} indicator fluo-4 (Molecular Probes, Eugene, OR). Slices were incubated with fluo-4-AM (2–5 mL of 2 mM dye were dropped over the striatum, attaining a final concentration of 2–10 mM and 0.01% of pluronic) for 20–30 min at room temperature. In these conditions, most of the cells loaded were astrocytes (Kang et al., 1998; Martin et al., 2007; Perea and Araque, 2007). Astrocytes were imaged using a CCD camera (ORCA-R^2 C10600-10B, Hamamatsu Photonics K.K., Hamamatsu City, Japan) attached to an upright microscope (Olympus BX51WI) equipped with 40× water-immersion objective. Cells were illuminated during 200 ms with a LED excitation system (pE-2, CoolLED Limited, Andover, UK) and images were acquired every 1 s. The LED excitation system and the CCD camera were controlled and synchronized by the NIS-Elements software (Nikon Corporation, Tokyo, Japan) that was also used for quantitative epifluorescence measurements. Methamphetamine was delivered by 2-s-duration pressure pulses (PMI-100 DAGAN, Minneapolis, MN) using a pulled capillary filled with METH (100 μM) dissolved in ACSF (the final METH concentration around the recorded cell was (15 μM). Ca^{2+} variations recorded at the soma of the cells were estimated as changes of the fluorescence signal over baseline ($\Delta F/F_0$) and cells were considered to respond to the METH puff when $\Delta F/F_0$ increased three times the standard deviation of the baseline.

Statistics

Data are presented as mean ± standard error of the mean (SEM). The results of rectal temperature measurements were analyzed using two-way analysis of variance (ANOVA) for repeated measures.

Data obtained from image analysis of striatal TH and DAT immunostaining were analyzed using two-way ANOVA. Relevant differences were analyzed pair-wise by post-hoc comparisons with Tukeys's test to determine specific group differences.

All statistical analyses were performed using SigmaStat 2.03 program, and the threshold for statistical significance was set at $P < 0.05$. Graphical representations were obtained using SigmaPlot 9.0 software.

RESULTS

METH Produces More Hyperthermia in $Nrf2^{-/-}$ Than in WT Mice

METH treatment (5 mg/kg, i.p., three injections given at 3-h-intervals) significantly increased rectal temperatures compared with saline-treated animals. A hyperthermic response was evident by 30 min after each injection of the drug and this increase was higher in $Nrf2^{-/-}$ mice than in WT. In WT mice, 5 mg/kg METH raised rectal temperature to a mean of 38.1°C with the first injection, 38.3°C with the second, and 37.7°C with the third injection. In $Nrf2^{-/-}$ mice, the mean temperature increased to 39.0°C, 38.8°C, and 38.2°C after the first, second, and third injections, respectively. All these values were statistically different from saline-treated animals (Fig. 1A).

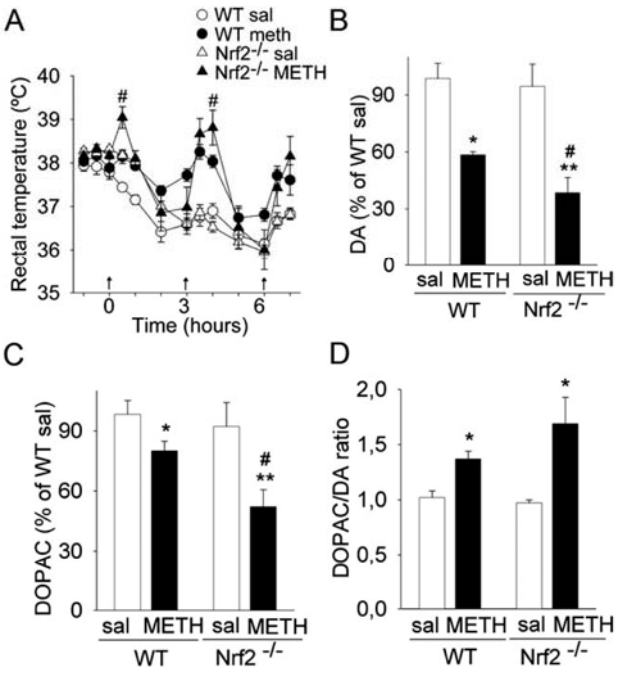

Fig. 1. Deficiency of Nrf2 enhances METH-induced hyperthermia and loss of striatal dopamine and DOPAC. **A**: METH (three injections of 5 mg/kg i.p., given at 3-h-intervals) increased rectal temperature in WT animals, peaking 30 min after each injection. This increase was higher in $Nrf2^{-/-}$ mice. Arrows indicate drug injection, n = 6–8. **B, C**: Histograms show striatal concentrations of dopamine (B) and DOPAC (C) as percentages of concentration of saline-treated WT animals (WT sal). **D**: DOPAC/DA ratio (mean ± SEM, n = 6–8) in the striatum of mice one day after METH administration. *$P < 0.01$, ** $P < 0.001$, compared to saline group; # $P < 0.05$ vs WT mice, two-way ANOVA followed by Tukey's test.

Nrf2 Deficiency Potentiates METH-Induced Striatal Dopamine Decrease

METH causes damage to the DA neuronal system, possibly via oxidative stress. Since Nrf2 regulates expression of genes that are protective against oxidative stress, we wanted to determine whether the absence of Nrf2 would increase loss of dopamine and its metabolites in the caudate-putamen. Twenty-four hours after METH administration, DA and its metabolite DOPAC were measured in the striatum and the DOPAC/DA ratio was determined (Fig. 1B–D). There was significant depletion of DA and DOPAC and an increase in the ratio

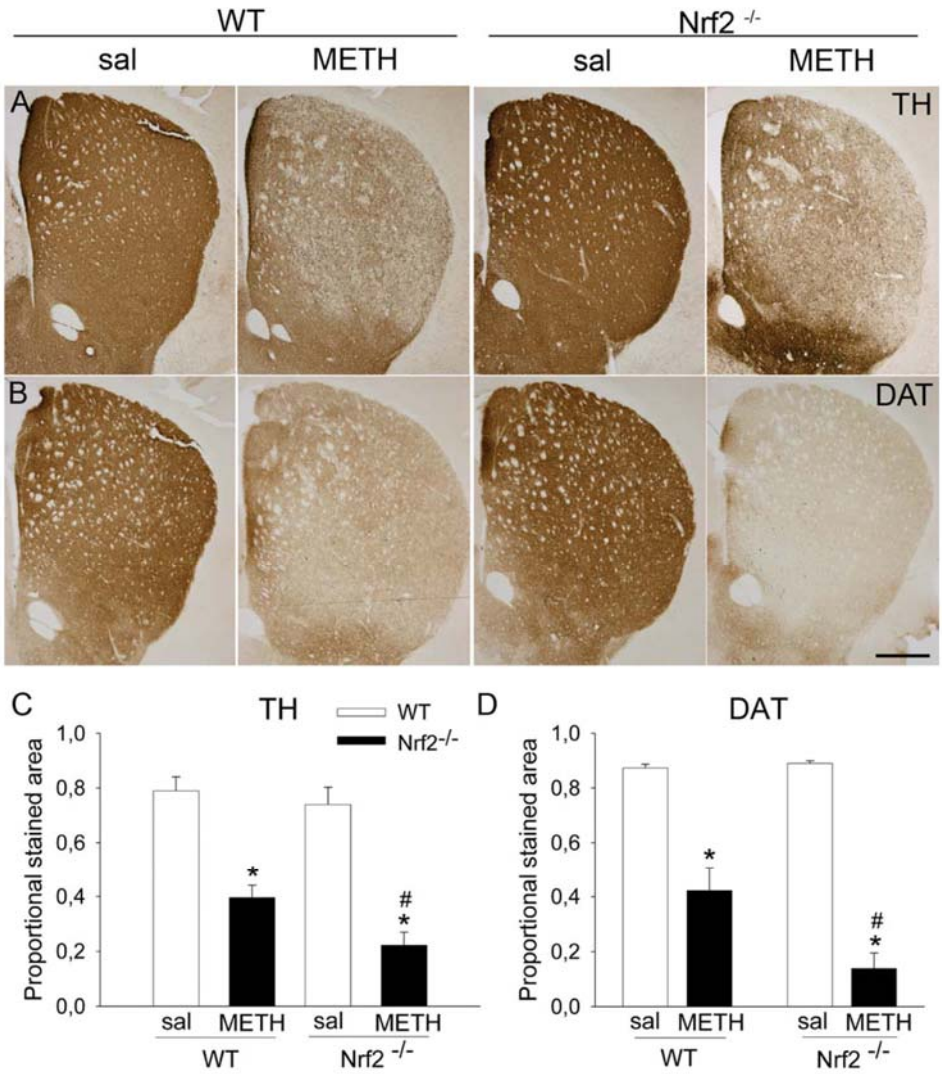

Fig. 2. METH induces greater TH and DAT fiber loss in the striatum of Nrf2$^{-/-}$ compared to WT animals. Photomicrographs of striatal sections stained for TH (**A**) and DAT (**B**) from mice one day after treatment with METH. **C, D**: Histograms show the proportional stained area of TH-ir (C) or DAT-ir (D) in the striatum. Data represent mean ± SEM, n = 6–8 per group. *$P < 0.05$ vs. saline; # $P < 0.05$ vs. WT, two-way ANOVA, followed by Tukey's test. Bar indicates 500 μm.

DOPAC/DA in the striatum of METH-treated mice. Compared with saline-treated mice, METH induced significant depletion of DA in both Nrf2$^{-/-}$ (61%, $P < 0.01$) and WT mice (42%, $P < 0.001$). Loss of DA was significantly greater in Nrf2$^{-/-}$ mice ($P < 0.05$). Similarly, METH decreased DOPAC levels compared with mice treated with saline by 40% ($P < 0.01$) in Nrf2$^{-/-}$ and 18% ($P < 0.001$) in WT mice. Again, the difference between the two genotypes treated with METH was significant ($P < 0.05$). Although it did not reach significance, Nrf2$^{-/-}$ mice always displayed a higher DOPAC/DA ratio than WT mice. In addition, the DOPAC/DA ratio 24 h after METH administration was significantly different from saline treated mice in both WT and Nrf2$^{-/-}$ mice ($P < 0.01$). These data demonstrate that dopaminergic damage is more extensive in Nrf2$^{-/-}$ mice than in their WT littermates.

METH-Induced TH and DAT Loss Is Exacerbated in Striatum of Nrf2$^{-/-}$ Mice

METH administration decreased TH and DAT fiber density in the mouse striatum one day after drug administration (Granado et al., 2010, 2011). Immunohistochemistry of brain sections through the caudate-putamen one day after METH administration revealed less TH and DAT immunoreactivity than in sections from saline-treated animals (Fig. 2A,B). Quantification demonstrated that METH administration to WT mice decreased TH immunoreactivity (ir) by 49.9% ($P < 0.001$) and DAT-ir by 51.6% ($P < 0.001$) compared with saline-treated mice (Fig. 2C,D). In METH-treated Nrf2$^{-/-}$ mice, TH-ir decreased by 69.9% ($P < 0.001$) and DAT-ir by 84.3% ($P < 0.001$) compared with saline-treated mice (Fig. 2C,D). The decreases in TH- and DAT-ir were significantly

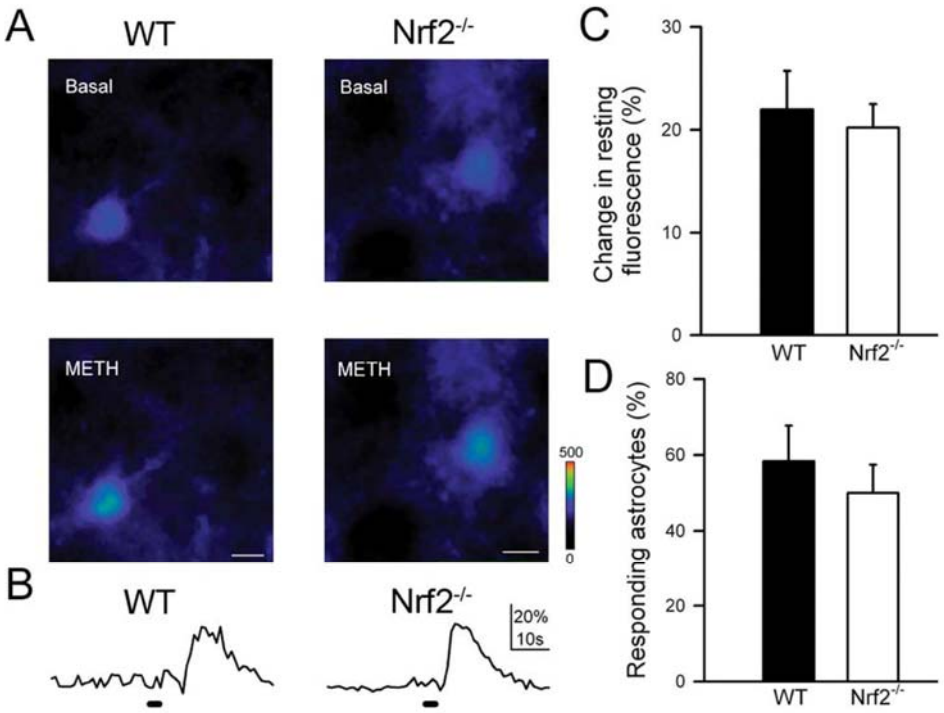

Fig. 3. Nrf2 deficiency does not modify the METH-induced increase in intracellular Ca^{2+} in striatal astrocytes. **A**: Pseudocolor images representing fluorescence intensities of a fluo-4 AM-filled astrocyte from the dorsolateral striatum before and after local application of METH delivered by pressure pulse from a micropipette. Scale bar, 10 μm. **B**: Astrocytic Ca^{2+} levels evoked by local application (horizontal bars) of METH. **C**, **D**: Relative fluorescence changes induced by METH and proportion of responding astrocytes in WT (black bars) and $Nrf2^{-/-}$ (white bars) mice. Error bars indicate SEM.

greater in $Nrf2^{-/-}$ than in WT mice ($P < 0.05$ for TH, $P < 0.001$ for DAT, two-way ANOVA).

As expected, one day of METH treatment had no effect on TH- and DAT-ir levels in the NAc of WT or $Nrf2^{-/-}$ mice (data not shown). Thus, the greatest neurotoxic effect of METH in $Nrf2^{-/-}$ mice was observed in the striatum, as is true for WT (Granado et al., 2010), and as has been shown for other amphetamine derivative drugs like MDMA (Granado et al., 2008a, b). Moreover, our data demonstrated that Nrf2 deficiency increased the neurotoxic effect of METH administration, primarily in the dorsal striatum.

In an attempt to dissociate neurotoxicity from hyperthermia in $Nrf2^{-/-}$, we carried out an additional experiment in which the ambient temperature was controlled at 21°C. In these conditions, only WT mice exhibited hyperthermia after the first injection of METH. Nevertheless, $Nrf2^{-/-}$ mice that did not show hyperthermia, still presented significantly greater reductions in striatal TH-ir one day after METH treatment than WT animals, indicating the role of the lack of this factor in potentiating METH-induced dopaminergic neurotoxicity independently of body temperature (Supp. Info. Fig. 1).

The Effect of METH on Striatal Gliosis Is Increased in $Nrf2^{-/-}$ Mice

To assess the functional integrity of astrocytes in $Nrf2^{-/-}$ mice, we measured intracellular Ca^{2+} signaling, a key element in astrocyte physiology, in response to METH in WT and $Nrf2^{-/-}$ mice. Astrocyte Ca^{2+} signal was determined from the mean resting fluorescence of Fluo-4 AM-filled astrocytes. The number of astrocytes that responded to METH was quantified in coronal sections from WT and $Nrf2^{-/-}$ striatum. METH increased the number of responding astrocytes by 50%–60% and the relative fluorescence signal by 20% within a few minutes of delivery to WT and $Nrf2^{-/-}$ mice (Fig. 3), indicating that Nrf2 deficiency does not impair the primary astrocytic response.

However, METH-induced neurotoxicity may be mediated by alterations of cellular redox status and induction of inflammatory genes. To test this hypothesis, we examined whether absence of Nrf2 affected METH-induced gliosis. Astroglia and microglia were examined with antibodies against glial fibrillar acidic protein (GFAP) and Mac-1 (CD11b), respectively. Immunofluorescence staining for GFAP demonstrated a small number of astrocytes in saline-treated WT and $Nrf2^{-/-}$ mice. Treatment with METH produced an increase in striatal GFAP expression in both genotypes, similar to that described for MDMA (Granado et al., 2008a, b, 2010). However, this increase was greater in $Nrf2^{-/-}$ mice than WT mice (Fig. 4A). When we examined the effects of METH on GFAP mRNA levels measured by qRT-PCR, we observed a significant twofold increase in $Nrf2^{-/-}$ animals compared with WT ($P < 0.05$, Fig. 4B). These data indicate that treatment with METH induces enhanced astrogliosis in the absence of Nrf2.

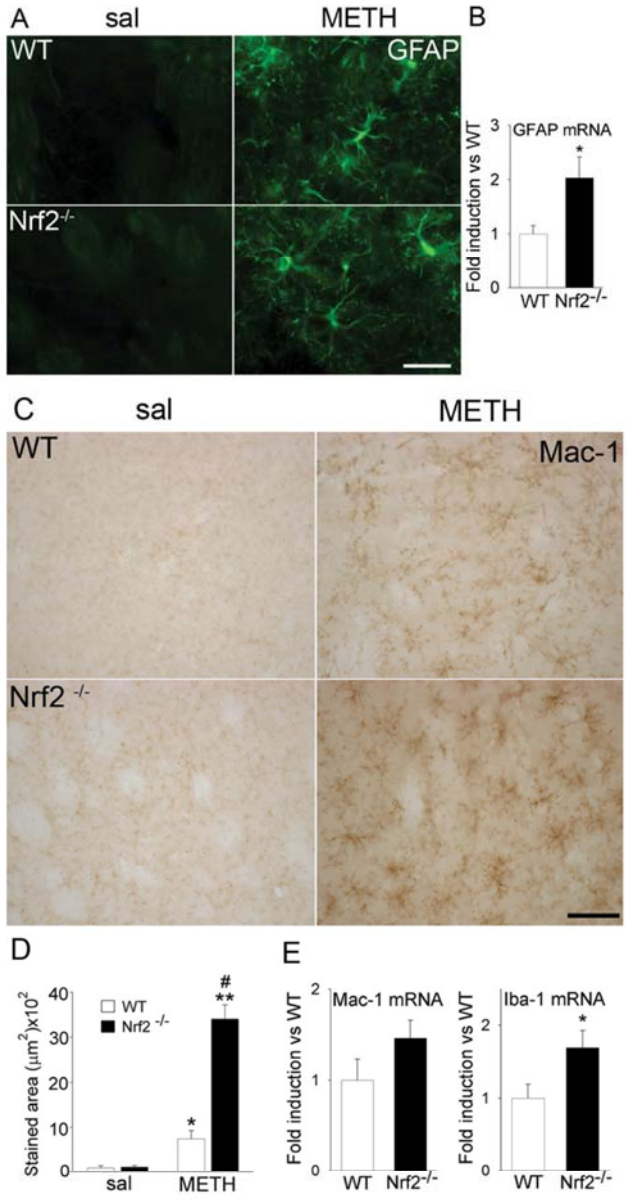

Fig. 4. Nrf2 deficiency increases gliosis induced by METH in the mouse striatum. **A, C**: Photomicrographs of striatal sections stained with GFAP (A) or Mac-1 (C) from WT (top row) and Nrf2$^{-/-}$ (bottom row) mice, one day after treatment with METH or saline. METH induced GFAP and Mac-1 expression in WT animals and this increase was higher in Nrf2$^{-/-}$ mice. Bar indicates 50 μm (A) or 100 μm (C). **B**: METH-induced GFAP mRNA levels were twice as high in Nrf2$^{-/-}$ as in WT mice. *$P < 0.05$ vs. WT mice, two-way ANOVA, followed by Tukey's test. **D**: Quantification of stained area of Mac1-ir. **E**: Striatal mRNA levels of Mac-1 and Iba-1 (determined by qRT-PCR) following METH administration were higher in Nrf2$^{-/-}$ than in WT mice, *$P < 0.05$ vs. WT mice, two-way ANOVA, followed by Tukey's test.

Immunohistochemistry for Mac-1 (CD11b) showed a small number of activated microglia in both WT and Nrf2$^{-/-}$ mice following treatment with saline. METH-treated animals exhibited an increased number of activated microglia in the striatum, and this increase was larger in Nrf2$^{-/-}$ than in WT mice (Fig. 4C). Quantification demonstrated that METH administration significantly ($P < 0.05$) increased Mac-1-ir and that this increase was even greater in Nrf2$^{-/-}$ mice ($P < 0.05$, two-way ANOVA), (Fig. 4D). Mac-1 mRNA levels were slightly, but not significantly, higher in METH-treated Nrf2$^{-/-}$ than WT animals (Fig. 4D). We also examined expression of Iba-1, another marker for microglial activation. Following METH administration, Iba-1 mRNA levels were significantly higher in Nrf2$^{-/-}$ WT mice than in WT (1.7-fold, $P < 0.05$, Fig. 4D). These data demonstrate a greater increase in METH-induced astrocytosis and microgliosis in Nrf2$^{-/-}$ mice than their WT littermates.

Nrf2 Deficiency Increases Expression of METH-Induced Proinflammatory and Oxidative Stress Markers in the Striatum

METH treatment increases the expression of microglia-associated factors, including TNF-α, IL-1β, and IL-15. We analyzed whether expression of these factors or of phase 2 enzymes was increased in Nrf2$^{-/-}$ mice. Quantitative-RT-PCR showed that under basal conditions Nrf2$^{-/-}$ mice expressed higher levels of TNF-α mRNA (Fig. 5A) compared with WT littermates. METH treatment induced a fivefold increase in TNF-α expression in WT mice and a 13.5-fold increase in Nrf2$^{-/-}$ mice one day after drug administration. This difference is significant ($P < 0.001$, two-way ANOVA), indicating that the proinflammatory effects of METH treatment are potentiated in the absence of Nrf2. Similar results were observed for IL-1β mRNA (data not shown). However, within the time-frame we examined, METH treatment did not induce any alteration in expression of the phase 2-related enzymes NQO1 and Gsta2 (data not shown). In addition, we analyzed the expression of antioxidant genes that are regulated by Nrf2, including the catalytic and modulatory subunits of γ-cysteine lygase (Gclc and Gclm), Cu/Zn-superoxide dismutase (Cu/Zn-SOD), Mn-superoxide dismutase (Mn-SOD), and glutathione peroxidase (GPx). qRT-PCR revealed a significant METH-induced increase in mRNA levels for all of these Nrf2-regulated genes except Gclc in WT mice but not in Nrf2$^{-/-}$ mice (Fig. 5B,C). Thus, Nrf2$^{-/-}$ mice treated with METH presented significantly lower levels of Gclm and GPx than WT animals. Levels of Cu/ZnSOD and MnSOD in Nrf2$^{-/-}$ METH treated mice also showed a tendency to be lower than in WT mice, although did not reach significance.

We also examined expression of IL-15, an early marker of neuroinflammation (Gomez-Nicola et al., 2008). One day after METH administration, we observed a greater increase in IL-15 expression levels in the striatum of Nrf2$^{-/-}$ mice than WT mice. This was evidenced by a higher number of striatal IL-15 positive cells showing engrossed cell body and numerous longer processes (Fig. 6A). To elucidate the identity of cells expressing IL-15, we performed double immunohistochemistry with antibody to IL-15 in combination with antibodies to either the astrocyte marker GFAP or to Iba-1, a marker of

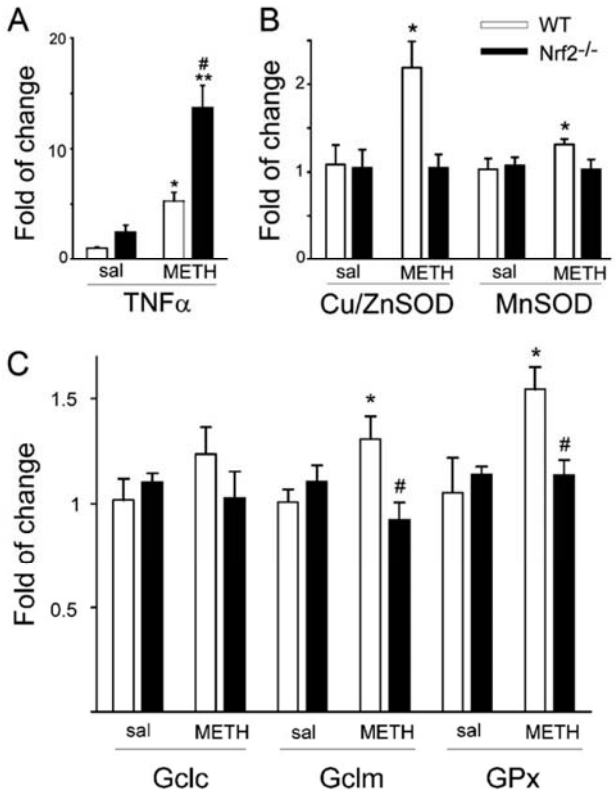

Fig. 5. The increase in METH-induced TNF-α expression in Nrf2-deficient mice may be because of lack of induction of Nrf2-regulated detoxification enzymes. **A**: Histogram shows fold induction of TNF-α mRNA expression in the striatum, one day after METH administration. METH induced a fivefold increase in TNF-α expression in WT mice and a 13.5-fold increase in $Nrf2^{-/-}$ mice. (mean ± SEM, n = 6–8 per group). **B and C**: Histograms show fold induction of mRNA for detoxification enzymes (B: Cu/Zn-SOD, Mn-SOD and C: Gclc, Gclm, GPx) in the striatum, one day after METH administration (mean ± SEM, n = 5 per group). *$P < 0.05$, ** $P < 0.001$, vs. saline group; # $P < 0.05$ vs. WT mice, two-way ANOVA, followed by Tukey's test.

reactive microglia. All IL-15-immunoreactive (IR) cells (red), colocalized with GFAP (green); however, not all GFAP-IR cells expressed IL-15 (Fig. 6B). Indeed, we found just 72% colocalization in WT animals treated with METH and a similar proportion, 76%, in $Nrf2^{-/-}$ mice. Moreover, Iba-1-IR increased after METH administration, and this increase was potentiated in $Nrf2^{-/-}$ mice (Fig. 6C). No Iba-1-IR cells expressed IL-15 in METH-treated WT or $Nrf2^{-/-}$ mice, despite the increased Iba-1 expression in $Nrf2^{-/-}$ mice (Fig. 6C). Together, these results suggest that Nrf2 mediates its neuroprotective effects via astrocytes.

Nrf2 Deficiency Potentiates METH-Induced Degeneration of Striatal Neurons

We previously reported that MDMA, another amphetamine derivative known to cause dopaminergic neurodegeneration, induced FluoroJade staining in the striatum. FluoroJade stains cell bodies, dendrites, and axon terminals of degenerating neurons without staining healthy neurons (Schmued et al., 1997; Granado et al., 2008a). One day after METH treatment, we observed some FluoroJade-stained neurons scattered throughout the striatum in WT mice, while saline-treated animals are devoid of staining. More neurons are stained with FluoroJade in $Nrf2^{-/-}$ mice after METH, suggesting that striatal neurons of $Nrf2^{-/-}$ mice are more vulnerable than those of WT mice to the neurotoxic effects of METH (Fig. 7).

Effects of METH on Gliosis in the Substantia Nigra in $Nrf2^{-/-}$ Mice

METH treatment not only increases gliosis in the caudate-putamen, but also in the substantia nigra, where dopamine cell bodies are located. We analyzed the impact of Nrf2 deficiency on METH-induced gliosis in the substantia nigra by looking at immunoflourescence for GFAP and Mac-1. We observed a similar small number of GFAP-ir astrocytes in saline-treated WT and $Nrf2^{-/-}$ mice. Treatment with METH produced an increase in GFAP-ir in the substantia nigra one day after treatment. This increase was larger in $Nrf2^{-/-}$ than WT mice (Fig. 8A). GFAP mRNA levels were slightly increased in $Nrf2^{-/-}$ mice compared with their WT littermates (Fig. 8C), although this increase did not reach statistical significance.

Mac-1 staining was increased following METH treatment in both $Nrf2^{-/-}$ and controls; however, Mac-1-ir and mRNA appeared to be induced to greater levels in $Nrf2^{-/-}$ mice compared with WT mice (Fig. 8B,D). mRNA for proinflammatory markers IL-1β (Fig. 8E) and TNF-α (Fig. 8F) were increased by METH, with a slightly, but not significantly, greater increase in $Nrf2^{-/-}$ mice compared with WT. Taken together, these results suggest that Nrf2 plays a more significant role in neuroprotection in the striatum than in the SN.

METH-Induced Loss of Dopaminergic Neurons in the SN Is Not Increased in $Nrf2^{-/-}$ Mice

To determine whether the increase in METH-induced striatal TH fiber loss we observed in $Nrf2^{-/-}$ corresponded to a bigger loss of dopaminergic cells in the SN of these animals, we assessed TH-ir in the SN using stereological methods to quantify dopaminergic neurons. SNpc dopaminergic neurons were identified by TH staining and were counterstained with Nissl. We observed a decrease in TH-ir in the SN *pars compacta* (SNpc; dopaminergic cell bodies) and in the *pars reticulata* (dopaminergic neuropil) one day after METH administration (Fig. 9A). The number of TH-ir neurons in the SN of METH-treated animals was significantly lower than in saline-treated animals in WT (79%) and $Nrf2^{-/-}$ (76%) mice ($P < 0.05$, post-hoc analysis for both genotypes compared to saline-treated animals, Fig. 9B). Similarly, the number of Nissl-stained SNpc neurons was significantly decreased in both genotypes compared with saline-treated animals (Fig. 9C). However, there were no

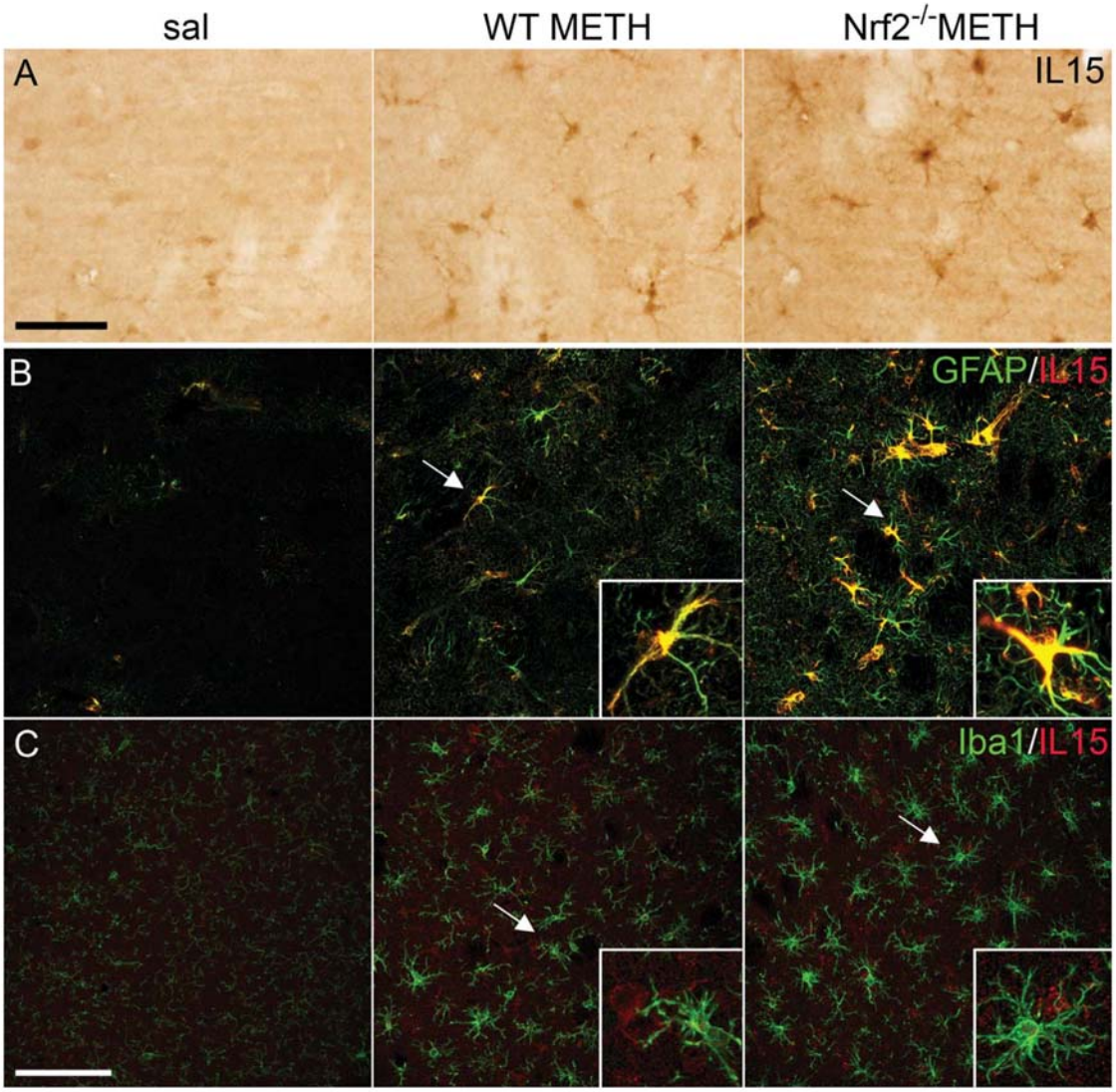

Fig. 6. Deficiency of Nrf2 enhances METH-induced IL-15 expression in the striatum. **A**: Photomicrographs of striatal sections stained for IL-15 from saline treated mice and WT and Nrf2$^{-/-}$ treated with METH. METH induced higher expression of IL-15 in Nrf2$^{-/-}$ mice than in WT mice. Bar indicates 100 μm. **B and C**: Sections were analyzed by double immunohistochemistry with antibodies to IL-15 (red) and to GFAP or Iba1 (green). Arrows indicate double-labeled neurons. Bar indicates 100 μm.

differences between METH-treated WT and Nrf2$^{-/-}$ mice in either TH or Nissl counts. Thus, at this time-point, loss of Nrf2 transcription factor does not potentiate METH-induced loss of dopamine neurons in the SNpc, despite producing stronger TH fiber loss in the striatum.

Apoptotic cell profiles were identified by Nissl staining in the SN of METH-treated WT and Nrf2$^{-/-}$ mice, further demonstrating that some dopaminergic neurons undergo cell death by apoptosis after METH treatment (Fig. 9D). An increase in FluoroJade staining in the SN following METH treatment further confirms the degeneration of neurons in this area as was described earlier (Granado et al., 2011). FluoroJade staining in the SN was similar in WT and Nrf2$^{-/-}$ mice (Fig. 9E).

DISCUSSION

Previous studies have shown that repeated administration of METH produced a hyperthermic response, accompanied by a loss of DA, TH, and DAT fiber loss in the striatum (Fantegrossi et al., 2008; Granado et al., 2010; O'Callaghan and Miller, 1994), a significant decrease in TH levels and DAT binding and protein levels in the striatum, and a concomitant neuronal loss in the SN. We found that the absence of Nrf2 transcription factor potentiated all of the following effects of METH in the striatum: TH- and DAT-ir loss, induction of reactive microglia and astrocytes, and an increase in striatal TNFα mRNA. In addition, Nrf2 mice exhibited significantly greater hyperthermia after METH injection than

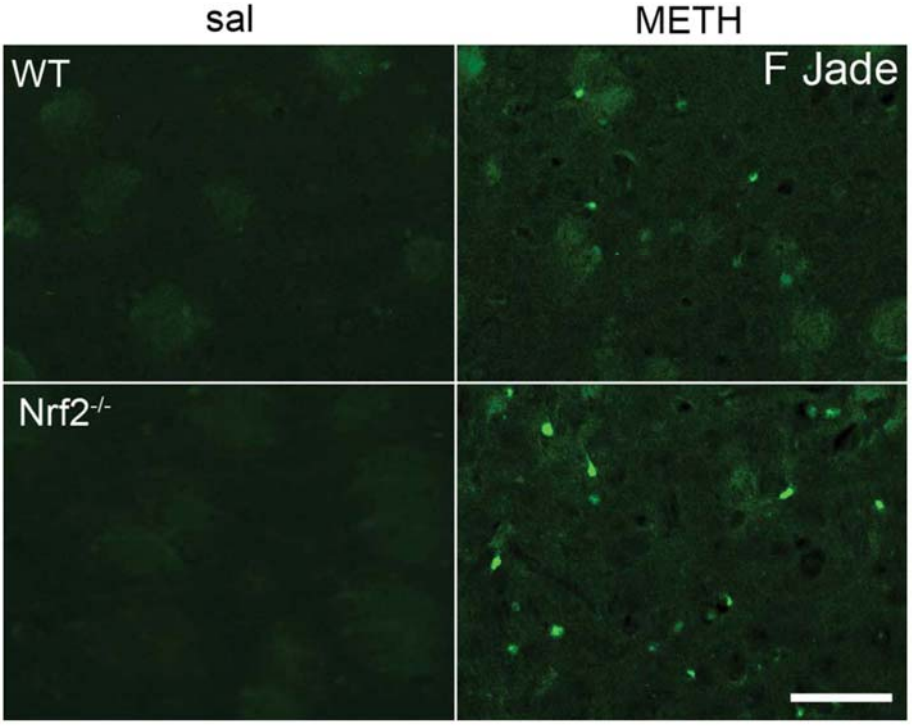

Fig. 7. Nrf2 deficiency potentiates degeneration of striatal neurons induced by METH. High power photomicrographs of striatal sections stained for FluoroJade from WT and Nrf2$^{-/-}$ mice one day after treatment with METH or saline. Note the increased FluoroJade signal in Nrf2$^{-/-}$ mice after METH treatment. Photomicrographs are representative of six to eight sections examined for each animal, five animals per group. Bar indicates 50 μm.

WT mice. By contrast, the degree of METH-induced dopaminergic cell loss in the SN was similar in Nrf2$^{-/-}$ and WT mice. Furthermore, the effect of METH on microglial and astroglial activation and IL-1β and TNFα mRNA levels in the SN showed a tendency to increase in Nrf2$^{-/-}$ mice compared with WT littermates.

Temperature dysregulation appears to be an important factor in the mediation of some toxic responses to METH. Hyperthermia facilitates METH-induced ROS production and increased oxidation of DA, which have been associated with the neurotoxic effects of this drug. In the current study, body temperature changes of Nrf2$^{-/-}$ animals were slightly above those of WT, along with increased degeneration in the striatum. It is possible that Nrf2$^{-/-}$ mice lacking Nrf2 transcription factor are more sensitive to temperature dysregulation after methamphetamine treatment because of reduced antioxidative defenses and increased oxidative stress responses. However, increased hyperthermia is not required for the potentiation of the neurotoxic effects of METH seen in Nrf2$^{-/-}$ mice. Because in experiments carried out at lower ambient temperature (21°C) in which Nrf2$^{-/-}$ mice did not showed higher body temperature than WT after METH, Nrf2$^{-/-}$ mice still had significantly more TH-fiber loss than WT mice. Moreover, other studies have shown that hyperthermia does not always correlate with METH-induced neurotoxicity. Experiments using classical pharmacology with reserpine and α-methyl tyrosine (Albers and Sonsalla 1995, Thomas et al., 2008), reviewed in Krasnova and Cadet (2009) or D2 receptor knock out mice (Granado et al., 2011) indicated that hyperthermia can contribute to, but is not solely responsible for the neurotoxicity induced by METH.

Nrf2$^{-/-}$ mice have exacerbated neurotoxicity after METH, particularly in the striatum, where we showed an increased TH-fiber loss 24 h after drug-treatment. A previous study in Nrf2$^{-/-}$ mice did not observe these differences (Pacchioni et al., 2007). This discrepancy may be because of a difference in timing: their experiments were done two weeks after drug administration, when dopaminergic recovery is highest. By contrast, our experiments were performed just 24 h after drug administration, when damage or loss of dopaminergic markers peaks, allowing us to see differences between the genotypes as we have shown previously for $D_2R^{-/-}$ mice (Granado et al., 2011). Consistent with our findings, dopaminergic neurons of Nrf2$^{-/-}$ mice were previously shown to be more sensitive to the MPTP neurotoxin used to model Parkinson's disease (Chen et al., 2009; Rojo et al., 2010). This sensitivity is evident through a wide range of MPTP doses (10–30 mg/kg, Chen et al., 2009). Nrf2 deficiency increases TH fiber loss in the mouse caudate-putamen following chronic MPTP administration because of decreased antioxidant defenses and increased inflammation.

Nrf2 is implicated in the synthesis of phase 2 detoxification enzymes that coordinate the protective response

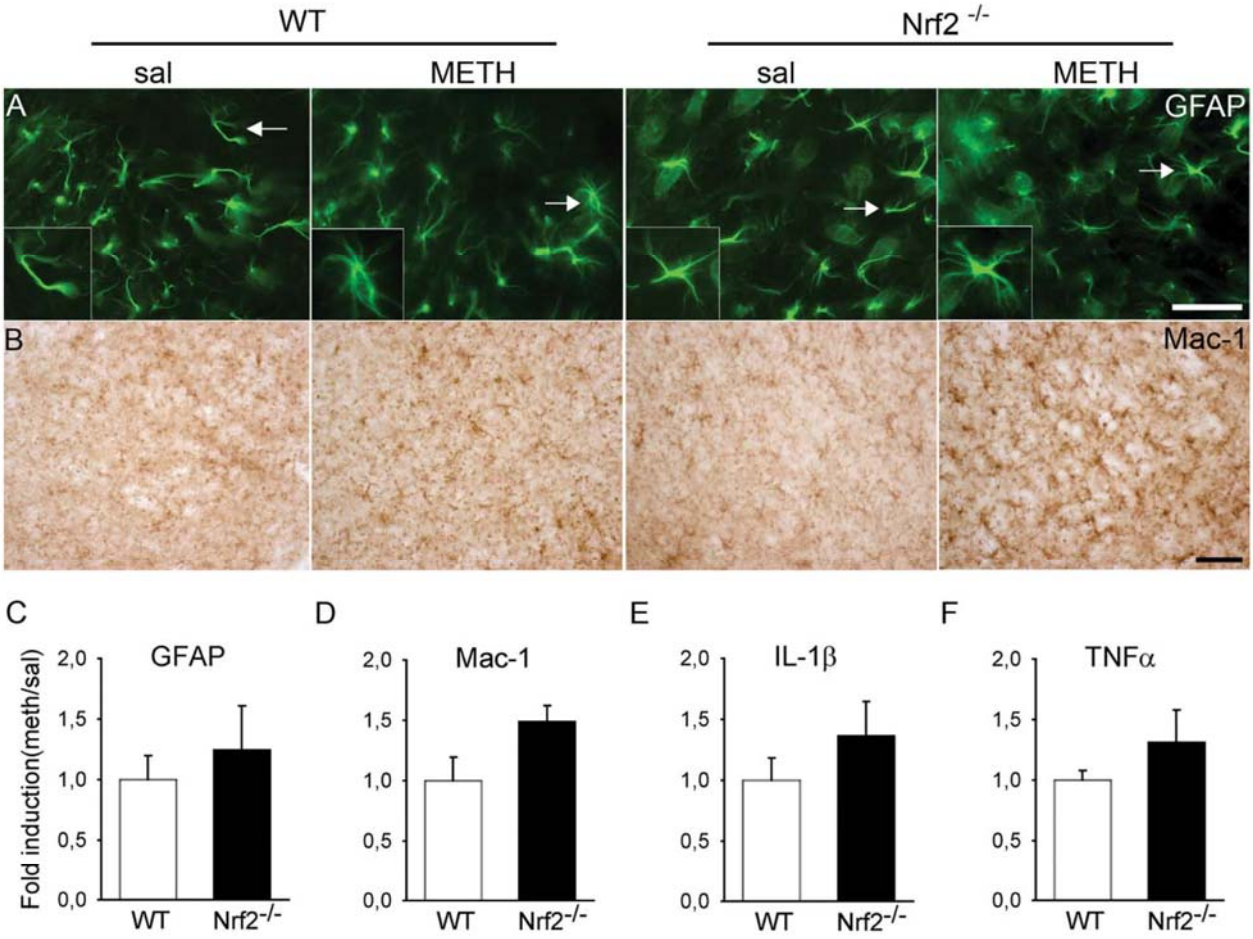

Fig. 8. METH-induced gliosis and expression of proinflammatory markers in the SN are higher in Nrf2 deficient mice compared to WT mice. **A, B**:. Sections of SN from WT and Nrf2$^{-/-}$ mice stained for GFAP (A) and Mac-1 (B) one day after treatment with METH or saline. Note that sections of Nrf2$^{-/-}$ mice show similar GFAP and Mac-1 staining to WT mice. Bars indicate 50 μm (A, B). **C–F**: Histogram shows fold induction of GFAP(C), Mac-1(D), IL-1β (E), and TNF-α (F) mRNA levels in the SN, one day after METH treatment. Slightly higher levels in Nrf2$^{-/-}$ compared with WT mice did not reach statistical significance (mean ± SEM, n = 6–8 per group).

to oxidative stress. Decreased expression of the phase 2 enzymes is likely one of the reasons that Nrf2$^{-/-}$ mice are more susceptible to MPTP (Chen et al., 2009; Rojo et al., 2010) and lipolysaccharide (Innamorato et al., 2008; Rangasamy et al., 2004; Thimmulappa et al., 2006a, b), toxins that generate ROS. It is likely that a similar mechanism occurs following METH administration in the absence of Nrf2: ARE-regulated genes in the striatum, including HO-1 and other antioxidant genes, are not induced as they are in WT mice, leading to increased oxidative stress, accumulation of ROS (Chen et al., 2009), and ultimately to dopamine fiber loss.

METH injections also cause reactive microgliosis and astrocytosis in the mouse striatum, peaking 1 and 3 days, respectively, after METH administration (Fantegrossi et al., 2008; Granado et al., 2010; Thomas et al., 2004; Zhu et al., 2005). Nrf2 is an important modulator of microglial dynamics and participates in prevention of inflammation by a mechanism that has not been elucidated. As expected, injection of METH produced an increase in astrogliosis in WT mice, indicated by an increase in GFAP mRNA and protein levels, which was exacerbated significantly in Nrf2$^{-/-}$ mice one day after METH. Furthermore, METH-treated Nrf2$^{-/-}$ mice expressed a greater increase than WT mice in striatal microglial and proinflammatory markers, in particular TNF-α, indicating that the inflammation caused by METH is enhanced in the absence of Nrf2. Higher levels of TNFα presented by Nrf2$^{-/-}$ in our experiments after METH treatment seem to be a consequence of the higher neurotoxicity rather than the cause (Nakajima et al., 2004; Lai et al., 2009). These results, in addition to the data obtained with Ca^{2+} signaling, indicate that the primary response of astrocytes to METH is similar in Nrf2$^{-/-}$ and WT mice. However, in the absence of Nrf2, the antioxidant capacity of the striatum is reduced, leaving neurons more vulnerable to progressive METH-induced increases in oxidative stress and inflammation, providing strong evidence for the role of Nrf2 in antioxidant and anti-inflammatory processes.

Previous studies showed that MPTP-induced toxicity was completely abolished in transgenic mice overex-

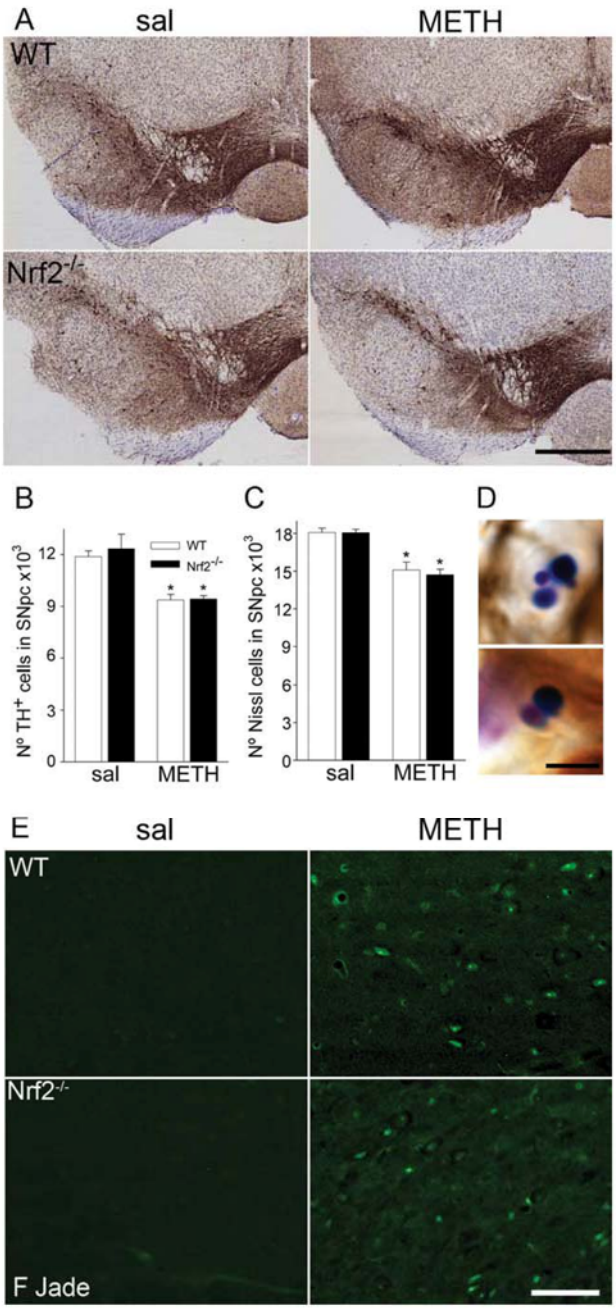

Fig. 9. METH induces a similar loss of dopaminergic neurons in SN of WT and Nrf2$^{-/-}$ mice. **A**: SN sections from WT and Nrf2$^{-/-}$ mice stained for TH 1 day after treatment with METH or saline. **B, C**: Histograms show number of TH-positive and Nissl-stained neurons in the SNpc of WT and Nrf2$^{-/-}$ mice (mean ± SEM, n = 3–4 per group) counted by stereology in midbrain sections obtained one day after METH treatment. **D**: Photomicrographs of Nissl-stained apoptotic bodies observed in the SN of WT and Nrf2$^{-/-}$ mice after one day of METH administration. **E**: Nigral sections from WT and Nrf2$^{-/-}$ mice stained with FluoroJade one day after saline (left panel) or METH (right panel) treatment. Photomicrographs are representative of four sections, taking both hemispheres, examined for each animal, five animals per group. * $P < 0.05$ vs. saline, two way ANOVA, followed by Tukey's test. Bars indicate 500 μm (A), 5 μm (D) or 50 μm (E).

pressing Nrf2 under the control of GFAP (Chen et al., 2009). In addition, transplanted Nrf2-expressing astrocytes in the striatum were able to protect against other dopaminergic neurotoxins, such as 6-OHDA, injected in the transplanted striatum (Jakel et al., 2007), further indicating that Nrf2 transcription factor activation in GFAP-positive cells is important for the survival of TH fibers in the striatum after dopaminergic injury.

In a recent study, Jayanthi et al. (2009) reported Nrf2 activation in the striatum of rats treated with METH. Our finding that Nrf2-deficient mice were more sensitive than WT to METH-induced striatal damage further demonstrates that Nrf2 activation is part of a defensive response. The Jayanthi et al. study also demonstrated METH-induced activation of the ER stress response. Based on their data, it is tempting to speculate that activation of the ER stress response leads to induction of Nrf2 in response to METH. Indeed, Diehl's group has demonstrated that PERK, a transmembrane protein kinase required for the cellular response to ER stress, phosphorylates and activates this transcription factor (Cullinan et al., 2003). In agreement with this hypothesis, we observed a small upregulation of CHOP, a critical ER response protein; however, we did not see a consistent increase in BIP, another ER stress marker (data not shown). The Jayanthi et al. study was in rats and used a different dosing paradigm and different time point for examination; any of these factors may account for the discrepancy between their results and ours. Further work will be required to compare the ER response reported in rat striatum with that of wild type mice and Nrf2-deficient mice.

In the substantia nigra, METH administration induced loss of TH cells to a similar degree in WT and Nrf2$^{-/-}$ mice one day after drug delivery. This cell loss was accompanied by an increase in astrogliosis and microgliosis, as well as proinflammatory cytokines, which were slightly, but not significantly, greater in the absence of Nrf2. Thus, at this time point, Nrf2 deficiency potentiates METH-induced neurotoxicity in the striatum, but not in the SN. It is possible that METH differentially actives Nrf2-ARE transcription pathways in the striatum and in the SN. In fact, other dopaminergic toxins like MPTP differentially modulate this pathway: MPTP decreases Nrf2 and NAD(P)H:quinone oxidoreductase-1 (NQO1) protein levels in the striatum, but significantly increases them in the SN (Chen et al., 2009). Thus, differential regulation of Nrf2 by METH in SN and striatum might explain the lack of effect of Nrf2$^{-/-}$ on neurotoxicity in the SN in our study.

In summary, we have shown that METH administration induced greater damage in striatum of Nrf2$^{-/-}$ mice than WT mice when examined one day after drug administration. In addition, cytokine mRNA levels, gliosis, and astrocytosis in the striatum were elevated to a greater extent in METH-treated Nrf2$^{-/-}$ mice than WT mice. Our data strongly support the hypothesis that METH produces dopaminergic neurotoxicity through a process involving inflammation and oxidative stress. In addition, they suggest that in WT animals, Nrf2 plays

an important protective role against dopaminergic neurotoxicity by modulating the inflammation and oxidative stress induced by METH.

ACKNOWLEDGMENTS

NGM is recipient of a Juan de la Cierva contract and ILB is recipient of a Ramón y Cajal contract and SAS is funded with a JAE predoctoral fellowship from the CSIC. The authors thank Emilia Rubio, Marco de Mesa, and Rosa Ana Ramírez for their technical support.

REFERENCES

Albers DS, Sonsalla PK. 1995. Methamphetamine-induced hyperthermia and dopaminergic neurotoxicity in mice: pharmacological profile of protective and nonprotective agents. J Pharmacol Exp Ther 275: 1104–1114.

Cadet JL, Jayanthi S, Deng X. 2005. Methamphetamine-induced neuronal apoptosis involves the activation of multiple death pathways. Neurotox Res 8:199–206.

Cadet JL, Krasnova IN, Jayanthi S, Lyles J. 2007. Neurotoxicity of substituted amphetamines: Molecular and cellular mechanisms. Neurotox Res 11:183–202.

Calkins MJ, Jakel RJ, Johnson DA, Chan K, Kan YW, Johnson JA. 2005. Protection from mitochondrial complex II inhibition in vitro and in vivo by Nrf2-mediated transcription. Proc Natl Acad Sci USA 102:244–249.

Chen PC, Vargas MR, Pani AK, Smeyne RJ, Johnson DA, Kan YW, Johnson JA. 2009. Nrf2-mediated neuroprotection in the MPTP mouse model of Parkinson's disease: Critical role for the astrocyte. Proc Natl Acad Sci USA 106:2933–2938.

Clark J, Simon DK. 2009. Transcribe to survive: Transcriptional control of antioxidant defense programs for neuroprotection in Parkinson's disease. Antioxid Redox Signal 3:509–528.

Cullinan SB, Zhang D, Hannink M, Arvisais E, Kaufman RJ, Diehl JA. 2003. Nrf2 is a direct PERK substrate and effector of PERK-dependent cell survival. Mol Cell Biol 23:7198–7209.

Darmopil S, Martín AB, De Diego IR, Ares S, Moratalla R. 2009. Genetic inactivation of dopamine D1 but not D2 receptors inhibits L-DOPA-induced dyskinesia and histone activation. Biol Psychiatry 66:603–613.

Darmopil S, Muñetón-Gómez VC, de Ceballos ML, Bernson M, Moratalla R. 2008. Tyrosine hydroxylase cells appearing in the mouse striatum after dopamine denervation are likely to be projection neurones regulated by L-DOPA. Eur J Neurosci 27:580–592.

Eisch AJ, Gaffney M, Weihmuller FB, O'Dell SJ, Marshall JF. 1992. Striatal subregions are differentially vulnerable to the neurotoxic effects of methamphetamine. Brain Res 598:321–326.

Fantegrossi WE, Ciullo JR, Wakabayashi KT, De La GR, Traynor JR, Woods JH. 2008. A comparison of the physiological, behavioral, neurochemical and microglial effects of methamphetamine and 3,4-methylenedioxymethamphetamine in the mouse. Neuroscience 151:533–543.

Gómez-Nicola D, Valle-Argos B, Pita-Thomas DW, Nieto-Sampedro M. 2008. Interleukin 15 expression in the CNS: Blockade of its activity prevents glial activation after an inflammatory injury. Glia 56:494–505.

Granado N, Ares-Santos S, O'shea E, Vicario-Abejón C, Colado MI, Moratalla R. 2010. Selective vulnerability in striosomes and in the nigrostriatal dopaminergic pathway after methamphetamine administration: Early loss of TH in striosomes after methamphetamine. Neurotox Res 18:48–58.

Granado N, Ares-Santos S, Oliva I, O Shea E, Martin ED, Colado MI, Moratalla R. 2011. Dopamine D2-receptor knockout mice are protected against dopaminergic neurotoxicity induced by methamphetamine or MDMA. Neurobiol Dis 42:391–403.

Granado N, Escobedo I, O'shea E, Colado MI, Moratalla R. 2008a. Early loss of dopaminergic terminals in striosomes after MDMA administration to mice. Synapse 62:80–84.

Granado N, Ortiz O, Suarez LM, Martin ED, Cena V, Solis JM, Moratalla R. 2008c. D1 but notD5 dopamine receptors are critical for LTP, spatial learning, and LTP-induced arc and zif268 expression in the hippocampus. Cereb Cortex 18:1–12.

Granado N, O'shea E, Bove J, Vila M, Colado MI, Moratalla R. 2008b. Persistent MDMA-induced dopaminergic neurotoxicity in the striatum and substantia nigra of mice. J Neurochem 107:1102–1112.

Innamorato NG, Rojo AI, Garcia-Yague AJ, Yamamoto M, de Ceballos ML, Cuadrado A. 2008. The transcription factor Nrf2 is a therapeutic target against brain inflammation. J Immunol 181:680–689.

Itoh K, Chiba T, Takahashi S, Ishii T, Igarashi K, Katoh Y, Oyake T, Hayashi N, Satoh K, Hatayama I, Yamamoto M, Nabeshima Y. 1997. An Nrf2/small Maf heterodimer mediates the induction of phase II detoxifying enzyme genes through antioxidant response elements. Biochem Biophys Res Commun 236:313–322.

Jakel RJ, Townsend JA, Kraft AD, Johnson JA. 2007. Nrf2-mediated protection against 6-hydroxydopamine. Brain Res 1144:192–201.

Jayanthi S, McCoy MT, Beauvais G, Ladenheim B, Gilmore K, Wood W 3rd, Becker K, Cadet JL. 2009. Methamphetamine induces dopamine D1 receptor-dependent endoplasmic reticulum stress-related molecular events in the rat striatum. PLoS One 4:e6092

Johnson JA, Johnson DA, Kraft AD, Calkins MJ, Jakel RJ, Vargas MR, Chen PC. 2008. The Nrf2-ARE pathway: An indicator and modulator of oxidative stress in neurodegeneration. Ann NY Acad Sci 1147:61–69.

Kang J, Jiang L, Goldman SA, Nedergaard M. 1998. Astrocyte-mediated potentiation of inhibitory synaptic transmission. Nat Neurosci 1:683–692.

Krasnova IN, Cadet JL. 2009. Methamphetamine toxicity and messengers of death. Brain Res Rev 60:379–407. Review.

Lai YT, Tsai YP, Cherng CG, Ke JJ, Ho MC, Tsai CW, Yu L. 2009. Lipopolysaccharide mitagates methamphetamine-induced striatal dopamine depletion via modulating local TNF-alpha and dopamine transporter expression. J Neural Transm 116:405–415.

Lo SC, Li X, Henzl MT, Beamer LJ, Hannink M. 2006. Structure of the Keap1:Nrf2 interface provides mechanistic insight into Nrf2 signaling. EMBO J 25:3605–3617.

Martín AB, Fernández-Espejo E, Ferrer B, Gorriti MA, Navarro M, Rodríguez de Fonseca F, Moratalla R. 2008. Expression and function of CB1 receptor in the rat striatum: Localization and effects on D1 and D2 dopamine receptor-mediated motor behaviors. Neuropsychopharmacol 33:1667–1679.

Martín ED, Buño W. 2005. Stabilizing effects of extracellular ATP on synaptic efficacy and plasticity in hippocampal pyramidal neurons. Eur J Neurosc 21:936–944.

Martín ED, Fernández M, Perea G, Pascual O, Haydon PG, Araque A, Ceña V. 2007. Adenosine released by astrocytes contributes to hypoxia-induced modulation of synaptic transmission. Glia 55:36–45.

Nakajima A, Yamada K, Nagai T, Uchiyama T, Miyamoto Y, Mamiya T, He J, Nitta A, Mizuno M, Tran MH, Seto A, Yoshimura M, Kitaichi K, Hasegawa T, Saito K, Yamada Y, Seishima M, Sekikawa K, Kim HC, Nabeshima T. 2004. Role of tumor necrosis factor-alpha in methamphetamine-induced drug dependence and neurotoxicity. J Neurosci 24:2212–2225.

O'Callaghan JP, Miller DB. 1994. Neurotoxicity profiles of substituted amphetamines in the C57BL/6J mouse. J Pharmacol Exp Ther 270:741–751.

Ortiz O, Delgado-García JM, Espadas I, Bahí A, Trullas R, Dreyer JL, Gruart A, Moratalla R. 2010. Associative learning and CA3-CA1 synaptic plasticity are impaired in D1R null, Drd1a$^{-/-}$ mice and in hippocampal siRNA silenced Drd1a mice. J Neurosci 30:12288–12300.

Pacchioni AM, Vallone J, Melendez RI, Shih A, Murphy TH, Kalivas PW. 2007. Nrf2 gene deletion fails to alter psychostimulant-induced behavior or neurotoxicity. Brain Res 1127:26–35.

Pavón N, Martín AB, Mendialdua A, Moratalla R. 2006. ERK phosphorylation and FosB expression are associated with L-DOPA-induced dyskinesia in hemiparkinsonian mice. Biol Psychiatry 59:64–74.

Perea G, Araque A. 2007. Astrocytes potentiate transmitter release at single hippocampal synapses. Science 317:1083–1086.

Rangasamy T, Cho CY, Thimmulappa RK, Zhen L, Srisuma SS, Kensler TW, Yamamoto M, Petrache I, Tuder RM, Biswal S. 2004. Genetic ablation of Nrf2 enhances susceptibility to cigarette smoke-induced emphysema in mice. J Clin Invest 114:1248–1259.

Rangasamy T, Guo J, Mitzner WA, Roman J, Singh A, Fryer AD, Yamamoto M, Kensler TW, Tuder RM, Georas SN, Biswal S. 2005. Disruption of Nrf2 enhances susceptibility to severe airway inflammation and asthma in mice. J Exp Med 202:47–59.

Ricaurte GA, Guillery RW, Seiden LS, Schuster CR, Moore RY. 1982. Dopamine nerve terminal degeneration produced by high doses of methylamphetamine in the rat brain. Brain Res 235:93–103.

Rodrigues TB, Granado N, Ortiz O, Cerdan S, Moratalla R. 2007. Metabolic interactions between glutamatergic and dopaminergic neurotransmitter systems are mediated through D(1) dopamine receptors. J. Neurosci Res 85:3284–3293.

Rojo AI, Innamorato NG, Martin-Moreno AM, De Ceballos ML, Yamamoto M, Cuadrado A. 2010. Nrf2 regulates microglial dynamics and

DISCUSIÓN

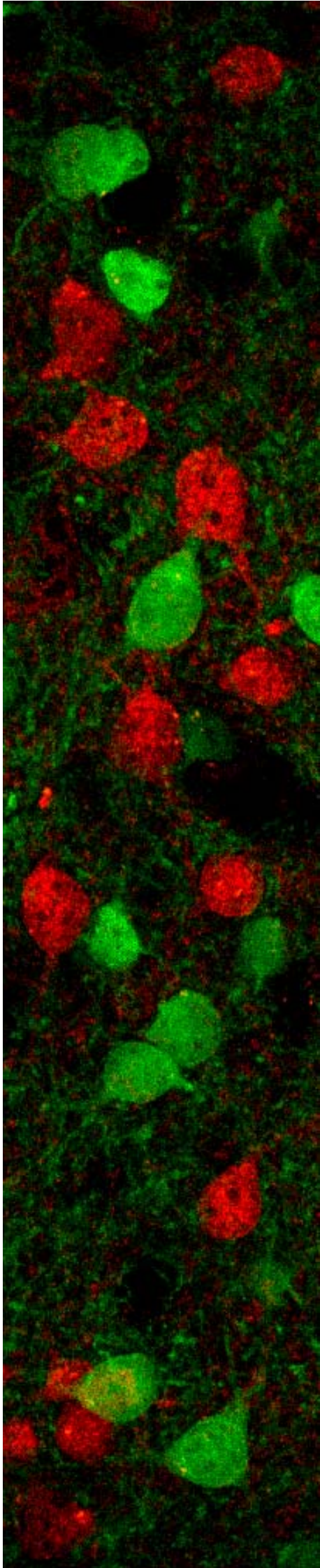

Foto de la página anterior: Sección de estriado de un ratón transgénico BAC D1-Tmt/D2-GFP en la que se ha hecho una tinción inmunofluorescente para las neuronas de proyección de la vía directa (D1-tmt, rojo) y para las de la vía indirecta (D2-GFP, verde) . Obsérvese que estas dos poblaciones no colocalizan.

La metanfetamina induce degeneración de terminales dopaminérgicos en el estriado

Los resultados de nuestros estudios afianzan trabajos previos realizados con otros métodos de plata que indican que la metanfetamina produce la destrucción y pérdida de terminales dopaminérgicos en el estriado (Ricaurte *et al*. 1982, 1984) y no una simple reducción en la expresión de marcadores dopaminérgicos. La pérdida de terminales TH-ir, junto con la presencia concomitante de terminales teñidos con plata y gliosis en el estriado (Fig. 1, 2 y 3, pág. 44, 46 y 47), revelan la degeneración selectiva de los terminales dopaminérgicos, 1 día después del tratamiento con metanfetamina. Estos resultados se confirmaron con microscopía electrónica que mostró fibras dopaminérgicas en degeneración, y terminales positivos para 3NT (Fig. 5, pág. 49) marcador de daño irreversible como consecuencia de formación de peroxinitritos (Imam *et al.* 2001).

Se ha planteado la hipótesis de que la metanfetamina puede causar la pérdida de terminales dopaminérgicos mediante la redistribución de la dopamina desde el entorno reductor del interior de las vesículas sinápticas al ambiente oxidante extravesicular intracelular (Krasnova y Cadet 2009). La dopamina citoplasmática se oxida fácilmente a especies reactivas como quinonas y peroxinitrito ,después de la combinación con el NO (Imam *et al.* 2001), que pueden contribuir a la interrupción de importantes procesos celulares incluyendo la función del axón (Hastings 2009), la bioenergética, la estabilidad de los microtúbulos, el tráfico de orgánulos y la autofagia, dando lugar a problemas de tráfico axonal, disfunción y degeneración (Burke y O 'Malley 2012; Krasnova y Cadet 2009; Yamamoto y Yang 2012). La administración de múltiples dosis bajas de metanfetamina (**3x5** ó **3x10**) resultó claramente más tóxica para los terminales dopaminérgicos en el estriado que la administración de una única dosis alta (**1x30**) (Fig. 1b, c, d, pág. 44). Esta disparidad podría deberse a los diferentes efectos de estos protocolos sobre el bloqueo del DAT o del VMAT-2, que resulta en la acumulación citosólica de la dopamina, que es mayor y de más duración en administraciones múltiples que en administraciones únicas de metanfetamina (Fleckenstein *et al.* 1999; Metzger *et al.* 2000). Además, la respuesta hipertérmica fue mayor y tuvo más picos con la administración de múltiples dosis bajas (**3x5** y **3x10**) que con la administración única de una dosis alta, aunque con este último régimen la hipertermia fue más sostenida (Fig. 1a pág. 44). Como ya se describió en la introducción y se discutirá más adelante, aunque la hipertermia puede potenciar los efectos neurotóxicos de la metanfetamina, no es la única responsable de neuropatología inducida por la metanfetamina (Albers y Sonsalla 1995; Ares-Santos *et al.* 2012, Urrutia *et al.* 2013).

La metanfetamina puede causar la muerte de neuronas estriatales

Estudios anteriores habían llegado a la conclusión de que la administración de metanfetamina (**3x10** ó **1x30**) induce degeneración de neuronas estriatales tan pronto como 1 día después del tratamiento (Tulloch *et al*. 2011; Zhu et al. 2006a, b) y todavía detectable a los 3 días (Fig. 2 a, b pág. 46). Sorprendentemente, observamos que el protocolo de **3x5** no indujo aumentos significativos en el número de neuronas estriatales en degeneración, mientras que los protocolos de **3x10** y **1x30** sí lo hicieron, y además no se observaron diferencias en el número de neuronas estriatales que degeneran entre los protocolos de **3x10** y **1x30**, a pesar de la diferencia significativa que presentan en sus efectos neurotóxicos sobre los terminales dopaminérgicos en el estriado (Fig. 1 pág. 44). Otros estudios han

señalado que la apoptosis estriatal es independiente de la respuesta hipertérmica, y que la administración de dosis bajas repetidas de metanfetamina (4x10mg/kg, en intervalos de 2h) es menos eficaz en la inducción de la muerte celular apoptótica, evaluada por tinción de TUNEL a las 24h del tratamiento, que dosis únicas administradas en bolus de 1x30mg/kg (Zhu *et al*. 2006a) .Esta conclusión concuerda con nuestros resultados.

Este es el primer estudio que demuestra que las neuronas que degeneran tras un tratamiento con metanfetamina se distribuyen por igual entre las neuronas de proyección de las vías directa, indirecta y otro tipo de neuronas estriatales (Fig. 2d pág. 46). Un tercio de las neuronas estriatales positivas para la plata no colocalizaron con D1/Tmt ni con D2/GFP (Fig. 2e, f pág. 46). Esto podría significar que algunas neuronas de proyección estriatal han perdido la expresión de proteínas Tmt o GFP antes de degenerar, o que se trata de interneuronas. Dado que las interneuronas comprenden una población de células mucho menor en el cuerpo estriado (5-10%) en relación a las neuronas de proyección (90-95%) (Kawaguchi *et al.* 1995), la equidad de poblaciones de células en degeneración (neuronas de proyección de las vías directa e indirecta y otras neuronas (probablemente las interneuronas) sugieren que las interneuronas son selectivamente más vulnerables a la metanfetamina. En esta línea, hay trabajos previos que muestran que las neuronas de proyección son menos vulnerables a la neurotoxicidad de metanfetamina que las interneuronas parvalbúmina o colinérgicas, aunque las interneuronas somatostatina son refractarias a la neurotoxicidad inducida por metanfetamina (Zhu *et al.* 2006b).

La metanfetamina induce muerte de neuronas dopaminérgicas en la SNpc

Este es también el primer estudio que proporciona evidencias sólidas y directas de la degeneración de las neuronas dopaminérgicas en la SNpc después de la exposición a la metanfetamina (Fig. 4 pág. 48), confirmado las sospechas suscitadas en estudios anteriores que mostraron reducciones en el número de neuronas TH positivas, y de células Nissl, junto con la presencia de cuerpos apoptóticos en esta área (Ares-Santos *et al.* 2012, Granado *et al.* 2011a, b; Sonsalla *et al.* 1996). Aunque se ha propuesto que la degeneración axonal, en lugar de la pérdida neuronal, desempeña el papel causal dominante en las manifestaciones clínicas de la enfermedad de Parkinson (Burke y O 'Malley, 2012), la pérdida permanente de una pequeña fracción de las células dopaminérgicas en la SNpc haría disminuir la capacidad de compensación y de protección frente a daños futuros (Switzer 1991). Ricaurte *et al.* 1982 ya utilizaron una técnica de plata (el método Fink-Heimer) para examinar si un régimen neurotóxico de metanfetamina producía degeneración de las neuronas dopaminérgicas de la SNpc en ratas, sin que encontraran pruebas de la pérdida de somas. Sin embargo y según nuestros resultados, el momento que escogieron para su estudio no era el óptimo, ya que buscaron degeneración terminal entre el estriado 4 días después del tratamiento, pero esperaron aproximadamente 6 semanas, para buscar la neurodegeneración en la SNpc "con el fin de dejar tiempo suficiente para que la degeneración retrógrada llegara hasta el cuerpo celular". En nuestro experimento de curso temporal, encontramos que la mayor degeneración de los cuerpos celulares de las neuronas se produce entre 1-3 días tras la administración de metanfetamina, en consonancia con otros estudios con técnicas de plata reducida que muestran que los cuerpos celulares en degeneración sólo pueden ser detectados poco después de la lesión, ya que los desechos se aclaran entre los 7-10 días (Switzer 2000).

Se observaron también varios axones degenerando en el haz prosencefálico medial (MFB) en su camino de la SNpc al estriado (Fig. 3, pág. 47), proporcionando pruebas de que la pérdida de neuronas observada en la SNpc podría ser debida a la degeneración retrógrada. Sin embargo, los axones en el MFB y las neuronas dopaminérgicas que degeneran en la SNpc tras la metanfetamina representan un pequeño porcentaje en comparación con el daño masivo de terminales observado en el estriado.

Curso temporal de la degeneración en la vía nigroestriatal

Nuestro experimento de curso temporal con el régimen de múltiples dosis bajas de metanfetamina (**3x5**) muestra que la degeneración de los terminales dopaminérgicos en el estriado y de los cuerpos celulares en la SNpc ya había comenzado a las 3-12 horas del tratamiento, y alcanza su máximo al día siguiente del tratamiento para los terminales y entre 1-3 días después del tratamiento para los cuerpos neuronales (Fig. 5a-g, pág. 49). A partir de este momento, el número de neuronas dopaminérgicas teñidas con plata disminuyó, pero siguió siendo significativo a los 7 y 30 días después del tratamiento en comparación con los animales tratados con salino. Dado que la tinción de plata empleada en el estudio sólo marca neuronas que están activamente degenerando, esto podría significar que algunas neuronas dañadas, que inicialmente sobreviven a la metanfetamina, acaban colapsándose y finalmente mueren (Fig. 5f, pág. 49). De acuerdo con lo anterior, no hubo recuperación en el número de neuronas TH-ir en la SNpc (que permanece reducido entre un 20-25% incluso 30 días después del tratamiento), lo que confirma la idea de que la pérdida de estas neuronas es permanente, a pesar de la recuperación parcial de los terminales dopaminérgicos que se produce en el estriado. Es probable que la principal fuente de recuperación de terminales TH-ir sea un crecimiento de terminales partir de las neuronas dopaminérgicas que sobreviven en la SNpc. A pesar de esta recuperación, la inmunorreactividad estriatal de TH permanece reducida (un 16%) 30 días después del tratamiento con la droga.

Los efectos neurotóxicos de la metanfetamina tienen como consecuencia deficiencias motoras transitorias

Los efectos neurotóxicos de la metanfetamina tuvieron consecuencias funcionales, aunque transitorias: se observó una drástica disminución del movimiento horizontal y vertical de los ratones y de su coordinación motora, 1 día después de la droga. Sin embargo, a los 7 días, los animales se habían recuperado de estos déficits motores. (Fig. 5, pág. 49) Aunque los efectos tóxicos sistémicos de la metanfetamina pueden contribuir a la pérdida selectiva de terminales dopaminérgicos (Halpin y Yamamoto 2012), las disfunciones motoras que observamos parecen deberse únicamente a la pérdida de terminales en el estriado, tal y como se ha demostrado en consumidores humanos de metanfetamina (Volkow *et al*. 2001a, b; McCann *et al*. 1998). El curso temporal de las deficiencias motoras fue paralelo al de la degeneración y recuperación parcial de los terminales dopaminérgicos, y el hecho de que las deficiencias motoras se recuperaran por completo sugiere que no se deben a la pérdida permanente de neuronas dopaminérgicas (20-25%) en la SNpc. Nuestros resultados con metanfetamina confirman una vez más que es necesario tener ciertos niveles de dopamina en el estriado para que la actividad y la coordinación motora sean normales (Rodrigues *et al*. 2007). Una vez que los terminales dopaminérgicos se han recuperado parcialmente, alcanzando al menos el 78% de la inervación vista en los salinos, ya producen suficiente dopamina para que la neurotoxicidad sea sub-

sintomática. Estos resultados están de acuerdo con lo que ocurre en los modelos animales de enfermedad de Parkinson, en los que se observan déficits motores tras una pérdida del 80% de la dopamina en el estriado y del 30-60% de las neuronas dopaminérgicas de la SNpc (Burke y O'Malley 2012; Fearnley y Lees 1991), lo que indica que la metanfetamina podría destruir muchas neuronas dopaminérgicas sin que se observaran síntomas de Parkinson (Davidson et al. 2001).

Mecanismo de degeneración de la vía nigroestriatal

La hipótesis con respecto a la degeneración de esta vía en la enfermedad de Parkinson es que las neuronas de la SNpc degeneran a través de una axonopatía retrógrada, en la que la degeneración comienza en el axón distal y continúa hacia el cuerpo neuronal (Burke y O'Malley 2012). Esta idea no pudo ser confirmada con nuestros resultados, que indican que estos dos procesos, la pérdida de terminales y de los cuerpos neuronales en la SNpc, ocurrieron simultáneamente. La degeneración de las neuronas y los terminales se empezó a observar a las 3-12h y llegó al máximo entre 1 y 3 días tras la metanfetamina, lo que nos hace pensar en un efecto directo de la droga sobre las neuronas y los terminales, en lugar de en una degeneración retrógrada como sugiere un informe anterior (Davidson *et al.* 2001). Varios datos constatan que los mecanismos moleculares de la degeneración axonal son distintos e independientes de los de la degeneración de los somas neuronales (Burke y O'Malley 2012; Coleman *et al.* 2005; Raff *et al.* 2002; Ries *et al.* 2008). Esta idea se refuerza por el hecho de que la inactivación genética del factor de transcripción Nrf2 potencia el daño de los terminales dopaminérgicos sin afectar la supervivencia de las neuronas en la SNpc (Granado *et al.* 2011b). En línea con esto, las mutaciones homocigotas dobles de las quinasas N-terminal c-jun (jnk) 2 y 3 (jnk2 y jnk3) dan lugar a la anulación completa de la apoptosis y a la supervivencia prolongada de toda la población de neuronas dopaminérgicas, sin ofrecer ninguna protección contra la degeneración axonal (Ries *et al*. 2008). Esta idea se ve reforzada por el hecho de que no se detectan diferencias significativas entre la degeneración neuronal, en la SNpc, inducida por la administración de una única dosis alta de metanfetamina y en la inducida por regímenes de múltiples dosis más bajas, a pesar de la gran influencia del régimen de dosificación en los efectos neurotóxicos de los terminales dopaminérgicos del estriado.

Los mecanismos que median la degeneración de las neuronas dopaminérgicas de la SNpc por metanfetamina parecen incluir más de una vía conocida de muerte celular. Anteriormente, habíamos observado la aparición de cuerpos apoptóticos en la SNpc detectados con tinción de Nissl después de la metanfetamina (Fig. 5 pág. 64 y Fig. 9, pág. 100) (Ares-Santos *et al.* 2012; Granado *et al.* 2011b). Más recientemente, también hemos observado neuronas necróticas eosinofílicas en esta área tras la administración de metanfetamina (Fig 4, pág 48). La necrosis y la apoptosis pueden ocurrir por separado como procesos independientes, en combinación, o como eventos secuenciales (Davidson *et al.* 2001). Los resultados de la investigación in vitro con modelos de cultivo de células dopaminérgicas apuntan a la activación de la cascada de la apoptosis que implica la caspasa-3 y la fragmentación del ADN en la neurodegeneración de estas células, y sugieren que otros factores pueden contribuir a la muerte celular, incluyendo el estrés del retículo endoplasmático (RE), la disfunción de la ubiquitina y el deterioro de la autofagia (Kanthasamy *et al.* 2011; Larsen *et al.* 2002). Serían necesarias nuevas investigaciones para caracterizar mejor el proceso que lleva a esta neurodegeneración y definir los distintos mecanismos que pueden mediar la neurodegeneración axonal y somática.

Similitudes con la neurotoxicidad observada en consumidores humanos de metanfetamina

Nuestros resultados son consistentes con artículos recientes que muestran que los consumidores de metanfetamina tienen un mayor riesgo de desarrollar la enfermedad de Parkinson (PD) (Callaghan *et al.* 2010, 2012), y con otros estudios que muestran déficits en la actividad motora asociados con pérdida de DAT en los núcleos caudado y putamen (Volkow *et al.* 2001a, b; McCann *et al.* 1998). Se ha descrito una recuperación parcial de los marcadores dopaminérgicos, similar a la que vemos en ratones, en el estriado de los consumidores humanos después de un tiempo de abstinencia (Volkow *et al.* 2001a). A pesar de ello, la persistencia de la pérdida de terminales de dopamina también se ha documentado después de 11 meses (Volkow *et al.* 2001a) ó 3 años de abstinencia (McCann *et al.* 1998), lo que concuerda con la persistencia de la pérdida de los terminales dopaminérgicos que vemos a los 30 días en nuestro modelo. Sin embargo, hasta la fecha, no hay evidencias anatómicas directas de la destrucción de neuronas dopaminérgicas en la SNpc de los consumidores humanos, aunque hay pruebas de cambios neurodegenerativos: por ejemplo, se ha visto una disminución específica de las neuronas pigmentadas en la SN de los consumidores de metanfetamina, similar a la observada en los pacientes de PD (Büttner y Weis 2006; Büttner 2011). Por otra parte, la morfología de la SN en individuos con historial de abuso de estimulantes, incluyendo la metanfetamina, es anormal, presentando cambios en la sonografía transcraneal asociados con una menor captación de dopamina en el estriado y un mayor riesgo para el desarrollo de PD (Todd *et al.* 2013). Además, la baja disminución (5%) en el marcador neuronal N-acetil aspartato descrita en el estriado de los consumidores de metanfetamina ya abstinentes (Ernst *et al.* 2000) está de acuerdo con nuestros resultados que indican muerte celular en el estriado en tasas muy bajas, pero significativas, (<0,17%, considerando una población de 1,72 millones de neuronas en el estriado de los ratones C57BL/6J [Rosen y Williams 2001]), después de la administración de metanfetamina.

La inactivación genética de los receptores D1 o D2 protege frente al daño dopaminérgico producido por metanfetamina

Los primeros estudios que implicaron a los receptores dopaminérgicos en los efectos neurotóxicos de la metanfetamina eran estudios farmacológicos que empleaban antagonistas de los receptores de las familias D1 o D2. Estos agentes protegen parcial o completamente frente a la toxicidad dopaminérgica inducida por la metanfetamina, y también evitan la respuesta hipertérmica. El pretratamiento con SCH 23390, (un antagonista de los receptores dopaminérgicos de la familia D1) o con eticlopride, raclopride o sulpiride (antagonistas de los receptores de la familia D2) atenúa la pérdida de dopamina y sus metabolitos y de los niveles de expresión y actividad de TH y DAT (Albers y Sonsalla 1995, Angulo *et al.* 2004; Broening *et al.* 2005; Metzger *et al.* 2000; O'Dell *et al.* 1993; Sonsalla *et al.* 1986; Xu *et al.* 2005). También se ha descrito que el SCH23390 y el raclopride previenen los aumentos de la proteína GFAP y la pérdida de neuronas estriatales inducidas por metanfetamina (Xu *et al*. 2005).

Sin embargo, los antagonistas farmacológicos empleados no son específicos y también bloquean otros receptores de la misma familia o de otro tipo, como es el caso del SCH23390 (Briggs *et al.* 1991; Millan *et al.* 2001). Por ello, estos resultados son inconclusos, ya que no dejan claro qué subtipos de receptores dopaminérgicos están involucrados en este proceso. Nuestros resultados

muestran por primera vez que los subtipos D1 y D2 están selectivamente implicados en la neurotoxicidad de la metanfetamina sobre los terminales y somas dopaminérgicos de la vía nigroestriatal. Así, la inactivación individual de estos receptores (D1 ó D2) protege frente a la neurotoxicidad dopaminérgica, evidenciada por la disminución en la pérdida de dopamina, TH y DAT en el estriado (Fig. 1,2 pág. 62,76 y 77). La falta del receptor D1 o del D2 bloquea también la pérdida de neuronas dopaminérgicas de la SNpc y evita la microgliosis y astrogliosis reactiva tanto en el estriado como en la SN tras la metanfetamina (Fig. 3, 5 pág. 63, 64 y Fig. 5, 6 y 8, pág. 80 y 82).

El bloqueo de la hipertermia inducida por la metanfetamina contribuye, aunque no justifica la protección conferida por la inactivación de los receptores D1 ó D2.

Nuestros resultados son consistentes con los estudios previos que muestran que los antagonistas farmacológicos de los receptores D1/D5 y D2/D3/D4 inhiben la hipertermia inducida por metanfetamina (Broening *et al.* 2005). De hecho, en los ratones $D1^{-/-}$ o $D2^{-/-}$, la primera inyección de la droga indujo una marcada hipotermia. Las dosis posteriores no provocaron aumentos significativos de la temperatura corporal (Fig. 1a, pág. 62 y Fig. 1 a pág. 76). Por lo tanto, parecía posible que los efectos protectores observados por la inactivación del receptor D1 o del receptor D2 se debieran a la hipotermia presentada tras la primera inyección de metanfetamina o a la ausencia de hipertermia tras las siguientes administraciones. Para dilucidar el papel de la respuesta térmica en la neuroprotección observada con la inactivación del receptor D1 o D2, se administró metanfetamina a ratones $D1^{-/-}$ y $D2^{-/-}$ en una sala a mayor temperatura ambiente (29-30ºC), condiciones que potencian la hipertermia y la neurotoxicidad de la metanfetamina (Bowyer *et al.* 1994; Granado *et al.* 2011a; Miller y O'Callaghan 2003). En estas condiciones, la metanfetamina indujo hipertermia en los animales $D1^{-/-}$, similar a la observada en animales WT tratados con metanfetamina en un ambiente a temperatura estándar (23ºC) (Fig. 6a, pág. 65). Estos resultados demuestran que el receptor D1 es necesario para que se produzca la respuesta hipertérmica de la metanfetamina a temperatura ambiente estándar (23 °C), pero no a 29 °C. Además, la neuroprotección proporcionada por la inactivación del receptor D1 no se observó cuando los animales $D1^{-/-}$ fueron tratados con la metanfetamina a 29°C y presentaron hipertermia (Fig. 6b,c pág. 65), apoyando la idea de que los efectos protectores de la inactivación del receptor D1 se deben, al menos en parte, a la falta de respuesta hipertérmica. Sin embargo, los ratones $D2^{-/-}$ presentaron hipotermia, incluso cuando la metanfetamina se administró a elevada temperatura ambiente (29-30 °C) (Fig. 3, pág. 78). La dificultad para separar la neuroprotección de la atenuación de hipertermia después de la inactivación del receptor D2 no permite tampoco descartar completamente que el receptor D2 tenga un papel específico en la neurotoxicidad inducida por metanfetamina, ya que es posible que la ausencia de la hipertermia medie la neuroprotección observada en ausencia del receptor D2. Lo que está claro es que la hipertermia inducida por metanfetamina requiere un receptor D2 funcional, mientras que otros miembros de esta familia de receptores, D3 y D4, no son necesarios para que se dé esta repuesta hipertérmica.

La temperatura corporal es un factor importante en las respuestas tóxicas a la metanfetamina (Krasnova y Cadet, 2009; Yamamoto *et al.* 2010) y se ha demostrado que potencia la función del DAT (Xie *et al.* 2000), y aumenta la producción de radicales libres y la oxidación de dopamina en el cerebro

(Kil *et al.* 1996; LaVoie y Hastings 1999; Spencer *et al.* 2002). Sin embargo, nuestros resultados están de acuerdo con la idea previamente expuesta de que la hipertermia puede contribuir, pero no es necesaria para la neurotoxicidad dopaminérgica inducida por la metanfetamina (Albers y Sonsalla 1995; Fumagalli *et al.* 1998; Granado *et al.* 2011a; Thomas *et al.* 2008b), ya que la inactivación de los receptores D1 ó D2 tiene un papel en la neuroprotección por mecanismos que van más allá de la prevención de la hipertermia inducida por metanfetamina: el tratamiento con reserpina produjo una marcada hipotermia en los animales WT y $D1^{-/-}$, y a pesar de ello potenció los efectos tóxicos de la metanfetamina sobre los terminales dopaminérgicos en ambos genotipos (Fig. 8 pág. 66) lo que indica que los efectos protectores de la inactivación del receptor D1 son el resultado de otros mecanismos distintos a la inhibición de la hipertermia. Un estudio posterior al nuestro ha mostrado que la administración intraestriatal de SCH23390 confiere protección frente a la toxicidad dopaminérgica inducida por metanfetamina en el estriado sin afectar a la respuesta hipertérmica, confirmando la idea de que el bloqueo del receptor D1 confiere protección por mecanismos independientes a la atenuación de la hipertermia (Friend y Keefe 2013). En el caso de los animales $D2^{-/-}$, ni siquiera el pretratamiento con reserpina fue capaz de abolir el efecto neuroprotector de la inactivación del receptor D2 (Fig. 4, pág. 79). Estos resultados sugieren que la neuroprotección conferida por la inactivación del receptor D2 no es completamente dependiente de la hipotermia ya que las temperaturas rectales tras la administración de metanfetamina de los ratones WT reserpinizados y la de los ratones $D2^{-/-}$ sin reserpinizar fueron muy similares, mientras que los efectos neurotóxicos fueron claramente diferentes en estos dos grupos.

La inactivación del receptor D1 reduce el contenido total de dopamina pero aumenta la dopamina vesicular

El menor contenido y reciclaje de dopamina que tienen los ratones $D1^{-/-}$ (Fig. 1a pág. 62) también puede ser determinantes en su resistencia a la neurotoxicidad de la metanfetamina, ya que se traducirían en un menor aumento de dopamina citosólica tras la administración de metanfetamina y por lo tanto, en menos sustratos para la generación de ROS inducida por metanfetamina (Cadet y Brannock 1998; Krasnova y Cadet 2009; LaVoie y Hastings 1999). Esta hipótesis se ve apoyada también por nuestros experimentos con αMPT, un agente farmacológico que bloquea la actividad de la TH inhibiendo la síntesis de dopamina y disminuyendo, por tanto, los niveles de la dopamina citosólica. El pretratamiento con αMPT, que protege contra la toxicidad de metanfetamina (Albers y Sonsalla 1995; Thomas *et al.* 2008b), induce efectos protectores más pronunciados en los ratones $D1^{-/-}$ que en los controles WT (Fig. 7 pág. 65). Esto puede deberse a la menor actividad de la TH, ya que la síntesis de dopamina también es menor en los ratones $D1^{-/-}$ que en los WT, como se muestra en nuestros experimentos por HPLC. Esto está de acuerdo con estudios previos que muestran que la αMPT es más eficaz bloqueando la actividad TH en ratones $DAT^{-/-}$ con menor contenido de dopamina (Jones *et al.* 1998). El menor contenido y reciclaje de dopamina observado en los $D1^{-/-}$ podrían ser el resultado de una disminución de la síntesis de dopamina en estos animales: es decir, la falta del receptor D1 podría cambiar la tasa de síntesis de dopamina, como se ha demostrado tras la manipulación de otros componentes del sistema dopaminérgico como con la inactivación del receptor D2 (Granado *et al.* 2011a; Tinsley *et al.* 2009) o del DAT (Jaber *et al.* 1999; Jones *et al.* 1998).

Otro posible mecanismo responsable de los efectos protectores observados en los ratones $D1^{-/-}$ podría estar relacionado con la diferente distribución de dopamina en el terminal, ya que como se ha descrito previamente, la dopamina citosólica está directamente implicada en los efectos neurotóxicos de la metanfetamina, mientras que la dopamina vesicular no está involucrada (Fumagalli *et al.* 1999; Thomas *et al.* 2008b). Para confirmar esta hipótesis, realizamos experimentos de voltametría cíclica (FSCV) para estudiar la liberación de dopamina en condiciones basales y en presencia de metanfetamina en ratones de ambos genotipos. Los ratones $D1^{-/-}$ presentan una mayor la liberación de dopamina que los ratones control tras un pulso eléctrico. El aumento de esta liberación inducido por la presencia de metanfetamina en el medio, también fue mayor en los ratones $D1^{-/-}$ que en los controles (Fig. 9, pág. 67). Estos resultados concuerdan con estudios anteriores que mostraron una mayor la liberación de dopamina tras el tratamiento con SCH23390 en presencia de metanfetamina (O'Dell *et al.* 1993). El pico de la liberación de dopamina es resultado del equilibrio entre los mecanismos de liberación sináptica y de recaptación de dopamina, mientras que el curso temporal de la subsiguiente disminución de los niveles de dopamina refleja la competencia entre los mecanismos de recaptación a través del DAT y de difusión (Bull *et al.* 1990; Wightman y Zimmerman, 1990). Por lo tanto, nuestros experimentos indican que los ratones $D1^{-/-}$ tienen una mayor liberación de dopamina vesicular y una menor capacidad de recaptación que los animales WT, a pesar del menor contenido de dopamina basal, lo que sugiere que los animales $D1^{-/-}$ almacenan más dopamina en las vesículas y, por lo tanto, tienen menor contenido de dopamina citosólica que los WT, proporcionando una posible explicación de por qué la metanfetamina induce un menor daño dopaminérgico en los ratones $D1^{-/-}$ (Ver figura 12, pág. 113).

El mayor contenido de dopamina vesicular en los ratones $D1^{-/-}$ también se pone de manifiesto en nuestro experimento con reserpina, que suprime la acumulación vesicular de monoaminas (Henry *et al.* 1987, 1998; Kirshner 1962 a, b). La liberación de la dopamina desde las vesículas al citosol, inducida por reserpina, hizo que los ratones $D1^{-/-}$ presentaran la misma neurotoxicidad dopaminérgica tras la metanfetamina que los WT (Fig. 8 pág. 66). Esta idea también concuerda con los datos obtenidos cuando se administró metanfetamina a alta temperatura ambiente, 29 ºC. En estas condiciones, los animales $D1^{-/-}$ presentaron hipertermia después de la segunda y tercera inyecciones de metanfetamina, muy similar a la observada en los animales WT tratados con metanfetamina a 23 ° C. Sin embargo, hubo una potenciación drástica de la neurotoxicidad en los animales $D1^{-/-}$ en comparación con los WT, a pesar de presentar respuestas hipertérmicas muy similares (Fig. 6, pág. 65). La mayor liberación de dopamina de los ratones $D1^{-/-}$, junto con el hecho de que la temperatura potencia la recaptación de dopamina a través del DAT (Volz *et al.* 2006), resultarían en mayores niveles citosólicos de dopamina, produciendo por lo tanto una potenciación de la neurotoxicidad dopaminérgica inducida por metanfetamina en los ratones $D1^{-/-}$ tratados con la droga a 29 °C.

La menor actividad del DAT en ausencia del receptor D2 es en parte responsable de la protección observada en los animales $D2^{-/-}$

Entre los posibles mecanismos independientes de la hipertermia que median la neuroprotección observada por la inactivación del receptor D2, hay pruebas fehacientes de que la actividad del DAT estriatal, que es crucial para la neurotoxicidad dopaminérgica (Fumagalli *et al.* 1998; Manning-Bog *et*

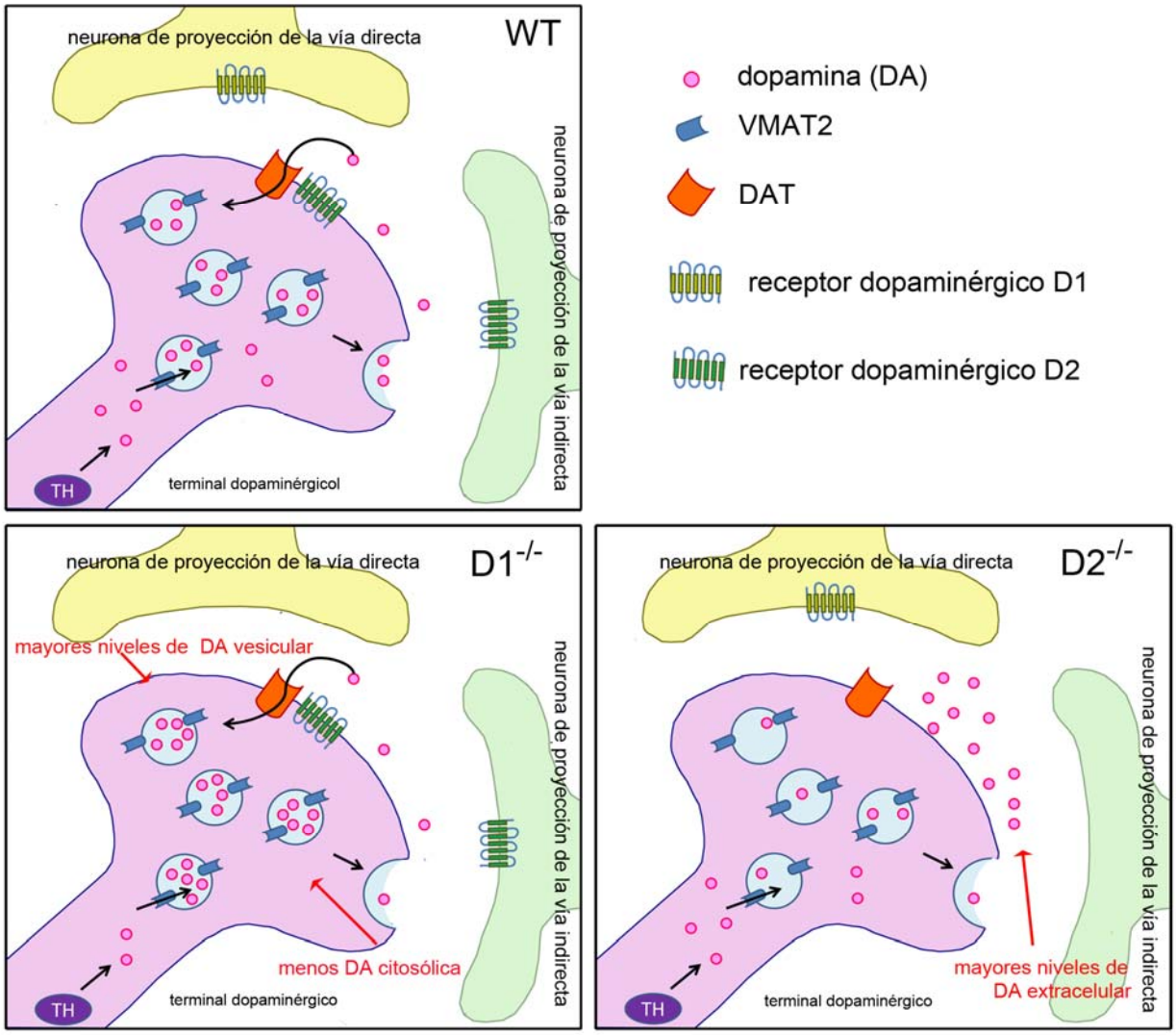

Figura 12. Distribución de dopamina en los terminales dopaminérgicos estriatales en animales WT, D1$^{-/-}$ y D2$^{-/-}$
Los animales D1$^{-/-}$ tienen menos dopamina estriatal, pero más dopamina vesicular y menos dopamina citosólica que los animales WT. Sin embargo, los animales D2$^{-/-}$ tienen menos dopamina citosólica y más dopamina extracelular que los animales WT. Esto puede deberse a su menor recaptación de dopamina dada la menor actividad del DAT en ausencia del receptor D2 (Modificado de Ares-Santos *et al*. 2013b).

al. 2007), está reducida en ausencia del receptor D2 (Dickinson *et al.* 1999; Afonso-Oramas *et al.* 2009). Esta disminución de la actividad DAT producida por la inactivación del receptor D2 disminuye la recaptación de dopamina, lo que resulta en menores niveles de dopamina citosólica que, como en el caso de la inactivación del receptor D1, parecen mediar la neuroprotección por la inactivación del receptor D2.

Además, los resultados de experimentos de voltametría muestran que la metanfetamina induce una liberación de dopamina significativamente menor en los animales D2$^{-/-}$, lo que indica que estos ratones tienen menos dopamina vesicular (Fig. 9 pág. 67). Esto concuerda con resultados de estudios previos que muestran que el tratamiento con eticlopride atenúa la liberación de dopamina inducida por metanfetamina (O'Dell *et al.* 1993). Esta hipótesis también coincide con la reducción de la neurotoxicidad inducida por metanfetamina observada en ratones D2$^{-/-}$ reserpinizados, en comparación con los controles WT, ya que la reserpina potencia la neurotoxicidad de la metanfetamina porque libera la dopamina vesicular al citosol (Albers y Sonsalla 1995; Henry *et al.* 1998).

Aunque los niveles basales de dopamina son similares en los ratones $D2^{-/-}$ y en los WT, los $D2^{-/-}$ muestran un mayor contenido de DOPAC y HVA que indica un mayor reciclaje de dopamina (datos no mostrados) (Ares-Santos *et al.* 2011¸ Tinsley *et al.* 2009). Además, los $D2^{-/-}$ tienen menos dopamina intracelular (con menos dopamina citosólica y vesicular) y mas dopamina en el espacio extracelular. Nuestros resultados indican que el menor contenido de dopamina vesicular y su menor liberación al citosol, junto con la menor recaptación parecen mediar la neuroprotección conferida por la inactivación del receptor D2 (Figura 12, pág. 113).

Relación entre el bloqueo de la apoptosis estriatal por inactivación de los receptores D1 o D2 y la protección del daño sobre los terminales dopaminérgicos

Como se ha descrito que el bloqueo de los receptores D1 y D2 con SCH23390 o raclopride bloquea la apoptosis estriatal inducida por metanfetamina (Xu *et al*.2005) y que esta apoptosis estriatal es anterior a la pérdida de terminales dopaminérgicos (Zhu *et al.* 2005), la atenuación de la muerte de neuronas estriatales inducida por metanfetamina por la inactivación del D1 o del D2 también podría contribuir a la neuroprotección presináptica observada en ratones $D1^{-/-}$ y $D2^{-/-}$. De acuerdo con esta idea, estudios anteriores han demostrado que el pretratamiento con SCH23390 reduce la expresión estriatal inducida por metanfetamina de varios genes relacionados con estrés del RE, como ATF4, ATF6, junto con la de proteínas de choque térmico involucradas en la apoptosis y en la muerte celular (Jayanthi *et al.* 2009). Además, el bloqueo de D1/D5 puede prevenir la neurotoxicidad estriatal al suprimir la activación de las caspasas 3 y 8, mediadores de la vía de muerte apoptótica dependiente de calcineurina/NFAT/FasL (Jayanthi *et al.* 2005; Krasnova y Cadet 2009). Por otra parte, el pretratamiento con raclopride atenúa parcialmente los aumento inducidos por metanfetamina en la expresión de la proteína CHOP, relacionada con estrés de RE, y de la caspasa 12 (Beauvais *et al*. 2011). Sin embargo, el estudio de Zhu *et al.* 2005 que propone que la muerte estriatal precede a la pérdida de neuronas dopaminérgicas, empleaba un protocolo de administración de una única dosis alta de metanfetamina (**1x30**) y veía un alto porcentaje de apoptosis estriatal a las 24h, mientras que la pérdida de terminales del estriado se apreciaba a las 24h pero era máxima a los 3d del tratamiento. Por el contrario, en nuestros estudios con animales $D1^{-/-}$ y $D2^{-/-}$ (Ares-Santos *et al.* 2012, Granado *et al.* 2011a) empleamos un régimen de administración de dosis bajas repetidas (**3x5**) de metanfetamina que no produce aumentos significativos en el numero de neuronas que degeneran en el estriado a las 24h mientras que produce una degeneración de terminales dopaminérgicos que comienza las 3-12h y es máxima a las 24h de la administración de la droga (Ares-Santos *et al.* 2013c). Por lo tanto, con nuestro régimen empleado no parece probable que el bloqueo de la apoptosis estriatal por inactivación de los receptores D1 ó D2 esté mediando la protección sobre los terminales dopaminérgicos, aunque esto sí podría suceder con el régimen de administración de una única dosis elevada (**1x30**).

El bloqueo de los aumento de expresión de iNOS puede contribuir a la protección por inactivación de los receptores D1 o D2

La administración de dosis bajas repetidas de metanfetamina produce aumentos en la expresión de la enzima óxido nítrico sintasa inducible (iNOS) en el estriado 1 día después de la administración de la droga, que no se dan en ausencia de los receptores D1 ó D2 (Fig. 4 pág. 64, Fig., 7,

pág. 81). Esta enzima, que apenas se expresa en condiciones basales y que es inducida por citoquinas durante reacciones infamatorias, puede producir grandes cantidades de NO que se han implicado de por sí en los efectos neurotóxicos de la metanfetamina (Itzhak *et al*. 1999). Pero además, el NO puede combinarse con superóxido para formar peroxinitrito, un potente oxidante que puede producir la nitración de proteínas, peroxidación de lípidos y daño al ADN y mediar la degeneración (Anderson e Itzhak 2006). Ya hemos comentado que se pueden observar terminales nitrados degenerando en el estriado de los ratones tratados con la droga (Fig. 5, pág. 49). La inactivación genética de los receptores D1 o D2 bloquea los aumentos inducidos por metanfetamina en los niveles de iNOS, lo cual podría explicar la atenuación del daño dopaminérgico en el estriado que se observa en estas condiciones. Sin embargo una revisión reciente concluye que el NO puede contribuir a la neurotoxicidad pero no es suficiente para provocarla (Friend *et al*. 2013).

Potenciación del daño inducido por metanfetamina a los terminales dopaminérgicos en ausencia de Nrf2

La falta de Nrf2 exacerba la neurotoxicidad de la metanfetamina, en particular en el estriado, donde potencia la pérdida de terminales dopaminérgicos, pero también de neuronas estriatales 24h después del tratamiento (Fig. 2 y 7, pág. 93, 98). En un estudio previo con ratones Nrf2$^{-/-}$ no se observó esta diferencia (Pacchioni *et al.* 2007). Esta discrepancia puede deberse a una diferencia en el tiempo en el que se observan los efectos: Pacchioni *et al* realizaron las determinaciones de los niveles de los marcadores dopaminérgicos dos semanas después de la administración de la metanfetamina, cuando ya hay una considerable recuperación dopaminérgica (Ares-Santos *et al.* 2013c). Por el contrario, nosotros evaluamos la integridad dopaminérgica a las 24 h de la administración de la droga, cuando el daño o la pérdida de marcadores dopaminérgicos es máxima (Fig. 5, pág. 49) (Ares-Santos *et al.* 2013c, 2012; Granado *et al.* 2011), lo que nos permite ver mejor las diferencias entre los genotipos.

La falta de Nrf2 potencia la neurotoxicidad estriatal por mecanismos independientes de la potenciación de la hipertermia

En nuestro estudio, los cambios de temperatura corporal de los animales Nrf2$^{-/-}$ fueron ligeramente superiores a los de los WT, y presentaron también una mayor degeneración en el estriado (Fig. 1a, pág. 92). Es posible que los ratones que carecen de factor de transcripción Nrf2 sean más sensibles a la desregulación de la temperatura corporal después del tratamiento con metanfetamina, debido a una reducción de sus defensas antioxidantes y a un aumento del estrés oxidativo. Sin embargo, el aumento de la hipertermia no es necesario para la potenciación de los efectos neurotóxicos de la metanfetamina que se observa en los ratones Nrf2$^{-/-}$, ya que en los experimentos llevados a cabo a temperatura ambiente ligeramente más baja (21 °C) los ratones Nrf2$^{-/-}$ no mostraron mayor hipertermia que los WT después de la administración de metanfetamina y, a pesar de ello, presentaron mayor pérdida de fibras TH en el estriado que los ratones WT.

El Nrf2 activa la defensa antioxidante para proteger frente a la neurotoxicidad estriatal de la metanfetamina

De acuerdo con nuestros resultados, las neuronas dopaminérgicas de los animales Nrf2$^{-/-}$ son

también más sensibles a la neurotoxina MPTP, usada como modelo de PD (Chen *et al.* 2009; Rojo *et al.* 2010). Esta sensibilidad es evidente con una amplia gama de dosis de MPTP (10-30 mg/kg, Chen *et al.* 2009). La deficiencia de Nrf2 aumenta la pérdida de fibras TH en el estriado del ratón después de la administración crónica de MPTP, debido a la disminución de las defensas antioxidantes y al aumento de la inflamación. El Nrf2 está implicado en la síntesis de enzimas de la fase 2 de desintoxicación que coordinan la respuesta protectora al estrés oxidativo. La disminución de la expresión de enzimas de la fase 2 es probablemente una de las razones por las que los ratones Nrf2$^{-/-}$ son más susceptibles a la neurotoxicidad inducida por MPTP y por lipopolisacárido, otras toxinas que también generan ROS (Chen *et al.* 2009; Innamorato *et al.* 2008; Rangasamy *et al.* 2004; Rojo *et al.* 2010; Thimmulappa *et al.* 2006 a, b). Es probable que un mecanismo similar se produzca después de la administración de metanfetamina en ausencia de Nrf2: Los genes regulados por los elementos de respuesta antioxidante (ERA) en el estriado, incluyendo HO-1 y otros genes antioxidantes como CuZnSOD, MnSOD, Gclm y GPx, se inducen en los WT pero no en los animales que carecen de Nrf2 tras el tratamiento con metanfetamina (Fig. 5 pág. 96), lo que lleva a un aumento del estrés oxidativo, a la acumulación de ROS (Chen *et al.* 2009) y, en última instancia, a la pérdida de terminales dopaminérgicos.

En un estudio reciente, Jayanthi *et al.* (2009) muestran la activación estriatal de Nrf2 tras el tratamiento con la metanfetamina. Nuestro hallazgo de que los ratones deficientes en Nrf2 son más sensibles que los WT al daño estriatal inducido por esta droga demuestra que la activación del Nrf2 es parte de una respuesta defensiva. El estudio de Jayanthi *et al*. también demuestra la activación, inducida por metanfetamina, de la respuesta de estrés de RE. En base a sus datos, resulta tentador especular que la activación de la respuesta de estrés de RE conduce a la inducción de Nrf2 estimulada por la metanfetamina. En efecto, el grupo de Diehl ha demostrado que PERK, una proteína quinasa necesaria para la respuesta celular al estrés de RE, fosforila y activa Nrf2 (Cullinan *et al.* 2003). De acuerdo con esta hipótesis, se observó un pequeño incremento de CHOP, una proteína crítica en la respuesta a estrés de RE. Sin embargo, no hemos visto un aumento consistente en BIP, otra proteína que marca estrés de RE (datos no mostrados). El estudio de Jayanthi *et al.* se hizo con ratas y usaba un paradigma diferente de dosificación y observaba los cambios a otros tiempos; cualquiera de estos factores puede dar cuenta de la discrepancia entre sus resultados y los nuestros. Además, será necesario seguir trabajando para comparar la respuesta de estrés de RE, vista en el estriado de rata, con la de los ratones WT y Nrf2$^{-/-}$.

La gliosis reactiva inducida por metanfetamina se atenúa con la inactivación de los receptores D1 ó D2 y se potencia en el estriado ausencia del Nrf2.

El tratamiento con metanfetamina y otros derivados anfetamínicos como el MDMA (o ´"extasis") producen aumentos en la reactividad microglial y astroglial que acompañan a la degeneración de terminales dopaminérgicos en el estriado. El estudio del curso temporal de la activación glial indica que la microglía tiene un pico de activación a las 24h del tratamiento con dosis bajas repetidas de estas drogas (Fig. 3 y 5, pág. 63 y 64, Fig. 6 y 8, pág. 80 y 82, Fig. 4 y 8, pág. 95 y 99). Como ya se explica en la introducción, esto puede ocurrir rápidamente después de ciertos tipos de daño en SNC y se considera un marcador farmacológico selectivo del daño en los terminales inducido

por anfetaminas (Thomas et al. 2004). Además, estas células presentan antígenos que se activan por inflamación, daño y enfermedad y secretan especies reactivas que incluyen prácticamente todas las especies reactivas implicadas en la neurotoxicidad inducida por los derivados anfetamínicos, incluyendo ROS, RNS (Cadet *et al.* 1994, 2007; Imam *et al.* 2001). Se ha sugerido que la activación microglial representa más que una respuesta al daño directo por la neurotoxicidad de las anfetaminas (Thomas et al 2004). Por otro lado, la activación de los astrocitos alcanza su máximo nivel entre 3 y 7 días después del tratamiento (Ares-Santos et al 2012, Granado et al 2008b, 2011a) resultados éstos que apoyan trabajos previos en la misma dirección (O'Callaghan Jensen 1992). La gliosis reactiva es considerada una reacción universal de daño en el SNC y se puede usar como marcador de daño neuronal (O'Callaghan y Sriram 2005). Parece que los astrocitos contrarrestan la actividad de la microglía, ya que pueden proteger contra la pérdida de neuronas dopaminérgicas y el estrés oxidativo inducido por MPTP directamente por eliminación de los radicales libres e indirectamente mediante el aumento glutationina, que tiene actividad antioxidante, pero también producen moléculas proinflamatorias que pueden favorecer o perpetuar los efectos neurotóxicos (Jia *et al.* 2009).

Como era de esperar, la gliosis reactiva es menor en los animales $D1^{-/-}$ y $D2^{-/-}$ que presentaron menor toxicidad dopaminérgica, mientras que se agrava significativamente en los ratones $Nrf2^{-/-}$, que presentan una pérdida mayor de terminales dopaminérgicos en el estriado. El Nrf2 es un importante modulador de la dinámica de microglial y participa en la prevención de la inflamación por un mecanismo que aún no ha sido dilucidado. Además, los ratones $Nrf2^{-/-}$ tratados con metanfetamina expresan un mayor incremento en marcadores microgliales y proinflamatorios, en particular TNF-α e IL -15, que los ratones WT, lo que indica que la inflamación causada por la metanfetamina es mayor en ausencia de Nrf2 (Fig. 4 pág. 93, fig. 5 pág. 96 y fig. 6 pág. 97). Los niveles más altos de TNFα en los ratones $Nrf2^{-/-}$ después del tratamiento con metanfetamina, parecen ser respuesta compensatoria al daño, y no la causa de la mayor neurotoxicidad ya que el pretratamiento con TNFα exógeno bloquea los efectos neurotóxicos de la metanfetamina mientras que los animales knock-out para TNFα muestran mayor toxicidad inducida por metanfetamina que los animales WT (Lai *et al.* 2009; Nakajima *et al.* 2004). Nuestros resultados demuestran por primera vez que el tratamiento con dosis bajas repetidas de metanfetamina produce aumentos en la expresión estriatal de IL-15, particularmente en los atrocitos (Fig 6, pág. 97). La IL-15 es una citoquina puede ser proinflamatoria e inducir gliosis reactiva (Gomez-Nicola *et al.* 2008, 2010), pero también es antiapoptótica y neurotrófica, y suprime la producción de óxido nítrico. La inactivación del receptor D2 previno los incrementos de IL-15 y la pérdida de terminales dopaminérgicos inducidos por metanfetamina en el estriado a las 24h del tratamiento con la droga, mientras que la falta de Nrf2 potenció la expresión de IL-15 y la pérdida de terminales dopaminérgicos y neuronas estriatales. Sin embargo, aún no está claro si los efectos proinflamatorios de IL-15 favorecen la neurorregeneración o si sus efectos proinflamatorios y antidegenerativos representan dos procesos paralelos (Pan *et al*. 2013).

Estos resultados, además de los datos obtenidos con imagen de señalización de Ca^{2+}, indican que la respuesta primaria de los astrocitos a la metanfetamina es similar en los ratones $Nrf2^{-/-}$ y WT (Fig. 3, pág. 82). Sin embargo, en ausencia de Nrf2, la capacidad antioxidante del estriado se reduce (Fig. 5, pág. 96), dejando neuronas más vulnerables al aumento progresivo del estrés oxidativo y la inflamación inducido por la metanfetamina, reflejando la enorme relevancia del Nrf2 en los procesos antioxidantes y antiinflamatorios. Estudios anteriores muestran que la toxicidad inducida por MPTP se

bloquea completamente en ratones transgénicos que sobreexpresan Nrf2 bajo el control de GFAP (Chen *et al.* 2009). Además, el transplante de astrocitos que expresan Nrf2 en el estriado protege contra otras neurotoxinas dopaminérgicas, como la 6-OHDA (Jakel *et al.* 2007), indicando aún más que la activación de Nrf2 en los astrocitos es importante para la supervivencia de las fibras TH en el estriado después de una lesión dopaminérgica.

La falta de Nrf2 no potencia la pérdida de neuronas dopaminérgicas en la SNpc inducida por metanfetamina

En la SN, la administración de metanfetamina indujo una pérdida similar de neuronas dopaminérgicas en ambos genotipos de ratones, WT y Nrf2$^{-/-}$, un día después de su administración (Fig. 9, pág. 100). Esta pérdida de células vino acompañada de un aumento en la astrogliosis y microgliosis, así como en la expresión de citoquinas proinflamatorias, que fue ligera pero no significativamente mayor, en ausencia de Nrf2 (Fig. 8, pág. 99). Por lo tanto, a las 24 h del tratamiento, la deficiencia de Nrf2 potencia la neurotoxicidad inducida por metanfetamina en el cuerpo estriado, pero no en la SN. Es posible que la metanfetamina active de diferente manera la vía ERA-Nrf2 en estriado y en SN. De hecho, otras toxinas dopaminérgicas como MPTP modulan de forma diferente esta vía: así el MPTP disminuye los niveles de proteína de Nrf2 y NQO1 en el estriado, pero los aumenta en la SN (Chen *et al.* 2009). En consecuencia, una diferente regulación de Nrf2 por parte de la metanfetamina en la SN y el estriado podría explicar la falta de efecto de la ausencia de Nrf2 en la neurotoxicidad en el SN en nuestro estudio.

En resumen, los datos presentados aquí proporcionan la primera evidencia anatómica de la degeneración de los cuerpos celulares de las neuronas dopaminérgicas de la SNpc tras la administración de metanfetamina en ratones, por lo que parece claro que sus efectos neurotóxicos son irreversibles a pesar de que exista cierta regeneración de los terminales dopaminérgicos en el estriado. Queda por determinar si se produce una degeneración similar de neuronas dopaminérgicas en la SNpc de los consumidores de metanfetamina humanos. Es probable que el menor contenido neuronal y el daño sufrido por la exposición a la metanfetamina de las neuronas que en principio sobreviven en la SNpc representen un factor de vulnerabilidad para futuras agresiones neurotóxicas (como el envejecimiento, la exposición a otras neurotoxinas o la presencia de factores de riesgo genéticos para la enfermedad de Parkinson). Sin embargo, como ocurre con otros factores de susceptibilidad para PD, el aumento de la susceptibilidad inducido por la metanfetamina para desarrollar esta enfermedad no significa que todos los usuarios de metanfetamina vayan a presentar PD en un futuro. La baja concordancia de esta enfermedad en pacientes de la misma familia y la baja penetrancia de algunas mutaciones descritas como factores de riesgo de PD, sugiere que es necesaria una combinación de agresiones o la interacción de varios factores predisponentes (“multiple hits hypothesis”) para acabar desarrollando PD (Sulzer et al. 2007). Nuestros resultados indican que el abuso de metanfetamina podría representar uno de estos factores, predisponiendo a los consumidores al desarrollo de PD. También queda demostrado que los receptores D1 y D2 están específicamente implicados en los efectos neurotóxicos de la metanfetamina, identificándolos como un importante objetivo para intervenciones terapéuticas relacionadas con la neurotoxicidad inducida por metanfetamina. La neuroprotección contra los efectos de esta droga observados en ausencia del receptor D1 se debe al

menor contenido estriatal de dopamina y a la mayor acumulación vesicular de dopamina que se dan cuando el receptor D1 está inactivado. En el caso de la ausencia del receptor D2, la protección contra la neurotoxicidad de la metanfetamina podría depender, al menos en parte, de la inhibición de la hipertermia inducida por metanfetamina, de la disminución de la actividad del DAT, y de los menores niveles de dopamina citosólicos y vesiculares. Por último, nuestros datos apoyan firmemente la hipótesis de que la metanfetamina produce neurotoxicidad dopaminérgica a través de un proceso que implica estrés oxidativo e inflamación y muestran que Nrf2 desempeña un importante papel al activar la defensa contra la neurotoxicidad sobre los terminales dopaminérgicos mediante la modulación de la inflamación y del estrés oxidativo inducidos por metanfetamina.

CONCLUSIONES

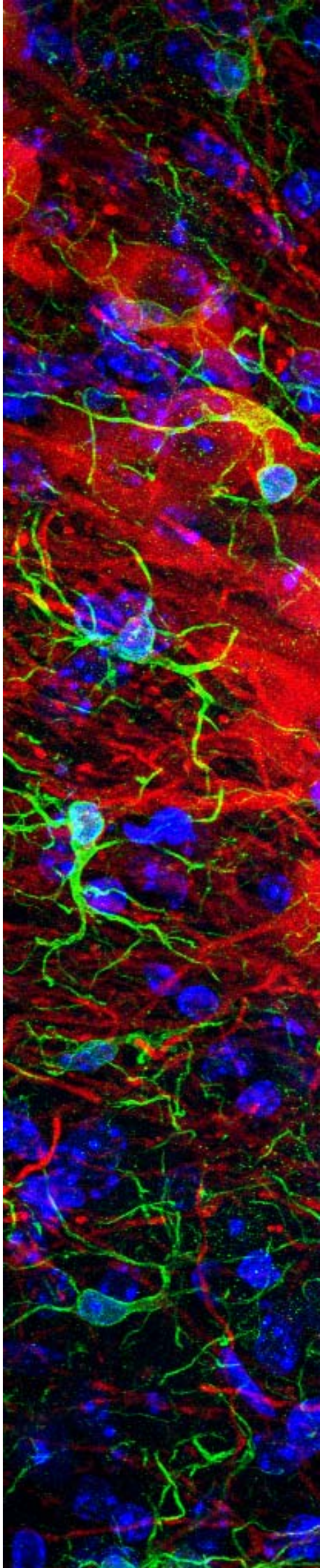

Foto de la página anterior: Sección de SN de ratón en la que se ha hecho una tinción inmunofluorescente para las neuronas dopaminérgicas (TH, rojo), para la microglía reactiva (Iba-1, verde) y se han teñido los núcleos celulares con DAPI (azul).

De los resultados obtenidos en la presente Tesis Doctoral se pueden extraer las siguientes conclusiones:

1. La metanfetamina induce una degeneración permanente de neuronas dopaminérgicas en la SNpc. El número de neuronas dopaminérgicas en esta área permanece reducido pasado incluso un mes desde la administración de la droga.
2. La muerte de estas neuronas tras la administración de metanfetamina se produce mediante necrosis y apoptosis.
3. La administración repetida de varias dosis bajas produce más neurotoxicidad sobre los terminales dopaminérgicos que una única dosis alta, aunque ambas producen un daño similar en la SN.
4. La degeneración de los terminales dopaminérgicos en el estriado inducida por la metanfetamina viene seguida de una reinervación progresiva, pero parcial, del estriado, ya que los déficits en la cantidad de terminales persisten incluso un mes después de la administración de la droga
5. La administración de metanfetamina produce déficits transitorios en la actividad y coordinación motora de los animales, coincidiendo con la degeneración de las terminales dopaminérgicas en el estriado. Estos déficits desaparecen con la recuperación parcial de dichas fibras.
6. La metanfetamina también produce la muerte de un bajo porcentaje (<0.17%) de neuronas estriatales. Las interneuronas parecen ser más vulnerables que las neuronas de proyección de las vías directa e indirecta, que degeneran por igual.
7. La administración de metanfetamina provoca un aumento de reactividad glial en estriado y SN, que sigue un patrón espacio temporal similar al de la neurotoxicidad.
8. El receptor dopaminérgico D1 está implicado en la neurotoxicidad que produce la metanfetamina. La inactivación del receptor D1 previene, en parte, este daño debido a que atenúa la respuesta hipertérmica, disminuye los niveles totales de dopamina y produce un cambio en la distribución de dopamina intracelular, aumentando la vesicular y disminuyendo la citosólica.
9. El receptor dopaminérgico D2 está implicado en la neurotoxicidad que produce la metanfetamina. La inactivación del receptor D2 previene este daño en parte por la inhibición de hipertermia, pero también porque su falta disminuye la actividad del DAT y por tanto disminuye la recaptación de dopamina, produciendo menores niveles de dopamina intracitosólicos.
10. El factor de transcripción Nrf2 está implicado en la protección frente al estrés oxidativo que produce la metanfetamina. La falta de Nrf2 potencia la neurotoxicidad en el estriado, aunque no en la SN. Esta potenciación de daño estriatal se debe a una falta de respuesta antioxidante al no activarse las enzimas de fase 2.

BIBLIOGRAFÍA

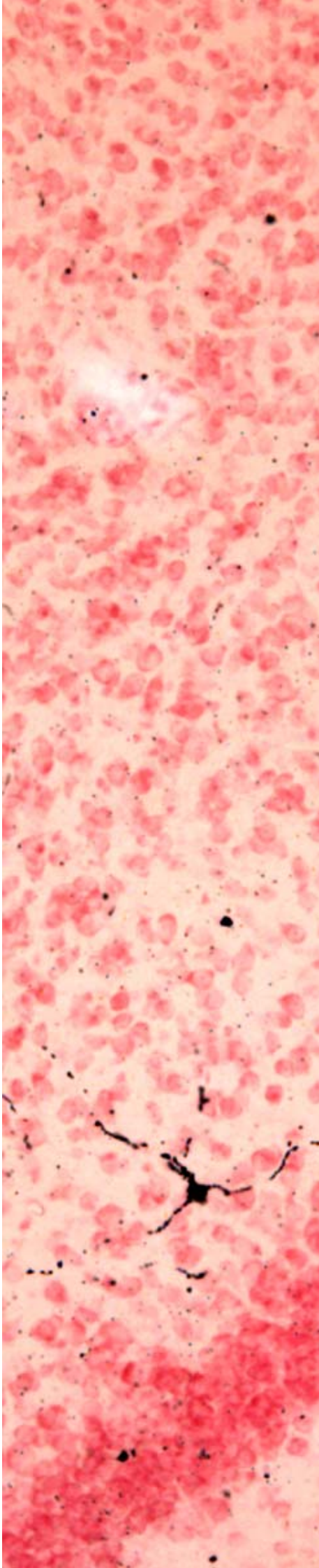

Foto de la página anterior: Neurona degenerando (negro) marcada con la tinción A-Cu-Ag en una sección de bulbo olfatorio teñida con Nissl con Neutral Red (rosa).

Afonso-Oramas, D., Cruz-Muros, I., Alvarez de la Rosa, D., Abreu, P., Giráldez, T., Castro-Hernández, J., Salas-Hernández, J., Lanciego, J.L., Rodríguez, M., González-Hernández, T., (2009). Dopamine transporter glycosylation correlates with the vulnerability of midbrain dopaminergic cells in Parkinson's disease. *Neurobiol. Dis*. **36**, 494–508.

Albers DS, Sonsalla PK. (1995). Methamphetamine-induced hyperthermia and dopaminergic neurotoxicity in mice: pharmacological profile of protective and nonprotective agents. *J Pharmacol Exp Ther.* **275**:1104-14.

Anderson KL, Itzhak Y. (2006). Methamphetamine-induced selective dopaminergic neurotoxicity is accompanied by an increase in striatal nitrate in the mouse. *Ann N Y Acad Sci*. **1074**:225-33.

Angulo JA, Angulo N, Yu J. (2004) Antagonists of the neurokinin-1 or dopamine D1 receptors confer protection from methamphetamine on dopamine terminals of the mouse striatum. *Ann N Y Acad Sci*; **1025**: 171–80.

Ares-Santos S, Granado N, Moratalla R. (2013a). Neurobiology of methamphetamine. Miller PM (Ed.). *Biological Research on Addiction: Comprehensive Addictive Behaviors and Disorders*. El Sevier Inc., San Diego: Academic Press. pp 579-591. Chapter 57. ISBN: 9780123983350.

Ares-Santos S, Granado N, Moratalla R. (2013b). Role of dopamine receptors in the neurotoxicity of methamphetamine. *J Intern Med*. **273**:437-53. Review.

Ares-Santos S, Granado N, Moratalla R. (2013c). Methamphetamine causes degeneration of dopamine cell bodies and terminals of the nigrostriatal pathway evidenced by silver staining. *Neuropsychopharmacology*. doi: 10.1038/npp.**2013**.307 . In press

Ares-Santos S, Granado N, Oliva I, O'Shea E, Martin ED, Colado MI, Moratalla R. (2012). Dopamine D (1) receptor deletion strongly reduces neurotoxic effects of methamphetamine. *Neurobiol Dis*. **45**:810-20.

Beaulieu JM, Gainetdinov RR. (2011). The physiology, signaling, and pharmacology of dopamine receptors. *Pharmacol Rev*. **63**:182-217. Review.

Beauvais G, Atwell K, Jayanthi S, Ladenheim B, Cadet JL. (2011). Involvement of dopamine receptors in binge methamphetamine-induced activation of endoplasmic reticulum and mitochondrial stress pathways. *PLoS One*. **6**(12):e28946

Beltramino CA, de Olmos JS, Gallyas F, Heimer L, Zaborszky L (1993). Silver staining as a tool for neurotoxic assessment. In: *Assessing Neurotoxicity of Drugs of Abuse,* Erinoff L (ed). National Institute of Drug Abuse Monograph 136, Rockville, Maryland, pp 101-126.

Bender C, de Olmos S, Bueno A, de Olmos J, Lorenzo A. (2010). Comparative analyses of the neurodegeneration induced by the non-competitive NMDA-receptor-antagonist drug MK801 in mice and rats. *Neurotoxicol Teratol*. **32**:542-50.

Bielschowsky M. (1904). Silberimpregnation der neurofibrillen. *J Psychol neurol* **3**: 169-188.

Black MM, Ansley HR. (1966). Histone specificity revealed by ammoniacalsilver staining. *J Histochem Cytochem.* **14**: 177-181.

Block, M.L., Hong, J.S. (2007). Chronic microglial activation and progressive dopaminergic neurotoxicity. *Biochem. Soc. Trans*. **35**, 1127–1132.

Bourne JA. (2001). SCH 23390: the first selective dopamine D1-like receptor antagonist. *CNS Drug Rev*. **7**: 399–414.

Bowyer JF, Davies DL, Schmued L, Broening HW, Newport GD, Slikker W Jr, Holson RR. (1994). Further studies of the role of hyperthermia in methamphetamine neurotoxicity. *J Pharmacol Exp Ther*. **268**:1571-80.

Breslow E. (1973). Metal-protein complexes. In: *Inorganic Biochemistry*, Eichhorn GL (ed). Elsevier, Amsterdam, The Netherlands, pp 227-249.

Briggs CA, Pollock NJ, Frail DE Paxson CL, Rakowski RF, Kang CH, Kebabian JW. (1991). Activation of the 5-HT1C receptor expressed in Xenopus oocytes by the benzazepines SCH 23390 and SKF 38393. *Br J Pharmacol* 1991; **104**:1038–44.

Broening HW, Morford LL, Vorhees CV. (2005). Interactions of dopamine D1 and D2 receptor antagonists with D-methamphetamine- induced hyperthermia and striatal dopamine and serotonin reductions. *Synapse (New York, N.Y.*). **56**: 84–93.

Bronstein DM, Hong JS (1995). Effects of sulpiride and SCH 23390 on methamphetamine-induced changes in body temperature and lethality. *J Pharmacol Exp Ther* **274:** 943–50.

Brown JM, Quinton MS, Yamamoto BK. (2005). Methamphetamine-induced inhibition of mitochondrial complex II: roles of glutamate and peroxynitrite. *J Neurochem.* **95:**429-36.

Brown JM, Riddle EL, Sandoval V, Weston RK, Hanson JE, Crosby MJ, Ugarte YV, Gibb JW, Hanson GR, Fleckenstein AE. (2002). A single

methamphetamine administration rapidly decreases vesicular dopamine uptake. *J Pharmacol Exp Ther*. **302**:497-501.

Bull DR., Palij P, Sheehan, MJ, Millar J, Stamford JÁ, Kruk ZL, Humphrey PP. (1990). Application of fast cyclic voltammetry to measurement of electrically dopamine overflow from brain slices in vitro. *J. Neurosci*. **32**, 37–44.

Burke RE, O'Malley K. (2012). Axon degeneration in Parkinson's disease. *Exp Neurol*. **246**:72-83.

Burrows KB, Gudelsky G, Yamamoto BK. (2000). Rapid and transient inhibition of mitochondrial function following methamphetamine or 3,4-methylenedioxymethamphetamine administration. *Eur J Pharmacol.* **398**:11-8.

Büttner A. (2011). The neuropathology of drug abuse. *Neuropathol Appl Neurobiol*. **37**:118-34. Review.

Büttner A, Weis S. (2006) Neuropathological alterations in drug abusers: the involvement of neurons, glial, and vascular systems. *Forensic Sci Med Pathol.* **2**: 115–26.

Cadet, J.L., Krasnova, I.N., Jayanthi, S., Lyles, J., (2007). Neurotoxicity of substituted amphetamines: molecular and cellular mechanisms. *Neurotox. Res*. **11**, 183–202.

Cadet JL, Jayanthi S, Deng X. (2003). Speed kills: cellular and molecular bases of methamphetamine-induced nerve terminal degeneration and neuronal apoptosis. *FASEB J.* **17**:1775-88. Review.

Cadet, J.L., Brannock, C. (1998). Free radicals and the pathobiology of brain dopamine systems. *Neurochem. Int*. **32**, 117–131.

Cadet, J.L., Ali, S., Epstein, C., (1994). Involvement of oxygen-based radicals in methamphetamine-induced neurotoxicity: evidence from the use of CuZnSOD transgenic mice. *Ann. N. Y. Acad. Sci.* **738**, 388–391.

Caligiuri MP, Buitenhuys C. (2005). Do preclinical findings of methamphetamine-induced motor abnormalities translate to an observable clinical phenotype? *Neuropsychopharmacology.* **30**:2125-34. Review

Callaghan RC, Cunningham JK, Sajeev G, Kish SJ. (2010). Incidence of Parkinson's disease among hospital patients with methamphetamine-use disorders. *Mov Disord*. **25**:2333-9.

Callaghan RC, Cunningham JK, Sykes J, Kish SJ. (2012). Increased risk of Parkinson's disease in individuals hospitalized with conditions related to the use of methamphetamine or other amphetamine-type drugs. *Drug Alcohol Depend.* **120**:35-40.

Callier S, Snapyan M, Le Crom S, Prou D, Vincent JD, Vernier P. (2003). Evolution and cell biology of dopamine receptors in vertebrates. *Biol Cell*. **95**:489-502. Review.

Cell Biology Promotion. http://www.cellbiol.net/ste/alpobesity3.php . Consultado por última vez el 3 de Diciembre de 2013.

Chan P, Di Monte DA, Luo JJ, DeLanney LE, Irwin I, Langston JW. (1994). Rapid ATP loss caused by methamphetamine in the mouse striatum: relationship between energy impairment and dopaminergic neurotoxicity. *J Neurochem*. **62:**2484-7.

Chen PC, Vargas MR, Pani AK, Smeyne RJ, Johnson DA, Kan YW, Johnson JA. (2009). Nrf2-mediated neuroprotection in the MPTP mouse model of Parkinson's disease: Critical role for the astrocyte. *Proc Natl Acad Sci USA* **106**:2933–2938.

Chen, J., Rusnak, M., Luedtke, R.R., Sidhu, A., (2004). D1 dopamine receptor mediates dopamine-induced cytotoxicity via the ERK signal cascade. *J. Biol. Chem.* **279**, 39317–39330.

Chu PW, Hadlock GC, Vieira-Brock P, Stout K, Hanson GR, Fleckenstein AE. (2010). Methamphetamine alters vesicular monoamine transporter-2 function and potassium-stimulated dopamine release. *J Neurochem*. **115**:325-32.

Clark J, Simon DK. (2009). Transcribe to survive: transcriptional control of antioxidant defense programs for neuroprotection in Parkinson's disease. *Antioxid Redox Signal*. **11**:509-28. Review.

Clark KH, Wiley CA, Bradberry CW. (2013). Psychostimulant abuse and neuroinflammation: emerging evidence of their interconnection. *Neurotox Res.* **23:**174-88.

Coleman M. (2005). Axon degeneration mechanisms: commonality amid diversity. *Nat Rev Neurosci*. **6**:889-98. Review.

Cruickshank CC, Dyer KR. (2009). A review of the clinical pharmacology of methamphetamine. *Addiction.* **104,** 1085-99. Review.

Cullinan SB, Zhang D, Hannink M, Arvisais E, Kaufman RJ, Diehl JA. (2003). Nrf2 is a direct PERK substrate and effector of PERK-dependent cell survival. *Mol Cell Biol*. **23**:7198–7209.

Darmopil S, Martín AB, De Diego IR, Ares S, Moratalla R. (2009). Genetic inactivation of dopamine D1 but not D2 receptors inhibits L-DOPA-induced dyskinesia and histone activation. *Biol Psychiatry*.**66:**603-13.

Davidson C, Gow AJ, Lee TH, Ellinwood EH. (2001). Methamphetamine neurotoxicity: necrotic and apoptotic mechanisms and relevance to human abuse and treatment. Brain *Res Brain Res Rev*. **36**:1-22. Review.

De Mei C, Ramos M, Iitaka C, Borrelli E. (2009). Getting specialized: presynaptic and postsynaptic dopamine D2 receptors. *Curr Opin Pharmacol*. **9**:53-8. Review

de Olmos JS, Beltramino CA, de Olmos de Lorenzo S. (1994). Use of an amino-cupric-silver technique for the detection of early and semiacute neuronal degeneration caused by neurotoxicants, hypoxia, and physical trauma. *Neurotoxicol Teratol.* **16**:545-61.

De Olmos JS. (1969). A cupric-silver method for impregnation of terminal axon degeneration and its further use in staining granular argyrophilic neurons. *Bran Behav Evol*. **2**: 213-237.

de Olmos S, Bender C, De Olmos JS, Lorenzo A. (2009). Neurodegeneration and prolonged immediate early gene expression throughout cortical areas of the rat brain following acute administration of dizocilpine. *Neuroscience.* **164**:1347-59.

Deng X, Cadet JL. (2000). Methamphetamine-induced apoptosis is attenuated in the striata of copper-zinc superoxide dismutase transgenic mice. *Brain Res Mol Brain Res.* **83:**121-4.

Dickinson, S.D., Sabeti, J., Larson, G.A., Giardina, K., Rubinstein, M., Kelly, M.A., Grandy, D.K., Low, M.J., Gerhardt, G.A., Zahniser, N.R., (1999). Dopamine D2 receptor-deficient mice exhibit decreased dopamine transporter function but no changes in dopamine release in dorsal striatum. *J. Neurochem*. **72**, 148–156.

Drug Enforcement Administration. http:// www.dea.gov y http://www.justice.gov/dea/ pr/multimedia-library/image-gallery/ images_methamphetamine.shtml. Consultado por última vez el 3 de diciembre de 2013

Eiland MM, Ramanathan L, Gulyani S, Gilliland M, Bergmann BM, Rechtschaffen A, Siegel JM. (2002). Increases in amino-cupric-silver staining of the supraoptic nucleus after sleep deprivation. *Brain Res*. **945**:1-8.

Eisch AJ, Marshall JF. (1998). Methamphetamine neurotoxicity: dissociation of striatal dopamine terminal damage from parietal cortical cell body injury. *Synapse.* **30**:433-45.

Elkashef A, Vocci F, Hanson G, White J, Wickes W, Tiihonen J. (2008). Pharmacotherapy of methamphetamine addiction: an update. *Subst Abus.* **29**:31-49.. Review.

Ernst T, Chang L, Leonido-Yee M, Speck O. (2000). Evidence for long-term neurotoxicity associated with methamphetamine abuse: A 1H MRS study. *Neurology.* **54**:1344-9.

Escubedo E, Guitart L, Sureda FX, Jiménez A, Pubill D, Pallàs M, Camins A, Camarasa J. (1998). Microgliosis and down-regulation of adenosine transporter induced by methamphetamine in rats. *Brain Res.* **814:**120-6.

Fearnley JM, Lees AJ. (1991). Ageing and Parkinson's disease: substantia nigra regional selectivity. *Brain.* **114**:2283-301.

Fink RP, Heimer L. (1967). Two methods for selective silver impregnation of degenerating axons and their synaptic endings in the central nervous system. *Brain Res.* **4:**369-74.

Fleckenstein AE, Haughey HM, Metzger RR, Kokoshka JM, Riddle EL, Hanson JE, Gibb JW, Hanson GR.. (1999). Differential effects of psychostimulants and related agents on dopaminergic and serotonergic transporter function. *Eur J Pharmacol;* **382**:45-9.

Fleckenstein AE, Metzger RR, Wilkins DG, Gibb JW, Hanson GR. (1997). Rapid and reversible effects of methamphetamine on dopamine transporters. J Pharmacol Exp Ther.;282:834-8.

Freeman HC (1973). Metal complexes of amino acid and peptides. In: *Inorganic Biochemistry*, Eichhorn GL (ed). Elsevier, Amsterdam, The Netherlands, pp 121-166.

Friend DM, Fricks-Gleason AN, Keefe KA. (2013). Is There a Role for Nitric Oxide in Methamphetamine-Induced Dopamine Terminal Degeneration? *Neurotox Res.* [Epub ahead of print]

Friend DM, Keefe KA. (2013). A role for D1 dopamine receptors in striatal methamphetamine-induced neurotoxicity. *Neurosci Lett*. doi:pii: S0304-3940(13)00772-6

Fumagalli, F., Gainetdinov, R.R., Wang, Y.M., Valenzano, K.J., Miller, G.W., Caron, M.G., (1999). Increased methamphetamine neurotoxicity in heterozygous vesicular monoamine transporter 2 knock-out mice. *J. Neurosci*. **19**, 2424–2431.

Fumagalli F, Gainetdinov RR, Valenzano KJ, Caron MG. (1998). Role of dopamine transporter in methamphetamine-induced neurotoxicity: evidence from mice lacking the transporter. *J Neurosci*. **18**:4861-9.

Glees P (1946). Terminal degeneration within the central nervous system as studied by a new silver method. *J Neuropathol Exp Neurol* **5**: 54-59.32.

Gomez-Nicola D, Valle-Argos B, Nieto-Sampedro M. (2010). Blockade of IL-15 activity inhibits microglial activation through the NFkappaB, p38, and ERK1/2 pathways, reducing cytokine and chemokine release. *Glia.* **58**:264-76.

Gómez-Nicola D, Valle-Argos B, Pita-Thomas DW, Nieto-Sampedro M. (2008). Interleukin 15 expression in the CNS: blockade of its activity prevents glial activation after an inflammatory injury. *Glia.* **56**:494-505.

Granado N, Ares-Santos S, Moratalla R. (2013a). Methamphetamine and Parkinson's disease. *Parkinsons Dis*. 2013:308052.

Granado N, Ares-Santos S, Moratalla R. (2013b). D1 but not D4 receptors are critical for MDMA-induced neurotoxicity. *Neurotoxicicty Research*. En prensa. DOI 10.1007/s12640-013-9438-8.

Granado N, Ares-Santos S, Oliva I, O'Shea E, Martin ED, Colado MI, Moratalla R. (2011a). Dopamine D2-receptor knockout mice are protected against dopaminergic neurotoxicity induced by methamphetamine or MDMA. *Neurobiol Dis.* **42**:391-403.

Granado N, Lastres-Becker I, Ares-Santos S, Oliva I, Martin E, Cuadrado A, Moratalla R. (2011b). Nrf2 deficiency potentiates methamphetamine-induced dopaminergic axonal damage and gliosis in the striatum. *Glia.* **59**:1850-63.

Granado N, Ares-Santos S, O'Shea E, Vicario-Abejón C, Colado MI, Moratalla R. (2010). Selective vulnerability in striosomes and in the nigrostriatal dopaminergic pathway after methamphetamine administration: early loss of TH in striosomes after methamphetamine. *Neurotox Res*. **18**:48-58.

Granado N, Escobedo I, O'Shea E, Colado I, Moratalla R. (2008a) Early loss of dopaminergic terminals in striosomes after MDMA administration to mice. *Synapse.***62:**80-4.

Granado N, O'Shea E, Bove J, Vila M, Colado MI, Moratalla R. (2008b). Persistent MDMA-induced dopaminergic neurotoxicity in the striatum and substantia nigra of mice. *J Neurochem.* **107:**1102-12.

Granado N, Ortiz O, Suárez LM, Martín ED, Ceña V, Solís JM, Moratalla R. (2008c). D1 but not D5 dopamine receptors are critical for LTP, spatial learning, and LTP-Induced arc and zif268 expression in the hippocampus. *Cereb Cortex.* **18:**1-12.

Gross NB, Duncker PC, Marshall JF. (2011). Striatal dopamine D1 and D2 receptors: widespread influences on methamphetamine- induced dopamine and serotonin neurotoxicity. *Synapse (New York, N.Y.)* **65**: 1144–55.

Hall ED, Andrus PK, Oostveen JA, Althaus JS, VonVoigtlander PF. (1996). Neuroprotective effects of the dopamine D2/D3 agonist pramipexole against postischemic or methamphetamine-induced degeneration of nigrostriatal neurons. *Brain Res*. **742**:80-8.

Halpin LE, Collins SA, Yamamoto BK. (2013). Neurotoxicity of methamphetamine and 3,4-methylenedioxymethamphetamine. *Life Sci*. doi:pii: S0024-3205(13)00401-3. 10.1016/ j.lfs.2013.07.014.

Halpin LE, Yamamoto BK. (2012). Peripheral ammonia as a mediator of methamphetamine neurotoxicity. *J Neurosci. **32:13155-63.***

Hart CL, Marvin CB, Silver R, Smith EE. (2012). Is cognitive functioning impaired in methamphetamine users? A critical review. *Neuropsychopharmacology*. **37**:586-608.

Hastings TG. (2009). The role of dopamine oxidation in mitochondrial dysfunction: implications for Parkinson's disease. *J Bioenerg Biomembr*. **41**:469-72

Henry JP, Sagné C, Botton D, Isambert MF, Gasnier B. (1998). Molecular pharmacology of the vesicular monoamine transporter. *Adv Pharmacol*. . **42**:236-9.

Henry JP, Gasnier B, Roisin MP, Isambert MF, Scherman D. (1987). Molecular pharmacology of the monoamine transporter of the chromaffin granule membrane. *Ann N Y Acad Sci.* **493**:194-206. Review.

Hirata H, Cadet JL. (1997). p53-knockout mice are protected against the long-term effects of methamphetamine on dopaminergic terminals and cell bodies. *J Neurochem*. **69**:780-90.

Hirata H, Ladenheim B, Carlson E, Epstein C, Cadet JL. (1996). Autoradiographic evidence for methamphetamine-induced striatal dopaminergic loss in mouse brain: attenuation in CuZn-superoxide dismutase transgenic mice. *Brain Res*. **714**:95-103.

Hotchkiss AJ, Gibb JW. (1980). Long-term effects of multiple doses of methamphetamine on tryptophan hydroxylase and tyrosine hydroxylase activity in rat brain. *J Pharmacol Exp Ther.* **214**:257-62

Huang YH, Tsai SJ, Su TW, Sim CB. (1999). Effects of repeated high-dose methamphetamine on local cerebral glucose utilization in rats. *Neuropsychopharmacology.* **21**:427–34.

Imam SZ, Newport GD, Itzhak Y, Cadet JL, Islam F, Slikker W Jr, Ali SF. (2001). Peroxynitrite plays a role in methamphetamine-induced dopaminergic neurotoxicity: evidence from mice lacking neuronal nitric oxide synthase gene or overexpressing copper-zinc superoxide dismutase. *J Neurochem*. **76**:745-9.

Innamorato NG, Rojo AI, Garcia-Yague AJ, Yamamoto M, de Ceballos ML, Cuadrado A. (2008). The transcription factor Nrf2 is a therapeutic target against brain inflammation. *J Immuno.* **181**:680–689.

Ito M, Numachi Y, Ohara A, Sora I. (2008). Hyperthermic and lethal effects of methamphetamine: roles of dopamine D1 and D2 receptors. *Neurosci Lett.* **438**: 327–9.

Itzhak Y, Martin JL, Ali SF. (2002). Methamphetamine -induced dopaminergic neurotoxicity in mice: long-lasting sensitization to the locomotor stimulation and desensitization to the rewarding effects of methamphetamine. *Prog Neuropsychopharmacol. Biol Psychiatry.* **26:**1177 -83.

Itzhak Y, Martin JL, Ail SF. (2000). nNOS inhibitors attenuate methamphetamine-induced dopaminergic neurotoxicity but not hyperthermia in mice. *Neuroreport.* **11**:2943-6.

Itzhak Y, Gandia C, Huang PL, Ali SF. (1998). Resistance of neuronal nitric oxide synthase-deficient mice to methamphetamine-induced dopaminergic neurotoxicity. *J Pharmacol Exp Ther.* **284:**1040-7.

Jaber M, Dumartin B, Sagné C, Haycock JW, Roubert C, Giros B, Bloch B, Caron MG. (1999). Differential regulation of tyrosine hydroxylase in the basal ganglia of mice lacking the dopamine transporter. *Eur J Neurosci.* **11**:3499-511.

Jakel RJ, Townsend JA, Kraft AD, Johnson JA. (2007). Nrf2-mediated protection against 6-hydroxydopamine. *Brain Res.* **1144**:192–201.

Jayanthi S, McCoy MT, Beauvais G, Ladenheim B, Gilmore K, Wood W 3rd, Becker K, Cadet JL. (2009). Methamphetamine induces dopamine D1 receptor-dependent endoplasmic reticulum stress-related molecular events in the rat striatum. *PLoS One*.**4**:e6092.

Jayanthi S, Deng X, Ladenheim B, McCoy MT, Cluster A, Cai NS, Cadet JL. (2005). Calcineurin/NFAT-induced up-regulation of the Fas ligand/Fas death pathway is involved inmethamphetamine-induced neuronal apoptosis. *Proc Natl Acad Sci U S A.* **102**:868-73.

Jayanthi S, Ladenheim B, Cadet JL. (1998). Methamphetamine-induced changes in antioxidant enzymes and lipid peroxidation in copper/zinc-superoxide dismutase transgenic mice. *Ann N Y Acad Sci*. **844:**92-102.

Jeng W, Ramkissoon A, Parman T, Wells PG. (2006). Prostaglandin H synthase-catalyzed bioactivation of amphetamines to free radical intermediates that cause CNS regional DNA oxidation and nerve terminal degeneration. *FASEB J*. **20:**638-50.

Jensen KF, Olin J, Haykal-Coates N, O'Callaghan J, Miller DB, de Olmos JS. (1993) Mapping toxicant-induced nervous system damage with a cupric silver stain: a quantitative analysis of neural degeneration induced by 3,4-methylenedioxymethamphetamine.*NIDA Res Monogr*. **136**:133-49; discussion 150-4.

Jia, Z., Zhu, H., Li, Y., Misra, H.P. (2009). Cruciferous nutraceutical 3H-1,2-dithiole-3- thione protects human primary astrocytes against neurocytotoxicity elicited by MPTP, MPP(+), 6-OHDA, HNE and acrolein. *Neurochem. Res*. **34**, 1924–1934.

Johnson JA, Johnson DA, Kraft AD, Calkins MJ, Jakel RJ, Vargas MR, Chen PC. (2008). The Nrf2-ARE pathway: an indicator and modulator of oxidative stress in neurodegeneration. *Ann N Y Acad Sci*. **1147**:61-9. Review.

Jones, S.R., Gainetdinov, R.R., Jaber, M., Giros, B., Wightman, R.M., Caron, M.G. (1998). Profound neuronal plasticity in response to inactivation of the dopamine transporter. *Proc. Natl. Acad. Sci. U. S. A*. **95**, 4029–4034.

Kanthasamy K, Gordon R, Jin H, Anantharam V, Ali S, Kanthasamy AG, Kanthasamy A. (2011). Neuroprotective effect of resveratrol against methamphetamine-induced dopaminergic apoptotic cell death in a cell culture model of neurotoxicity. *Curr Neuropharmacol*. **9**:49-53.

Kawaguchi Y, Wilson CJ, Augood SJ, Emson PC. (1995). Striatal interneurones: chemical, physiological and morphological characterization. *Trends Neurosci*. **18**:527-35. Review. Erratum in: *Trends Neurosci* 1996;**19**:143.

Kelly KA, Miller DB, Bowyer JF, O'Callaghan JP. (2012). Chronic exposure to corticosterone

enhances the neuroinflammatory and neurotoxic responses tomethamphetamine. *J Neurochem*. **122**:995-1009.

Kil HY, Zhang J, Piantadosi CA (1996). Brain temperature alters hydroxyl radical production during cerebral ischemia/reperfusion in rats. *J Cereb Blood Flow Metab*; **16**: 100– 6.

Kim H, Jhoo W, Shin E, Bing G. (2000). Selenium deficiency potentiates methamphetamine-induced nigral neuronal loss; comparison with MPTP model*. Brain Res*. **862**:247-52.

Kirshner N. (1962). Uptake of catecholamines by a particulate fraction of the adrenal medulla. *Science.* **135**:107-8.

Kita T, Wagner GC, Nakashima T. (2003). Current research on methamphetamine-induced neurotoxicity: animal models of monoamine disruption. *J Pharmacol Sci*. **92**:178-95. Review.

Koda, LY, Gibb, JW. (1973). Adrenal and striatal tyrosine hydroxylase activity after methamphetamine. *J Pharmacol Exp Ther*. **185,** 42-8.

Kogan FJ, Nichols WK, Gibb JW. (1976). Influence of methamphetamine on nigral and striatal tyrosine hydroxylase activity and on striatal dopamine levels. *Eur J Pharmacol*. **36**:363-71.

Konuma. K. (1994). Use and abuse of amphetamine in Japan., *Amphetamine and Its Analogs*. A.K. Cho, D.S. Segal (Eds.). Academic Press, San Diego, CA. pp. 415–438

Kramer JC, Fischman VS,. Littlefield DC. (1967) Amphetamine abuse: pattern and effects of high doses taken intravenously. *J. Am. Med. Assoc*. **201**: 305–309

Krasnova IN, Cadet JL. (2009). Methamphetamine toxicity and messengers of death. *Brain Res Rev.* **60**:379-407. Review.

Lai YT, Tsai YP, Cherng CG, Ke JJ, Ho MC, Tsai CW, Yu L. (2009). Lipopolysaccharide mitagates methamphetamine-induced striatal dopamine depletion via modulating local TNF-alpha and dopamine transporter expression. *J Neural Transm*. **116**:405–415.

Larsen KE, Fon EA, Hastings TG, Edwards RH,Sulzer D. (2002). Methamphetamine-induced degeneration of dopaminergic neurons involves autophagy and upregulation of dopamine synthesis. *J Neurosci.* **22:**8951-60.

LaVoie MJ, Card JP, Hastings TG. (2004). Microglial activation precedes dopamine terminal pathology in methamphetamine-induced neurotoxicity. *Exp Neurol.* **187**:47-57.

LaVoie MJ, Hastings TG. (1999). Dopamine quinone formation and protein modification associated with the striatal neurotoxicity of methamphetamine: evidence against a role for extracellular dopamine. *J Neurosci.* **19:**1484-91.

Leigh GJ (1990). *Nomenclature of Inorganic Chemistry (recommendations 1990) - The Red Book*. Blackwell Science. IBSN 0-63202-4941

Leonard C (1981). Silver degeneration methods. In: *Current Trends in Morphological Techniques*, Johnson JE Jr (ed). CRC Press, Boca Raton, Florida, pp 93-140.

Li X, Wang H, Qiu P, Luo H. (2008). Proteomic profiling of proteins associated with methamphetamine-induced neurotoxicity in different regions of rat brain. *Neurochem. Int*. **52**: 256–264.

Liesegang RE (1911). Die kolloid-chemie der histologischen silberfarbung. *Kolloid Beitr* **3**: 1-46.

Lin LY, Di Stefano EW, Schmitz DA, Hsu L, Ellis SW, Lennard MS, Tucker GT, Cho AK. (1997). Oxidation of methamphetamine and methylenedioxymethamphetamine by CYP2D6. *Drug Metab Dispos*. **25**: 1059-64.

Lo SC, Li X, Henzl MT, Beamer LJ, Hannink M. (2006). Structure of the Keap1:Nrf2 interface provides mechanistic insight into Nrf2 signaling. *EMBO J.* **25**:3605-17.

Manning-Boğ, A.B., Caudle, W.M., Perez, X.A., Reaney, S.H., Paletzki, R., Isla, M.Z., Chou, V.P., McCormack, A.L., Miller, G.W., Langston, J.W., Gerfen, C.R., Dimonte, D.A., (2007). Increased vulnerability of nigrostriatal terminals in DJ-1-deficient mice is mediated by the dopamine transporter. *Neurobiol. Dis*. **31**, 334–341.

Markkanen E, Hübscher U, van Loon B. (2012). Regulation of oxidative DNA damage repair: the adenine:8-oxo-guanine problem. *Cell Cycle*. **11**:1070-5.

McCann UD, Wong DF, Yokoi F, Villemagne V, Dannals RF, Ricaurte GA. (1998). Reduced striatal dopamine transporter density in abstinent methamphetamine and methcathinone users: evidence from positron emission tomography studies with [11C]WIN-35,428*. J Neurosci.* **18:**8417-22.

Medina L, Figueredo-Cardenas G, Reiner A. (1996). Differential abundance of superoxide dismutase in interneurons versus projection neurons and in matrix versus striosome neurons in monkey striatum. *Brain Res.***708**:59-70.

Metzger RR, Haughey HM, Wilkins DG, Gibb JW,

Hanson GR, Fleckenstein AE. (2000). Methamphetamine-induced rapid decrease in dopamine transporter function: role of dopamine and hyperthermia. *J Pharmacol Exp Ther*. **295**:1077-85.

Millan MJ, Newman-Tancredi A, Quentric Y, Cussac. (2001). D. The "selective" dopamine D1 receptor antagonist, SCH23390, is a potent and high efficacy agonist at cloned human serotonin 2C receptors. *Psychopharmacology*. **156**: 58–62.

Miller DB, O'Callaghan JP. (2003). Elevated environmental temperature and methamphetamine neurotoxicity. *Environ Res*. **92**:48-53.

Moratalla R, Ares-Santos, Granado N, .(2014). Neurotoxicity of methamphetamine. Kostrzewa, Richard M. (Ed.). *Handbook of Neurotoxicity*. Springer-Verlag New York Inc. ISBN 978-1-4614-7458-6. In press.

Nakajima A, Yamada K, Nagai T, Uchiyama T, Miyamoto Y, Mamiya T, He J, Nitta A, Mizuno M, Tran MH, Seto A, Yoshimura M, Kitaichi K, Hasegawa T, Saito K, Yamada Y, Seishima M, Sekikawa K, Kim HC, Nabeshima T. (2004). Role of tumor necrosis factor-alpha in methamphetamine-induced drug dependence and neurotoxicity. *J Neurosci.* **24**:2212-25.

Nash JF, Yamamoto BK. (1992). Methamphetamine neurotoxicity and striatal glutamate release: comparison to 3,4-methylenedioxymethamphetamine. *Brain Res.* **581:**237-43

National Antidrug Strategy. http://www.nationalantidrugstrategy.gc.ca/prevention/parents/talking-aborder.html . Consultado por última vez el 3 de diciembre de 2013.

Nauta WJH, Gygax PA (1951). Silver impregnation of degenerating axon terminals in the central nervous system (1) Technic (2) Chemical notes. *Stain Technol* **26**: 5-11.

Newton TF, Kalechstein AD, Duran S, Vansluis N, Ling W. (2004). Methamphetamine abstinence syndrome: preliminary findings. *Am J Addict.* **13**:248-55.

Observatorio Europeo de las Drogas y las Toxicomanías (2013). *Informe Europeo Sobre Drogas: tendencias y novedades*. Luxemburgo: Oficina de Publicaciones de la Unión Europea. ISBN 978-92-9168-612-4. doi:10.2810/882.

O'Callaghan JP, Sriram K. (2005). Glial fibrillary acidic protein and related glial proteins as biomarkers of neurotoxicity. *Expert Opin Drug Saf.* **4**:433-42. Review.

O'Callaghan JP, Miller DB. (1994). Neurotoxicity profiles of substituted amphetamines in the C57BL/6J mouse. *J Pharmacol Exp Ther*. **270**:741-51.

O'Callaghan JP, Jensen KF. Enhanced expression of glial fibrillary acidic protein and the cupric silver degeneration reaction can be used as sensitive and early indicators of neurotoxicity. *Neurotoxicology.* **13**:113-22. Review.

O'Dell SJ, Weihmuller FB, Marshall JF. (1991). Multiple methamphetamine injections induce marked increases in extracellular striatal dopamine which correlate with subsequent neurotoxicity. *Brain Res.* **564**:256-60.

O'Dell SJ, Weihmuller FB, Marshall JF. (1993). Methamphetamine induced dopamine overflow and injury to striatal dopamine terminals: attenuation by dopamine D1 or D2 antagonists. *J Neurochem;* **60**: 1792–9

Ortiz O, Delgado-García JM, Espadas I, Bahí A, Trullas R, Dreyer JL Gruart A, Moratalla R. (2010). Associative learning and CA3-CA1 synaptic plasticity are impaired in D1R null, Drd1a-/- mice and in hippocampal siRNA silenced Drd1a mice. *J Neurosci.* **30**:12288-300.

Pacchioni AM, Vallone J, Melendez RI, Shih A, Murphy TH, Kalivas PW. (2007). Nrf2 gene deletion fails to alter psychostimulant-induced behavior or neurotoxicity. *Brain Res*. **1127**:26–35.

Pan W, Wu X, He Y, Hsuchou H, Huang EY, Mishra PK, Kastin AJ. (2013). Brain interleukin-15 in neuroinflammation and behavior. *Neurosci Biobehav Rev*. **37**:184-92.

Photobucket. http://s466.photobucket.com/user/kikifraser/media/DARTs%20Video%20Project/Drug%20Pictures/drugs7.jpg.html . Consulttado por última vez el 3 de Diciembre de 2013.

Raff MC, Whitmore AV, Finn JT. (2002). Axonal self-destruction and neurodegeneration. *Science.* **296**:868-71.

Rangasamy T, Guo J, Mitzner WA, Roman J, Singh A, Fryer AD, Yamamoto M, Kensler TW, Tuder RM, Georas SN, Biswal S. (2005). Disruption of Nrf2 enhances susceptibility to severe airway inflammation and asthma in mice. *J Exp Med.* **202**:47–59.

Ricaurte GA, Guillery RW, Seiden LS, Schuster CR, Moore RY. (1982) Dopamine nerve terminal degeneration produced by high doses of methylamphetamine in the rat brain. *Brain Res*. **235**:93-103.

Ricaurte GA, Seiden LS, Schuster CR. (1984). Further evidence that amphetamines produce long-lasting dopamine neurochemical deficits by destroying dopamine nerve fibers. *Brain Res*. **303**:359-64.

Ries V, Silva RM, Oo TF, Cheng HC, Rzhetskaya M, Kholodilov N, Flavell RA, Kuan CY, Rakic P, Burke RE (2008). JNK2 and JNK3 combined are essential for apoptosis in dopamine neurons of the substantia nigra, but are not required for axon degeneration. *J Neurochem.* **107**:1578-88.

Rodrigues TB, Granado N, Ortiz O, Cerdán S, Moratalla R. (2007). Metabolic interactions between glutamatergic and dopaminergic neurotransmitter systems are mediated through D(1) dopamine receptors. *J Neurosci Res*. **85:**3284-93.

Rojo AI, Innamorato NG, Martin-Moreno AM, De Ceballos ML, Yamamoto M, Cuadrado A. (2010). Nrf2 regulates microglial dynamics and neuroinflammation in experimental Parkinson' s disease. *Glia* **58**:588–598.

Rosen GD, Williams RW. (2001). Complex trait analysis of the mouse striatum: independent QTLs modulate volume and neuron number. *BMC Neurosci*. **2**:5.

Satoh T, Okamoto SI, Cui J, Watanabe Y, Furuta K, Suzuki M, Tohyama K, Lipton SA. (2006). Activation of the Keap1/Nrf2 pathway for neuroprotection by electrophilic [correction of electrophillic] phase II inducers. *Proc Natl Acad Sci U S A*. **103:**768-73.

Sattler R, Tymianski M. (2000). Molecular mechanisms of calcium-dependent excitotoxicity. *J Mol Med (Berl).* **78**:3-13. Review.

Schep LJ, Slaughter RJ, Beasley DM. (2010). The clinical toxicology of metamfetamine. *Clin Toxicol (Phila).* **48**:675-94. Review.

Seiden LS, Sabol KE, Ricaurte GA. (1993). Amphetamine: effects on catecholamine systems and behavior. *Annu Rev Pharmacol Toxicol.* **33**:639-77. Review.

Seiden LS, Commins DL, Vosmer G, Axt K, Marek G. (1988). Neurotoxicity in dopamine and 5-hydroxytryptamine terminal fields: a regional analysis in nigrostriatal and mesolimbic projections. *Ann N Y Acad Sci*. **537**:161-72. Review.

Seiden LS, Fischman MW, Schuster CR. (1976) Long-term methamphetamine induced changes in brain catecholamines in tolerant rhesus monkeys. Drug *Alcohol Depend*. **1**:215-9.

Sonsalla PK, Jochnowitz ND, Zeevalk GD, Oostveen JA, Hall ED. (1996). Treatment of mice with methamphetamine produces cell loss in the substantia nigra. *Brain Res.* **738**:172-5.

Sonsalla PK, Nicklas WJ, Heikkila RE. (1989). Role for excitatory amino acids in methamphetamine-induced nigrostriatal dopaminergic toxicity. *Science.* **243:**398-400.

Sonsalla PK, Gibb JW, Hanson GR. (1986.) Roles of D1 and D2 dopamine receptor subtypes in mediating the methamphetamine-induced changes in monoamine systems. *J Pharmacol Exp Ther*. **238**:932-7.

Spencer JPE, Whiteman M, Jenner P, Halliwell (2002). B. 5-s- Cysteinyl-conjugates of catecholamines induce cell damage, extensive DNA base modification and increases in caspase-3 activity in neurons. *J Neurochem*; **81:** 122**–**9.

Sriram K, Miller DB, O'Callaghan JP. (2006). Minocycline attenuates microglial activation but fails to mitigate striatal dopaminergic neurotoxicity: role of tumor necrosis factor-alpha. *J Neurochem.* **96**:706-18.

Sulzer D. (2007). Multiple hit hypotheses for dopamine neuron loss in Parkinson's disease. *Trends Neurosci.* **30**:244-50.

Sulzer D, Sonders MS, Poulsen NW, Galli A. (2005). Mechanisms of neurotransmitter release by amphetamines: a review. *Prog Neurobiol.* **75:**406 -33.

Sulzer D, Rayport S. (1990). Amphetamine and other psychostimulants reduce pH gradients in midbrain dopaminergic neurons and chromaffin granules: a mechanism of action. *Neuron*;**5**:797–808.

Switzer RC 3rd. (2000). Application of silver degeneration stains for neurotoxicity testing. *Toxicol Pathol*. **28**:70-83. Review.

Switzer RC 3rd. (1993). Silver staining methods: their role in detecting neurotoxicity. *Ann N Y Acad Sci*. **679**:341-8.

Switzer RC III (1991). Strategies for assessing neurotoxicity. *Neurosci Biobehav Rev* **15**: 89-93.

Switzer RC 3rd, Merril CR, Shifrin S. (1979). A highly sensitive silver stain for detecting proteins and peptides in polyacrylamide gels. *Anal Biochem*. **98**:231-7.

The DB-DRD4 Database Project, Bioinformatics Research Laboratory, IBI Biosolutions Pvt. Ltd. India http://www.ibibiobase.com/projects/db-drd4/drd4_pathway.htm . Consultado por última vez el 3 de diciembre de 2013.

Thimmulappa RK, Lee H, Rangasamy T, Reddy SP, Yamamoto M, Kensler TW, Biswal S. (2006a).

Nrf2 is a critical regulator of the innate immune response and survival during experimental sepsis. *J Clin Invest*. **116**:984–995.

Thimmulappa RK, Scollick C, Traore K, Yates M, Trush MA, Liby KT, Sporn MB, Yamamoto M, Kensler TW, Biswal S. (2006b). Nrf2-dependent protection from LPS induced inflammatory response and mortality by CDDO-imidazolide. *Biochem Biophys Res Commun* **351**:883–889.

Thomas DM, Dowgiert J, Geddes TJ, Francescutti-Verbeem D, Liu X, Kuhn DM. (2004). Microglial activation is a pharmacologically specific marker for the neurotoxic amphetamines. *Neurosci Lett.* **367:**349-54.

Thomas, D.M., Francescutti-Verbeem, D.M., Kuhn, D.M., (2008a) Methamphetamine-induced neurotoxicity and microglial activation are not mediated by fractalkine receptor signaling. *J. Neurochem*. **106**, 696–705.

Thomas, D.M., Francescutti-Verbeem, D.M., Kuhn, D.M., (2008b). The newly synthesized pool of dopamine determines the severity of methamphetamine-induced neurotoxicity. *J. Neurochem*. **105**, 605–616.

Tinsley, R.B., Bye, C.R., Parish, C.L., Tziotis-Vais, A., George, S., Culvenor, J.G., Li QX, Masters CL, Finkelstein DI, Horne MK. (2009). Dopamine D2 receptor knockout mice develop features of Parkinson disease. *Ann. Neurol*. **66**, 472–484.

Todd G, Noyes C, Flavel SC, Della Vedova CB, Spyropoulos P, Chatterton B, Berg D, White JM. (2013). Illicit stimulant use is associated with abnormal substantia nigra morphology in humans. PLoS One. 8:e56438.

Tulloch I, Afanador L, Mexhitaj I, Ghazaryan N, Garzagongora AG, Angulo JA. (2011). A single high dose of methamphetamine induces apoptotic and necrotic striatal cell loss lasting up to 3 months in mice. *Neuroscience*. **193**:162-9.

UNODC (2013). World drug report. (United Nations publication, Sales No. E.13.XI.6). http:// www.unodc.org/unodc/secured/wdr/wdr2013/ World_Drug_Report_2013.pdf

Urrutia A, Rubio-Araiz A, Gutierrez-Lopez MD, ElAli A, Hermann DM, O'Shea E, Colado MI. (2013). A study on the effect of JNK inhibitor, SP600125, on the disruption of blood-brain barrier induced by methamphetamine. *Neurobiol Dis*. **50**:49-58.

Usiello A, Baik JH, Rougé-Pont F, Picetti R, Dierich A, LeMeur M, Piazza PV, Borrelli E. (2000). Distinct functions of the two isoforms of dopamine D2 receptors. *Nature.* **408**:199-203.

Venton BJ, Zhang H, Garris PA, Phillips PE, Sulzer D, Wightman RM. (2003). Real-time decoding of dopamine concentration changes in the caudate-putamen during tonic and phasic firing. *J Neurochem*. **87**:1284-95.

Volkow ND, Chang L, Wang GJ, Fowler JS, Franceschi D, Sedler M, Gatley SJ, Miller E, Hitzemann R, Ding YS, Logan J.(2001a). Loss of dopamine transporters in methamphetamine abusers recovers with protracted abstinence. *J Neurosci.* **21**:9414-8.

Volkow ND, Chang L, Wang GJ, Fowler JS, Leonido-Yee M, Franceschi D, Sedler MJ, Gatley SJ, Hitzemann R, Ding YS, Logan J, Wong C, Miller EN. (2001b). Association of dopamine transporter reduction with psychomotor impairment in methamphetamine abusers. *Am J Psychiatry.* **158**:377-82.

Volkow ND, Chang L, Wang GJ, Fowler JS, Franceschi D, Sedler MJ, Gatley SJ, Hitzemann R, Ding YS, Wong C, Logan J. (2001c). Higher cortical and lower subcortical metabolism in detoxified methamphetamine abusers. *Am J Psychiatry*. **158**:383-9.

Volz, T.J., Hanson, G.R., Fleckenstein, A.E. (2006). Measurement of kinetically resolved vesicular dopamine uptake and efflux using rotating disk electrode voltammetry. *J. Neurosci. Methods.* **155**, 109–115.

Wagner GC, Carelli RM, Jarvis MF. (1986). Ascorbic acid reduces the dopamine depletion induced by methamphetamine and the 1-methyl-4-phenyl pyridinium ion *Neuropharmacology*. **25**:559-61

Wagner GC, Ricaurte GA, Seiden LS, Schuster CR, Miller RJ, Westley J. (1980). Long-lasting depletions of striatal dopamine and loss of dopamine uptake sites following repeated administration of methamphetamine. *Brain Res*. **181**:151-60.

Wang Q, Shin EJ, Nguyen XK, Li Q, Bach JH, Bing G Kim WK, Kim HC, Hong JS. (2012). Endogenous dynorphin protects against neurotoxin-elicited nigrostriatal dopaminergic neuron damage and motor deficits in mice. *J Neuroinflammation.* **13**;9:124.

White NM, Hiroi N. (1998). Preferential localization of self-stimulation sites in striosomes/patches in the rat striatum. *Proc Natl Acad Sci U S A*. **95**:6486-91.

Wightman, R.M., Zimmerman, J.B., (1990). Control of dopamine extracellular concentration in rat striatum by impulse flow and uptake. *Brain Res. Rev*. **15**, 135–144.

Wikimedia Commons. http://en.wikipedia.org/wiki/File:Suspectedmethmouth09-19-05.jpg . Consultado por última vez el 3 de Diciembre de 2013.

Wise RA. (2009). Roles for nigrostriatal--not just mesocorticolimbic--dopamine in reward and addiction. *Trends Neurosci.* **32**:517-24.

Woolverton WL, Ricaurte GA, Forno LS, Seiden LS. (1989). Long-term effects of chronic methamphetamine administration in rhesus monkeys. *Brain Res*.**486:**73-8.

Xie T, McCann UD, Kim S, Yuan J, Ricaurte GA. (2000). Effect of temperature on dopamine transporter function and intracellular accumulation of methamphetamine: implications for methamphetamine-induced dopaminergic neurotoxicity. *J Neurosci.* **20**:7838-45.

Xu W, Zhu JPQ, Angulo JA. (2005). Induction of striatal pre- and postsynaptic damage by methamphetamine requires the dopamine receptors. *Synapse (New York, N.Y.).* **58:** 110–21.

Yamamoto BK, Yang FC. (2012). Methamphetamine-induced oxidation of proteins and alterations in protein processing. *Neuropsychopharmacology.* **37**:298-9.

Yamamoto BK, Moszczynska A, Gudelsky GA. (2010). Amphetamine toxicities: classical and emerging mechanisms. *Ann N Y Acad Sci.* **1187**:101-21

Yamamoto BK, Zhu W. (1998). The effects of methamphetamine on the production of free radicals and oxidative stress. *J Pharmacol Exp Ther.* **287:**107-14.

Zhu JP, Xu W, Angulo N, Angulo JA. (2006a). Methamphetamine-induced striatal apoptosis in the mouse brain: comparison of a binge to an acute bolus drug administration. *Neurotoxicology.* **7**:131-6.

Zhu JP, Xu W, Angulo JA. (2006b). Methamphetamine -induced cell death: selective vulnerability in neuronal subpopulations of the striatum in mice. *Neuroscience*. **140**:607-22.

Zhu, JP, Xu W, Angulo JA. (2005). Disparity in the temporal appearance of methamphetamine-induced apoptosis and depletion of dopamine terminal markers in the striatum of mice. *Brain Res.* **1049**, 171–181.

OTRAS PUBLICACIONES

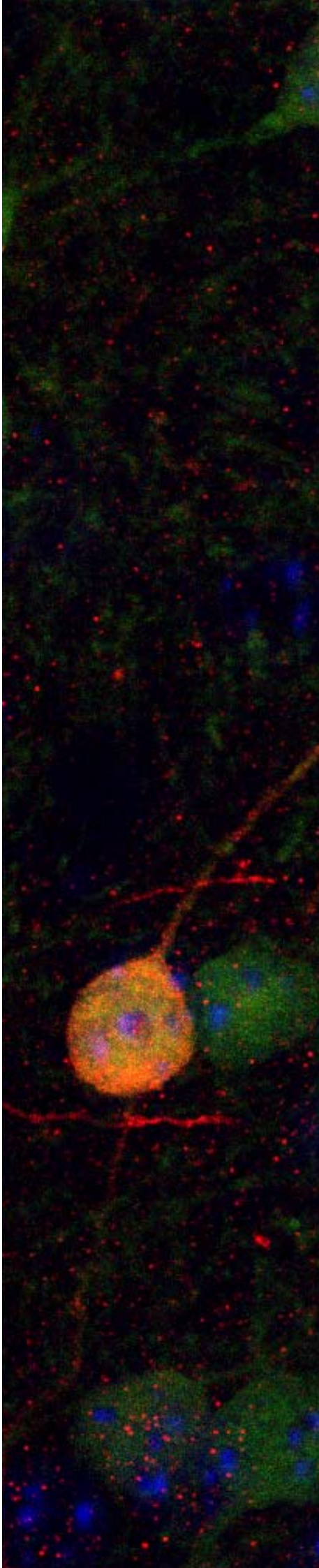

Foto de la página anterior: Sección de estriado de un ratón transgénico BAC D1-Tmt/D2-GFP tratado con metanfetamina (1x30) en la que se ha hecho una tinción inmunofluorescente para TH (rojo) y para las neuronas de proyección de la vía indirecta (D2-GFP, verde) y se han teñido los núcleos celulares con DAPI (azul). Obsérvese en amarillo una neurona de proyección de la vía indirecta que expresa TH tras el tratamiento con metanfetamina.

I. Genetic Inactivation of Dopamine D1 but Not D2 Receptors Inhibits L-DOPA–Induced Dyskinesia and Histone Activation. Darmopil S, Martín AB, Ruiz de Diego I, Ares S, Moratalla R *Biological Psychiatry.* 2009. 63:603-13.

Genetic Inactivation of Dopamine D1 but Not D2 Receptors Inhibits L-DOPA–Induced Dyskinesia and Histone Activation

Sanja Darmopil, Ana B. Martín, Irene Ruiz De Diego, Sara Ares, and Rosario Moratalla

Background: Pharmacologic studies have implicated dopamine D1-like receptors in the development of dopamine precursor molecule 3,4-dihydroxyphenyl-L-alanine (L-DOPA)-induced dyskinesias and associated molecular changes in hemiparkinsonian mice. However, pharmacologic agents for D1 or D2 receptors also recognize other receptor family members. Genetic inactivation of the dopamine D1 or D2 receptor was used to define the involvement of these receptor subtypes.

Methods: During a 3-week period of daily L-DOPA treatment (25 mg/kg), mice were examined for development of contralateral turning behavior and dyskinesias. L-DOPA-induced changes in expression of signaling molecules and other proteins in the lesioned striatum were examined immunohistochemically.

Results: Chronic L-DOPA treatment gradually induced rotational behavior and dyskinesia in wildtype hemiparkinsonian mice. Dyskinetic symptoms were associated with increased FosB and dynorphin expression, phosphorylation of extracellular signal-regulated kinase, and phosphoacetylation of histone 3 (H3) in the lesioned striatum. These molecular changes were restricted to striatal areas with complete dopaminergic denervation and occurred only in dynorphin-containing neurons of the direct pathway. D1 receptor inactivation abolished L-DOPA-induced dyskinesias and associated molecular changes. Inactivation of the D2 receptor had no significant effect on the behavioral or molecular response to chronic L-DOPA.

Conclusions: Our results demonstrate that the dopamine D1 receptor is critical for the development of L-DOPA-induced dyskinesias in mice and in the underlying molecular changes in the denervated striatum and that the D2 receptor has little or no involvement. In addition, we demonstrate that H3 phosphoacetylation is blocked by D1 receptor inactivation, suggesting that inhibitors of H3 acetylation and/or phosphorylation may be useful in preventing or reversing dyskinesia.

Key Words: Dopaminergic denervation, dynorphin, ERK1/2, FosB, Parkinson's disease, phosphoacetylated histone 3

Parkinson disease (PD) is caused by degeneration of midbrain dopaminergic neurons that project to the striatum. Despite extensive investigation and new therapeutic approaches, the dopamine precursor molecule 3,4-dihydroxyphenyl-L-alanine (L-DOPA) remains the most effective and most commonly used noninvasive treatment for PD. However, chronic treatment and disease progression lead to changes in the brain's response to L-DOPA, resulting in a lower therapeutic window and the appearance of abnormal involuntary movements. These movements, known as dyskinesias, interfere significantly with normal motor activity and are associated with changes in striatal gene expression.

Our hypothesis is that these changes are the result of intermittent stimulation of supersensitive dopamine receptors in denervated striatal neurons (1). These receptors have increased coupling to $G\alpha_{olf}$ (2), resulting in greater stimulation of adenylyl cyclase, which activates the extracellular signal-regulated kinase (ERK) pathway (3) and triggers posttranslational modification of histones (4), leading to gene transcription (5). All dopamine receptor (R) subtypes (D1-D5) are present in the striatum, although D1R and D2R are the most abundant. These two dopamine receptors exhibit opposite functions, and their expression is segregated: D1R and D2R are expressed in neurons of direct and indirect striatal output pathways, respectively. Some molecular changes correlated with dyskinesias such as increased FosB and dynorphin expression are confined to D1R-containing neurons, whereas p-ERK and Nurr1 expression have been described in both D1R- and D2R-containing neurons (6,7). Although dopamine receptors are clearly involved in dyskinesias, the contribution of each dopamine receptor subtype has not been demonstrated definitively, and the signaling pathways that trigger long-term changes that maintain dyskinesias are not fully defined.

Pharmacologic studies implicate both the D1/D5 and D2/D3 receptor families in the development of dyskinesias. In patients, chronic treatment with a nonselective dopamine agonist with a short plasma half-life is more likely to induce dyskinesia than treatment with D2R agonists with long plasma half-lives (8). In rodents, dyskinesias can be induced by D1-type (D1/D5) or D2-type (D2/D3) agonists (9–12) with D1/D5 agonists having the most powerful dyskinetogenic effect (7,12,13). Consistent with this, D1/D5 antagonists are more effective inhibitors of L-DOPA-induced dyskinesia than D2 antagonists (7,12–14).

Because D1 receptors greatly outnumber D5 receptors in the striatum, it is tempting to assume that the striatal actions of mixed D1/D5 ligands are due to the D1 receptor. However, there are several examples in which the less abundant dopamine receptor is the major player for specific functions. In the hippocampus, D5R are much more abundant than D1R, but the D5 receptors do not play a role in spatial learning or hippocampal long-term potentiation, whereas D1 receptors are critical in these processes (15). In addition, within the striatum itself, where D1 is predominant, D1 and D5 receptors are equally required for striatal

From the Cajal Institute, Consejo Superior de Investigaciones Científicas and Centro de Investigación Biomédica en Red para Enfermedades Neurodegenerativas, Instituto de Salud Carlos III, Madrid, Spain.
Address correspondence to Rosario Moratalla, Ph.D., Cajal Institute, Avenida Dr. Arce 37, 28002 Madrid, Spain. E-mail: moratalla@cajal.csic.es.
Received Feb 12, 2009; revised Apr 7, 2009; accepted Apr 17, 2009.

0006-3223/09/$36.00
doi:10.1016/j.biopsych.2009.04.025

BIOL PSYCHIATRY 2009;66:603–613

II. Selective vulnerability in striosomes and in the nigrostriatal dopaminergic pathway after methamphetamine administration: early loss of TH in striosomes after methamphetamine. Granado N, Ares-Santos S , O'Shea E, Vicario-Abejón C, Colado MI, Moratalla R. *Neurotoxicity Research.* 2010.18:48-58.

VOLUME 18 NUMBER 1 • JULY 2010

Neurotoxicity Research

Official Journal of the Neurotoxicity Society

Special Issue: Fourth Neurotoxicity Society Meeting, Arica, Chile, April 24–26, 2009

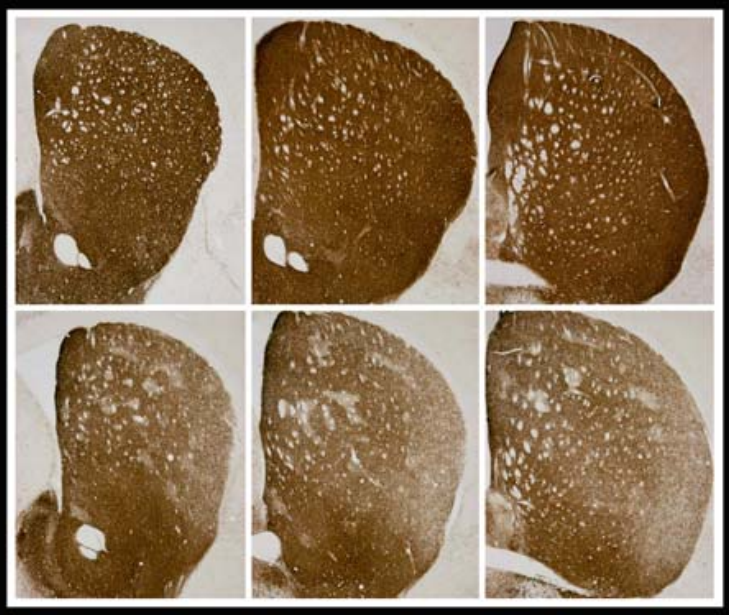

Springer

12640 • ISSN 1029-8428
18(1) 1–106 (2010)

Neurotox Res
DOI 10.1007/s12640-009-9106-1

Selective Vulnerability in Striosomes and in the Nigrostriatal Dopaminergic Pathway After Methamphetamine Administration

Early Loss of TH in Striosomes After Methamphetamine

Noelia Granado · Sara Ares-Santos · Esther O'Shea · Carlos Vicario-Abejón · M. Isabel Colado · Rosario Moratalla

Received: 1 July 2009 / Revised: 30 July 2009 / Accepted: 21 August 2009

Abstract Methamphetamine (METH), a commonly abused psychostimulant, causes dopamine neurotoxicity in humans, rodents, and nonhuman primates. This study examined the selective neuroanatomical pattern of dopaminergic neurotoxicity induced by METH in the mouse striatum. We examined the effect of METH on tyrosine hydroxylase (TH) and dopamine transporter (DAT) immunoreactivity in the different compartments of the striatum and in the nucleus accumbens. The levels of dopamine and its metabolites, 3,4-dihidroxyphenylacetic acid and homovanillic acid, as well as serotonin (5-HT) and its metabolite, 5-hydroxyindolacetic acid, were also quantified in the striatum. Mice were given three injections of METH (4 mg/kg, i.p.) at 3 h intervals and sacrificed 7 days later. This repeated METH injection induced a hyperthermic response and a decrease in striatal concentrations of dopamine and its metabolites without affecting 5-HT concentrations. In addition, the drug caused a reduction in TH- and DAT-immunoreactivity when compared to saline-treated animals. Interestingly, there was a significantly greater loss of TH- and DAT-immunoreactivity in striosomes than in the matrix. The predominant loss of dopaminergic terminals in the striosomes occurred along the rostrocaudal axis of the striatum. In contrast, METH did not decrease TH- or DAT-immunoreactivity in the nucleus accumbens. These results provide the first evidence that compartments of the mouse striatum, striosomes and matrix, and mesolimbic and nigrostriatal pathways have different vulnerability to METH. This pattern is similar to that observed with other neurotoxins such as MPTP, the most widely used model of Parkinson's disease, in early Huntington's disease and hypoxic/ischemic injury, suggesting that these conditions might share mechanisms of neurotoxicity.

Keywords TH · DAT · Striosomes · Matrix · Striatum · Neurotoxicity · Dopamine · Parkinson's disease

Abbreviations

METH	Methamphetamine
PB	Phosphate buffer
PBST	Phosphate sodium buffer with Triton X-100
DA	Dopamine
TH	Tyrosine hydroxylase
DAT	Dopamine transporter
MOR-I	Opioid μ receptor
DOPAC	3,4-Dihidroxyphenylacetic acid
HVA	Homovanillic acid
5-HT	Serotonin
5-HIAA	5-Hydroxyindolacetic acid
MDMA	3,4-Methylenedioxymethamphetamine
MPTP	1-methyl-4-phenyl-1,2,3,6-tetrahydropyridine

In memoriam to Dr. J.A. Burzaco for his dedication to Parkinson's patients.

N. Granado · S. Ares-Santos · C. Vicario-Abejón · R. Moratalla (✉)
Instituto Cajal, Consejo Superior de Investigaciones Científicas (CSIC), Avda. Dr. Arce 37, 28002 Madrid, Spain
e-mail: moratalla@cajal.csic.es

N. Granado · S. Ares-Santos · C. Vicario-Abejón · R. Moratalla
CIBERNED, Instituto de Salud Carlos III, Madrid, Spain

E. O'Shea · M. I. Colado
Departamento de Farmacologia, Facultad Medicina, Universidad Complutense, 28040 Madrid, Spain

Published online: 04 September 2009

III. The role of dopamine receptors in the neurotoxicity of methamphetamine (review). Ares-Santos S*, Granado N*, Moratalla R. *Journal of Internal Medicine* . 2013. 273: 467-53

Review

Journal of INTERNAL MEDICINE

Click here for more articles from the Ceccatalli symposium

doi: 10.1111/joim.12049

The role of dopamine receptors in the neurotoxicity of methamphetamine

S. Ares-Santos[1,2]*, N. Granado[1,2,3]* & R. Moratalla[1,2]

From the [1] Instituto Cajal, Consejo Superior de Investigaciones Científicas, CSIC, [2]CIBERNED, ISCIII, and [3]Facultad de Medicina, Universidad Complutense de Madrid, Madrid, Spain

Abstract. Ares-Santos S, Granado N, Moratalla R (Instituto Cajal, Consejo Superior de Investigaciones Científicas, CSIC, Madrid; CIBERNED, ISCIII, Madrid; Universidad Complutense de Madrid, Madrid, Spain). The role of dopamine receptors in the neurotoxicity of methamphetamine. (Review). *J Intern Med* 2013; **273**: 437–453.

Methamphetamine is a synthetic drug consumed by millions of users despite its neurotoxic effects in the brain, leading to loss of dopaminergic fibres and cell bodies. Moreover, clinical reports suggest that methamphetamine abusers are predisposed to Parkinson's disease. Therefore, it is important to elucidate the mechanisms involved in methamphetamine-induced neurotoxicity. Dopamine receptors may be a plausible target to prevent this neurotoxicity. Genetic inactivation of dopamine D1 or D2 receptors protects against the loss of dopaminergic fibres in the striatum and loss of dopaminergic neurons in the substantia nigra. Protection by D1 receptor inactivation is due to blockade of hypothermia, reduced dopamine content and turnover and increased stored vesicular dopamine in D1R $^{-/-}$ mice. However, the neuroprotective impact of D2 receptor inactivation is partially dependent on an effect on body temperature, as well as on the blockade of dopamine reuptake by decreased dopamine transporter activity, which results in reduced intracytosolic dopamine levels in D2R$^{-/-}$ mice.

Keywords: amphetamine derivatives, designer drugs, dopamine, drug addiction, Parkinson's disease, psychostimulants.

Introduction

The most recent estimates from The United Nations Office on Drugs and Crime (UNODC) indicate that there are between 14.3 million and 52.5 million users of the psychostimulant methamphetamine and other amphetamine-type stimulant drugs worldwide, making these the second most widely consumed drugs of abuse after cannabis [1]. Methamphetamine poses a serious international public health concern due to its high potential for addiction and the risk of long-lasting neurological impairment [2]. Methamphetamine is a neurotoxic drug that causes, amongst other effects, deficits in and alterations to dopaminergic pathways in the brain. Repeated administration of methamphetamine to mice causes neurodegeneration of dopaminergic axon terminals in the striatum, producing reductions in striatal tyrosine hydroxylase (TH; the rate-limiting enzyme for dopamine synthesis) and dopamine transporter (DAT), accompanied by reductions in the striatal levels of dopamine and its metabolites 3,4-dihidroxyphenylacetic acid (DOPAC) and homovanillic acid (HVA) [3–6]. This dopamine axonal loss can be detected as early as 24 h after exposure to the drug. Although some days later there is a partial recovery of striatal TH and DAT immunoreactivity, the recovery is not complete and some loss persists for long periods [3, 5, 6]. This persistent loss of dopamine axons has been correlated with dopamine cell body loss in the substantia nigra pars compacta (SNpc), demonstrated by rigorous stereological measurement of cell count with both TH and Nissl staining. This has been further supported by staining with cell death markers such as FluoroJade and by detection of apoptotic cell bodies, an irrefutable marker of cell death [3, 5–8].

Recent evidence demonstrates that methamphetamine primarily affects the nigrostriatal dopaminergic pathway, whereas the mesolimbic pathway is more resistant, as demonstrated by the finding that TH levels in the nucleus accumbens of rodents are not affected by methamphetamine [4] paralleling the situation in Parkinson's disease where the

*These authors contributed equally.

IV. Methamphetamine and Parkinson's Disease (review). Granado N*, Ares-Santos S*, Moratalla R. *Parkinson's Disease.* 2013:308052

* equal contribution

Hindawi Publishing Corporation
Parkinson's Disease
Volume 2013, Article ID 308052, 10 pages
http://dx.doi.org/10.1155/2013/308052

Review Article

Methamphetamine and Parkinson's Disease

Noelia Granado,[1,2,3] Sara Ares-Santos,[1,2] and Rosario Moratalla[1,2]

[1] *Instituto Cajal (CSIC), Avenida Doctor Arce 37, 28002 Madrid, Spain*
[2] *CIBERNED, Instituto de Salud Carlos III, Madrid, Spain*
[3] *Facultad de Medicina, Universidad Complutense de Madrid, Madrid, Spain*

Correspondence should be addressed to Rosario Moratalla; moratalla@cajal.csic.es

Received 20 August 2012; Accepted 22 October 2012

Academic Editor: José Manuel Fuentes Rodríguez

Parkinson's disease (PD) is a neurodegenerative disorder predominantly affecting the elderly. The aetiology of the disease is not known, but age and environmental factors play an important role. Although more than a dozen gene mutations associated with familial forms of Parkinson's disease have been described, fewer than 10% of all cases can be explained by genetic abnormalities. The molecular basis of Parkinson's disease is the loss of dopamine in the basal ganglia (caudate/putamen) due to the degeneration of dopaminergic neurons in the substantia nigra, which leads to the motor impairment characteristic of the disease. Methamphetamine is the second most widely used illicit drug in the world. In rodents, methamphetamine exposure damages dopaminergic neurons in the substantia nigra, resulting in a significant loss of dopamine in the striatum. Biochemical and neuroimaging studies in human methamphetamine users have shown decreased levels of dopamine and dopamine transporter as well as prominent microglial activation in the striatum and other areas of the brain, changes similar to those observed in PD patients. Consistent with these similarities, recent epidemiological studies have shown that methamphetamine users are almost twice as likely as non-users to develop PD, despite the fact that methamphetamine abuse and PD have distinct symptomatic profiles.

1. Parkinson's Disease

Parkinson's disease (PD) is the second most common neurodegenerative disorder after Alzheimer's disease, affecting an estimated 7 to 10 million people worldwide. Incidence of the disease increases with age. PD usually affects people over the age of 50, but an estimated 4% of PD cases is diagnosed before the age of 50. Early in the course of the disease, the most obvious symptoms are movement-related. These include shaking, rigidity, slowness of movement, and difficulty with walking and gait. Later, cognitive and behavioral problems may arise, with dementia commonly occurring in the advanced stages of the disease. Other symptoms include sensory, sleep, and emotional problems. PD is caused by degeneration of midbrain dopaminergic neurons that project to the striatum. The loss of striatal dopamine is responsible for the major symptoms of the disease. Although a small proportion of cases can be attributed to known genetic factors, most cases of PD are idiopathic. While the aetiology of dopaminergic neuronal demise is elusive, a combination of genetic susceptibilities, age, and environmental factors seems to play a critical role [1]. Dopamine degeneration process in PD involves abnormal protein handling, oxidative stress, mitochondrial dysfunction, excitotoxicity, apoptotic processes, and microglial activation/neuroinflammation.

2. Epidemiology and Pharmacology of Methamphetamine Use

Methamphetamine is an addictive, highly water-soluble CNS (central nervous system) stimulant. It belongs to the group of synthetic drugs chemically related to amphetamine; however, its effects on the CNS are much more pronounced than those of the parent compound. Abuse of these illegal psychostimulants has become an international public health problem, with an estimated 14 to 52 million amphetamine-type stimulant users worldwide, exceeding the total number of cocaine

V. Neurobiology of Methamphetamine. Ares-Santos S, Granado N, Moratalla R. *Biological Research on Addiction*. Chapter 57. 579-91.

From Ares-Santos, S., Granado, N., Moratalla, R., 2013. Neurobiology of Methamphetamine.
In: Biological Research on Addiction:Comprehensive Addictive Behaviors and Disorders.
Elsevier Inc., San Diego: Academic Press, pp. 579–591.
ISBN: 9780123983350

CHAPTER

57

Neurobiology of Methamphetamine

Sara Ares-Santos, Noelia Granado, Rosario Moratalla

Instituto Cajal, Consejo Superior de Investigaciones Científicas, CSIC, and CIBERNED, ISCIII, Madrid, Spain

OUTLINE

BACKGROUND AND HISTORY

Methamphetamine (METH) is an extremely potent synthetic psychostimulant compound used worldwide, primarily as a recreational drug. This drug has high addictive potential and abuse can result in severe psychological and physical dependence. It is, therefore, classified as a Schedule II drug under the Convention on Psychotropic Substances. Other drugs in this category are cocaine and phencyclidine (PCP). Most nonmedical METH comes from illegal laboratories, where it is commonly made by the reduction of ephedrine or pseudoephedrine in a simple process. This simplicity of synthesis seems to have contributed to its popularity: It has replaced cocaine, heroin, and marijuana as the recreational drug of choice in many countries.

Structurally, METH (*N*-methyl-1-phenylpropan-2-amine) is closely related to phenylethylamine, amphetamine, and dopamine (Fig. 57.1). There are quite a few amphetamine derivatives, reflecting the many chemical variations that can be made from the naturally occurring substance phenylethylamine. Amphetamine has an additional methyl group ($-CH_3$) and the addition of a second methyl group in the basic nitrogen leads to METH. Alterations to the benzene ring yield methylenedioxymethamphetamine (MDMA), most commonly known as "ecstasy," and methylenedioxyamphetamine (MDA), also known as the love drug or Eva (Fig. 57.1). Another naturally derived compound, cathinone, is chemically similar to ephedrine and the main component of Khat, abundant in East Africa and the Arabian Peninsula. Like most of these compounds, METH contains a chiral carbon atom, and therefore exists as

Biological Research on Addiction, Volume 2
http://dx.doi.org/10.1016/B978-0-12-398335-0.00057-1

Biological Research on Addiction, First Edition, 2013, 579–591

VI. Neurotoxicity of Methamphetamine. Moratalla R, Ares-Santos S, Granado N. *Handbook of Neurotoxicity*. In press.

Comp. by: Udayasankar Stage: Proof Chapter No.: 123 Title Name: HbNT
Date:6/9/13 Time:09:07:28 Page Number: 1

Neurotoxicity of Methamphetamine

Rosario Moratalla, Sara Ares-Santos, and Noelia Granado

Contents

Abstract

Recreational consumption of the highly addictive psychostimulant methamphetamine is becoming a serious public health problem worldwide. Recent estimates indicate that methamphetamine abuse has increased in the last decade and that only cannabis is used by a greater number of consumers. Despite its popularity, methamphetamine is a known neurotoxin that damages dopaminergic terminals

R. Moratalla (✉) • S. Ares-Santos • N. Granado
Instituto Cajal, Consejo Superior de Investigaciones Científicas, CSIC, and CIBERNED, ISCIII, Madrid, Spain
e-mail: moratalla@cajal.csic.es; moratalla@cajal.csic.es; moratalla@cajal.csic.es

R.M. Kostrzewa (ed.), *Handbook of Neurotoxicity*, DOI 10.1007/978-1-4614-5836-4_123,

VII. D1 but not D4 dopamine receptors are critical for MDMA-induced neurotoxicity in mice. Granado N, Ares-Santos S, Moratalla R. *Neurotoxicity*. Research In press. DOI 10.1007/s12640-013-9438-8

Neurotox Res
DOI 10.1007/s12640-013-9438-8

ORIGINAL ARTICLE

D1 but not D4 Dopamine Receptors are Critical for MDMA-Induced Neurotoxicity in Mice

N. Granado · S. Ares-Santos · R. Moratalla

Received: 2 April 2013 / Revised: 17 October 2013 / Accepted: 29 October 2013

Abstract MDMA, an addictive psychostimulant-consumed worldwide, has the ability to induce neurotoxic effects and addiction in laboratory animals and in humans through its effects on monoaminergic systems. MDMA-induced neurotoxicity in mice occurs primarily in dopaminergic neurons and does not significantly affect the serotonergic system. As the neurotoxic effects of MDMA in mice involve excessive dopamine (DA) release, DA receptors are highly likely to play a role in MDMA neurotoxicity, but the specific dopamine receptor subtypes involved have not previously been determined definitively. In this study, dopamine D1 and D4 receptor knock-out mice ($D1R^{-/-}$ and $D4R^{-/-}$) were used to determine whether these receptors are involved in MDMA neurotoxicity. D1R inactivation attenuated MDMA-induced hyperthermia, decreased the reduction of dopamine and dopamine metabolite levels, and protected against dopamine terminal loss and reactive astrogliosis as determined in the striatum, 7 days after MDMA treatment. In sharp contrast, inactivation of D4R did not prevent hyperthermia or the neurotoxic effects of MDMA. Altogether, these results indicate that D1R, but not D4R, plays a significant role in the dopaminergic striatal neurotoxicity observed after exposure to MDMA.

Keywords Amphetamine derivatives · Methamphetamine · Methcathinone · DAT · Drug addiction · Parkinson's disease · Striatum · TH

Abbreviations

D1R	D1 dopamine receptor
D4R	D4 dopamine receptor
$D1R^{-/-}$	D1 dopamine receptor knockout
$D4R^{-/-}$	D4 dopamine receptor knockout
DA	Dopamine
DAT	Dopamine transporter
DOPAC	3,4-Dihidroxyphenylacetic acid
HVA	Homovanillic acid
5-HT	Serotonin
5-HIAA	5-Hydroxyindolacetic acid
MDMA	3,4-Methylenedioxymethamphetamine
PB	Phosphate buffer
PBST	Phosphate sodium buffer with triton
TH	Tyrosine hydroxylase

Introduction

(±)3,4-Methylenedioxymethamphetamine (MDMA or ecstasy) is a synthetic amphetamine derivative and a psychostimulant drug with addictive potential (Cottler et al. 2009). Use of MDMA and its analogs is estimated at levels comparable to those of cocaine use, with between 10.5 and 28 million users worldwide in 2010 (UNODC World Drug Report 2012). The use of "ecstasy" is particularly common among young people and the drug is frequently used in dance club settings where experienced users often take several dosages at spaced intervals during a given evening (i.e., "stacking" Parrott 2005).

N. Granado · S. Ares-Santos · R. Moratalla (✉)
Instituto Cajal, Consejo Superior de Investigaciones Científicas, CSIC, Avd. Dr. Arce 37, 28002 Madrid, Spain
e-mail: moratalla@cajal.csic.es

N. Granado · S. Ares-Santos · R. Moratalla
CIBERNED, Instituto de Salud Carlos III, Madrid, Spain

Published online: 21 November 2013